

THESE DE DOCTORAT DE

L'UNIVERSITE DE NANTES

ECOLE DOCTORALE N° 602

Sciences pour l'Ingénieur

Spécialité : « *Génie des Procédés et Bioprocédés* »

Par

« **Guillaume TANGUY** »

« **Biocompatible extraction of β -carotene from *Dunaliella salina*** »

Thèse présentée et soutenue à « Saint-Nazaire », le « 23/06/2022 »

Unité de recherche : Laboratoire GEPEA UMR CNRS 6144

Rapporteurs avant soutenance :

Filipa Lopes Professeur des universités, Centrale-Supélec
Nathalie Bourgougnon Professeur des universités, Université Bretagne Sud

Composition du Jury :

Président : Nathalie Bourgougnon Professeur des universités, Université Bretagne Sud

Examineurs : Justine Marchand Maître de conférences, Le Mans Université
 Miriam Phélippé Docteur, Aqua Eco Culture

Dir. de thèse : Luc Marchal Professeur des universités, Polytech Nantes
Co-dir. de thèse : Benoît Schoefs Professeur des universités, Le Mans Université
Encadrant de thèse : Olivier Goncalves Professeur des universités, IUT de Nantes

Remerciements

L'aboutissement de mes travaux de thèse est une grande joie. Les efforts déployés doivent beaucoup aux personnes qui m'ont conseillé, soutenu et motivé au cours de ces nombreuses années pour m'aider à affirmer ma passion de la science et les microalgues, intrigantes et fascinantes à la fois.

Je tiens à exprimer toute ma reconnaissance aux directeurs successifs du laboratoire GEPEA : Messieurs Jack Legrand, Pascal Jaouen et Jérémy Pruvost pour m'avoir accueilli au sein de leur équipe. Je tiens à remercier Madame Nathalie Bourgougnon, Professeur des universités, à l'Université Bretagne Sud et Madame Filipa Lopes, Professeur des universités à Centrale-Supélec pour avoir accepté d'être rapporteurs de mes travaux. Je vous remercie pour les rapports, les échanges approfondis lors de la soutenance et les suggestions pertinentes pour améliorer le manuscrit lors des corrections. Merci Madame Lopes pour nos échanges très approfondis sur l'activité métabolique des microalgues à certains moments de ma thèse. Je remercie Justine Marchand, maître de conférences à Le Mans Université et Miriam Phélippe, docteur à Aqua Eco Culture pour avoir accepté d'examiner mon mémoire et de faire partie de mon Jury de thèse.

Un grand merci à mes directeurs de thèse, Monsieur Luc Marchal, Professeur des universités à Polytech Nantes et Benoît Schoefs, Professeur des universités à Le Mans Université. Merci pour m'avoir accordé votre confiance sur ce sujet de recherche passionnant, merci pour nos nombreuses discussions de haute qualité scientifique, merci de votre soutien constant, merci de m'avoir fait découvrir la richesse et l'exigence de la science. J'en sors affûté et encore plus curieux. Un grand merci également à Olivier Goncalves, professeur des universités, IUT de Nantes pour ta sympathie, ton soutien et tes nombreux conseils.

Je tiens, en particulier, à témoigner ma gratitude et ma reconnaissance à toute l'équipe du GEPEA. Merci à tous. Laurette pour ton accueil chaleureux. Delphine et Laurence pour votre sympathie et votre soutien. Hélène pour tes conseils sur l'électronique. Guillaume pour ton aide pratique, le scotch c'est la vie ! Sébastien pour ton temps accordé sur la CPC. Raphaëlle pour tes conseils sur la culture, je suis bien armé pour la suite ! Carole pour tes conseils professionnel et personnel percutant. Merci également aux enseignants chercheurs du laboratoire qui ont répondu à mes nombreuses questions : Guillaume Cogne, Mariana Titica, Dominique Grizeau, Catherine Dupré, Caroline Gentric, Estelle Couallier, Walid Blel, Anthony Masse. Merci au personnel de Le Mans Université pour m'avoir accueilli à plusieurs reprises dans votre laboratoire. Merci Justine, Brigitte et Hélène.

Je remercie tous mes collègues doctorant pour tous ces moments colorés : Merci Asma, Armel, Antoine, Dounia, Sara, Vladimir, Philippe, Antoinette, Alexandra, Rémy, Jérémy, Fernando, Shu-Li, Eglantine, Rosine.

Finalement, je dédie ce travail à ma famille qui m'a beaucoup soutenu durant ce parcours. Merci Maman, papa et à mes frères Mathieu, Julien et Romain.

List of scientific communications

- “Granulo-selective extraction of beta-carotene from *Dunaliella salina*- new contribution”
Journée scientifiques d’AMI (European Congress of Applied Biotechnology), G.Tanguy, O. Goncalves, L.Marchal, B.Schoefs, Florence, Italy (Juin 2018).
- “Granulo-selective extraction of beta-carotene from *Dunaliella salina*- new contribution”
Journée scientifiques d’AMI (European Congress of Applied Biotechnology), G.Tanguy, O. Goncalves, L.Marchal, B.Schoefs, Florence, Italy (Juin 2019). La MER XXL
- “Granulo-selective extraction of beta-carotene from *Dunaliella salina*- new contribution”
ECAB 5 (European Congress of Applied Biotechnology), G.Tanguy, O. Goncalves, L.Marchal, B.Schoefs, Florence, Italy (Septembre 2019).
- “Extraction biocompatible de β -carotène de *Dunaliella salina* -nouvelle contribution ”
congrès SFGP (Société Française de Génie des Procédés), G.Tanguy, O. Goncalves, L.Marchal, B.Schoefs, Nantes, France (Octobre 2019).
- Tanguy, G.; Legat, A.; Gonçalves, O; Schoefs, B.; Marchal, L. Selection of culture conditions and cell morphology for biocompatible extraction of β -carotene from *Dunaliella salina*. *Mar. Drugs* **2021**, *19*(11), 648. <https://doi.org/10.3390/md19110648> (Published)

Table of content

<i>Résumé en français</i>	1
Introduction du sujet	2
Objectifs de l'études.....	4
Principaux résultats et discussion	6
<i>General introduction</i>	1
<i>Chapter 1. Production and biorefining of β-carotene from Dunaliella salina</i>	7
1 The β -carotene	8
1.1 Chemical structure	8
1.2 Role in microalgae.....	9
1.3 Metabolism in animals.....	9
1.4 Industrial application of β -carotene	10
1.4.1 Food and feed.....	10
1.4.2 Medical sector	11
1.4.3 Cosmetic industries	11
1.5 Industrial production.....	12
1.5.1 Global market.....	12
1.5.2 Chemical production	12
1.5.3 Biological production.....	13
2 Production of β -carotene from <i>Dunaliella salina</i>	15

2.1	<i>Dunaliella salina</i>	15
	2.1.1 Morphology	15
	2.1.2 Taxonomy	15
	2.1.3 Ecology.....	16
	2.1.4 Reproduction and life cycle	18
2.2	Microalgal metabolism	19
	2.2.1 Photosynthesis	19
	2.2.2 Respiration	22
2.3	Carotenogenesis in <i>Dunaliella</i>	23
	2.3.1 Anabolic pathway	23
	2.3.2 Stress detection.....	23
	2.3.3 Intracellular reorganisation.....	24
	2.3.4 Factors influencing accumulation.....	25
3	Mass culture of <i>Dunaliella</i>	34
	3.1 Industrial producers	34
	3.2 Open culture systems.....	35
	3.3 Closed Culture System: Photobioreactor (PBR)	36
4	Industrial biorefining of β -carotene from <i>Dunaliella</i>	40
	4.1 Harvesting.....	40
	4.1.1 Coagulation-flocculation	40
	4.1.2 Flottation.....	<i>Erreur ! Signet non défini.</i>

4.1.3	<i>Sedimentation</i>	41
4.1.4	<i>Centrifugation</i>	41
4.1.5	<i>Adsorption</i>	42
4.2	<i>Dewatering</i>	42
4.2.1	<i>Sun drying</i>	43
4.2.2	<i>Freeze drying</i>	43
4.2.3	<i>Spray drying</i>	43
4.3	<i>Extraction</i>	44
4.3.1	<i>Organic solvent</i>	44
4.3.2	<i>Edible oil</i>	44
4.3.3	<i>Supercritical CO₂</i>	45
5	<i>Milking of microalgae</i>	47
5.1	<i>The milking concept</i>	47
5.2	<i>Pulsed electric field</i>	49
5.3	<i>Mechanical extraction</i>	50
5.4	<i>Spontaneous oozing</i>	51
5.5	<i>Biocompatible organic solvents</i>	53
5.5.1	<i>Solvent partitioning and toxicity</i>	53
5.5.2	<i>Effect of extraction on cell viability</i>	55
5.5.3	<i>Stimulation and inhibition of cell growth</i>	58
5.5.4	<i>Membrane permeabilization</i>	60

5.5.5 Mechanism of extraction	61
6 Viability and vitality of microalgae	62
6.1 Cell density	62
6.2 Biological activity.....	64
6.2.1 Autofluorescence	66
6.2.2 Permeability	67
6.2.3 Enzymatic activity.....	68
6.2.4 Cell division cycle.....	69
Chapter 2. Material and methods.....	72
1 Cultivation	73
1.1 Strain and growth conditions	73
1.2 Production of β -carotene enriched biomass.....	73
1.3 Culture in photobioreactor.....	76
2 Extraction.....	77
2.1 Solvent choice.....	77
2.2 Optimization of the extraction in Falcon	78
3 Analysis	80
3.1 Photosynthetic parameters	80
3.1.1 Oxygen production	80
3.1.2 Photosynthetic activity.....	81
3.2 β -carotene by spectrophotometry	82

3.2.1	<i>Mass balance with n-decane</i>	84
3.3	Dry weight	85
3.4	Characterization of cell morphology	85
3.4.1	<i>Counting chamber</i>	85
3.4.2	<i>Cell fixation</i>	86
3.4.3	<i>Automated particle analysis</i>	88
3.4.4	<i>Digital imaging accuracy</i>	88
3.4.5	<i>Size measurement</i>	90
3.4.6	<i>Shape factors</i>	91
3.5	Biological activity	92
3.5.1	<i>Enzymatic activity</i>	92
3.5.2	<i>Permeability</i>	92
3.5.3	<i>Phase of cell division cycle</i>	93
3.5.4	<i>β-carotene fluorescence</i>	94
Chapter 3. Effects of n-decane exposure on metabolic activity of <i>Dunaliella salina</i>		95
1	Introduction	96
2	Materiel et methods	98
2.1	Strain and pre-culture	98
2.2	In-situ mixing experiment	98
2.3	Characterization of the impact on cell biology	99
2.3.1	<i>Growth ability after extraction</i>	99

2.3.2	<i>Oxygen production and consumption</i>	99
2.3.3	<i>Enzymatic activity</i>	100
2.3.4	<i>Permeability</i>	101
2.3.5	<i>Phase of cell division cycle</i>	101
2.3.6	<i>β-carotene fluorescence</i>	102
2.4	Instrument for fluorescence measurement.....	102
2.4.1	<i>Spectrofluorimetry</i>	102
2.4.2	<i>Epifluorescence microscopy</i>	102
2.4.3	<i>Flow cytometry</i>	103
2.5	Statistics.....	105
2.5.1	<i>Population analysis</i>	105
2.5.2	<i>Single cells analysis</i>	105
3	Results and discussion	106
3.1	Characterization of the microalgae population.....	106
3.1.1	<i>Photosynthetic oxygen production and respiration</i>	106
3.1.2	<i>Cell permeability to Propidium Iodide</i>	108
3.1.3	<i>Enzymatic activity</i>	109
3.1.4	<i>Growth after solvent exposure</i>	109
3.2	Single cell characterization.....	110
3.2.1	<i>Cytometry measurements with fluorescein</i>	110
3.2.2	<i>Epifluorescence measurement with CTC</i>	111

3.2.3	<i>Single cell permeability with Sytox Green</i>	113
3.2.4	<i>Cell cycle analysis</i>	114
3.2.5	<i>β-carotene content</i>	117
3.3	Comparison of characterization methods	119
4	Conclusion	121
Chapter 4. Selection of culture conditions and cell morphology for biocompatible extraction of β-carotene from <i>Dunaliella salina</i>*		123
1	Introduction.....	124
2	Material and methods.....	126
2.1	Strain and cultures in flask	126
2.2	Culture in photobioreactor.....	127
2.3	In situ extraction experiment	128
2.4	Characterization of the aqueous and solvent phases	128
2.4.1	<i>Photosynthetic activity</i>	128
2.4.2	<i>β-carotene quantification in biomass</i>	129
2.4.3	<i>Dry mass</i>	130
2.4.4	<i>Cell density, volume and circularity</i>	130
2.4.5	<i>Cell membrane permeabilization</i>	133
2.4.6	<i>Statistics and plots</i>	135
3	Results and discussion	135
3.1	β -carotene extraction from cells	135

3.2	Impact of β -carotene extraction on photosynthetic activity	137
3.3	Impact of n-decane treatment on cell integrity	137
3.4	Impact of the cell size distribution	139
3.5	Influence of volume and circularity on cell disruption.....	141
3.6	Cell permeabilization with solvent	144
4	Conclusions.....	147
	<i>General discussion</i>	148
	<i>Conclusion and perspectives</i>	155
	Conclusion.....	156
	Perspectives	157
	Conclusion.....	159
	Perspectives	160
	<i>Appendixes 188</i>	
	Appendix 1	189
	Appendix 2	193
	Fluorescence measurement	193
	<i>Fluorescence principle</i>	193
	<i>Spectrofluorometer</i>	194
	<i>Epifluorescence microscope</i>	195
	<i>Flow cytometer</i>	196

List of figures

Figure 1.1 – Structures of all- <i>trans</i> - β -carotene and its four major <i>cis</i> -isomers (Jing <i>et al.</i> , 2012).	8
Figure 1.2 – Summary of β -carotene metabolism (D’Ambrosio <i>et al.</i> , 2011).....	10
Figure 1.3 – Global β -carotene market share by source in 2016 (Grand View Research, 2018).	12
Figure 1.4 – β -carotene content in selected fruits and vegetables (Bogacz-Radomska and Harasym, 2018).	13
Figure 1.5 – Light micrographs of <i>Dunaliella</i> species and stages of <i>Dunaliella</i> life cycle (the length of the cells is given in parentheses), (Borowitzka and Siva, 2007).	17
Figure 1.6 – Photosynthetic antenna and reactions and its localization on the thylakoid membrane of the chloroplast (Joyard and Morot-Gaudry, 2020).....	20
Figure – 1.7 Calvin Cycle	21
Figure 1.8 – The carotenoid biosynthetic pathway (Gateau <i>et al.</i> , 2016).	23
Figure 1.9 – Ultrastructure of <i>Dunaliella salina</i> under growth conditions (a) and under stressful conditions (b), (Polle <i>et al.</i> , 2020).....	25
Figure 1.10 – Comparison of nutrient intake of culture media used for <i>Dunaliella</i> culture....	31
Figure 1.11 – Photographs of two industrial production methods of the species <i>Dunaliella salina</i> . (a) Open pond in Australia at Western Technologies, (b) Raceway in Israel at Nature Beta Technologies.	35
Figure 1.12 – Closed cultivation system of microalgae in a bag photobioreactor (a), (Koller, 2015) an air lift photobioreactor (b), (Lindblad <i>et al.</i> , 2019) and a tubular photobioreactor (c), (Alaswad <i>et al.</i> , 2015).	38

Figure 1.13 – Relation between the light absorption conditions (represented by the irradiance field $G(z)$) and corresponding mean biomass volumetric productivities ($\langle rx \rangle$). The three typical cases of light-attenuation conditions are represented: full light absorption (Case A), luminostat (Case B) and kinetic regimes (Case C) (Pruvost and Cornet, 2012).....	39
Figure 1.14 – Biorefining process of β -carotene used in industrial production (Hosseini Tafreshi and Shariati, 2009).	46
Figure 1.15 – Scheme presenting milking as an alternative to current processes. (Top): Current processes are systems that require starting new microalgal cultures for each batch of metabolites, with fresh nutrients; (Bottom): Milking only requires inputs of carbon dioxide and water used up in producing metabolites, and thus is closer to a closed system (Vinayak <i>et al.</i> , 2015). HVM : high value metabolites.	48
Figure 1.23 – The electroporation mechanism of microalga cell membrane (Joannes <i>et al.</i> , 2015).....	50
Figure 1.24 – Stimulation of astaxanthin production after extraction with gold nano-scalpel incision (Praveenkumar <i>et al.</i> , 2015).	51
Figure 1.25 – Colony of <i>Botryococcus Braunii</i> with natural oil bodies oozing in the extracellular matrix. Due to the flattening by the microscope cover glass, hydrocarbons are exuded from extracellular matrices (Hirano <i>et al.</i> , 2019).....	52
Figure 1.26 – <i>Diadesmis confervaceae</i> in solitary and chain forms as observed under 100 \times oil immersion. Note oozed oil droplets in panel C. Cf. (Vinayak <i>et al.</i> , 2014). Scale bar: 10 μ m.	52
Figure 1.16 – Schematic diagram of the principle in the liquid biphasic system (Khoo <i>et al.</i> , 2020).....	53
Figure 1.17 – Droplet of n-decane in a <i>Dunaliella salina</i> culture (a), <i>Dunaliella salina</i> cell in n-decane (b), (Kleinegris <i>et al.</i> , 2011b).	54

Figure 1.18 – Phase separation of lipids milking in <i>Chlorella vulgaris</i> with (a) 10% tetradecane (b) 20% dodecane after 2nd cycle of extraction (Atta <i>et al.</i> , 2016).	55
Figure 1.19 – Principle of extraction in a two-phase photobioreactor.	57
Figure 1.20 – Impact of biocompatible extraction on <i>Dunaliella salina</i> cells in the literature.	59
Figure 1.21 – Solvent membrane poration : a) The membrane is fluid, b) The solvent diffuses into the membrane, c) The transmembrane gradient creates a reversible pore, and d) The membrane integrity is breached.	60
Figure 1.22 – Scanning electron microscope of <i>Dunaliella salina</i> cell cultivated in medium saturated in dodecane. A vesicle which is located between the cell and the chloroplast membrane (A) and another vesicle which seems to be being released from the cells of <i>D. salina</i> (B) are shown.	62
Figure 1.27 – Present standard methods for detecting and evaluating microbes, including microalgae. Optical measurements, the electrical sensing zone method, the conventional plate count method, and weight measurements are categorized. The automated cell counter marked with an asterisk means a device without fluorescence detection (Takahashi, 2020).	63
Figure 1.28 – Confidence limits of the cell counting method regarding the number of cells counted (Lund, 1958).	64
Figure 1.29 – The measurement of single cell parameters, viability and vitality definitions (Hyka <i>et al.</i> , 2013).	65
Figure 1.30 – Living 3-month-old <i>Chroococcidiopsis</i> 041 CCALA laboratory culture (a) simultaneously stained with SYTOX Green (b), CTC (c) and DAPI (d) dyes and showing pigment autofluorescence (e) and classification of cells according to the selected criteria.	66
Figure 1.31 – Phase of the cell division cycle, the histogram shows a population analysis color coded by phase (“Cell Cycle Assay Principle - Beckman Coulter,” n.d.).	70

Figure 2.1 – Selected culture conditions (a) and protocol of production of β -carotene enriched biomass (b).....	75
Figure 2.2 – Culture system in photobioreactor.....	76
Figure 2.3 – Solvent physicochemical characteristic (“CRC Handbook of Chemistry and Physics, 2009–2010, 90th ed.,” 2009).	77
Figure 2.4 – Set up for extraction of β -carotene with organic solvent by stirring falcon tube on a vortex.....	78
Figure 2.5 – The volume needed for analysis (a) Experimental plan to select operatory conditions of extraction in falcon tube (b).	79
Figure 2.6 – Transverse section through a Clark (Rank) oxygen electrode (“Oxygen electrodes Electroanalytical techniques,” n.d.).....	80
Figure 2.7 – Measurement of photosynthetic activity (Roháček, 2010).	81
Figure 2.8 – Extraction of β -carotene with methanol. Effect of one, two or three extraction cycle on the extraction yield of β -carotene (a). Effect of incubating conditions with methanol on β -carotene extraction yield (b).....	83
Figure 2.9 – The repartition of β -carotene between cells and the n-decane for increasing stirring time (a) and the calibration made in the lab for spectrophotometric measurement of β -carotene concentration in the n-decane, with $R^2>0.99$ (b).....	84
Figure 2.10 – Nageotte counting chamber.	86
Figure 2.11 – Choice of fixative agents for cell counting size and fluorescence measurements of <i>Dunaliella salina</i>	87
Figure 2.12 – Principle of pixel representation of a particle (INRA, 2021).	88
Figure 2.13 – Relative error on the estimation of cell volume regarding diameter for different resolution of image.....	89

Figure 2.14 – Cell volume calculation from cross section for sphere and prolate spheroid shapes (Sun and Liu, 2003).....	90
Figure 2.15 – The different size parameters of a particle and shape factors.....	91
Figure 3.1 – The gating strategy in cytometric analysis. Cells outside the focus were not considered (a), isolated cells were analysed (b), cells with a chlorophyll content were kept (c).	104
Figure 3.2 – Effect of n-decane stirring on the oxygen productivity (a), on the permeability (b) and on the enzymatic activity (c) of <i>Dunaliella salina</i> with and without n-decane stirring for 120 s for cells grown in erlenmeyer (GE) and stressed in erlenmeyer (SE).	107
Figure 3.3 Growth ability of stressed cells in erlenmeyer (SE) after n-decane mixing for 120s in nitrogen depleted and nitrogen repleted medium.....	110
Figure 3.4 – Effect of n-decane stirring on esterases activity of stressed cells in erlenmeyer (SE). Cytogram of untreated stressed cells (a) and stressed cells exposed to 120s n-decane stirring (b). Cells were stained with fluorescein diacetate (FDA).....	111
Figure 3.5 – Bright field picture of <i>Dunaliella salina</i> untreated stressed cell (a,b) and after 120s stirring with n-decane (c,d). Enzymatic activity of <i>Dunaliella salina</i> is indicated by the blue fluorescence intensity of CTC (formazan) (b,d). Scale bars in white indicate 50µm. The normalized enzymatic activity distribution is plot in cell frequency (e).....	112
Figure 3.6 – Bright field picture of <i>Dunaliella salina</i> untreated stressed cell (a,b) and after 120s stirring with n-decane (c,d). Permeability of <i>Dunaliella salina</i> to Sytox Green is indicated by the green fluorescence intensity (b,d). Scale bars in white indicate 50µm. The normalized permeability distribution is plot in cell frequency (e).	114
Figure 3.7 – Bright field picture of <i>Dunaliella salina</i> untreated stressed cell (a,b) and after 120s stirring with n-decane (c,d). DNA content of <i>Dunaliella salina</i> is indicated by the blue fluorescence intensity of DAPI (b,d). Scale bars in white indicate 50µm. The normalized DNA	

distribution is plot in cell frequency (e). The phase of cell division is indicated by dashed lines.	116
Figure 3.8 – Scatter plot of β -carotene content (x-axis) and volume (y-axis) for untreated stressed cells (a), after n-decane stirring for 120s (b).	118
Figure 3.9 – Comparison of the characterization methods used to access biological parameters such as permeability, activity, cell cycle.....	120
Figure 4.1 – Biocompatibility of n-decane treatment. Photosynthetic activity (a-b) before stirring (0s) and after 120 s mixing time for (a) grown cells (GE) and (b) stressed cells (SE). Biomass integrity (%) (c-e) expressed as cell density (control: stirring without solvent), biomass volume, dry weight and β -carotene content for GE (c), SE (d) and SPBR (e) cells with solvent mixing time. Scale bars indicate standard deviation error (n=3).	136
Figure 4.2 – Cell volume dependant disruption for (GE) grown cells (a,d,g), (SE) stressed cells (b,e,h) and (SPBR) stressed cells in erlenmeyer (c,f,i). Box plot of the distribution (a-c). Cumulated cell density per volume class (d-f). Cell disruption rate by volume class (μm^3) after 240s (g-i). Scale bars indicate standard error (n=3). Median and third quartile of the distribution were more affected than first quartile ($p < 0.05$).....	140
Figure 4.3 – Effect of n-decane extraction on circularity and volume. Density scattering plots of grown cells (GE), (a-d) for 0s (a), 45 s (b), 120s (c) and 240s (d), stressed cells in erlenmeyer (SE), (e-h) for 0s (e), 45s (f), 120s (g) and 240s (h) and stressed cells in PBR (SPBR), (i-l) for 0s (i), 45s (j), 120s (k) and 240s (l).....	142
Figure 4.4 – The index of potential disruption. Cumulated cell density per circularity class (a-c) for (a) grown cells (GE), (b) stressed cells (SE) and (c) SPBR cells. Disruption yield (%) per index of potential disruption class (IPCD), (d-f) for GE cells (d), SE cells (e) and SPBR cells (f). Scale bars indicate standard deviation (n=3). The higher the IPCD the higher the disruption yield ($p < 0.05$).....	143

Figure 4.5 – Membrane permeabilization with n-decane of SPBR+E cells. Pictures of the different permeabilization categories of cells (a), black line represent 20µm. Cell abundance (%) in disrupted cells (DC), non-affected cells (NA), irreversibly permeabilized cells (IP) and reversibly permeabilized cells (RP) for the different extraction time (b). Biocompatibility index throughout the treatment (c). Density scatter plots of non-affected cells (d) and naturally permeabilized cells (e). Cell disruption yield per index of potential disruption (IPCD), (f).	145
Figure 5.1 Influence of β-carotene extraction with n-decane on the metabolic activity of <i>Dunaliella salina</i>	152
Figure 5.2 Suggested strategy for the optimization of culture conditions of <i>Dunaliella salina</i> to improve the biocompatibility of β-carotene extraction.	153
Figure 5.1– The stokes wavelength shift in fluorescence phenomenon, the excited the excited electrons emit a particle with different wavelength.	193
Figure 5.2 – A spectrofluorometer Horiba fluoromax plus.....	194
Figure 5.3 – Rays of light in an epifluorescence microscope (a) and a Nikon TiE eclipse inverted epifluorescence microscope (b).....	195
Figure 5.4 – Cytometry working principle. Multiple laser source excites the sample, the fluorescence intensity is then read by a photodiode detector (a). An imaging flow cytometry Amnis Image Stream Mk II (b) and a laser flow cytometer BD Accuri C6 plus (c).	196

List of tables

Table 1.1 – Carotenoid content in the selected microalgae species (Ambati <i>et al.</i> , 2019).	14
Table 1.2 – Highest carotenoids content reported in <i>Dunaliella salina</i> cell.	26
Table 1.3 – <i>Dunaliella tertiolecta</i> P-molar formula	30
Table 1.4 – Commercial producers of β -carotene from <i>Dunaliella</i> (Del Campo <i>et al.</i> , 2007).34	
Table 4.1 – Cell response to the staining with Evans blue.	133

List of abbreviations

CLD: cytoplasmic lipid droplet

CTC: 5-Cyano-2,3-Ditolyl Tetrazolium Chloride

DAPI: 4',6-diamidino-2-phenylindole

DC: disrupted cells

DNA: deoxyribonucleic acid

FDA: fluorescein diacetate

GE: grown in erlenmeyer

HVM: high value metabolites

IP: irreversibly permeabilized

NA: non-affected

NADPH: Nicotinamide adenine dinucleotide phosphate

NAT-P: naturally permeabilized

NPQ: non photochemical quenching

PBR: photobioreactor

PEF: pulsed electric field

PFD: photon flux density

PI: propidium iodide

PSII: photosystem II

ROS: reactive oxygen species

RP: reversibly permeabilized

SE: stressed in erlenmeyer

SPBR: stressed in photobioreactor

Résumé en français

Introduction du sujet

Les microalgues sont des organismes unicellulaires microscopiques qui opèrent la photosynthèse pour extraire de l'énergie et des substances de leur environnement (Scarsini *et al.*, 2019). Pendant le processus de croissance, 1 kg de microalgues capte environ 1,8 kg de CO₂ de l'atmosphère (Iglina *et al.*, 2022). En outre, le rendement de production des microalgues par hectare est plus de 20 fois supérieur à celui des plantes (Benedetti *et al.*, 2018). Certaines des biomolécules naturelles produites par les microalgues ne peuvent pas être synthétisées chimiquement aujourd'hui, car elles nécessitent l'action d'enzymes spécifiques (Alder *et al.*, 2012). La ressource microalgale est une source de nouveaux composés pour de nombreuses applications industrielles : alimentation humaine, alimentation animale, pharmacie, cosmétique et énergie (Mimouni *et al.*, 2012). Parmi les biomolécules extraites des microalgues, les caroténoïdes occupent une place historique et prépondérante (Scarsini *et al.*, 2020) car ils présentent des propriétés uniques comme la provitamine A, des activités antioxydantes et de protection de la peau (Gateau *et al.*, 2016). Le puissant effet antioxydant des caroténoïdes, comme le β -carotène, est dû au piégeage des radicaux libres. Son effet positif sur la santé a été prouvé dans le traitement d'un grand nombre de maladies avec des activités antidiabétiques, antitumorales, anti-inflammatoires et des bénéfices pour la fonction cognitive (Gateau *et al.*, 2016).

La viabilité économique de la production de métabolites produits à partir des microalgues représente un défi biotechnologique qu'il convient de relever. En effet, les microalgues sont des microorganismes à croissance lente (0,05 jour⁻¹ pour *Isochrysis galbana* et 1,2 jour⁻¹ pour *Scenedesmus* sp.), (Darvehei *et al.*, 2018) par rapport aux levures (9,6 jours⁻¹ pour *Saccharomyces cerevisiae*), (Boender *et al.*, 2009) et aux bactéries (18,5 jours⁻¹ pour *Escherichia coli*), (Paalme *et al.*, 1997). Les coûts de production actuels associés aux

métabolites de microalgues sont plus élevés que pour les levures et les bactéries avec qui elles vont rentrer en compétition commerciale. La disponibilité de la lumière au sein des réacteurs est un verrou technique majeur pour l'industrialisation de la production autotrophe de microalgues qui nécessitent des designs spécifiques de bioréacteurs (Pruvost *et al.*, 2016). Afin d'industrialiser la production de substances à hautes valeurs ajoutées, l'amélioration de la productivité et de la reproductibilité des processus de culture et d'extraction est obligatoire (Guedes *et al.*, 2011). La compréhension du métabolisme des microalgues et des processus de production est donc une étape clé.

Chez certains taxons de microalgues, l'application couplée d'un appauvrissement en azote et d'un stress lumineux élevé déclenche la réorientation du métabolisme carboné vers l'accumulation massive de métabolites secondaires. Par exemple, la microalgue verte *Dunaliella*, qui se trouve naturellement dans de nombreux marais salants, accumule du β -carotène jusqu'à 14% de son poids sec (Ben-Amotz *et al.*, 1988 ; da Silva et Lombardi, 2020). Les procédés actuels de fractionnement des microalgues nécessitent plusieurs étapes en aval telles que la déshydratation, le séchage, l'extraction par solvant et la purification des biomolécules cibles (Vinayak *et al.*, 2015). De plus, ils génèrent des résidus qui doivent être traités. La plupart de ces étapes sont très consommatrices en temps et en énergie (Hosseini Tafreshi et Shariati, 2009), ce qui peut mettre en péril la viabilité écologique et économique de ces procédés, à moins que le prix de ces biomolécules soit très élevé. La réduction des résidus de production par des méthodes d'extraction *in situ*, dites de traite, a été proposée. Cela inclut l'utilisation de prétraitements telles que des impulsions électriques (Zhang *et al.*, 2020 ; Gateau *et al.*, 2021) ou des fréquences de résonance (Vinayak *et al.*, 2017), et de solvants biocompatibles (Frenz *et al.*, 1989 ; Hejazi *et al.*, 2002 ; León *et al.*, 2003 ; Atta *et al.*, 2016). Chez *Dunaliella*, en comparant la solubilité du β -carotène, la capacité d'extraction par solvant

et la biocompatibilité des solvants organiques, León *et al.* (2003) ont établi que le meilleur compromis pour l'extraction biocompatible du β -carotène est obtenu en utilisant des solvants hydrophobes présentant un $\log P_{\text{octanol}}$ autour de 5 comme le n-décane, à condition que le rapport solvant/culture (v/v) reste inférieur à 1. Cependant, pour *Dunaliella*, le n-décane a été considéré comme non compatible (Hejazi et al, 2002) avec une corrélation directe entre la destruction des cellules et l'extraction du β -carotène (Kleinegris *et al.*, 2011b), ou biocompatible (Mojaat *et al.*, 2008) avec une fraction plus élevée de β -carotène extrait par rapport au taux de destruction des cellules. En général, il a été rapporté que l'extraction des lipides des microalgues avec un solvant organique dépend du temps de contact et de la surface entre le milieu et le solvant organique, mais plus le taux d'extraction est élevé, plus la biocompatibilité est faible (Frenz *et al.*, 1989 ; Hejazi *et al.*, 2003 ; Atta *et al.*, 2016 ; Miazek *et al.*, 2017).

Objectifs de l'étude

Alors que de nombreuses études se sont concentrées sur la sélection des solvants et les conditions opératoires de l'extraction, l'effet des conditions de culture sur les caractéristiques à l'échelle de la cellule et, *de facto*, sur la biocompatibilité de l'extraction reste peu étudié. Les méthodes les plus courantes de suivi des cultures consistent à mesurer des caractéristiques moyennes de la population (densité cellulaire, poids sec, teneur en pigments, activité photosynthétique), ce qui peut conduire à des informations biaisées qui ne rendent pas compte de l'hétérogénéité de la culture. Les études environnementales et toxicologiques du phytoplancton fournissent des informations de base sur les mécanismes de toxicité des substances et leur impact sur les activités métaboliques et l'intégrité biologique (Hyka *et al.*, 2013). Les outils développés peuvent être appliqués pour la compréhension du mécanisme de toxicité d'un traitement de bioraffinage. En dehors des conditions de laboratoire, la variabilité

de la croissance est causée par des conditions non homogènes, la disponibilité des nutriments, la compétition et la prédation. Dans les conditions de laboratoire, les cultures microbiennes présentent toujours un degré élevé d'hétérogénéité en termes de taux de croissance et de résistance au stress (Adler *et al.*, 2007).

Il est généralement admis que parmi les premiers signes mesurables de la mort cellulaire figurent la perte ou la réduction de l'intégrité de la membrane et de l'activité métabolique (Caron et Badley, 1995 ; Hyka *et al.*, 2013). Ainsi, l'activité enzymatique qui représente l'intensité du métabolisme (vitalité) et le contenu en ADN qui montre la capacité de la cellule à poursuivre sa croissance (viabilité) pourraient influencer la biocompatibilité unicellulaire à l'extraction par du solvant organique.

D. salina est une microalgue sans paroi cellulaire, ce qui signifie que les cellules sont limitées par une membrane plasmique mince et élastique (Dodge, 1973) qui agit comme la seule barrière sélective aux composés (León *et al.*, 2001). Par principe, l'extraction ne peut être biocompatible pour une cellule que si la perméabilisation de sa membrane est réversible. Or les membranes cellulaires sont les endroits préférentiels où les solvants organiques, comme les n-alcanes, peuvent s'accumuler (Bar, 1988), perturbant la fluidité membranaire (Sikkema *et al.*, 1995) et conduisant à la perméabilisation de la membrane (Lorente De Nó, 1934). Ainsi, le volume cellulaire et la circularité qui quantifient la morphologie de la membrane cellulaire et la perméabilité naturelle qui qualifie l'intégrité de la membrane cellulaire pourraient influencer le processus de perméabilisation et la biocompatibilité qui en résulte.

•

Il en résulte les questions scientifiques suivantes auxquelles cette thèse apporte des éléments de réponses :

- Est-ce que le solvant a une toxicité préférentielle sur une sous population de cellules ??
- Quel est l'impact de l'extraction de β -carotène sur l'activité métabolique des cellules ?
- Existe-t-il des conditions de cultures plus favorables pour que l'extraction soit biocompatible ?

Principaux résultats et discussion

Les résultats obtenus dans cette thèse montre qu'un critère d'extraction biocompatible retenu dans la littérature est que la proportion de β -carotène extraite doit être supérieure à la proportion de cellules détruites par l'extraction. Dans ces conditions, on peut faire l'hypothèse que tous les métabolites ont été extraits des cellules perturbées et que la quantité restante de métabolites a été extraite des cellules intactes. Pour les cellules cultivées, l'extraction a été tout au long légèrement biocompatible avec une récupération jusqu'à 60% dans le n-décane pour 45% de cellules perturbées. Pour les cellules stressées après 240s, l'extraction était efficace mais peu biocompatible : jusqu'à 88% de récupération des caroténoïdes pour 87% de déstructuration cellulaire. Il est intéressant de noter que pour les cellules stressées en photobioréacteur (SPBR) après 120s, la récupération des caroténoïdes était de 30 % pour 15 % de destruction des cellules. Même si le critère de biocompatibilité a été rempli, il apparaît globalement qu'un rendement d'extraction élevé est lié à une destruction cellulaire plus importante. Ceci confirme la corrélation entre l'extraction du β -carotène et la mort cellulaire, et la perturbation cellulaire comme condition préalable à l'extraction du β -carotène, atteinte par plusieurs autres études (Kleinegris et al., 2011b; Miazek et al., 2017)

De l'analyse de l'impact de l'extraction sur la distribution de la taille des cellules, le résultat principal est que le taux de destruction des cellules augmente linéairement ($R^2 > 0.99$) avec le volume des cellules. Il a été validé que les cellules les plus grandes ont une teneur en caroténoïdes plus élevée. Par conséquent, le taux d'extraction des cellules stressées en erlenmeyer (SE) était plus rapide que celui des cellules cultivées en erlenmeyer (GE) car elles étaient plus grandes. En considérant que la taille des gouttelettes de n-décane est d'environ 1mm de diamètre pendant l'extraction (mesure au microscope, données non montrées), la différence de diamètre des cellules (4 à 25 μ m) n'est pas significative pour aboutir à un mécanisme sélectif basé sur la probabilité de contact entre les cellules et les gouttelettes de solvant. On peut en conclure que, pour une condition de culture donnée, une cellule plus grande nécessite moins d'énergie pour se briser. Un meilleur critère pour vérifier la biocompatibilité serait que la proportion de β -carotène extraite doit être supérieure à la proportion de perte de volume cellulaire. Cependant, il faut vérifier qu'il est effectivement possible d'extraire le β -carotène des cellules survivantes sur un nombre significatif de cellules. La seule façon de réaliser ce test est d'opérer l'extraction et la mesure de biocompatibilité sur une seule cellule, éventuellement avec des techniques microfluidiques.

Une circularité faible était associée à un faible taux de survie. La circularité était plus faible pour les cellules SE, ce qui se traduit par un indice de destruction cellulaire (IPCD) plus élevé pour SE. La diminution transitoire de la circularité pour un temps de contact court avec le solvant (moins de 45s) a induit une distorsion de la cellule qui peut être due à une altération de la membrane cellulaire peut être une conséquence de la perméabilisation de la cellule. Pour les cellules GE et SE, la contribution de la perméabilisation naturelle à la fragilité des cellules n'a pas été mesurée. La perméabilisation des cellules augmente avec l'exposition au n-décane, comme le montre la coloration à l'iodure de propidium et la mesure avec un spectrofluoromètre.

L'utilisation du SYTOX Green, compatible avec le spectre des microalgues, et l'analyse unicellulaire ont montré au contraire que la perméabilité des cellules diminue après exposition au n-décane. Au-dessus du seuil de 20% de perméabilité, plus la perméabilité est élevée, plus la perturbation est importante. Ce résultat contraste avec l'augmentation de la perméabilité due à l'exposition aux solvants organiques rencontrée dans la littérature, souvent mesurée en moyenne sur la population. Or, le mécanisme de la toxicité des solvants organiques est basé sur la formation de pores dans la membrane. Les cellules qui sont naturellement perméabilisées sont plus proches du seuil critique de la surface des pores sur la membrane et plus sujettes à la perturbation cellulaire. La mesure unicellulaire de la perméabilisation réalisée avec le colorant bleu Evans a confirmé les résultats et a permis de mettre en évidence le mécanisme de perturbation cellulaire. La proportion de cellules naturellement perméabilisées était élevée pour les cultures de cellules en erlenmeyer. Un temps d'exposition supérieur à 45s a conduit à une diminution des cellules avec intégrité membranaire (non affectées) et de l'indice de biocompatibilité. Les cellules perméabilisées naturellement sont perturbées en premier, mais elles sont considérées comme des cellules mourantes non viables, leur mort ne diminuant pas efficacement la biocompatibilité. Par conséquent, le traitement peut être considéré comme principalement biocompatible pour un temps d'extraction très court, c'est-à-dire <45s. En résumé, les cellules naturellement perméabilisées sont perturbées en premier, et les cellules non affectées semblent suivre un processus de perméabilisation graduel : perméabilisation réversible → perméabilisation irréversible → cellules détruites. La présence de cellules perméabilisées de manière réversible n'est que transitoire car sa proportion diminue lorsque le temps de traitement dépasse 20s.

La production d'oxygène diminue légèrement de 20% en moyenne. L'absence de diminution de Fv/Fm après 120s de mélange indique que le solvant n'a pas altéré de manière significative la

machinerie photosynthétique. Nos résultats confirment la faible toxicité du n-décane sur l'activité photosynthétique des cellules GE et SE atteinte par plusieurs autres études (par exemple, (Hejazi *et al.*, 2002 ; León *et al.*, 2003)). Comme mesuré avec le colorant CTC, l'activité respiratoire est stimulée, probablement en raison d'un échange plus élevé à travers la membrane. Cette méthode a confirmé la faible toxicité du n-décane sur l'activité photosynthétique. L'exposition au n-décane diminue l'activité estérase des cellules cultivées et stressées, mesurée en moyenne par spectrofluorimétrie. En ce qui concerne l'impact de l'exposition au n-décane sur le cycle de division cellulaire, les cellules qui n'étaient pas en cours de division cellulaire étaient plus susceptibles d'être perturbées. En effet, la croissance a été arrêtée en raison d'un mauvais fonctionnement des cellules ou de conditions de culture défavorables (pH, nutriment, lumière). Dans l'ensemble, les résultats suggèrent que les cellules faibles, qui étaient déjà perméabilisées et incapables de poursuivre la division cellulaire, ont été perturbées de manière préférentielle.

En comparant les résultats des études précédentes et les nôtres, on peut conclure qu'une faible concentration et une courte exposition ont stimulé la cellule, qu'une concentration élevée et une courte exposition ont légèrement inhibé la survie des cellules et qu'une exposition à long terme a eu un effet toxique élevé sur les cellules. La mort sélective des cellules non viables à l'intérieur de la culture et l'augmentation des échanges à travers la membrane perméabilisée pourraient expliquer la stimulation métabolique après l'exposition au solvant organique qui a été rapportée dans la littérature.

Le cas idéal pour la traite du β -carotène pourrait être que toutes les molécules soient extraites de toutes les cellules sans mort cellulaire, puis que les cellules réaccumulent, le plus rapidement possible, les molécules extraites. Les cellules utilisent les caroténoïdes comme une protection contre la lumière. Ainsi, une quantité minimale doit être laissée dans les cellules. Comme la

mort cellulaire survient sur des cellules fragiles, les cellules doivent repousser pour maintenir une densité cellulaire constante et éviter l'effondrement de la culture. Les cellules doivent alors être recyclées dans un milieu contenant de l'azote. Pour répondre à ce besoin, deux procédés sont possibles : (i) il y a une étape de relaxation avec un milieu enrichi en azote pour déclencher la croissance des cellules, ou (ii) un seul photobioréacteur est utilisé avec un milieu limité en azote pour maintenir la croissance. Cette deuxième solution peut permettre d'obtenir des cellules moins fragiles car elles disposeraient de suffisamment de matière pour le maintien des cellules par rapport au milieu appauvri.

En conclusion, les conditions de culture influencent fortement la morphologie cellulaire et la robustesse des cellules de *Dunaliella salina* à l'extraction du β -carotène. Les cellules survivantes étaient petites ($<600\mu\text{m}^3$), avec une circularité élevée (0.7-0.9) et non perméabilisées naturellement. Cette découverte ouvre de nouveaux schémas de production de caroténoïdes basés sur la culture de cellules robustes enrichies en β -carotène dans des conditions contrôlées, telles que le pH, le mélange et le CO_2 dans le photobioréacteur, afin d'assurer une extraction biocompatible.

General introduction

Climate change and biodiversity losses have raised awareness about the consumption of renewable products and natural substances. These environmental impacts are largely attributable to greenhouse gas emissions and chemical pollution from anthropic activities, such as extracting and refining materials and chemicals from the environment and transporting them to consumers. Consumption of organic foods and natural products has been shown to have many advantages over conventional and synthetic products, such as improved health and increased environmental sustainability (Mie *et al.*, 2017).

Microalgae are microscopic unicellular organisms that operate photosynthesis to extract energy and substances from their environment (Scarsini *et al.*, 2019). During the growth process, 1 kg of microalgae captures 1,8 kg of CO₂ from the atmosphere. Unlike terrestrial plants, that need watering, microalgae grow in water that can be reused several times. In addition, microalgae production yield per acre is >20 times higher than that for plants (Benedetti *et al.*, 2018). Microalgae form a polyphyletic group of organisms. The number of species is estimated to be between 30,000 and 1,000,000 (Guiry, 2012). Along with their long and complex evolution, microalgae have acquired the capacity to produce a wide spectrum of natural products (proteins, antioxidants, drugs, omega-3 oil, biofuel and pigments), (Mimouni *et al.*, 2012; Rajvanshi *et al.*, 2019). Because it is not widely explored, microalgal resource may be the source of new compounds that exhibit higher activity. Some of these natural biomolecules cannot be chemically synthesized today. The targeted applications are numerous and span many industries: food, feed, pharmaceuticals, cosmetics and energy (Mimouni *et al.*, 2012).

However, the economic viability of the metabolites produced from microalgae is a biotechnological challenge that needs to be addressed. Indeed, microalgae are slow growth microorganisms (0.05day⁻¹ for *Isochrysis galbana* and 1.2day⁻¹ for *Scenedesmus sp.*), (Darvehei *et al.*, 2018) compared to yeast (9.6day⁻¹ for *Saccharomyces cerevisiae*), (Boender *et al.*, 2009)

and bacteria (18.5day^{-1} for *Escherichia coli*), (Paalme *et al.*, 1997). The light availability within the reactors is a major bottleneck in the industrialization of autotrophic production of microalgae (Pruvost *et al.*, 2016). In order to unlock the potential of microalgae and industrialize the production of high-value substances, the improvement of the productivity and the reproducibility of cultivation and extraction processes is mandatory (Guedes *et al.*, 2011). The understanding of the microalgal metabolism and production processes is thus a key step.

In a few microalgae taxa, the coupled application of nitrogen depletion and high light stress triggers the reorientation of the carbon metabolism toward the massive accumulation of secondary metabolites. For example, the green microalga *Dunaliella*, accumulates β -carotene up to 14% of its dry weight (Ben-Amotz *et al.*, 1988; da Silva and Lombardi, 2020). Current microalgal fractionation processes require several downstream steps such as dewatering, drying, solvent extraction, and purification of the target biomolecules (Vinayak *et al.*, 2015). More than that, they generate residues that need to be treated. Most of these steps are time- and energy- intensive (Hosseini Tafreshi and Shariati, 2009), which can jeopardize the ecological and economic viability of these processes unless the prices of such biomolecules is very high. Reduction of production residues with *in situ* extraction methods, referred as milking, have been proposed. This includes the use of pre-treatments such as electric pulses (Zhang *et al.*, 2020; Gateau *et al.*, 2021) or resonance frequencies (Vinayak *et al.*, 2017), and biocompatible solvents (Frenz *et al.*, 1989; Hejazi *et al.*, 2002; León *et al.*, 2003; Atta *et al.*, 2016). In *Dunaliella*, by comparing β -carotene solubility, solvent extraction ability and biocompatibility of organic solvents, León *et al.* (2003) established that the best compromise for β -carotene biocompatible extraction is achieved using hydrophobic solvents exhibiting a $\log P_{\text{octanol}}$ around 5 as *n*-decane, provided that the solvent/culture ratio (v/v) remains less than 1. However, for *Dunaliella*, *n*-decane was considered noncompatible (Hejazi *et al.*, 2002) with a direct

correlation between cell destruction and β -carotene extraction (Kleinegris *et al.*, 2011b), or biocompatible (Mojaat *et al.*, 2008) with a higher fraction of β -carotene extracted compared to cell destruction rate. Generally, it has been reported that lipid extraction from microalgae with organic solvent depends on the contact time and area between the medium and the organic solvent, but the higher the extraction rate, the lower the biocompatibility (Frenz *et al.*, 1989; Hejazi *et al.*, 2003; Atta *et al.*, 2016; Miazek *et al.*, 2017).

While many studies have focused on solvent selection and extraction operating conditions, there is a lack of understanding of the effect of culture conditions on single-cell characteristics and, de facto, on the extraction biocompatibility. The most common method for monitoring cultures is to measure the average characteristic of the population (cell density, dry weight, pigment content, photosynthetic activity), which can lead to biased information that is not rendering culture's heterogeneity. Environmental and toxicological studies of phytoplankton provide basic information on the toxicity of substances and treatments on microalgae (Adler *et al.*, 2007; Hyka *et al.*, 2013). Outside of laboratory conditions, growth variability is caused by non-homogeneous conditions, nutrient availability, competition, and predation. Under laboratory conditions, microbial cultures still exhibit high degree of heterogeneity in terms of growth rate and stress resistance.

There is a general consensus that among the first measurable signs of cell death are the loss or reduction of membrane integrity and metabolic activity (Caron and Badley, 1995; Hyka *et al.*, 2013). Thus, the enzymatic activity that represents the intensity of metabolism (vitality) and DNA content that shows the cell ability to pursue growth (viability) could influence single-cell biocompatibility of organic solvent.

D. salina is a cell wall less microalga meaning that the cells is limited by a thin and elastic plasma membrane (Dodge, 1973) that acts as the sole selective barrier to compounds (León *et*

al., 2001). In theory, the extraction can only be biocompatible for a cell if its membrane permeabilization is reversible. Indeed, cell membranes are the preferential places where organic solvents, like *n*-alkanes, can accumulate (Bar, 1988), perturbing membrane fluidity (Sikkema *et al.*, 1995) and leading to membrane's permeabilization (Lorente De Nó, 1934). Therefore, the morphology and the permeability of the cell membrane could influence the permeabilization process and the resulting biocompatibility.

This thesis aims to study the biocompatible extraction of β -carotene from the model organism *Dunaliella salina* with the organic solvent *n*-decane. The understanding of individual cell characteristics' impact on the extraction biocompatibility constitutes tools for decision making in the design of biocompatible extraction.

The first chapter consists in a literature review addressing the potential and the challenges of industrial production of β -carotene from *Dunaliella salina*. Emphasis is set on the milking concept i.e., the biocompatible extraction, especially using organic solvents.

The second chapter deals with (i) the development and implementation of a robust methodology for the production and extraction of carotenoids from *D. salina* and (ii) the characterization of the single-cell reaction to organic solvent exposure as well.

The third chapter investigates the influence of *n*-decane exposure on the biological function, that characterize the biological activity of individual cells of *D. salina*.

The fourth chapter is devoted to a selection of culture conditions in Erlenmeyer and Photobioreactor to obtain appropriate cell morphology that ensures biocompatible extraction of β -carotene extraction from *D. salina*.

General introduction

Then, a general discussion draws together the main findings of the thesis and establishes the significance of the work. Finally, the manuscript ended with the conclusion and perspectives to summarize the work and make recommendations for future work.

Chapter 1.

*Production and biorefining of β -
carotene from Dunaliella salina*

1 The β -carotene

1.1 Chemical structure

β -carotene is devoid of oxygen and is composed of 40 carbon atoms chained together with alternating single and double unsaturated bonds and a β -ionone rings at both ends of the molecule (Figure 1.1). This structural arrangement makes β -carotene a hydrophobic member of the carotene sub-family of carotenoids characterized by a high antioxidant activity. β -carotene molecule was isolated for the first time from carrots in 1837 by Wackenroder (Sourkes, 2009). Several isomers of β -carotene exist: all-*trans* is the predominant form found in nature but the 9-*cis* one has the most potent antioxidant activity (Ye *et al.*, 2008).

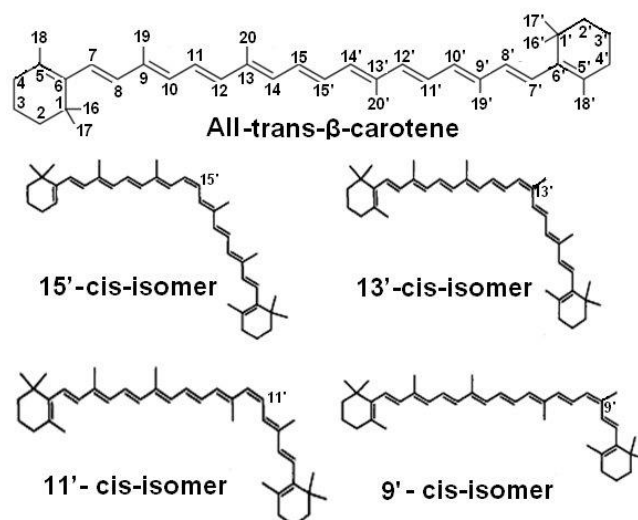


Figure 1.1 – Structures of all-*trans*- β -carotene and its four major *cis*-isomers (Jing *et al.*, 2012).

1.2 Role in microalgae

Primary β -carotene play a significant role in the photosynthetic process as a photon collector and energy transmitter in the pigment-protein complex of the photosystem I and II (Takaichi, 2011). β -carotene protect chlorophyll from excess light by providing shading, dissipating heat and limiting the formation of reactive oxygen species (ROS), (Shaish *et al.*, 1993). β -carotene stabilizes protein folding in the photosynthetic apparatus and protects chlorophylls, lipids, proteins and DNA from oxidative damage by quenching singlet oxygen arising from sunlight absorption by pigments (Ahmed *et al.*, 2015). β -carotene can also be found in the eyespot (stigma) of flagellated microalgae to show the cell the direction and intensity of light (Arrieta *et al.*, 2017). The cell is then able to approach light (positive phototaxis) or to move away from it (negative phototaxis).

1.3 Metabolism in animals

β -carotene is metabolized by the human body in vitamin A (Figure 1.2). In animals, β -carotene can be enzymatically cleaved in two molecules of retinaldehyde or in one β -ionone and one apocarotenal which is then converted to retinaldehyde. Retinaldehyde can be oxidized to generate all-trans retinoic acid, the biologically active form of vitamin A or it can be reduced to retinol, its alcohol form, commonly referred as vitamin A (D'Ambrosio *et al.*, 2011). Retinol can be esterified in retinyl ester, the storage form of vitamin A in different tissue like liver, lung and adipose. Its further release in the body is controlled by nutrient need.

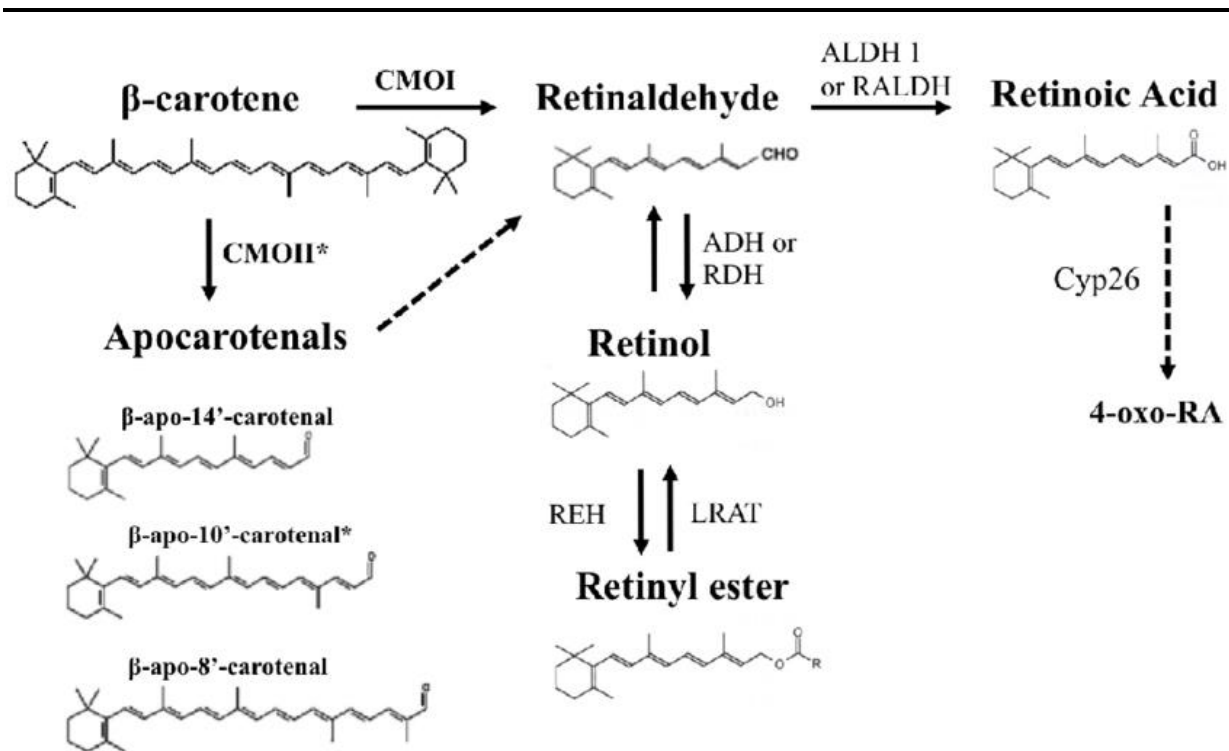


Figure 1.2 – Summary of β -carotene metabolism (D'Ambrosio *et al.*, 2011)

1.4 Commercial application of β -carotene

1.4.1 Food and feed

Carotenoids cannot be synthesized by animal cells and therefore must be acquired through the alimentation. In western countries, β -carotene contributes to about 30% of the dietary intake in vitamin A and is the most abundant or the sole source of vitamin A in developing countries (Shete and Quadro, 2013). β -carotene is used in the food industry (food additive E160a(iv)) for pigmenting product like margarine, butter, bakery products, sugar confectionery, meat, pasta and egg products, deserts and mixes, dairy and related products, fruit juices and beverages, canned soups, preserves and syrups (Delgado Vargas *et al.*, 2010). It is also used as a food additive in

children food to increase vitamin content. In the feed industry β -carotene is added to animal feed for the pigmentation of fish, sea fruits, egg yolk and chicken meat (Solymosi *et al.*, 2015).

1.4.2 Medical sector

The uptake of β -carotene occurs in the duodenum of the small intestine on the same receptor as that of vitamin E (α -tocopherol). The in vivo absorption yield of carotenoids like β -carotene is in general estimated to be 5-22%. Vitamin A, which derives from β -carotene is involved in bone growth and eyes' pigment synthesis. Its positive effect on health has been proven through the treatment of a wide number of diseases with antidiabetic, antitumor, anti-inflammatory activities and benefits for cognitive function (Gateau *et al.*, 2016; Torregrosa-Crespo *et al.*, 2018). Its antioxidant property mediates the harmful effects of free radicals and hence can potentially protect humans from compromised immune response, premature aging, certain cancers, cardiovascular diseases, and/or arthritis. People with erythropoietic protoporphyria, a rare genetic condition that causes painful sun sensitivity, as well as liver problems, are often treated with β -carotene to reduce sun sensitivity. However, there is also some evidence that when smokers, so as people who are exposed to asbestos, take β -carotene supplements, their risk of lung cancer is increased (Druesne-Pecollo *et al.*, 2010).

1.4.3 Cosmetic industries

β -carotene is used in the manufacturing of sunscreen. It protects the skin from oxidation and UV damage, by antioxidant and photo-oxidative protection mechanism. β -carotene can be found in other cosmetic product to prevent skin aging.

1.5 Industrial production

1.5.1 Global market

Synthetic β -carotene is worth 750\$. kg^{-1} and depending on the level of purity, natural β -carotene is sold between 300-3000€. kg^{-1} (Gateau *et al.*, 2016). The global β -carotene market represented 180 M€ in 2010, 520 M\$ in 2020 and is expected to increase to 720 M\$ by 2027 (Marino *et al.*, 2020; Kunal Ahuja and Amit Rawat, 2021). The market value is more important for microalgae than for synthetic products (Figure 1.3). Chemical synthesis produces only trans isomers and accounts for 85% of the market volume (Shaish *et al.*, 2006).

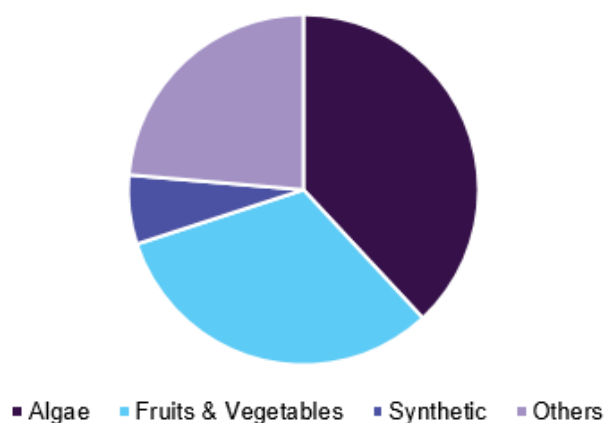


Figure 1.3 – Global β -carotene market share by source in 2016 (Grand View Research, 2018).

1.5.2 Chemical production

Since 1950, chemical synthesis has been used in the production of β -carotene via Wittig reactions or Grignard compounds (Bogacz-Radomska and Harasym, 2018). The Wittig reaction combine two phosphonium salt molecules and one dialdehyde molecule. Then, the reaction

products undergo an isomerization reaction leading notably to the formation of β -carotene. The Grignard compounds are organometallic molecule that react in presence of one moles of diketone and two moles of methanol to obtain carotenoids (Britton *et al.*, 1996; Alvarez *et al.*, 2014). There is evidence that synthetic β -carotene induce carcinogenic activity (Black 2004). This was a fundamental reason to search for a method to produce β -carotene from natural ressources because these compounds can be found in a wide variety of vegetables and microorganisms

1.5.3 Biological production

Vegetables such as carrots, pumpkins, spinach and tomatoes are natural sources of β -carotene, the most popular one being the orange carrot (Figure 1.4). Carotenoids are contained in thylakoid membranes of plant cells and in the membrane of the carrot's root cell. Carotenoids can be extracted from plants with physicochemical processes. The main drawback of the carotenoids production from vegetables is the expensive extraction cost and seasonal variability of the production. (Bogacz-Radomska and Harasym, 2018).

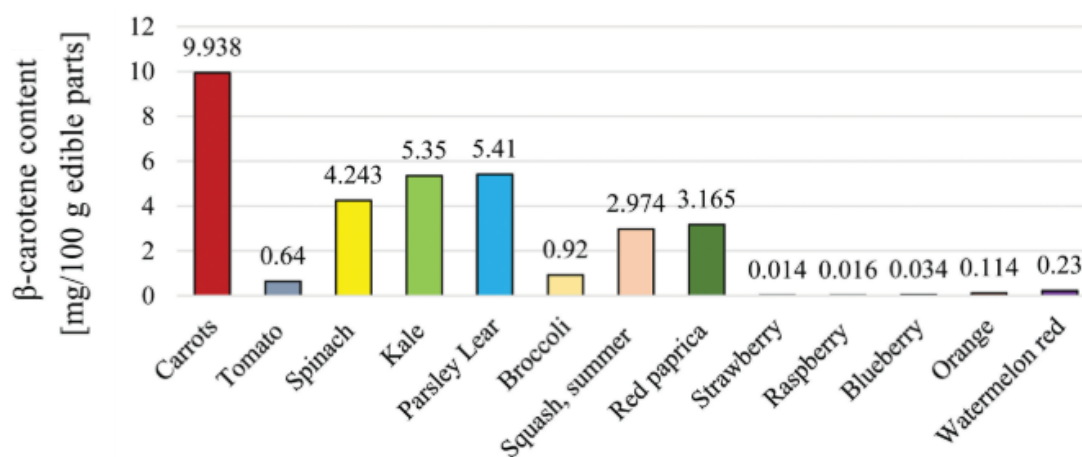


Figure 1.4 – β -carotene content in selected fruits and vegetables (Bogacz-Radomska and Harasym, 2018).

Micro-organisms, such as yeast and microalgae, can be used for the industrial production of carotenoids. For example, the mold *Blakeslea trispora* produces 1% in dry weight of β -carotene (Choudhari and Singhal, 2008). Microalgae of the genus *Dunaliella* are the most important source for the industrial production of natural β -carotene (Lamers *et al.*, 2008). *Dunaliella salina* can accumulate up to 10-14% of its dry weight in carotenoids (Table 1.1) compared to less than 1% for other microalgae (Ben-Amotz *et al.*, 1982; Ambati *et al.*, 2019). The proportion of 9-*cis*- β -carotene observed in microalgae is the highest among photosynthetic organisms. The extracted β -carotene has a typical composition of 42% all-*trans*-, 41% 9-*cis*-, 10% 15-*cis*- and 6% other isomers (Borowitzka and Borowitzka, 1989).

Table 1.1 – Carotenoid content in the selected microalgae species (Ambati *et al.*, 2019).

Algal species	^a Pigment (%)	^a Major pigment or total carotenoids	References
<i>Haematococcus pluvialis</i>	3–7%	AX	Hata <i>et al.</i> , 2001; Steinbrenner <i>et al.</i> , 2001; Kang <i>et al.</i> , 2005; Nobre <i>et al.</i> , 2006; Ceron <i>et al.</i> , 2007; Ranga Rao <i>et al.</i> , 2011; 2014a; Regnier <i>et al.</i> , 2015;
<i>Chlorella vulgaris</i>	12.5% TC	AX	Mendes <i>et al.</i> , 1995; Cha <i>et al.</i> , 2008
<i>Chlorella vulgaris</i>	55.5% TC	AX	Mendes <i>et al.</i> , 2003; Singh and Gu, 2010; Chacon-Lee <i>et al.</i> , 2010; Cha <i>et al.</i> , 2010
<i>Chlorella zofingiensis</i>	0.7%	AX	Bar <i>et al.</i> , 1995
<i>Coelastrrella striolata</i> Var. <i>multistriata</i>	0.15%	AX	Abe <i>et al.</i> , 2007
<i>Dunaliella salina</i>	3–13%	BC	El-Baz <i>et al.</i> , 2002;
<i>Chlorella zofingiensis</i>	0.9%	BC	Bar <i>et al.</i> , 1995
<i>Coelastrrella striolata</i> Var. <i>multistriata</i>	0.7%	BC	Abe <i>et al.</i> , 2007
<i>Spirulina platensis</i>	70–80% TC	BC	Miranda <i>et al.</i> , 1998; El-Baky <i>et al.</i> , 2003; Jaime <i>et al.</i> , 2005; Ranga Rao <i>et al.</i> , 2010
<i>Chlorella pyrenoidosa</i>	0.2–0.4%	LT	Wu <i>et al.</i> , 2007
<i>Botryococcus braunii</i>	0.16%	LT	Tonegawa <i>et al.</i> , 1998
<i>Botryococcus braunii</i>	75% TC	LT	Ranga Rao <i>et al.</i> , 2006; 2007a; 2010a; 2010b; 2013b
<i>Chlorella vulgaris</i>	45% TC	LT CX	Mendes <i>et al.</i> , 2003; Singh and Gu, 2010; Chacon-Lee <i>et al.</i> , 2010; Cha <i>et al.</i> , 2010
<i>Phaeodactylum tricornutum</i>	1.65%	FX	Ragni <i>et al.</i> , 2007; Kim <i>et al.</i> , 2012; Dambek <i>et al.</i> , 2012
<i>Isochrysis aff. galbana</i>	1.8%	FX	Kim <i>et al.</i> , 2012
<i>Cylindrotheca closterium</i>	0.5%	FX	Rijstenbil <i>et al.</i> , 2003
<i>Odontella aurita</i>	2.2%	FX	Xia <i>et al.</i> , 2013
<i>Coelastrrella striolata</i> Var. <i>multistriata</i>	4.7%	CX	Abe <i>et al.</i> , 2007
<i>Chlorella zofingiensis</i>	25% TC	CX	Bar <i>et al.</i> , 1995
<i>Chlorella vulgaris</i>	36% TC	CX	Li <i>et al.</i> , 2002; Singh <i>et al.</i> , 2010; Chacon-Lee <i>et al.</i> , 2010; Kong <i>et al.</i> , 2012
<i>Botryococcus braunii</i>	0.17%	ECN	Tonegawa <i>et al.</i> , 1998
<i>Nannochloropsis</i> sps	0.1%	TC	Lubian <i>et al.</i> , 2000; Macias-Sanchez <i>et al.</i> , 2005; Forjan <i>et al.</i> , 2007; Nobre <i>et al.</i> , 2013; Solovchenko <i>et al.</i> , 2014
<i>Scenedesmus</i> sps	0.69%	TC	Qin <i>et al.</i> , 2008; Ceron <i>et al.</i> , 2008; Pirastru <i>et al.</i> , 2012; Chan <i>et al.</i> , 2013; Guedes <i>et al.</i> , 2013; Ho <i>et al.</i> , 2014;
<i>Chlorococcum</i> sps	0.25%	TC	Zhang and Lee, 1997; Zhang <i>et al.</i> , 997; Masojidek <i>et al.</i> , 2000; Yuan <i>et al.</i> , 2002; Sivathanu and Palaniswamy, 2012;

^acarotenoid contents in algae species varied upon their culture conditions; AX, astaxanthin; BC, β -carotene; LT, lutein; CX, canthaxanthin; ECN, echineone; TC, total carotenoids.

2 Production of β -carotene from *Dunaliella salina*

2.1 *Dunaliella salina*

2.1.1 Morphology of *Dunaliella*

Dunaliella is a genus of unicellular green microalga with an ovoid shape and two flagella (Figure 1.5a), (Borowitzka and Siva, 2007). Distinction between *Dunaliella* species is mainly based on morphological characteristics: shape can vary from ellipsoid to spherical, pyriform or fusiform (Figure 1.5a-j). Cells are radially symmetrical, bilateral or slightly asymmetrical. The cell size is influenced by the culture conditions especially light intensity. The cell size of *Dunaliella* is also inversely correlated with growth rate (Uriarte *et al.*, 1993). The inner structure is similar to other microalga: it contains a single-cup shaped chloroplast (with a pyrenoid), a nucleus, mitochondria and vacuoles (Polle *et al.*, 2020). The *Dunaliella* genus particularity is the absence of cell wall, it has only a plasma membrane enveloped in a thin, flexible and extensible mucilaginous envelope (Ben-Amotz and Avron, 1979). The flexibility of the envelope allows the cell to adjust its size rapidly to adapt to fluctuating environmental conditions such as salinity, in order to avoid osmotic shock (Einsparh *et al.*, 1988; Yao *et al.*, 2016).

2.1.2 Taxonomy

Different species are identified depending on the ecological niche, the morphology and the ability to produce specific compounds (Figure 1.5a-j). The specie Dunaliella salina is widely known for

its ability to accumulate large quantities of β -carotene under stressful conditions. The specie was first observed in 1838 in saltern evaporation ponds in the south of France by Michel Felix Dunal. In 1905, Teodoresco demonstrated that the specie was different from known species and proposed the name *Dunaliella* (Teodoresco, 1905), for a review see Oren, (2005). It is a member of Chlorophyta, genus *Dunaliella*, placed in the class Chlorophyceae, order *Dunaliellales* and family Polyblépharidaceae.

2.1.3 Ecology

Dunaliella salina has been identified on all continents, except the Arctic and Antarctic ones (Oren, 2005). *Dunaliella salina* is a halophile organism that can withstand high salinity. As an extremophile specie, it can survive under extreme environmental conditions (extreme light intensity or extreme temperature, high salinity, lack or excess of nutrients). It is the main specie of microalga living in salt pounds (Borowitzka, 1981).

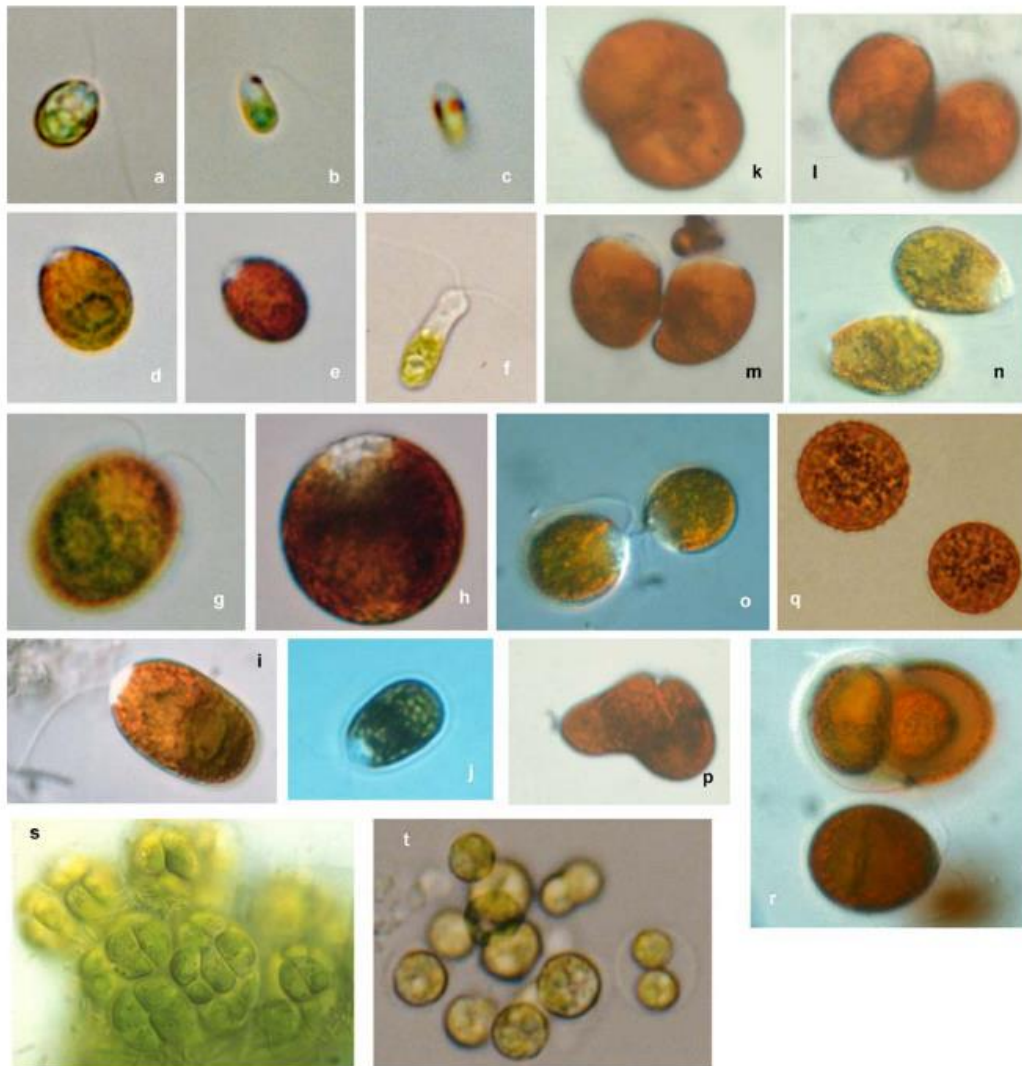


Figure 1.5 – Light micrographs of *Dunaliella* species and stages of *Dunaliella* life cycle (the length of the cells is given in parentheses). (I) Basic morphology of *Dunaliella* spp.: (a) *Dunaliella* *quartolecta* (MUR191=CCAP 19/10) (8 μ m); (b) *D. primolecta* (MUR55=CCAP 11/43) showing single prominent stigma (6 μ m); (c) *D. bioculata* (MUR26) showing the 2 distinct stigmas (6 μ m); (d) *D. salina* (MUR9) grown at 0.86 M NaCl (13 μ m); (e) *D. salina* (MUR9) grown at 5.17 M NaCl–note darker red colour (13 μ m); (f) *Dunaliella* sp.? (MUR202) showing typically elongated cell form and absence of a stigma (12 μ m); (g) *D. salina* (MUR10) grown at 0.86 M NaCl (20 μ m); (h) *D. salina* (MUR23) grown at 5.17 M NaCl (24 μ m); (i) *D. salina*–field sample from Hutt Lagoon (23 μ m); (j) *D. salina* (MUR200=CCAP 19/30) grown at 5.17 M NaCl (16 μ m). (II) Cell division in *D. salina*: (k–m) sequential stages of cytokinesis (all cells approx. 21 μ m long); (n) final stage just before cell separation–cells are still connected by a thin cytoplasmic bridge and are rotating around each other. (III) Stages of life cycle of *D. salina* mainly taken from field samples:(o) early stage of mating showing appressed flagella and mating tube between the two cells (22 μ m); (p) mid stage of gamete fusion and formation of zygote (21 μ m); (q) aplanospores with rough wall (22 μ m); (r) germinating aplanospore with 2 emerging cells and motile vegetative cell below (vegetative cell 24 μ m long); (s) palmella stage of *D. viridis* (field sample) (~12 μ m long); (t) palmella stage *D. viridis* var. *palmelloides* (Borowitzka and Siva, 2007).

2.1.4 *Reproduction and life cycle*

2.1.4.1 Vegetative reproduction

The reproduction of *Dunaliella* cells can happen with sexual or vegetative (asexual) reproduction. Vegetative reproduction occurs by the scission where the cell volume increases with a formation of a longitudinal division plane. This reproduction begins with nuclear division, followed by chloroplast and pyrenoid division until the daughter cells remain connected by only a thin, colorless cytoplasmic bridge (Figure 1.5k-m). At this point, a second flagellum appears, and the cells separate. When environmental conditions become harsh (desiccation, extreme pH and high light intensity), some *Dunaliella* species lose their two flagella to develop the "palmella" form. This form consists of non-mobile round cells. During this formation, the microalgae secrete a mucous layer in which they divide, forming an accumulation of green cells (Figure 1.5s,t).

The formation of aplanospore, vegetative cysts, was reported in old, nutrient depleted cultures of *D. salina* by Leonardi and Cáceres, (1997). It was found that reduced salinity, nitrogen depletion, cool temperatures, short daylength and the presence of sulphate were required for aplanospore formation in *D. salina* (Borowitzka and Huisman, 1993). Aplanospores have a thick a very resistant two layered rugose wall (Figure 1.5q).

2.1.4.2 Sexual reproduction

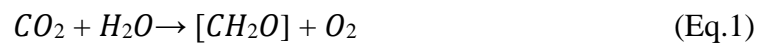
Mating occurs between two different strains called + and -. Cells start the mating process by joining their flagella on the tips (Figure 1.5o). Then, the + gamete produces a thin mating tube between which connects to the – gamete. The fusion of the two cells results in a planozygote with four flagella and then forms a thick wall. Germination of the zygote led to the formation of

4-8 cells in most cases (16-32 in rare cases). The zygote wall finally breaks to release the daughter cells.

2.2 Microalgal metabolism

2.2.1 Photosynthesis

The photosynthetic reaction is usually described by the following simplified equation:



This process converts light energy (photons) into chemical energy (ATP and NADPH) then used by cells to synthesize organic carbon from inorganic carbon (CO_2 or other form of dissolved inorganic carbon). This conversion is made possible by the succession of two types of reactions: clear reactions (or photochemical) and dark (or biochemical) reactions.

2.2.1.1 Light reaction

The clear reactions take place in the thylakoid membranes located in the chloroplast of microalgae cells (Figure 1.6). The thylakoid membranes possess photosynthetic pigments grouped into photosystems. There are two categories of photosystems: photosystem I (PSI) and photosystem II (PSII) that absorb light at slightly different wavelengths. Each photosystem has an antenna, made up of pigments like chlorophyll that capture the energy of the photons, and a reaction center which transfers this energy to a primary electron acceptor.

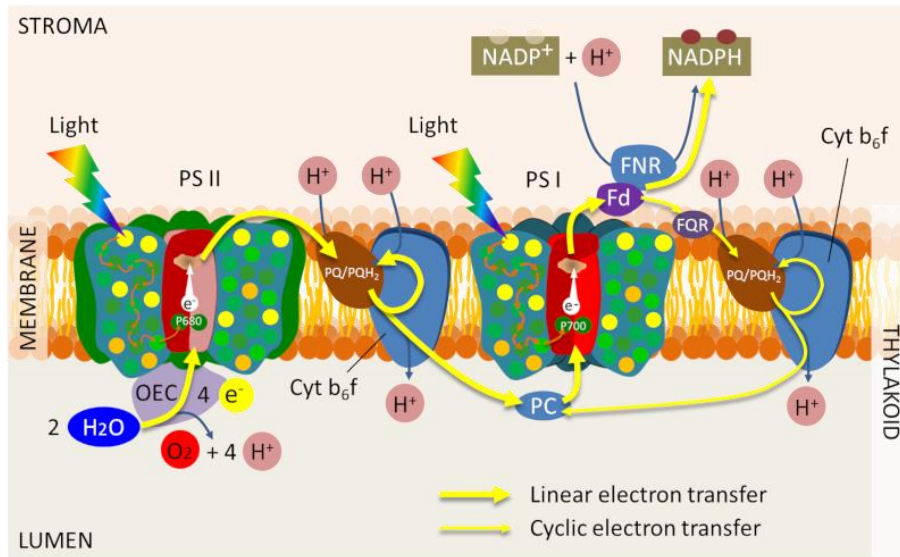


Figure 1.6 – Photosynthetic antenna and reactions and its localization on the thylakoid membrane of the chloroplast (Joyard and Morot-Gaudry, 2020).

Initially, the transfer takes place from the PSII branch to its reaction center. The latter then yields two electrons to the primary acceptor which transmits them to a chain of electron carriers, directing these electrons to the PSI.

As electrons pass through the cytochrome b₆f complex, H⁺ protons are pumped from the stroma to the intrathylakoid space. The reaction center having to recover the lost electrons, this one thus goes, by via an enzyme, to split a molecule of water, thus releasing two electrons, captured by the reaction center, as well as oxygen and protons. While the PSII loses two electrons, the PSI also loses two electrons under the action of photons. It then hands them over to a second transport chain. The last electron carrier of this second transport chain is an enzyme called NADP-reductase. This enzyme will transfer electrons to NADP⁺ contained in the stroma, which by accepting these two electrons, will bond with hydrogen to form NADPH, H⁺. The protons then accumulated in the intrathylakoid space will tend to return towards the stroma (due to the gradient). However, this can only be done by ATP-synthase (the membrane of the thylakoid

being impermeable to protons). An ATP molecule is then synthesized thanks to the flux of protons generated by assembling a molecule of ADP and an inorganic phosphate.

The molecules of ATP and NADPH,H⁺ will ultimately be used in the Calvin cycle (dark reactions).

2.2.1.2 Calvin cycle

Called dark reactions, all the reactions related to carbon fixation take place through a cycle called the Calvin cycle. This cycle takes place in the stroma and uses the energy stored during the clear phase in the form of ATP and NADPH,H⁺ to fix inorganic carbon and synthesize organic carbon. The first step in this cycle is the synthesis of 2 3-phosphoglycerate (3PGA) from CO₂ and ribulose-1,5-biphosphate (RuBP), a reaction triggered by an enzyme, RuBisCO. This phase is called: carbon fixation phase.

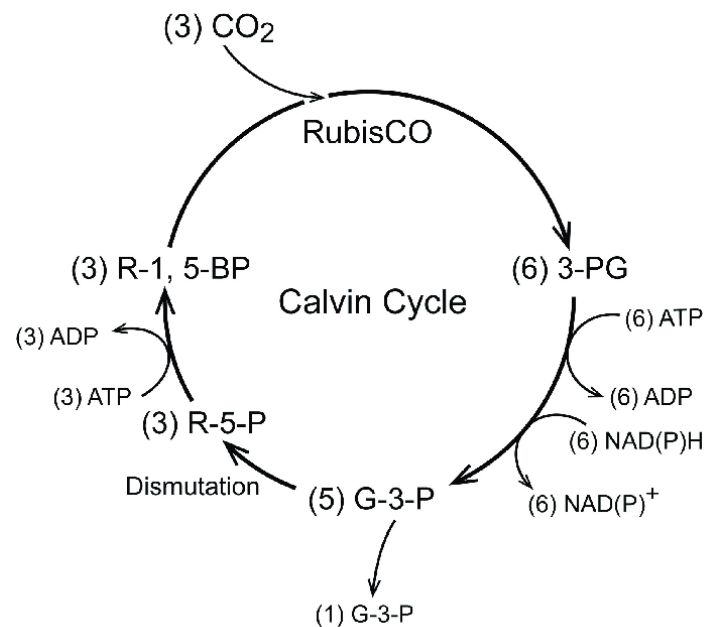


Figure – 1.7 Calvin Cycle

The second phase is called the reduction phase. During this phase, each molecule of 3PGA receives an additional phosphate from ATP (synthesized in the clear phase), then a electron pair donated by the NADPH,H⁺ molecule reduces the 1,3-biphosphoglycerate molecule to G3P, donating a phosphate group.

The G3P molecule is a three-carbon sugar. For twelve moles of G3P synthesized, only two are transported to the sugar metabolic pathway, the rest being directed to the third phase of the cycle, the regeneration of RuBP. This last phase completes the Calvin cycle by synthesizing RuBP molecules from G3P under the action of ATP in order to regenerate the first CO₂ acceptor.

2.2.2 Respiration

In the dark, mitochondrial respiration is the dominant activity because there is no photosynthesis in the chloroplast. However, the latter remains metabolically active to convert the carbohydrates produced by the Calvin reaction into other sugars exported to the cytosol (Hoefnagel *et al.* 1998). Mitochondrial respiration takes place in 3 major steps. First the glycolysis that takes place in the cytoplasm in anaerobiosis. Products of this glucose breakdown enter the mitochondria where the second and third stage occur. During the Krebs cycle or citric acid cycle, pyruvate from glycolysis is converted into acetyl CoA, point start of the Krebs cycle, with the release of a first molecule of CO₂. Finally, the oxidative phosphorylation requires a series of enzymes called ETC (electron transport chain). It is an aerobic process that produces the majority of ATP. The two previous steps serve as support for this last step. All the H⁺ produced from the Krebs cycle will thus be used in oxidative phosphorylation.

2.3 Carotenogenesis in *Dunaliella*

2.3.1 Anabolic pathway

Carotenoid backbone formation starts by the condensation of two geranylgeranyl diphosphate molecules into phytoene (Figure 1.8). The phytoene synthase enzyme (CRTB) catalyzes the reaction. Then, the phytoene desaturase (CRTQ) adds double bonds to the molecule resulting in Lycopene formation. Finally, α -carotene and β -carotene derive from the different cyclizing of the end of lycopene with the LCYE and LCYB enzyme, respectively (Bertrand, 2010).

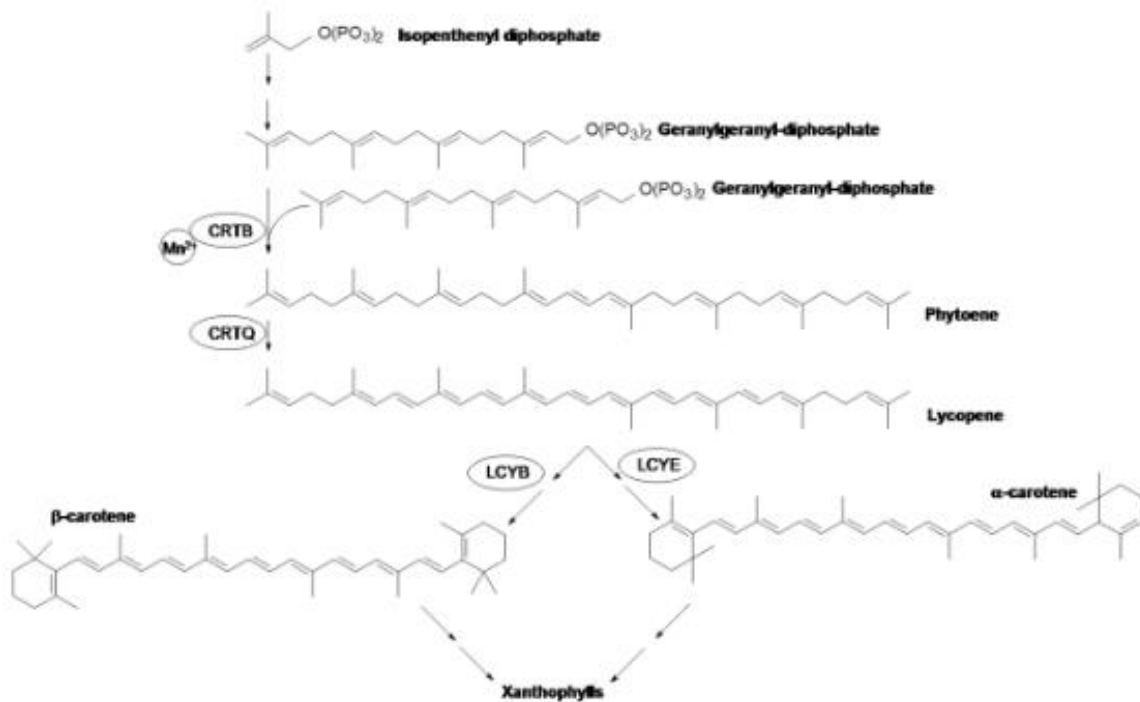


Figure 1.8 – The carotenoid biosynthetic pathway (Gateau *et al.*, 2016).

2.3.2 Stress detection

It is widely accepted that β -carotene accumulation occurs under culture conditions that reduce the growth rate such as high light, extreme temperatures, high salinity and nitrogen limitation or

depletion (Ben-Amotz and Avron, 1983). When the cell is exposed to light, photosynthetic reactions fix carbon dioxide and produce dioxygen as a by-product. The resulting high concentration of oxygen and the onset of environmental disturbance can form reactive oxygen species (ROS) and free radicals that cause oxidative stress. ROS such as singlet oxygen are likely to be involved in the signaling process that lead to β -carotene accumulation, although the mechanism is not yet understood (Lamers *et al.*, 2008).

2.3.3 Intracellular reorganization

Under stress conditions, the β -carotene content and the volume of cell increase while the chlorophyll content decreases (Ben-Amotz and Avron, 1983; Borowitzka and Borowitzka, 1990; Hejazi and Wijffels, 2003; Lamers *et al.*, 2010). The stressed cells have greatly reduced amounts of thylakoid membranes and greatly increased numbers of β -carotene globules (or oil bodies), turning the cell color from green to orange (Figure 1.9).

At the early stages of stress, cytoplasmic lipid droplets (CLD) are produced in the endoplasmic reticulum mostly by the incorporation of new synthesized fatty acids (Varsano *et al.*, 2003). β -carotene is accumulated in globules in the interthylakoid space of the chloroplast and frequently laid side-by-side along the thylakoid membrane surface, indicating exchange of molecules between β -carotene globules and thylakoid membranes. It has been reported that the location close to the plasma membrane would allow to absorb excess light before it can damage the photosynthetic apparatus of cells (Ben-Amotz *et al.*, 1989). Most of the oil bodies' lipids are made from the hydrolysis of chloroplast membrane's lipids and in part by a continual transfer of TAG or fatty acids from cytoplasmic lipid droplets (CLD) (Davidi *et al.*, 2014). CLD are composed of linoleic, palmitic, and myristic acid, which are also of biotechnological interest. β -carotene globules have an average diameter of 150nm and contain 65% β -carotene in dry weight

and are composed at 90 % of neutral lipids, including saturated fatty acids (Lers *et al.*, 1990; Kleinegris *et al.*, 2010b). Neutral lipids allow the isolation of hydrophobic carotenoids from the hydrophilic cell environment. Moreover, amphiphilic proteins such as oleoresin stabilize the membrane of the globules.

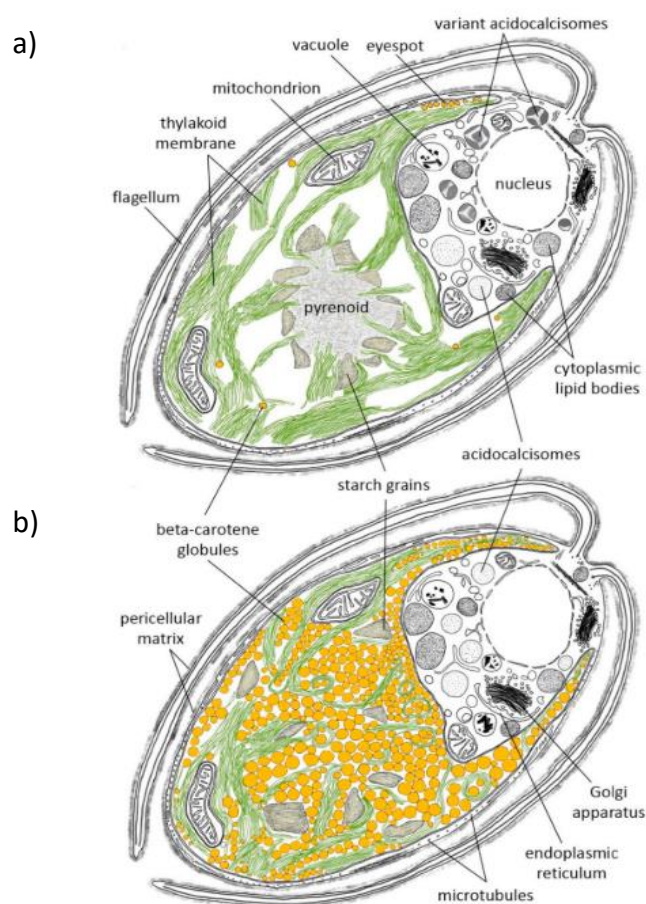


Figure 1.9 – Ultrastructure of *Dunaliella salina* under growth conditions (a) and under stressful conditions (b), (Polle *et al.*, 2020).

2.3.4 Factors influencing accumulation

Due to the inverse correlation between cell growth and β -carotene accumulation, the β -carotene production process is often separated in two distinct steps: growth and accumulation to improve

the overall performance of the β -carotene production (Ben-Amotz, 1995). β -carotene accumulation is commonly triggered by stress in salinity, high or low light and nitrogen depletion or a combination of them. The intracellular level of accumulation is also highly strain dependent.

2.3.4.1 Strains

Depending on the environmental conditions, strains of *Dunaliella salina* have adapted and contain varying amounts of β -carotene (Çelekli and Dönmez, 2006; Borowitzka and Siva, 2007). The Table 1.2 summarizes the seven strains with the highest reported β -carotene content. Even though the CCAP 19/18 is not the highest carotenoids producer with 70pg cell⁻¹, it is the most widely referenced in scientific literature for its ease of cultivation (Oren, 2005; Mojaat *et al.*, 2008; Polle *et al.*, 2020).

Table 1.2 – Highest carotenoids content reported in *Dunaliella salina* cell.

Strain	CCAP 19/18	UTEX 2538	CCAP 19/30	MUR 8	Lake Tuz, Turkey (1991)	MUR 22	MUR 23
β -carotene (pg/cell)	70	90	95	149	261	550	836
Reference	Mojaat et al., 2008	García- González et al., 2005	Coesel et al., 2008	Borowitzka et al., 2007	Çelekli and Dönmez, 2006b	Borowitzka et al., 2007	Borowitzka et al., 2007

2.3.4.2 Salinity

Salinity is a critical factor affecting biomass and β -carotene productions. Cell growth rate steadily increases with the rise of the salinity from 2.5 to 4.5% (Abu-rezq *et al.*, 2010). According to the strains, the optimal salinity for growth oscillates between 5 and 15% (Cifuentes *et al.*, 2001). Borowitzka, (1981) determines that the optimal salinity is 12%. Ben-Amotz and Avron, (1983) shown that the higher the salinity (in the range 1 to 4 M NaCl i.e. 16% to 65% in salinity), the higher the β -carotene to chlorophyll ratio. Farhat *et al.* (2011) reported that the highest cell density and intracellular β -carotene content was obtained between 1.5 and 3.0 M NaCl. Although the reported optimal salinity are different, it seems that a concentration of 2M NaCl would be appropriate to achieve the maximum β -carotene amount (Jesus *et al.*, 2010). Besides high salinity can reduce the presence of predators in the culture medium but can cause corrosion issues (Harvey and Ben-Amotz, 2020).

2.3.4.3 Macroelements

The nutrients required for microalgae are generally divided into two categories: macroelements and microelements. The most important macroelements are carbon, nitrogen, phosphorus, and sulphur. They are often in concentration range up to few g L⁻¹.

- Carbon

Carbon is the skeleton of organic molecules such as sugars, starch, lipids and phospholipids. Carbon input is crucial for growth as well as for accumulation. Inorganic carbon source can be supply as CO₂ gas, this allows to regulate the pH, or bicarbonate to ensure an initial amount of carbon (Hosseini Tafreshi and Shariati, 2009). Organic carbon can be added to the culture, such as acetate. Coupled with a supplementation of Fe²⁺ it maintained a high growth rate under β -carotene accumulation (Mojaat Guemir, 2008). The supplementation of relatively high amount

of organic carbon caused an increase in the C/N ratio and led to a relative nitrogen deficiency. However, organic carbon can favor the growth of detrimental heterotrophic bacteria.

- Nitrogen

Nitrogen is an important element present in amino acids, the building blocks of proteins. Nitrogen is involved in many cellular processes such as cell division. Low nitrate concentration negatively affected growth, but enhanced carotenoid accumulation (Marín *et al.*, 1998). In batch culture of a wild isolated *D.salina* cultured under low light, higher growth rate was obtained with higher nitrate concentration (0.9mM) and the highest carotenoids intracellular content were obtained with the lower nitrate concentration (0.2mM), (Pasqualetti *et al.*, 2010). Çelekli and Dönmez, (2006) reported that with an initial nitrate concentration of 5mM (in the range 1-17mM NaNO₃) the intracellular content in β -carotene was the highest (up to 261pg cell⁻¹). In continuous turbidostat experiments, the production of β -carotene started to increase immediately after total nitrogen depletion (Lamers *et al.*, 2012). During the first 4h, the production rates of β -carotene and cell volume increased proportionally. The switch from moderate to massive increase in β -carotene productivity after 12h coincided with the decrease of growth rate.

- Phosphorus

Phosphorus is essential to cellular metabolism through enzyme production, phospholipids and cell energy molecules, the adenosine triphosphates (ATP). Wongsansilp *et al.* (2016) showed that cell density increases with NaH₂PO₄ concentration (0-290 μ M) and the intracellular β -carotene content increase with phosphate depletion (up to 8.21pg cell⁻¹). Limitation or deficiency of KH₂PO₄ (0.1 and 0.0mM) also increase the β -carotene content compared to repleted artificial sea water medium (ASW), (Phadwal and Singh, 2003).

- Sulphur

Sulphur key functions include enzyme reactions and protein synthesis. A starvation in sulphur lead to a decreased growth rate but a doubling in β -carotene in the biomass (up to 15mg gDW⁻¹), (Khademi *et al.*, 2018). A limitation obtained with 6 μ M of MgSO₄ lead to an increase from 0.77 to 0.92pg cell⁻¹ compared to a sufficient amount of 48 μ M (Giordano *et al.*, 2000). It was shown that a depletion in sulphur by a substitution of MgSO₄ to MgCl₂ results in 3 times more intracellular β -carotene compared to repleted medium (Lv *et al.*, 2018).

2.3.4.4 Microelements

Microelements in culture medium include various metals like magnesium, potassium, copper, iron, zinc, etc., and vitamins in mg/L scale concentration. By comparing nitrogen depletion coupled to 16 different micro-nutrient depletion, Saha *et al.* (2013) reported that a maximum of 133% and 128% increase was observed under PAR high-light stress and ZnMnFe-depletion conditions, respectively, on day 10 compared to day zero of stress. On the 5th day after stress induction, the highest carotenoid content (2.26 mg/l) was recorded in the absence of Zn, Mn, Fe, and nitrogen, while the lowest carotenoid content (1.63 mg/l) was recorded in the absence of Mn and nitrogen.

2.3.4.5 Cultivation medium

To optimize growth, a comparison of the mineral composition of different culture media was made in relation to the biomass needs. Mineral needs of the culture are estimated with the elemental composition of the biomass (Figure 2.2). The P-molar formula of *Dunaliella tertiolecta* a microalgae from the same genus as *Dunaliella salina* was chosen (Ho *et al.*, 2003).

Table 1.3 – *Dunaliella tertiolecta* P-molar formula

(Coeff. 1)	$C_{222}N_{38}P_1S_{0.28}Fe_{11.3}Mn_{1.9}Zn_{1.49}Cu_{0.67}Co_{0.01}K_{0.36}Mg_{0.37}Ca_{0.019}Mo_{0.011}Sr_{0.081}Cd_{0.1}$	(Ho et al., 2003)
------------	---	-------------------

The molar weight of the biomass M_b was calculated as the sum of the products of p-molar coefficients of atoms N_x with the molar weight of atoms M_x (Eq. 2.1). The mineral input of the different media (Eq. 2.2) was calculated as the molar concentration of the medium divided by the molar concentration needed to produce 1 g/L of biomass (Eq. 2.3). With C_x : Concentration of atom X (g/L), M_x : Molar weight of atom X (g/mol), C_b : Concentration of biomass (g/L), M_b : Molar weight of biomass (g/mol), N_x : coefficient of the atom X in the P-molar formula, m: number of atoms in the P-molar formula.

$$M_b \text{ (g/mol)} = \sum_{X_1}^{X_m} N_{X_i} * M_X = 4365 \quad (\text{Eq. 2.1})$$

$$\text{Medium input}_X(\%) = \frac{\frac{C_X}{M_X}}{\frac{C_b}{M_b \cdot N_X}} \cdot 100 \quad (\text{Eq. 2.2})$$

$$\text{Target: } C_b \text{ (g/L)} = 1 \quad (\text{Eq. 2.3})$$

The results presented in Figure 1.10 indicate that some media contain quantities much greater than the requirements, providing up to 500% of the requirements. In contrast, Provasoli enriched seawater (Gómez and González, 2005), F/2 (Wongsansilp *et al.*, 2016) and Walne media (Helena *et al.*, 2016) contain, in theory, an insufficient mineral intake for the cultivation of *D. salina*. Boron, that is present in most of the mediums was not measured for the p-molar formula of *Dunaliella*. Cadmium, a highly toxic metal, is absent from the culture media and strontium is only present in the Conway. This latter showed 1.5 and 1.4 times higher lipid content than in the biomass grown with Johnson- and F/2, respectively (Colusse *et al.*, 2020). It is the media that fills most of the biomass needs. The Ramaraj medium was designed based on the modified

Johnsons medium with altering the concentration of $MgSO_4$, $NaHCO_3$ and addition of $NaVO_3$ and elimination of $MgCl_2$ (Sathasivam and Juntawong, 2013).

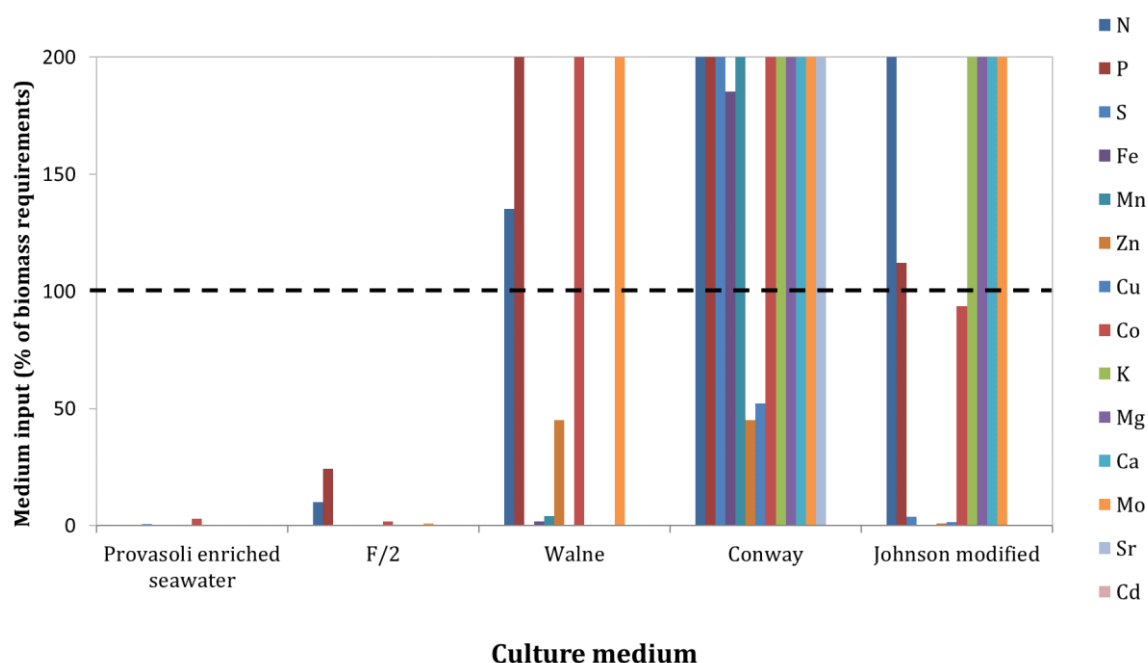


Figure 1.10 – Comparison of nutrient intake of culture media used for *Dunaliella* culture.

Modified Johnson fill an important part of the needs (Johnson *et al.*, 1968), it is the most widely used for the cultivation of *D.salina* (León *et al.*, 2003; Mojaat *et al.*, 2008) where it gave the best results in terms of β -carotene production, with 261pg/cell (Çelekli and Dönmez, 2006). Modified Johnson lack copper, zinc, and cobalt to fulfil biomass need but this micronutrient depletion might enhance β -carotene production as shown with copper and zinc depletion by Saha *et al.* (2013). Thus, modified Johnson is recommended for the culture of *D. salina*. In the case of a higher concentration of the biomass targeted N, S and P concentration can be proportionally increased.

2.3.4.6 Light

In microalgae, light is the key energy source for photosynthetic process to sustain the growth. In open pools, sunlight is the only source of light, whereas in photobioreactors, source of light can be supplied by fluorescence lamps and sunlight (Ben-Amotz and Levy, 1996) and LED panels more recently (Helena *et al.*, 2016). Cell growth rate increased from 50 to 800 $\mu\text{mol m}^{-2} \text{s}^{-1}$, remained constant at a maximum in the range of 800-1,500 $\mu\text{mol m}^{-2} \text{s}^{-1}$, and declined due to photoinhibition in the range of 1500-3000 $\mu\text{mol m}^{-2} \text{s}^{-1}$ (Baroli and Melis, 1996). In turbidostat experiment, Lamers *et al.* (2010) reported an increase in β -carotene accumulation when the light intensity was increased stepwise from 150 to 650 $\mu\text{mol m}^{-2} \text{s}^{-1}$. They reported a strong β -carotene induction 4 days after the stress application. It has been shown that after 84 hours of exposure to UV-A (320-400 nm) cells accumulate 3 times more β -carotene than under normal growth conditions (Salguero *et al.*, 2005). In day-night cycles, the maximum level is reached at irradiance peak (Phillips *et al.*, 1995). To improve the understanding and study the stress conditions of *D. salina*, there is a need for well-defined and controlled light regime. In most studies on carotenogenesis by *D. salina*, batch cultivations have been applied. The algal cells cultured in batch will experience changing light conditions throughout the experiment as a result of increased absorption by the increasing cell density and by the pigment accumulation in the culture (Lamers *et al.*, 2008).

2.3.4.7 Temperature

The temperature stimulates various intracellular processes by affecting the function of intracellular enzymes. *Dunaliella salina* is found in waters ranging from 0 to 40°C. The optimal growth temperature is between 20°C-40°C depending on strains and environmental conditions (Subba Rao, 2009). Between 20 and 23°C, the growth rate of *Dunaliella salina* increased

compared to higher temperature (Abu-rezq *et al.*, 2010). A study carried on seven strains of *D. salina* shown that the highest cell density and the highest β -carotene production rate (37.8 mg L^{-1}) was at 26°C (Gómez and González, 2005). On a large scale and in open outdoor ponds, due to technical limitations, the decline of temperature at night reduces the growth rate and cellular efficiency (Pourkarimi *et al.*, 2020). In *D. salina*, Ben-Amotz (1996) concluded that the 9-*cis*- to all-*trans* β -carotene ratio increased from 0.5 to 2 when the temperature drop from 30°C to 10°C . However, Orset and Young, (1999) found that β -carotene level remained constant by temperature decline from 34°C to 17°C and Gómez and González, (2005) reported that the temperature decrease from 26 to 15°C did not affect this ratio.

2.3.4.8 pH

pH of culture medium is among the most significant environmental factors affecting the microalgae culture. During microalgal growth, the pH increases due to the consumption of CO_2 and the modification of the bicarbonate equilibrium in culture media. At high pH values, there is a high risk of salt precipitation and flocculation phenomena in algae biomass. Control of the pH of outdoor ponds can be performed by either CO_2 gas injection or HCl addition (Pourkarimi *et al.*, 2020). *Dunaliella* species can live in a wide range of pH: from 1 to 11. Its optimal pH for growth is 9 to 11. Ying *et al.*, (2014) showed that the highest growth rate was obtained at pH = 7 (with a level of 5% CO_2). The optimal pH for high β -carotene content is 7 (Abu-rezq *et al.*, 2010).

3 Mass culture of *Dunaliella*

3.1 Industrial producers

The first industrial producers of β -carotene from *D. salina* were Western Biotechnology, Ltd., and Betatene, Ltd., in Australia, and Nature Beta Technologies (NBT) in Eilat in Israel since around 1985. In 1997, Western Biotechnology and Betatene were acquired by Cognis Nutrition and Health. Cognis, which is the major producer of natural β -carotene from *D. salina* in the world was then bought by BASF. Nowadays, the production plants of β -carotene operate in Israel, China, USA, and Australia. The main company is Betatene Ltd (Melbourne, Victoria), which produces more than 80% of world production in open ponds (Curtain, 2000).

Table 1.4 – Commercial producers of β -carotene from *Dunaliella* (Del Campo *et al.*, 2007).

Company	Location	Culture area (ha)	β -carotene production (tonnes per year)	Culture system
Betatene http://www.betatene.com.au	Australia	400	13–14	Extensive unmixed ponds
Western Biotechnology http://www.cognis.com	Australia	240	4–6	Extensive unmixed ponds
AquaCarotene http://www.aquacarotene.com	Australia	na	na	Extensive unmixed ponds
Cyanotech http://www.cyanotech.com	Hawaii	na	na	Raceways ponds
Inner Mongolia Biological Eng.	China	na	na	Raceways ponds
Nature Beta Technologies http://www.chlostanin.co.jp	Israel	5	3–4	Raceways ponds
Tianjin Lantai Biotechnology	China	na	na	Raceways ponds
Parry Agro Industries http://www.murugappa.com/0_our_companies/parry_agro.htm	India	na	na	Raceways ponds

na Information not available

Microalgae remain currently expensive to produce; many efforts are under way to cut down cost to unlock mass cultivation of these organisms. Different systems have been designed for the growth and handling of microalgae on a large scale, they can be classified in open culture and closed culture systems.

3.2 Open culture systems

The geographical location of the culture site and the corresponding environmental conditions, such as sunshine, temperature, land cost and availability in water play a key role in the productivity and optimization parameters of the system, which is the reason why cultures are mainly carried out in Australia and Israel (Del Campo *et al.*, 2007). Extensive culture of *Dunaliella salina* is generally made in lagoons or raceways.

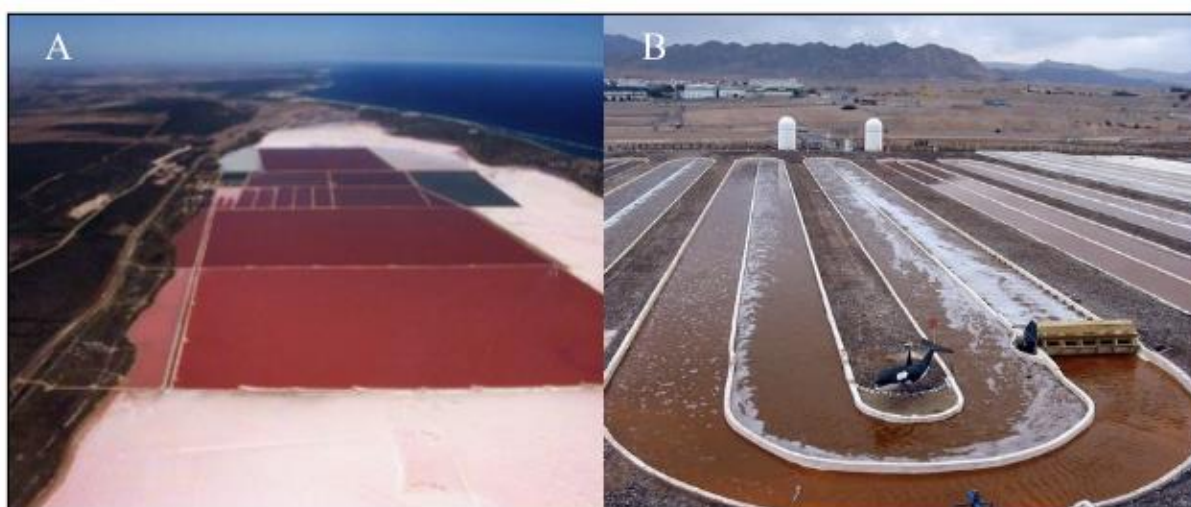


Figure 1.11 – Photographs of two industrial production methods of the species *Dunaliella salina*. (a) Open pond in Australia at Western Technologies, (b) Raceway in Israel at Nature Beta Technologies.

Lagoons consists of natural or artificial open basins of several hectares about 20 cm in depth and located by the sea to be easily supplied with water (Figure 1.11a). Due to evaporation, the high salinity is controlled only by the addition of seawater. The agitation is carried out by wind and thermal convection. The water depth in the different tanks should be sufficient to ensure good agitation without depriving the algae from light at the bottom of the tank (Borowitzka, 1999; García-González *et al.*, 2003). This form of extensive culture is inexpensive but allows only low cell densities (approximately $0.1\text{-}0.2\text{g L}^{-1}$), (Pulz, 2001). The production yield highly relies on

environmental conditions and varies throughout the year. Open ponds, with simple or no process control, represent the conventional method used in commercial production plants for *Dunaliella* (Borowitzka and Borowitzka 1988).

To improve the production, other companies have used raceways 2–10 m wide and 15–30 cm deep, running as simple loops or as meandering systems where mixing is done with paddle wheels (Figure 1.11b). The flow created ($0.2\text{--}0.5\text{ m s}^{-1}$) allows cells to remain in suspension improving mass transfer (Del Campo *et al.*, 2007). Each unit covers an area of several hundred to a few thousand square meters. Given the high cost of land in regions of operation (mostly United States and Israel) the pond area and volume are reduced compared to lagoons. CO_2 sparging supply inorganic carbon and also regulate the pH. These systems achieve higher cell densities and a higher β -carotene concentration (Ben-Amotz, 1995). The production cost is estimated at 26 \$ kg^{-1} (Y. Shen *et al.*, 2009).

Open culture systems are operated in open air and therefore are subject to contamination and variations in culture conditions. The nutrient competition and predation, due to the open-air nature of this system, only allow the culture of strains with weed-like behavior (e.g. *Chlorella*) or extremophile strains as *Spirulina* (*Arthrospira*) or *Dunaliella* (Del Campo *et al.*, 2007). In lagoons and raceways, low biomass concentrations induce high harvesting costs (Hosseini Tafreshi and Shariati, 2009).

3.3 Closed Culture System: Photobioreactor (PBR)

The need to control the culture conditions has led to the development of closed systems, dedicated to the culture of photosynthetic microorganisms and called photobioreactors. Various configurations of PBR (Photobioreactor) exist, ranging from simple floor-mounted bags to more sophisticated designs (Figure 1.12). For the last fifty years, tubular photobioreactors and

rectangular photobioreactors technologies have been the most widely developed systems for industrial production of microalgae (Pruvost *et al.*, 2016). The use of closed photobioreactors allows to avoid the contamination of the reactor by other strains or predators. In addition, the growth conditions of microalgae can be optimized and controlled by the regulation of pH with CO₂ bubbling, agitation and temperature stabilization more efficiently than in open systems (Del Campo *et al.*, 2007). The agitation and gas exchange in the reactor can be achieved simultaneously by injecting air with the "air lift" technology.

Even so, the main limitation of the development of microalgae production processes is the light availability. Regardless of the light source nature (natural or artificial, spectral composition, intensity), the light intensity decreases very rapidly in the reactor depth due to the light absorption by cells and by the self-shading. Therefore, the light quantity is not homogeneous, and cells will receive varying amount of light in function of their trajectory in the reactor. To be efficient, photobioreactors must have a large ratio between illuminated surface and culture volume which makes it difficult to scale up to a large volume at low cost. To run optimally, those systems must be operated to absorb all the incident light but should not have a dark zone ($\gamma=1$), (Figure 1.13). With closed systems, biomass concentration can reach 2-8g L⁻¹, (Pulz, 2001). Closed systems remain interesting for the cultivation of certain species that produce high value metabolites, such as carotenoids.

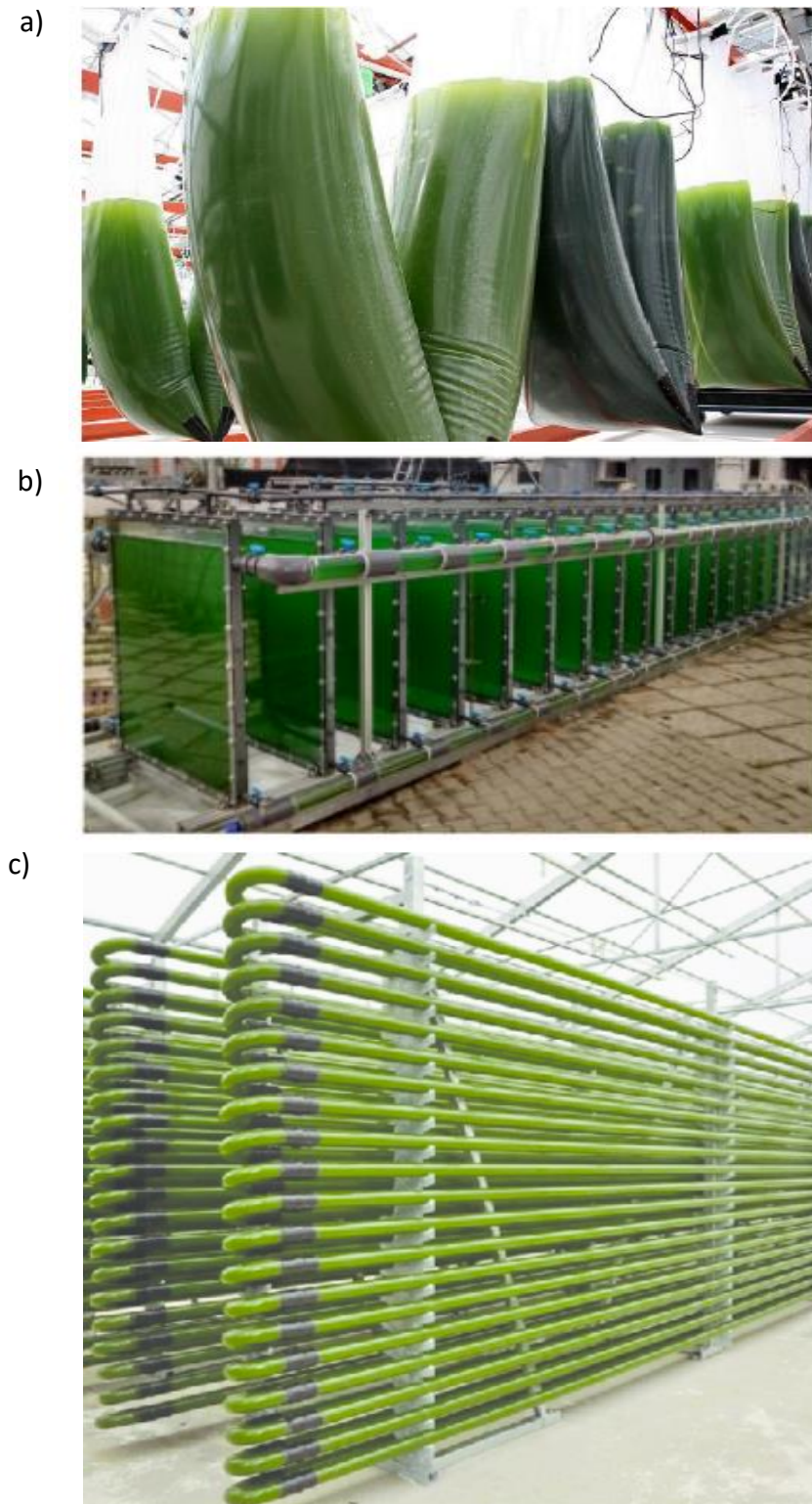


Figure 1.12 – Closed cultivation system of microalgae in a bag photobioreactor (a), (Koller, 2015) an air lift photobioreactor (b), (Lindblad *et al.*, 2019) and a tubular photobioreactor (c), (Alaswad *et al.*, 2015).

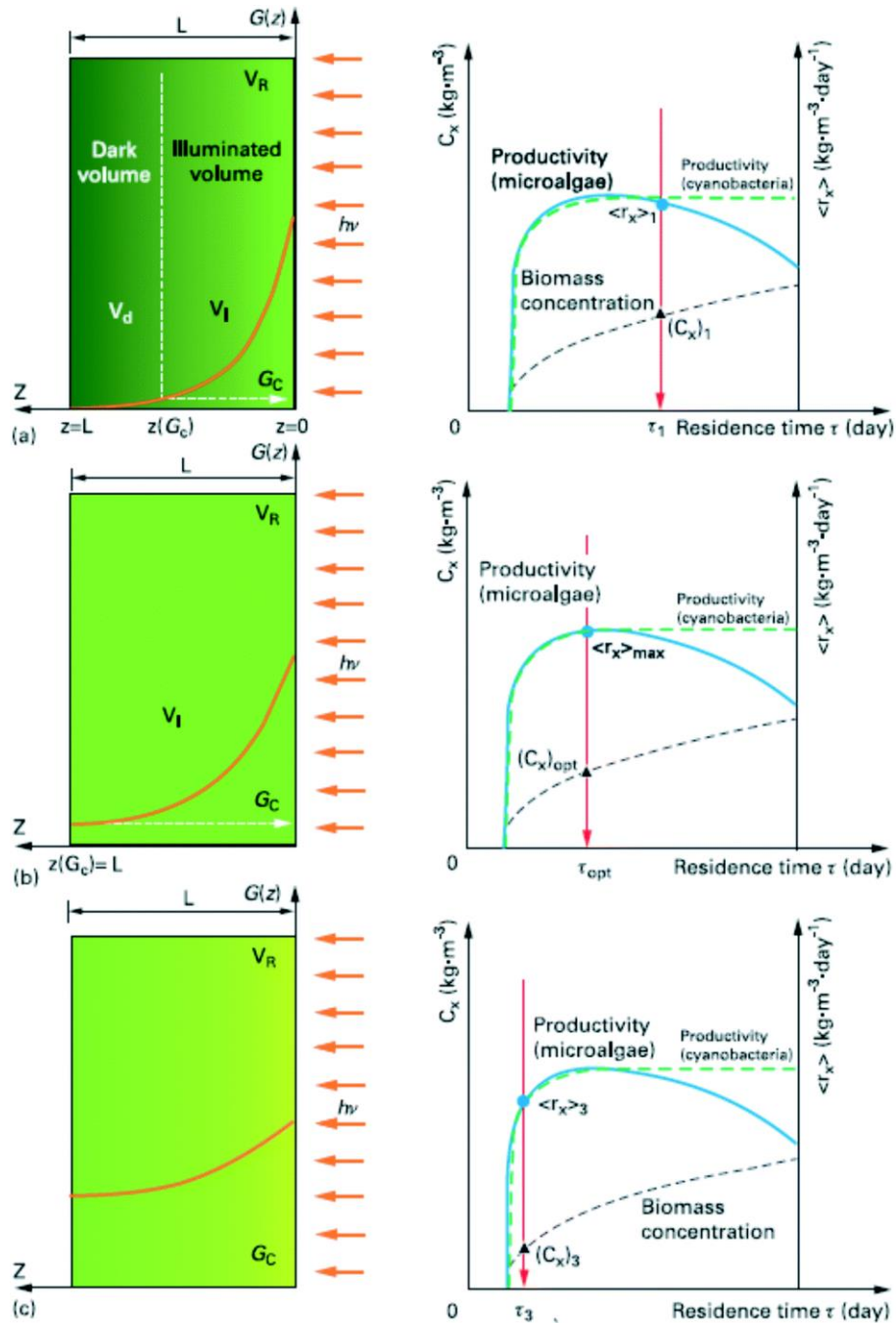


Figure 1.13 – Relation between the light absorption conditions (represented by the irradiance field $G(z)$) and corresponding mean biomass volumetric productivities ($\langle r_x \rangle$). The three typical cases of light-attenuation conditions are represented: full light absorption (Case A), luminostat (Case B) and kinetic regimes (Case C) (Pruvost and Cornet, 2012).

4 Industrial biorefining of β -carotene from *Dunaliella*

Biomass from the closed system culture process is more concentrated but more expensive to produce compared to an open system. The downstream biorefinery strategy must therefore be based on these cost characteristics, the product and the desired purity (Figure 1.14).

4.1 Harvesting

Cell harvesting of *Dunaliella salina* is a critical operation that requires particular attention. First, this strain lacks a rigid cell wall and is only protected by a plasma membrane; second, the salinity of the media which is high can provoke the corrosion of the material; and third, *Dunaliella* is generally cultured outdoor thus culture exhibits low cell density.

4.1.1 Coagulation-flocculation

The formation of microalgal aggregates can be promoted by microalgae cells themselves (autoflocculation) or using additional flocculants.

In conditions such as extreme temperatures or pH or nutrient conditions, some living organisms exude EPS (polysaccharides, uronic acid, pyruvic acid) which can lead to microalgal flocculation (Lee *et al.*, 2009). Flocculants can be chemical like multivalent metal salts such as ferric chloride, aluminum sulfate and ferric sulfate, prepolymerized metal salts, polyelectrolytes. Natural polymeric flocculants like Chitosan have also given positive results (Molina Grima *et al.*, 2003). However, the presence of the flocculating chemicals is often not considered as a safe impurity

and the removal from the final product is not an easy task. The flocculation by increasing the pH with NaOH has been proven to be an effective method (Horiuchi *et al.*, 2003).

After the formation of microalgae flocs, cells can be separated from the media by flotation, sedimentation, centrifugation or filtration.

4.1.2 Flotation

Flotation takes advantage of microalgae's natural low density and self-floating tendency (Garg *et al.*, 2012). It can be realized by gas assisted flotation like air. However due to the repulsive interaction between the bubble and the microalgae, the adhesion of cell to bubbles is low. The use of flocculation pretreatment improves the efficiency of flotation.

4.1.3 Sedimentation

Sedimentation is the simplest method to separate microalgae cells from the culture medium since it uses only the gravitational force and is additive free. It has a clear advantage in terms of cost (Li *et al.*, 2020; Najjar and Abu-Shamleh, 2020).

4.1.4 Centrifugation

Centrifugation is a separation technique that use centrifugal acceleration to separate the microalgae from the medium. The size of the algae and their difference in density with the medium are therefore also the essential parameters of centrifugal separation. Studies show that for some microalgae, between 90% and 100% of the algal material can be recovered in less than 5 min of treatment (Chen *et al.*, 2011; Heasman *et al.*, 2000).

However, due to shearing forces, fragile strains are disrupted by this process Knuckey *et al.* (2006). Despite expensive investment, and high demand in energy, labour and maintenance, centrifugation has been claimed to be one of the most effective harvesting methods for high value metabolites production chain.

4.1.5 Adsorption

This is the method used to harvest *Dunaliella salina* in the industrial process developed in Australia from diluted cultures in shallow ponds. *Dunaliella salina* tends to become hydrophobic beyond a NaCl concentration of 3 M. Curtain & Snook (1985) were inspired by this characteristic to propose a harvesting method which puts the algal suspension in contact with an adsorbent having a hydrophobic surface. In the patent in question, they also provide for the desorption of the algae by washing with fresh water or with a brine of less salinity. They also protect an integrated method of processing algal material. The latter consists in recovering the content of the algae during their adhesion to the hydrophobic surfaces, by bringing the coupling into contact with a solvent. This solvent allows the rupture of the microalgal membrane and the extraction of the compounds of interest, in particular β -carotene. From a technological point of view, the algal suspension can pass through a bed of hydrophobic particles, this is called hydrophobic filtration. Algae are retained in the bed and eluted sequentially by adding water or less concentrated brine. Another method is adsorption on low density particles followed by flotation recovery and solvent extraction.

4.2 Dewatering

The resulting microalgae paste is washed and then dehydrated by various methods such as spray drying, drum drying, freeze-drying or fluidized bed drying to extend the shelf-life of the biomass.

The culture medium freed of microalgae can be reused for the next culture or used as fertilizer.

To obtain a uniform and stable powder drum drying, spray drying and freeze-drying are generally used (Hosseini Tafreshi and Shariati, 2009).

4.2.1 Sun drying

Sun drying of *Dunaliella* may degradate the β -carotene molecules, which are photosensitive.

4.2.2 Freeze drying

At the laboratory scale, freeze-drying is most convenient because of its high yield of recovery but spray drying is less expensive than freeze-drying in large-scale commercial production

4.2.3 Spray drying

Finally, several types of *Dunaliella* food products have been manufactured by spray dring (Tanaka, 1990). An alternative product is a spraydried biomass powder. β -carotene is very susceptible to oxidative degradation. Indeed, it has been reported that spray-drying using conventional air as the drying gas can result in 45% oxidation of carotenoids from an algal feed.

4.3 Extraction

The result of the previous steps is a *D. salina* powder that can be directly marketed as such in capsule form, conditioned in vacuum bag or used for a final carotenoid extraction step. The extraction is carried out using organic solvents, edible oil or pressurized fluid (e.g., supercritical CO₂). The different forms obtained will contain a mixture of carotenoids ranging from 4% for *D. salina* powder to 9-cis β -carotenes of high purity obtained with organic solvents and chromatographic instruments (Hosseini Tafreshi and Shariati, 2009).

4.3.1 Organic solvent

Organic solvent extraction of carotenoids is the most employed method industrially. It can be realized with the help of organic solvents such as hexane, ethanol, chloroform and diethyl ether, directly in edible oil (Perrin and Examiner-John Rollins, 1985). The presence of organic solvent residues from petrochemical origin can be repulsive to the consumer, so the β -carotene in edible oil is preferred in the case of a direct human consumption.

4.3.2 Edible oil

During this process, a mixture of the organic phase with the aqueous suspension is carried out at high temperature ($\approx 120^\circ\text{C}$) in order to increase the solubility of β -carotene, to reduce the viscosity of the oil and to improve the extraction by promoting cell lysis. To increase the extraction yield, the cells are destroyed before the addition of solvent. After extraction, the two phases are separated by microfiltration or by ultrafiltration. The β -carotene extract is sold as a mixture in oil with a concentration variant of 1 to 20%. The edible oils used contain natural tocopherol which can improve the antioxidant properties and the stability of the product

4.3.3 Supercritical CO₂

The supercritical CO₂ is rather a good solvent for non-polar compounds and is nontoxic. As such it can be a good greener alternative to organic solvent extraction technology. When heated and pressurized CO₂ become supercritical, having the hydrophobicity of water but a viscosity close to vapor. After depressurization, CO₂ becomes gaseous and is then spontaneously separated from the extracted phase which allows the production of solvent free extracts when a co-solvent is not required. However, the extraction yield of carotenoids from a biomass with high water content with supercritical CO₂ is low consequently biomass would need to be dried, which is energy intensive.

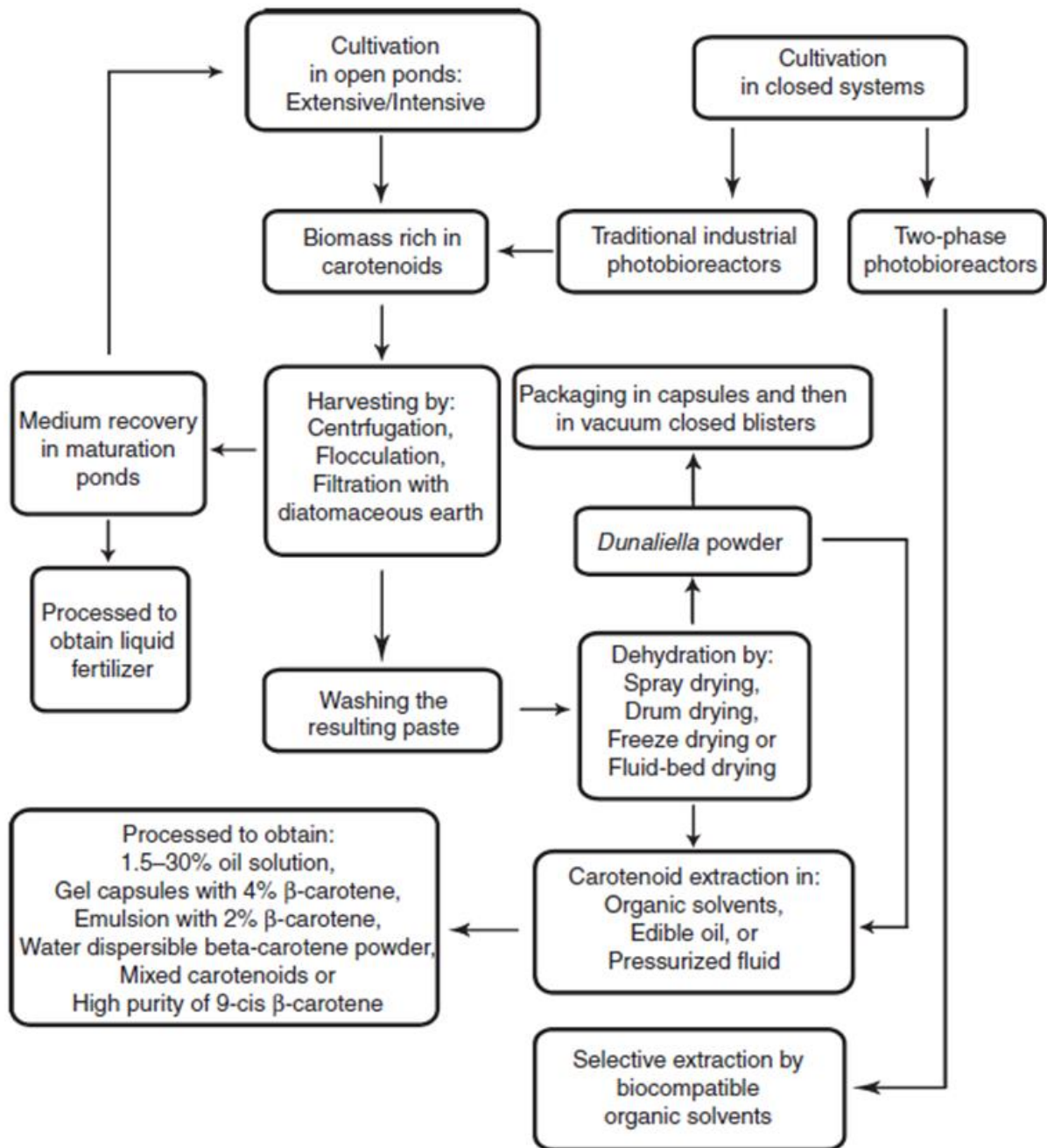


Figure 1.14 – Biorefining process of β -carotene used in industrial production (Hosseini Tafreshi and Shariati, 2009).

5 Milking of microalgae

5.1 The milking concept

The concept of “milking” of microalgae was first introduced by Frenz *et al.* in 1989 to describe the extraction of hydrocarbons from *Botryococcus Braunii* without cell death, realized by a short time exposure to hexane. The term ‘milking’ refers to the analogy of the extraction of dairy milk from cows, that are not killed in the process (Ramachandra *et al.*, 2009). It specifies that cells should not be killed during the extraction. In the literature, the “milking” (Hejazi, 2003) is also referred as “biocompatible extraction” (Mojaat *et al.*, 2008), “non-destructive extraction” (Moheimani *et al.*, 2013), “extraction without cell death” (Atta *et al.*, 2016), “in situ extraction” (Nezammahalleh *et al.*, 2017) or “extraction with retention of viability” (Hejazi *et al.*, 2002).

Vinayak *et al.* (2015) pointed out the need to clarify the terminology between milking, extraction and secretion with the following definitions:

- “Milking as the removal of a specific set of products without killing the organism, in such a way that it can be milked again at a later time.”
- “Extraction as the removal of a specific set of products without concern about the survival of the organism, generally leaving an organic residue.”
- “Secretion or spontaneous oozing as the active dumping of a specific set of products by an organism into its surrounding environment.”

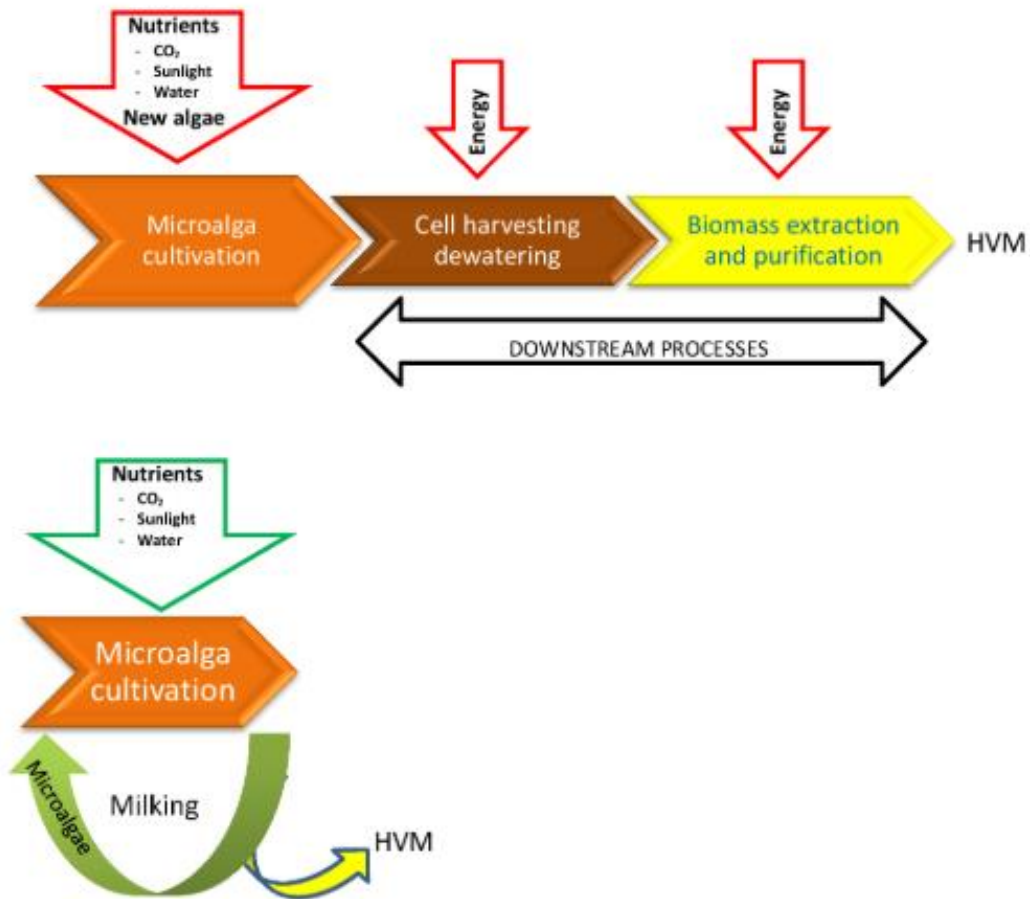


Figure 1.15 – Scheme presenting milking as an alternative to current processes. (Top): Current processes are systems that require starting new microalgal cultures for each batch of metabolites, with fresh nutrients; (Bottom): Milking only requires inputs of carbon dioxide and water used up in producing metabolites, and thus is closer to a closed system (Vinayak *et al.*, 2015). HVM: high value metabolites.

Hence, the milking provides many advantages over traditional biorefining strategies of metabolites from microalgae (Vinayak *et al.*, 2015), (Figure 1.15). The microalgae can be envisioned as a production catalyst, a “factory” that can be used several times to produce specific chemicals. The circular use of matter might unlock saving of water (not contaminated by cell residue), fertilizers (e.g. nitrogen and phosphorus) and energy (light, agitation, harvesting, dewatering, purification) in bio production processes (Chaudry *et al.*, 2015).

5.2 Pulsed electric field

When exposed to high electric fields, the membrane permeability of microorganism increases during a phenomenon called electroporation. Historically, electroporation has been applied to allow genetic modification by the insertion of new genetic material inside the cells. Depending on the treatment, electroporation can be reversible or irreversible. Reversible permeabilization occurs when the cell membrane can be resealed, it is widely use in medical application for genetic modification or drug injection inside targeted cells. On the contrary irreversible permeabilization happens when the recovery of membrane integrity is not possible, it is widely applied for microbial inactivation in food industries and to kill pathogens in wastewater treatments, for the extraction of intracellular metabolites such as pigments, proteins and lipids (Joannes *et al.*, 2015).

In practice, two electrodes are placed between the cell suspension, the application of the pulsed electric field (PEF) will start to distract the polar bonds that hold the molecules together, which forms the microalga outer surface (Figure 1.16). If the electric fields surpass the critical strength of the cell membrane, the non-covalent interaction that bonds the bilayer together will be overcome, resulting in the formation of pores. Electric pulses are characterized by length, intensity, polarity, frequency of repetition. It was shown that an electric field of 20-25kV cm⁻¹ results mostly in irreversible permeabilization of *Chlorella vulgaris* (Luengo *et al.*, 2014). Lower electric field of 10kV cm⁻¹ could withstand 50 pulses of 3 μ s. The use of PEF higher than 15kV cm⁻¹ and 15 μ s significantly increase the extraction of metabolites from *C. vulgaris*. The application of PEF at 1 kV cm⁻¹ allowed the biocompatible extraction of 46% of the total proteins from living cells of *Haematococcus Pluvialis* (Gateau *et al.*, 2021).

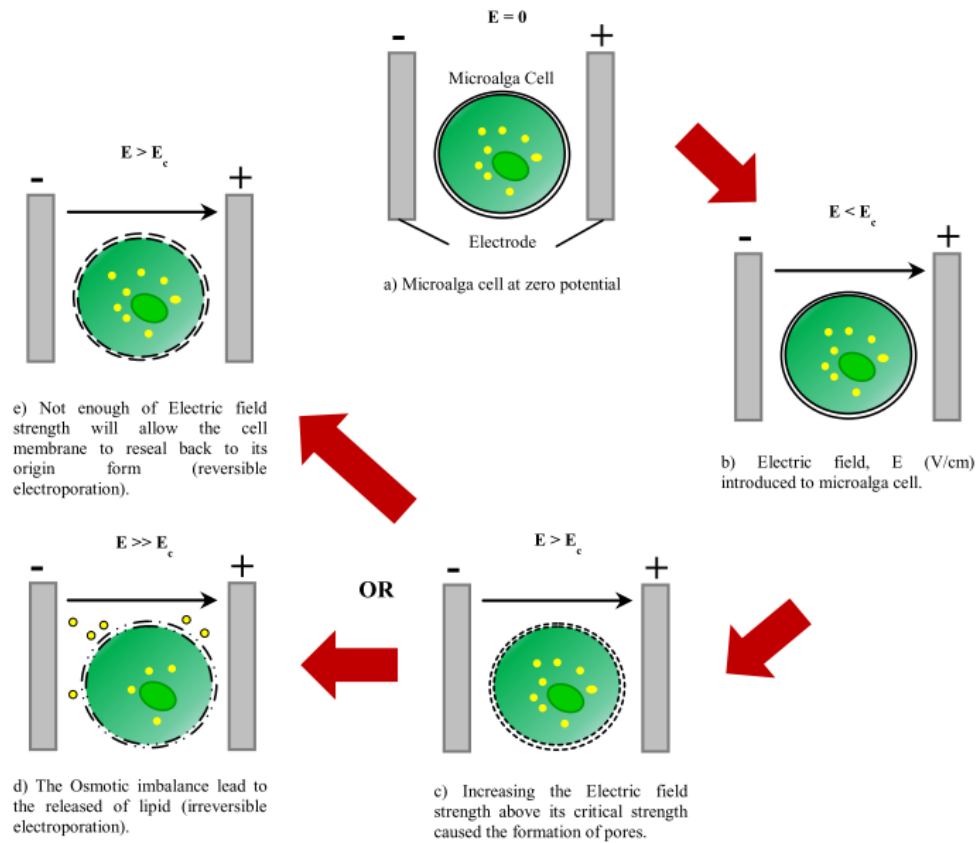


Figure 1.16 – The electroporation mechanism of microalga cell membrane (Joannes *et al.*, 2015).

5.3 Mechanical extraction

Different mechanical methods show the possibility to extract metabolites without cell disruption. However, these technics were realized at the microscale and remain complex to scale up. When mechanical pressure was applied on a cover slip above the microalga *Terpsinoë musica*, cells released oil and were not visibly broken (Vinayak *et al.*, 2015). The original extraction of astaxanthin from *Haematococcus Pluvialis* with gold nano scalpel provoke a remarkable overaccumulation of this carotenoid, the intracellular concentration was multiplied by two in the cell after wound healing in 12 days (Praveenkumar *et al.*, 2015), (Figure 1.17).

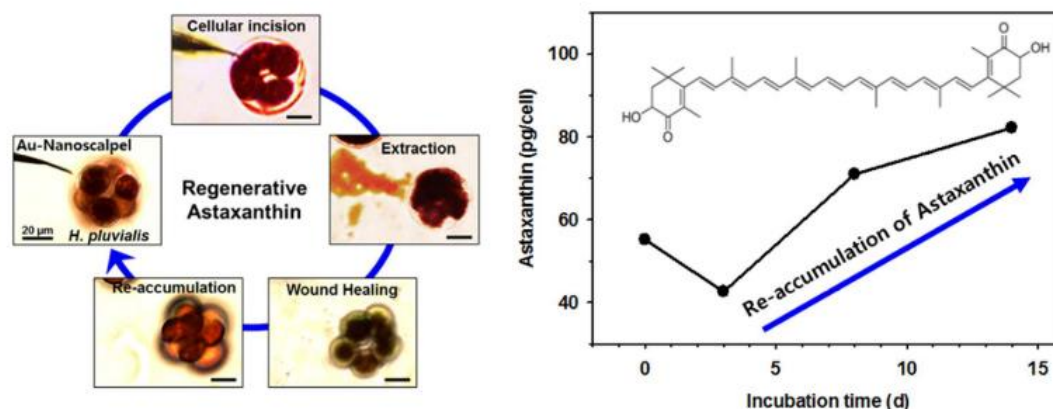


Figure 1.17 – Stimulation of astaxanthin production after extraction with gold nano-scalpel incision (Praveenkumar *et al.*, 2015).

5.4 Spontaneous oozing

The microalgae *Botryococcus Braunii* is well known for its ability to secrete oil in the extracellular matrix of the colony (Figure 1.18) in contrast to most other oleaginous microalgae that accumulate lipids in the cytoplasm (Hirano *et al.*, 2019). In fact, this alga contributed significantly to the generation of petroleum : fossils of this strain have been identified in oil shales and their hydrocarbons are a major component of crude oils (Glikson *et al.*, 1989). However, the slow growth rate of *Botryococcus Braunii* is a major bottleneck for its implementation for the production of biofuel feedstock (Metzger and Largeau, 2005).

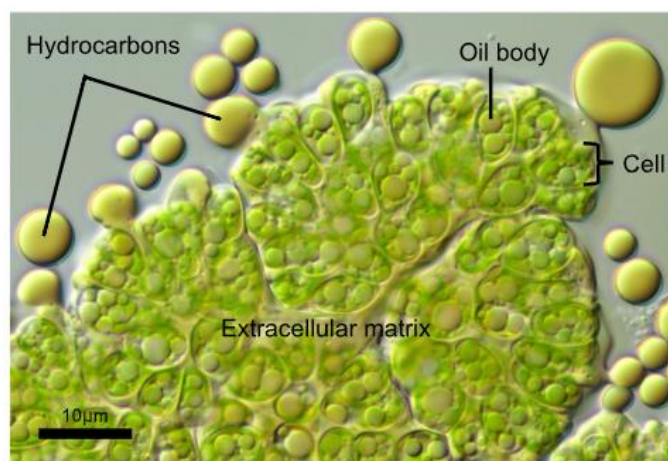


Figure 1.18 – Colony of *Botryococcus Braunii* with natural oil bodies oozing in the extracellular matrix. Due to the flattening by the microscope cover glass, hydrocarbons are exuded from extracellular matrices (Hirano *et al.*, 2019).

Recently, the secretion of lipid droplets into the culture medium from the diatom *Diadlesmis confervaceae* Kützing was reported by Vinayak *et al.* (2014), (Figure 1.9). This small diatom strain (14–18 μ m long and 6–7 μ m width), which has a 14.6% lipid content, accumulates the lipid droplets in the chloroplasts or in the cytoplasm. However, the oozing mechanism is not yet determined.

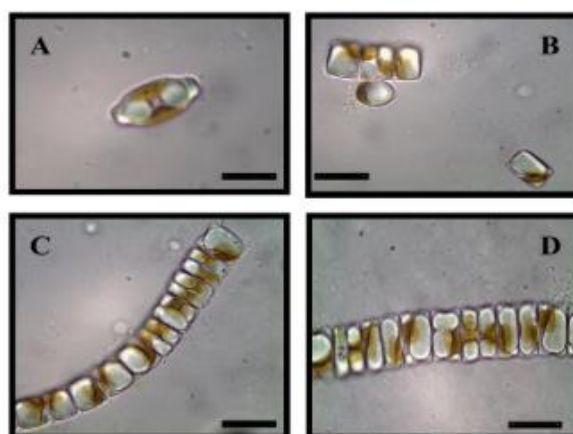


Figure 1.19 – *Diadlesmis confervaceae* in solitary and chain forms as observed under 100 \times oil immersion. Note oozed oil droplets in panel C. Cf. (Vinayak *et al.*, 2014). Scale bar: 10 μ m.

5.5 Biocompatible organic solvents

5.5.1 Solvent partitioning and toxicity

Hydrophobic and hydrophilic solvents typically do not mix when the solubility between each other is low, they form two distinct liquid phases when insert in the same container. During contact between the two phases, the solutes in solutions migrate from one phase to the other (Figure 1.20). They gradually equilibrate according to their solubility in each phase, their concentration and the temperature. The coefficient P is then defined as the ratio between the concentration of a solute X in the upper and in the lower phase of a two-phase equilibrium system.

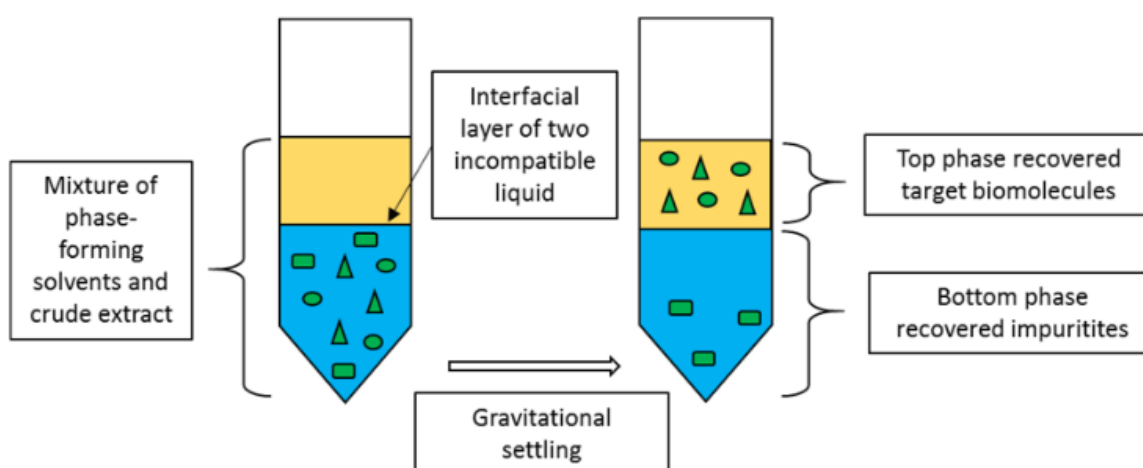


Figure 1.20 – Schematic diagram of the principle in the liquid biphasic system (Khoo *et al.*, 2020).

The coefficient P_{oct} of a compound is its partition coefficient between water and octanol. Harrop *et al.*, (1992) and Nikolova and Ward, (1993) have shown that a solvent is toxic to a micro-organism when $\log(P_{\text{oct}}) < 4$. Thus, biocompatible solvents are rather apolar.

For organic solvents, the longer the carbon chain, the more apolar the molecule. Brink and Tramper, (1985) have shown that solvents with a molecular weight greater than 150g/mol are

generally applicable for biocompatible extraction. In particular, alkanes, from hexane to hexadecane, are biocompatible (Sikkema *et al.*, 1995). Osborne *et al.* observed that the partition coefficient of a solvent between aqueous phase and the membrane follows a Collander-type relationship (Equation 1) as a function of $\log(P_{\text{Oct}})$, with R assumed constant for all the solvents (Lorente De N3, 1934).

$$\log([solv]_{\text{aq,cr}}) = \log\left(\frac{[solv]_{\text{mem,cr}}}{R}\right) - A \cdot \log(P_{\text{Oct}}) \quad (\text{Eq. 1.1})$$

With R: membrane / octanol partition coefficient of the system, $R=0,19$

A: deviation of solvent-membrane and solvent-octanol interaction

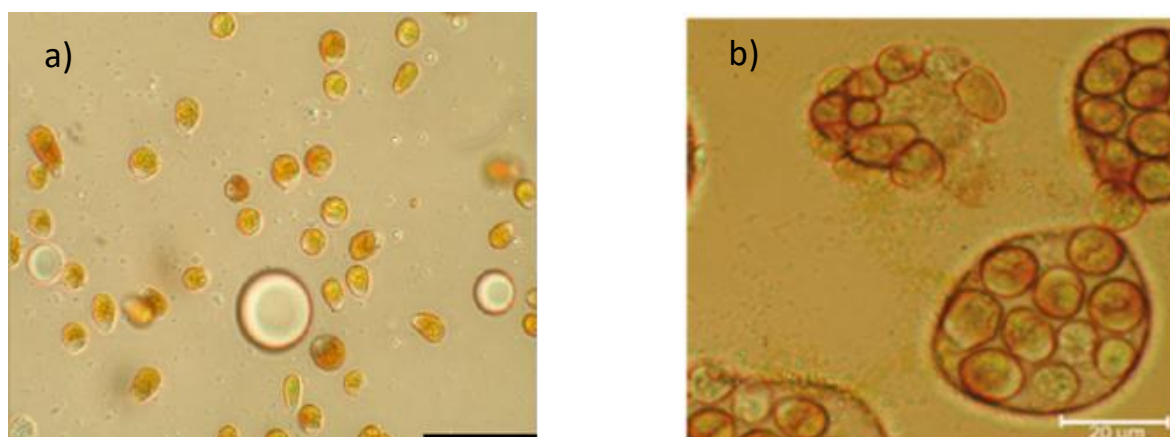


Figure 1.21 – Droplet of n-decane in a *Dunaliella salina* culture (a), *Dunaliella salina* cell in n-decane (b), (Kleinegris *et al.*, 2011b).

Although some solvents have a critical aqueous concentration for the membrane, it is never reached for very apolar solvents (Mojaat *et al.*, 2008). However, when the concentration is sufficient to form a separate phase, it may exert phase toxicity, due to direct contact between the cells and the solvent at the interface (Figure 1.21).

5.5.2 Effect of extraction on cell viability

In 1989, Frenz *et al.* reported that hexane enabled the *in situ* collection of the hydrocarbons from *Botryococcus Braunii*. This hydrophobic fraction is naturally excreted in the extracellular matrix of the colony during cultivation. The short contact time (10-120min) allowed the cells to recuperate and resume growth without negative effect after extraction of hydrocarbons. Heptane was reported to be less toxic than hexane to *B. Braunii* enabling contact time up to 20min without a loss of viability (Moheimani *et al.*, 2013). The long-term milking of hydrocarbons from *B. Braunii* was run through a 6-week continuous cultivation, with very short (15s twice a day) contact time between solvent and culture. However, the viability was highly strain-dependent as only one *Botryococcus* strain survived to hexane treatment (Griehl *et al.*, 2015).

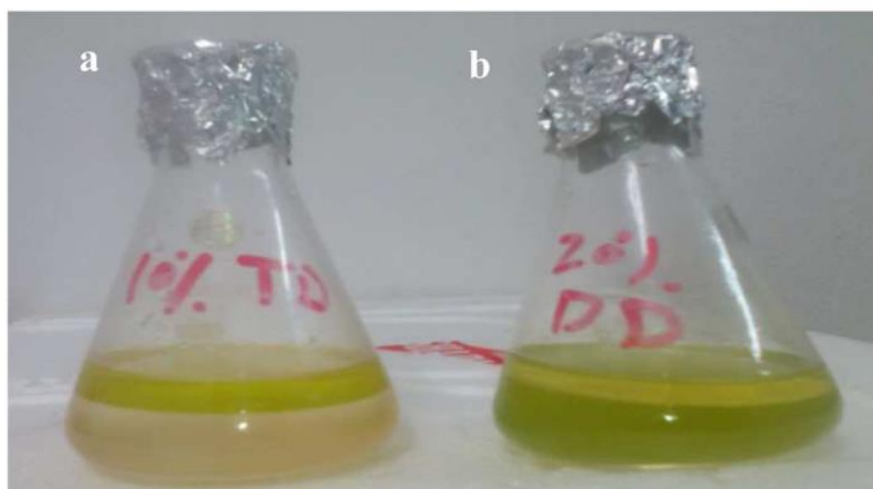


Figure 1.22 – Phase separation of lipids milking in *Chlorella vulgaris* with (a) 10% tetradecane (b) 20% dodecane after 2nd cycle of extraction (Atta *et al.*, 2016).

The extraction of lipids from *Chlorella vulgaris* has been carried out using n-hexane, n-octane and n-decane with extraction rate of 8%, 6% and 4% after 20min, respectively. Organic solvents, n-octane and n-decane, did not cause ionic leakage from cells, confirming that cell membranes

maintained their selective permeability. The lowest inhibitory effect on cell viability after 50min mixing with the solvent was obtained with n-decane (Li *et al.*, 2015). In another study, the milking of lipids from *Chlorella vulgaris* was conducted in 4 cycles with a dodecane and tetradecane layer added in the culture flask and replace each 7 days with a culture replenishment (Figure 1.22). The lipid recovery decrease from 45% at the first cycle to 25% at the fourth cycle, a stimulation on cell growth was reported after 7 days, but the contribution of solvent to the OD750nm was not measured, (Atta *et al.*, 2016).

In *Dunaliella salina*, by comparing β -carotene solubility, solvent extraction ability and biocompatibility of organic solvents, León *et al.* (2003) established that the best compromised for β -carotene biocompatible extraction is achieved with hydrophobic solvents exhibiting a log P_{octanol} around 5 like *n*-decane, provided that the solvent/culture ratio (v/v) remains less than 1. In another study, *n*-decane was considered as noncompatible with a total loss of oxygen production after 24h (Hejazi *et al.*, 2002). On the opposite, dodecane, tetradecane and hexadecane, provoked only a decrease in photosynthetic activity between 5-15% and microscopic observation confirmed the high viability of cells exposed to these solvents. Other authors reported that the photosynthetic activity of *Dunaliella salina* did not decrease after a 15min incubation with decane, dodecane and hexadecane (Mojaat *et al.*, 2008). The extraction biocompatibility was demonstrated with proportionally more β -carotene extracted than cells disrupted. Interestingly, a 10% increase of photosynthetic activity occurred upon contact with decane. The addition of the co-solvent dichloromethane to decane multiplied by 6 the extraction ability of the organic solvent. The addition of this polar solvent to the organic phase increased the solubility of β -carotene but, however, increased cell death. Another study relate direct correlations between cell destruction and β -carotene extraction when dodecane was directly used or supplemented with concentration of dichloromethane of 1,2% and 5% (v/v) and sparged

(300mL L⁻¹ min⁻¹) through the culture media (Kleinegris *et al.*, 2011b), (Figure 1.23). Continuous *in situ* extraction of β -carotene from *Dunaliella salina* was achieved with an equilibrium between cell growth and cell death (Kleinegris *et al.*, 2011a). However, a major part of β -carotene produced came from net production of the enriched biomass. Microscope observation showed that no cell survived in the emulsion formed due to the presence of a high concentration of solvent droplet, which result in phase toxicity. In addition, the high intensity of light applied to the culture to induce the production of β -carotene results in significant degradation of carotenoids in the extract that recirculated through the photobioreactor (Hejazi, 2003).

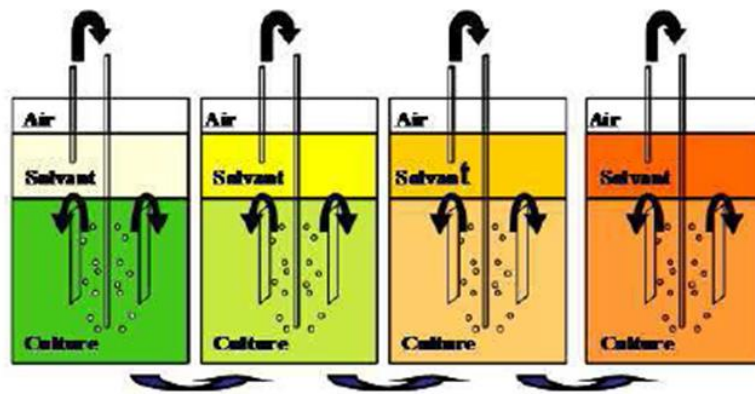


Figure 1.23 – Principle of extraction in a two-phase photobioreactor.

Altogether, it has been concluded that lipid extraction from microalgae with organic solvents depends on the contact time and area between the culture media and the organic solvent, but the higher the extraction, the lower the biocompatibility (Frenz *et al.*, 1989; Hejazi *et al.*, 2003; Atta *et al.*, 2016; Miazek *et al.*, 2017). While many studies focus on solvent choice and extraction operating conditions there is a lack of understanding of the impact of extraction on the single cell characteristics (Figure 1.24). This is particularly important due to the various culture conditions applied that might have results in very different single cell characteristics that are not investigated

or reported. When the extraction is coupled to the cell culture, the evaluation of cell viability is not possible because of cell growth happening at the same time than cell death due to solvent toxicity. Only the stimulating or inhibiting effect of solvent exposition on the cell growth rate can be evaluated.

5.5.3 Stimulation and inhibition of cell growth

When cultured for 72h with n-decane a slight induction of carotenogenesis was reported in *Dunaliella salina* (León *et al.*, 2003). The cultivation of *Dunaliella salina* in turbidostatic photobioreactor with bubbling of n-dodecane provoked an increase of cell density compared to control but it decreased the intracellular concentration of β -carotene (Kleinegris *et al.*, 2011a). The cultivation of *Chlorella vulgaris* (a microalgae that has a cell wall) with 10% n-dodecane and agitated by magnetic stirring provoked an increase in optical density and dehydrogenase activity (Atta *et al.*, 2016). However, the presence of solvent droplet in the medium could also contribute to the increase in optical density. There is a positive effect of solvent on growth and accumulation of metabolites (Vinayak *et al.*, 2015). At low concentration, it can stimulate biomass growth whereas at high concentration it is more suitable for extraction operations due to phase toxicity (Miazek *et al.*, 2017), (Figure 1.24).

Chapter 1: Production and biorefining of β -carotene from *Dunaliella salina*

Cultivation			Extraction						Impact					Reference
Culture system	Stress	Product	Solvent	Culture and extraction	Agitation	Contact time	Solvent ratio (v/v)	Extraction yield	Cell viability	Growth rate	Metabolites productivity	Biological activity	Permeability	
PBR batch	No	Carotenoids	n-Decane	Coupled	Stirring 70rpm	7d	12%	/	X	-	/	0% b	/	Hejazi et al, (2002)
PBR batch	No	Carotenoids	n-Dodecane	Coupled	Stirring 70rpm	"	12%	23%	X	+	114%	83% b	/	"
PBR batch	N depletion	β -Carotene	n-Decane	Decoupled	Solvent bubbling	72h	5%	/	/	92%	120%	111% b	/	Leon et al, (2003)
PBR batch	N depletion	β -Carotene	n-Decane	Decoupled	Solvent bubbling	100h	30%	8%	/	/	/	/	/	"
PBR batch	N depletion	β -Carotene	n-Decane	Decoupled	Shaking 200rpm	24h	30%	20%	/	/	/	/	/	"
PBR continuous	N depletion	β -Carotene	n-Decane	Decoupled	Stirring 800rpm	15min	50%	/	/	/	/	110% a	/	Mojaat et al, (2008a)
PBR continuous	N depletion	β -Carotene	n-Decane	Decoupled	Shaking 500rpm	24h	50%	10%	/	/	/	/	/	"
PBR continuous	N depletion	β -Carotene	n-Decane + 0,19 M CHCl ₂	Decoupled	Shaking 500rpm	24h	50%	60%	/	/	/	/	/	"
PBR continuous	N depletion	β -Carotene	n-Decane	Decoupled	CPC 800rpm	/	50%	23%	85%	/	/	/	/	Mojaat et al, (2008b)
PBR continuous	N depletion	β -Carotene	95% n-Decane + 5% CHCl ₂	Decoupled	CPC 800rpm	/	50%	37%	80%	/	/	/	/	"
PBR turbidostat	High light	β -Carotene	n-Dodecane	Coupled	Bubbling	6d	28,6 % min ⁻¹	9%	X	73%	59%	/	/	Kleinegris et al. (2011a)

" idem as above
 / Not communicated
 a Fv/Fm
 b O₂ production
 X Non mesurable

Figure 1.24 – Impact of biocompatible extraction on *Dunaliella salina* cells in the literature.

5.5.4 Membrane permeabilization

When solvent molecules meet the bilayer membrane, they are blocked by the aliphatic part and intercalates between the phospholipids (Salter and Kelt, 1995). The presence of the solvent disturbs the fluidity of the membrane (Figure 1.25) which normally allows the cell to adapt to the surrounding hydrodynamics.

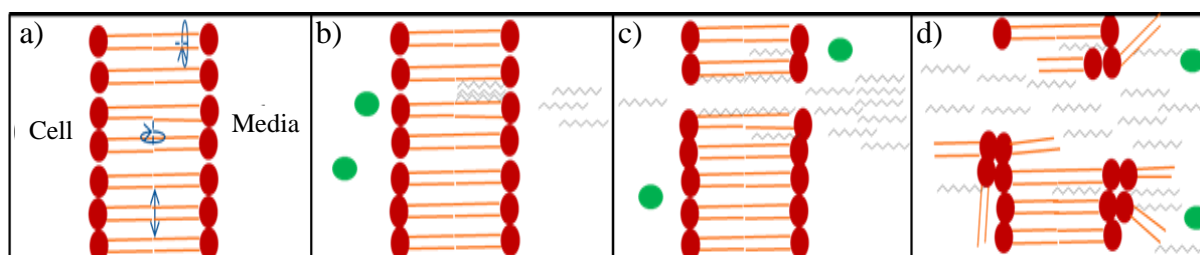


Figure 1.25 – Solvent membrane poration: a) The membrane is fluid, b) The solvent diffuses into the membrane, c) The transmembrane gradient creates a reversible pore, and d) The membrane integrity is breached.

Indeed, membranes are the preferential place where the organic solvent will accumulate (McIntosh *et al.*, 1980). The accumulation of molecules in the membrane increases the osmotic pressure (Sikkema *et al.*, 1992). When the transmembrane pressure increases, pores appear across the membrane. The pores created are, at first, hydrophobic, most of them resealed due to the fluctuations (fluidity) of the phospholipids. Even so, if their sizes exceed a critical radius, the pores will persist. If the surface of pores on the cell membrane is too high, the membrane will be irreversibly destabilized, and the cell will lyse. The toxicity will then depend on the concentration and the time of exposure of the cells to the solvent. Solvents with a carbon number below 10 diffuse less rapidly in the membrane compared to longer chains, this delay the formation of irreversible pores (Gillet, 2015).

5.5.5 Mechanism of extraction

Literature studies shown that membrane are the preferential places where organic solvents can accumulate, resulting in the formation of holes through the phenomenon of permeabilization (McIntosh *et al.*, 1980). The membrane permeabilization by the solvent will increase the transport of chemicals across each side of the membrane. The solvent could then enter the cell and diffuse into the chloroplast membrane to reach the oil bodies that contain the β -carotene. This explains how the solvent can reach the β -carotene. Hejazi *et al.*, (2004) have suggested two possible mechanism by which the β -carotene can exit from *Dunaliella salina* cell (Figure 1.26). The disturbance caused by the presence of organic solvent moves the globules of β -carotene to the space between the chloroplast membranes and the cell membrane, from there the globules are released by exocytosis (i). It has already been shown that the membrane of *D. salina* has natural ongoing endo and exocytosis activities as reported by Ginzburg *et al.*, (1998). Another mechanism is the release of β -carotene due to globule alteration, then the molecules diffuse across the chloroplast membrane and subsequently across the cell membrane to reach the medium (ii).

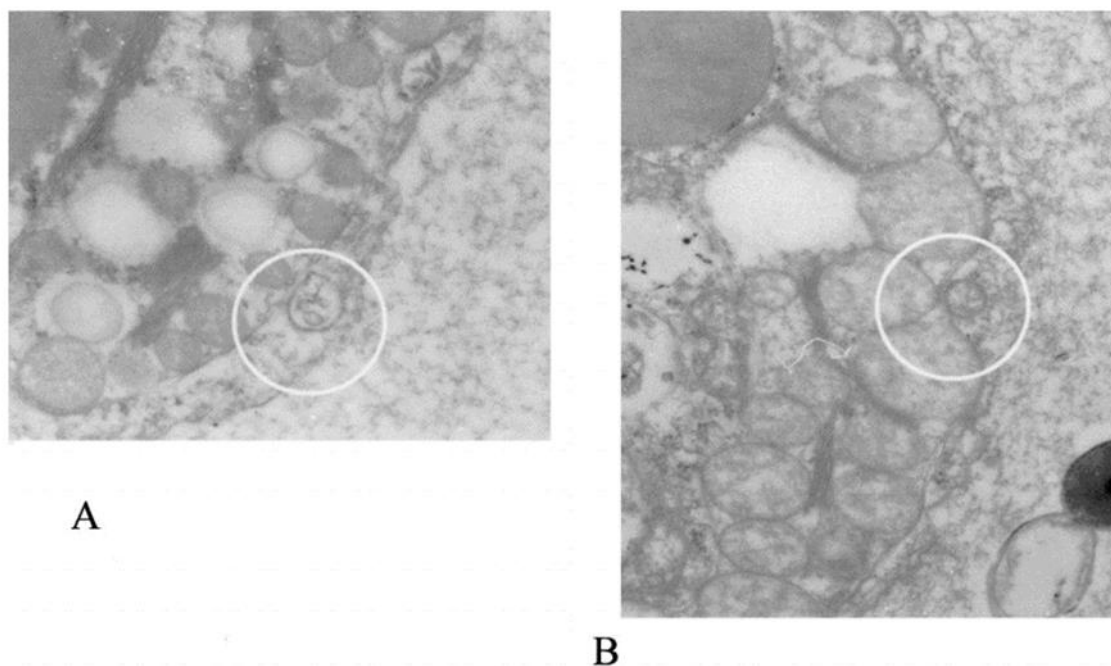


Figure 1.26 – Scanning electron microscope of *Dunaliella salina* cell cultivated in medium saturated in dodecane. A vesicle which is located between the cell and the chloroplast membrane (A) and another vesicle which seems to be being released from the cells of *D. salina* (B) are shown.

6 Viability and vitality of microalgae

6.1 Cell density

Cell density of microbial organisms can be measured with various methods such as weight measurement, electrical sensing, plate counting and optical measurement (Figure 1.27). Among them, cell counting under microscope is a fast and affordable method, widely used for the characterization of microbial density from environmental, laboratory or industrial culture samples. This method consists in a deposition of a sample under a known depth glass microscope

chamber and enumeration of individual cell by an operator or by image analysis (e.g. with an automated cell counter).

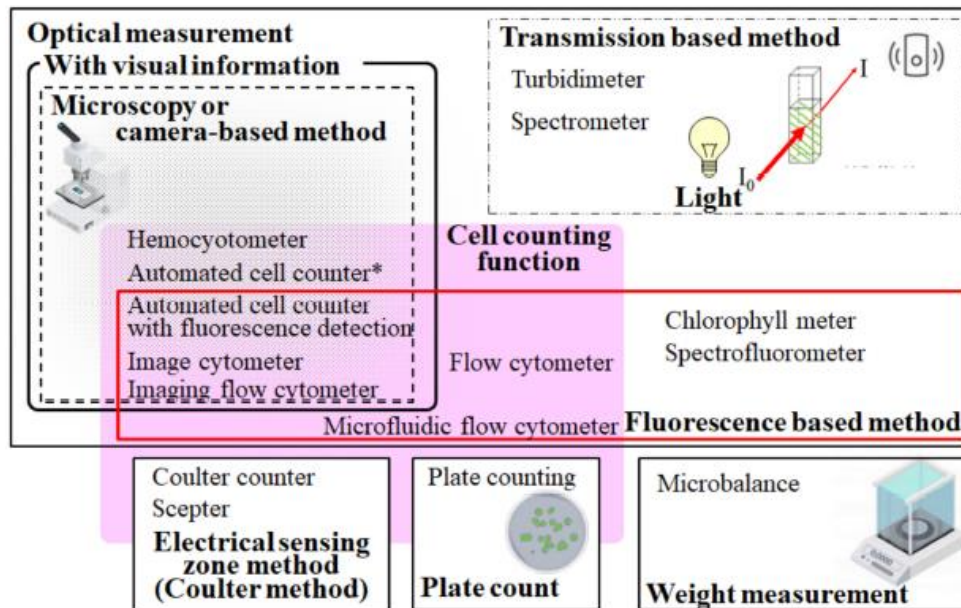


Figure 1.27 – Present standard methods for detecting and evaluating microbes, including microalgae. Optical measurements, the electrical sensing zone method, the conventional plate count method, and weight measurements are categorized. The automated cell counter marked with an asterisk means a device without fluorescence detection (Takahashi, 2020).

The method accuracy is central to ensure non-biased data. The organisms must be homogeneously distributed in the counting chamber. The density must be set in the recommended range. The usual protocol is to count 300 cells on a given number of squares (10 to 25). The counting error is frequently between 20 and 30% (Figure 1.28). This might be considered acceptable for culture monitoring were doubling of the microalgal population happens within days but insufficient for the biocompatibility characterization of organic solvents extraction of metabolites from cells.

Approximate 0.95 confidence limits		
Number of organisms counted	Expressed as percentage of count	Range
4	$\pm 100\%$	0—8
16	$\pm 50\%$	8—24
100	$\pm 20\%$	80—120
400	$\pm 10\%$	360—440
1,600	$\pm 5\%$	1,520—1,680
10,000	$\pm 2\%$	9,800—10,200
40,000	$\pm 1\%$	39,600—40,400

Figure 1.28 – Confidence limits of the cell counting method regarding the number of cells counted (Lund, 1958).

6.2 Biological activity

The need to understand the biological impact of the culture conditions or the toxicity of a substance on microalgae led to consider the potential heterogeneity of the treatment on subcategories of the population. Indeed, it is possible to distinguish between living and dead cells (non-viable) in a microbial culture. A cell can be (i) vital and viable, (ii) vital with reduced viability (e.g., consequence of a toxic substance), (iii) vital but without viability (e.g., because of total consumption of a nutrient) and (iv) non-vital and non-viable (death), (Figure 1.29). However, (Tashyreva *et al.*, 2013) developed a practical method with three fluorochromes and coined that a cell can have a reduced viability but still be metabolically active (Figure 1.30). Consequently, despite its frequent use in the literature, cell death, viability, vitality or viable-but-not-culturable (VBNC) states are not easily defined terms.

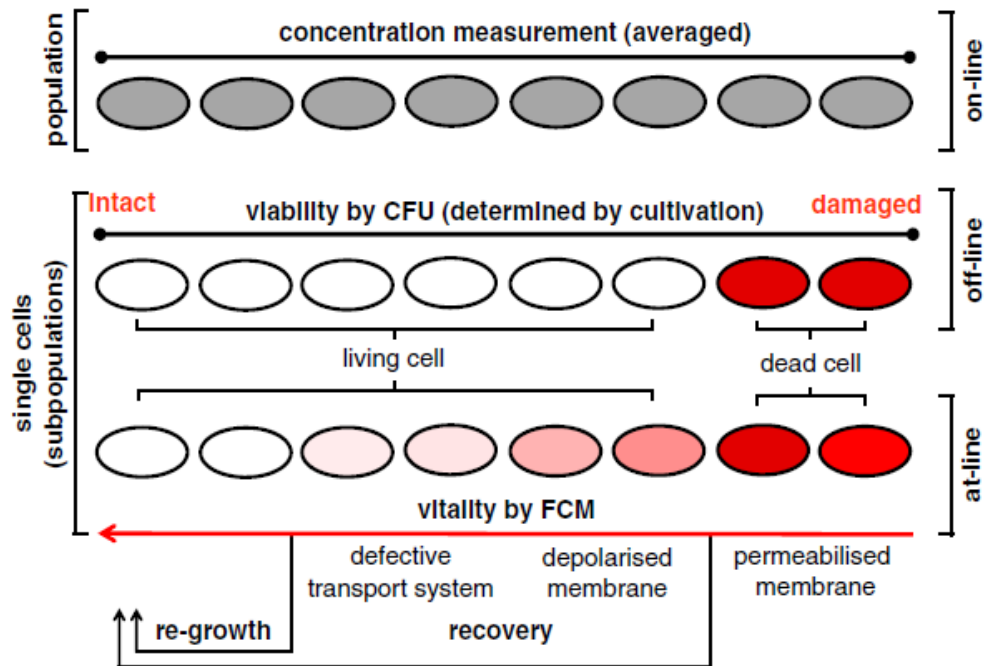
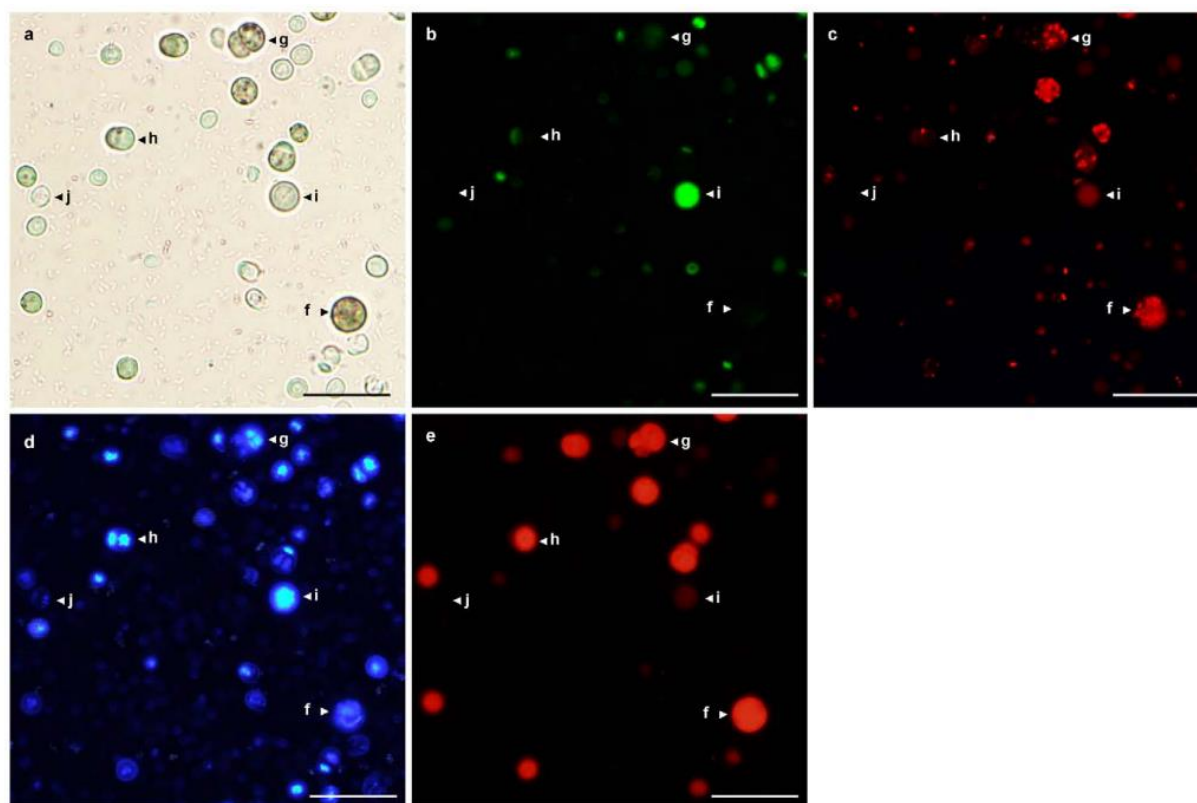


Figure 1.29 – The measurement of single cell parameters, viability and vitality definitions (Hyka *et al.*, 2013).

Generally, cell death is accompanied by a series of process which one of the first is the loss or reduction of membrane integrity (viability). A key point to emphasize is that the techniques most widely used to count dead cells are based on their membrane permeability. Viability can also be measured with the content of nucleic acid in cells that represent the reproduction ability. A second process that accompanied cell death is the reduction of metabolic activity (vitality). It is often based on enzymatic activity, in particular the dehydrogenases or the esterases. In microalgae the chlorophyll fluorescence can serve to measure the photosynthetic activity. In the following parts the different stains and method will be presented.



Physiological state of a cell	CTC reduction	SYTOX Green positive	DAPI positive	Photosynthetic pigments	Fig. 2, marked as
Active and intact (living healthy cell)	+	-	+	+	f
Injured but active (living injured or apoptic cell)	+	+	+	+/-	g
Metabolically inactive but intact (presumably dormant cell)	-	-	+	\pm /-	h
Inactive and injured (nucleoid-containing dead cells)	-	+	+	\pm /-	i
Non-nucleoid-containing dead cells	-	-	-	-	j

Figure 1.30 – Living 3-month-old *Chroococidiopsis041* CCALA laboratory culture (a) simultaneously stained with SYTOX Green (b), CTC (c) and DAPI (d) dyes and showing pigment autofluorescence (e) and classification of cells according to the selected criteria.

6.2.1 Autofluorescence

The fluorescent pigments present in microalgae are chlorophylls, carotenoids and in some species phycobiliproteins (Hyka *et al.*, 2013). The content is taxon-specific and depends on the culture

conditions (irradiance, nutrient concentration, temperature, pH, presence of photosynthetic inhibitors). Pigment fluorescence account for most of the endogenous fluorescence. There is also fluorescence due to molecules such as reduced pyridine nucleotides, flavins, tryptophan and elastin (Shapiro, 2005).

Chlorophyll fluoresces bright red with an emission peak at 580 nm. Chlorophyll fluorescence can be used to quantify vitality under certain growing conditions. Sato *et al.*, (2004) used a dual-fluorescence viability assay on ethanol treated *Chlamydomonas reinhardtii* with chlorophyll autofluorescence to count living cells and SYTOX green to count dead cells and correlated the results with plate counting. Jamers *et al.*, (2009) assess the toxicity of cadmium exposition on *Chlamydomonas reinhardtii* by measuring a decrease in chlorophyll fluorescence.

Under normal culture conditions, a lot of chlorophyll is present but in the case of stress some carotenoid algae will accumulate carotenoids. Carotenoids fluoresce in green, however, Kleinegris *et al.* (2010b) reported that the quantification was not possible. The pigment composition of the microalgae makes it possible to choose the appropriate fluorochromes to avoid the superposition of spectra, which would overestimate the measurement.

6.2.2 Permeability

A widely used dye for the determination of cells with compromised cell membrane is Evans Blue. Zhang *et al.*, (2011) measured the absorbance of Evans Blue on *Nannochloropsis sp.* cultivated with organic solvent. They showed that solvents with $\log P_{oct} < 5.5$ provoke an increase in dye absorption by the cells and thus in the permeability of the membrane. Gateau *et al.*, (2021) used Evans Blue to follow the permeabilized process of *Haematococcus pluvialis* along a treatment with Pulsed Electric Field by counting cell in the different categories: naturally permeabilized (stained in fresh culture), reversibly permeabilized (stained by addition before PEF) and

irreversible permeabilized (stained by addition after PEF) and non-affected cells (non-stained). Bicas *et al.*, (2015) determined the percentage of dead cells in *Botryococcus braunii* culture with Methylene Blue uptake.

The permeability of the membrane can also be measured by labelling nucleic acids with fluorescent polar molecules. Due to their hydrophilic nature, it only penetrates cells with permeabilized membranes. These fluorochromes are intercalated on DNA base pairs with little or no sequence specificity and according to a stoichiometry of one molecule for 4-5 base pairs (Hyka *et al.*, 2013). They fluoresce weakly in solution but when bound to a nucleic acid they emit 20 to 30 times greater intensity. There are many markers that emit green fluorescence (PICO green, SYBR Green I or II, SYTO 9, SYTO 13, SYTOX-green, TOTO-1, TO-PRO-1, YOYO-1, YO-PRO-1) or red fluorescence (propidium iodide). Dyes such as Trypan blue (McGahon *et al.*, 1995) or erythrosine B (Bochner *et al.*, 1989) were also used.

The use of propidium iodide (PI), is limited for microalgae because its spectrum overlaps with the chlorophyll one (Brussaard *et al.*, 2001), (Veldhuis *et al.*, 2001). Anyhow, it has been used to measure cell viability in several studies where the authors do not describe any interference or quenching with autofluorescence (Luengo *et al.*, 2014). In *Chlorella vulgaris*, the effect of pulsed electric fields was studied by varying the intensity and exposure time. It has been shown that pore formation can be reversible. That is to say, the inclusion of propidium iodide (PI) is lower (or even null) if added after treatment than before. The amount of PI included after addition has been correlated with the number of dead cells.

6.2.3 *Enzymatic activity*

Non-specific esterase activity is the most common way to measure the overall enzymatic activity of cells. For its detection apolar and non-fluorescent molecules of the fluorescein diacetate family

(FDA, cFDA, CMFDA) or calcein acetomethyl ester (Calcein-AM) are used (Jochem, 1999). Fluorochromes used must freely penetrate cell membranes (Brookes *et al.* 2000). In the intracellular medium, molecules from the fluorescein diacetate family are hydrolyzed by non-specific esterases, which are produced by the respiratory activity of cells, to polar fluorescein and fluorescein. The marker effectively measures the activity of the esterases, i.e., the hydrolysis rate which is a limiting factor compared to membrane penetration.

Fachet *et al.*, (2016) showed that in *Dunaliella salina* stressed with high light and nitrogen depletion and after 7 days of cultivation, two separate sub-populations were detected; about 50% of the culture emitted a lower fluorescent signal than the other half. FDA was used by Hejazi in flow cytometry to distinguish between viable (living) and dead (unruptured) cells but does not allow counting of cells that have lost their integrity. The number of cells marked by FDA has been correlated with cell digestion, which is a technique that measures the mass of cells with damaged membranes in certain microalgae including *Dunaliella tertiolecta* (Zetsche and Meysman, 2012).

6.2.4 Cell division cycle

The content of nucleic acids depends on the phases of the cycle (Figure 1.31). Reserve molecules are formed during the G2/M phase (Kwok and Wong, 2010), (Müller *et al.*, 2010; Vicker *et al.*, 1988; Yanpaisan *et al.*, 1999). Some agents intercalate on the G/C base pairs of nucleic acids but not A/T, so it labels DNA and RNA. They bind to DNA bases with little or no sequence specificity and with a stoichiometry of one molecule per 4-5 base pairs. Because of its hydrophobic character, it freely penetrates cells. It fluoresces weakly in solution but when it is bound to a nucleic acid it emits an intensity 20-30 times more important. The most widely used fluorochromes for DNA content measurement emit blue fluorescence (4'-6-diamidino-2-

phenylindole (DAPI) and Hoechst 33342). Veldhuis *et al.*, (2001) used DAPI staining and cytometry to determine the fragmentation of the genomic DNA during phytoplankton automortality.

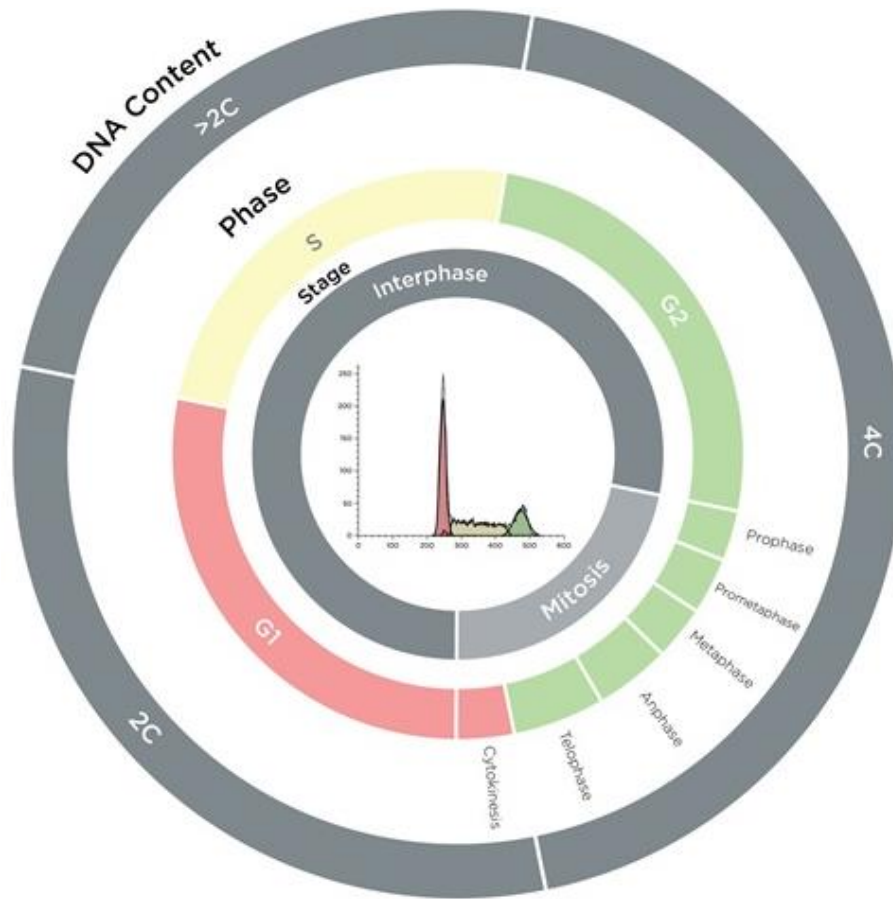


Figure 1.31 – Phase of the cell division cycle, the histogram shows a population analysis color coded by phase (“Cell Cycle Assay Principle - Beckman Coulter,” n.d.).

Chapter 2.

Material and methods

1 Cultivation

1.1 Strain and growth conditions

The green microalga *Dunaliella salina* CCAP 19/18 was cultivated in 500mL glass erlenmeyer fed with 200mL of Johnson growth medium modified according to Çelekli and Dönmez, (2006). Cultures were grown in a thermostated room ($20\pm 2^{\circ}\text{C}$) under a continuous photon flux density ($35\pm 5\mu\text{mol m}^{-2} \text{s}^{-1}$) and agitated manually once a day. The cultures were subcultured in fresh medium every four weeks.

Due to the lack of cell wall in *Dunaliella salina* magnetic stirring cause irreversible cell disruption within 3 days. As a result, the stirring was done manually twice a day. After 8 growth cycles (8 months), cultures reached higher density than previously. Culture in erlenmeyer was successful therefore the first extraction was realized on that biomass.

1.2 Production of β -carotene enriched biomass

The selected culture conditions are summarized in the

Figure 2.1a. The protocol for lipid accumulation described by Taleb, (2015) was adapted to trigger β -carotene accumulation in *Dunaliella salina*. Grown cells were harvested in sterile Falcon tube, centrifuged ($6000\times g$, 10°C , 10min), resuspended in a glass erlenmeyer in the same medium but free of nitrogen (nitrogen depleted medium) and continuously illuminated from the

bottom using a photon flux density (PFD) of $800\mu\text{mol m}^{-2} \text{s}^{-1}$ provided by LED panels (neutral white, 4000–4500K) for four weeks (

Figure 2.1b).

a)

Parameters	Conditions		Comments
Strain	<i>Dunaliella salina</i> CCAP 19/18		<i>Widely studies type</i>
Medium	Modified Johnson		<i>High β-carotene concentration</i>
Salinity	10%		<i>Limit salinity to avoid corossion</i>
N,S,P concentration	Proportionnal to biomass concentration		<i>Goal: 1g/L</i>
Agitation	Manual		<i>Avoid cell breaking</i>
CO ₂	1g/l of NaHCO ₃		<i>Carbon supplementation</i>
Culture state	Growth	Stress	<i>To trigger β-carotene accumulation</i>
Light intensity ($\mu\text{mol photons PAR/m}^2/\text{s}$)	35 (top)	800 (side)	Light stress
NaNO ₃ (mM)	17	0	Nitrogen depletion

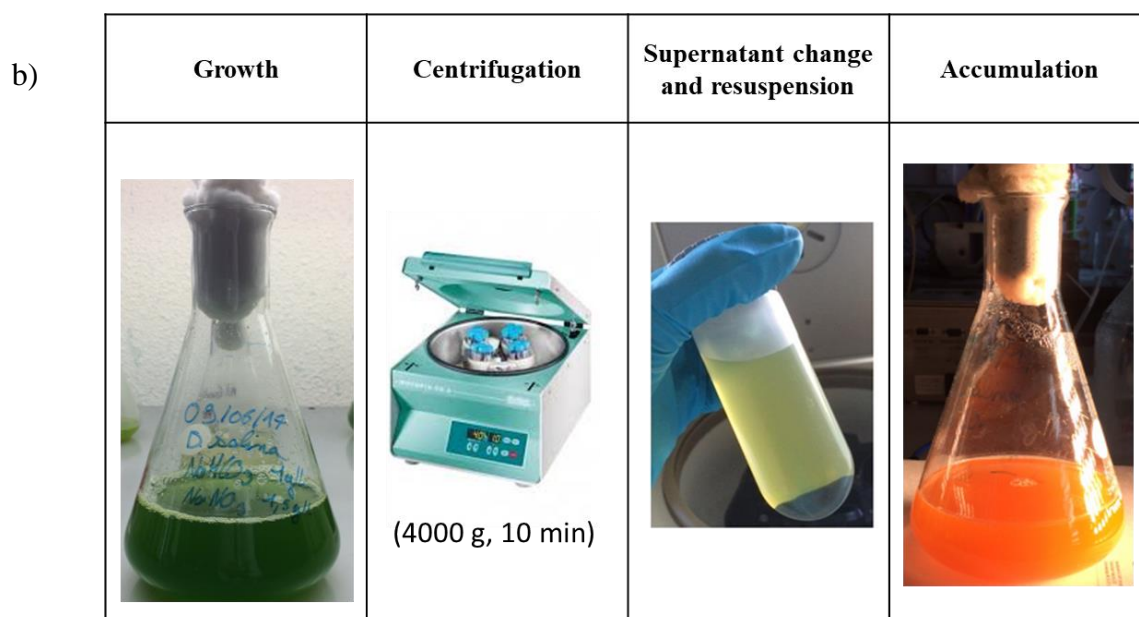


Figure 2.1 – Selected culture conditions (a) and protocol of production of β -carotene enriched biomass (b).

1.3 Culture in photobioreactor

Cells were produced in photobioreactor (PBR) in batch culture. A volume of 100mL of the grown cells were added into 1L airlift flat panel PBR (Figure 2.2) in the previous medium with doubled concentration of nitrogen, sulphur and phosphorus and maintained at pH=7.5 and at $400\pm 35\mu\text{mol m}^{-2} \text{s}^{-1}$ supplied by LED panels (neutral white, 4000–4500K) to reach a cell density of $8.2 \cdot 10^6 \text{ cell mL}^{-1}$ after one week in batch culture. Then, cells were harvested from the reactor, centrifuged ($6000 \times g$, 10°C , 10min), and resuspended in nitrogen free medium in PBR for one week, as described in the previous section, but the PFD was increased to $1200\mu\text{mol m}^{-2} \text{s}^{-1}$. The culture in photobioreactor crashed several times before the air flow adjustments were found.

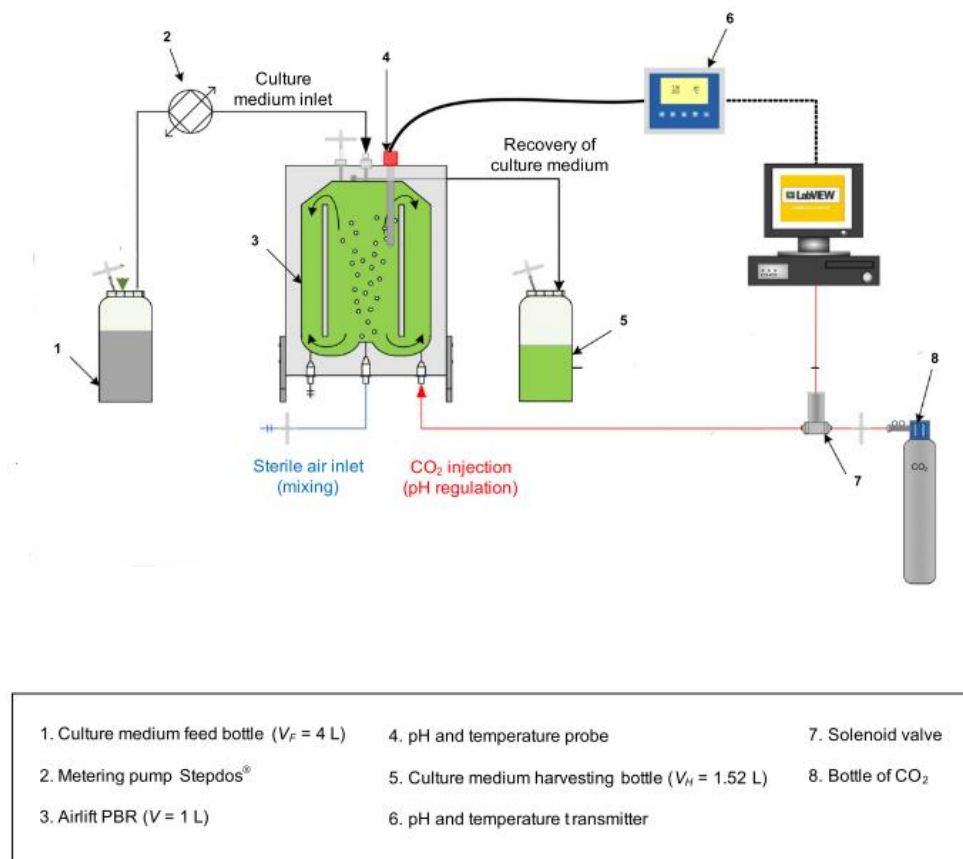


Figure 2.2 – Culture system in photobioreactor.

2 Extraction

2.1 Solvent choice

To choose the best suitable solvent, a list of ideal characteristics was summarized:

- (1) Low viscosity: low energy to mix the two phases
- (2) Low solubility in water: to avoid residual concentration after extraction
- (3) Relative density difference greater than 0.15: to ensure fast separation of the two phases
- (4) Low boiling point: limit energy consumption to back extract the β -carotene extracted
- (5) High molecular weight $>150\text{g/mol}$ and $\log P > 4$ is more biocompatible

Solvent	$\log P$	Molecular weight, M_w	Max. solubility in water (mg L^{-1})
Hexanol	2.03	102.174	5.90×10^3
Heptanol	2.62	116.201	3.27×10^3
Octanol	3.07	130.228	0.46×10^3
Hexane	4.00	86.175	9.80×10^3
Heptane	4.50	100.202	2.42×10^3
Octane	5.15	114.229	0.73
Nonane	5.65	128.255	0.17
Decane	6.25	142.282	1.50×10^{-2}
Dodecane	6.60	170.334	0.37×10^{-2}
Tetradecane	7.60	198.388	0.23×10^{-2}
Hexadecane	8.80	226.441	0.40×10^{-2}

Figure 2.3 – Solvent physicochemical characteristic (“CRC Handbook of Chemistry and Physics, 2009–2010, 90th ed.,” 2009).

Figure 2.3 summarizes the physicochemical properties of organic solvent used for extraction of lipids from microalgae (Zhang *et al.*, 2013). The *n*-decane has a viscosity of 0.838 mPa s at 25 °C (0.890 mPa s at 25 °C for water), low solubility in water ($1.50 \times 10^{-2} \text{ mg L}^{-1}$), a relative density of 0.70 (water density=1.0), a boiling point of 174 °C, a $\log P_{\text{oct}} > 5$. Although it is not suitable for

food or nutraceutical applications, it was primary used in the milking studies. In consequence *n*-decane is a good compromise regarding the five criteria.

2.2 Optimization of the extraction in Falcon

In the literature, solvent extraction has been implemented with solvent bubbling in the culture or by adding a static upper phase in the culture with or without an agitation. Here are the goals to set up an experiment (Figure 2.4) which: (1) perform the extraction separately from the cultivation step (2) on a small scale to quickly perform series and (3) with sufficient volume for the analysis (Figure 2.5 a).

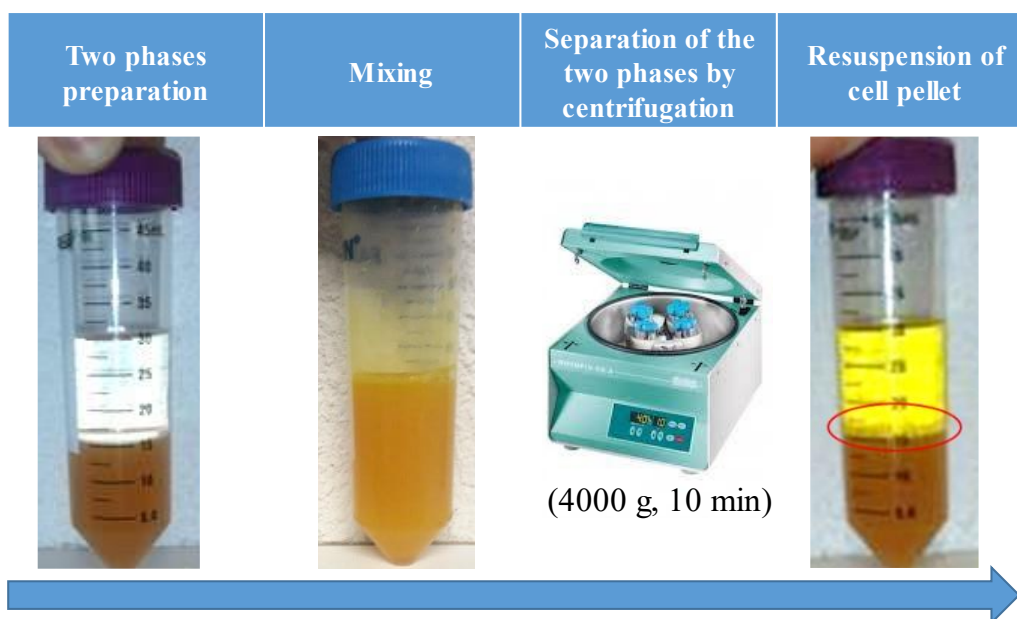


Figure 2.4 – Set up for extraction of β -carotene with organic solvent by stirring falcon tube on a vortex.

The Falcon tube was chosen as the container because it is widely used in scientific laboratories. Then, the vortex agitator was chosen to ensure reproducible agitation. To validate the model, an experimental plan has been developed with different sizes of tube, fillings of tube, solvent ratio

and agitation frequency (Figure 2.5b). The stirring time was arbitrary set at 2 min. The precise objective was to obtain sufficient agitation to ensure a significant extraction yield within a few minutes to achieve series.

a)

Planned analysis	Volume needed (mL/ sample)
Cell density	0,5
Pigments	0,5
Dry weight	5
Lipids	4
Total	10
Security margin	20%
Minimum volume	12 mL

b)

Falcon tube	25 mL	50 mL		
<i>Results</i>	-	+		
Solvent ratio	0,2	0,5	0,8	
<i>Results</i>	++	+	-	
Frequency	15 Hz	20 Hz	25 Hz	
<i>Results</i>	-	+	++	
Filling volume	24:50 mL	30:50 mL	40:50 mL	50:50mL
<i>Results</i>	+++	++	+	--

Figure 2.5 – The volume needed for analysis (a) Experimental plan to select operatory conditions of extraction in falcon tube (b).

The selected configuration is 50 mL Falcon tube, 0.5 solvent ratio, 25 Hz and a filling volume of 24 mL. The tube must contain air inside for the vortex flow to form and a solvent ratio of 0.5 give quite good apparent results with the yellowing of the *n*-decane. After stirring with the solvent, the emulsion was not separating itself within minutes, it was decided to centrifuge the tube to stop the contact between the two phases. After centrifugation, a non demixable emulsion remains at the interface of the two phases (Circled in red in Figure 2.4).

3 Analysis

3.1 Photosynthetic parameters

3.1.1 Oxygen production

To measure photosynthetic activity, the release of oxygen was measured using a Clark electrode (Figure 2.6). Nitrogen gas was bubbled to decrease the oxygen level. When the oxygen level rises, the data acquisition started recording. The curve was smoothed with a mean point every 10s. After 5 minutes, the light was turned off and data were recorded for another 5min. Oxygen production and oxygen consumption are obtained by linear regression of the oxygen concentration within the measurement chamber.

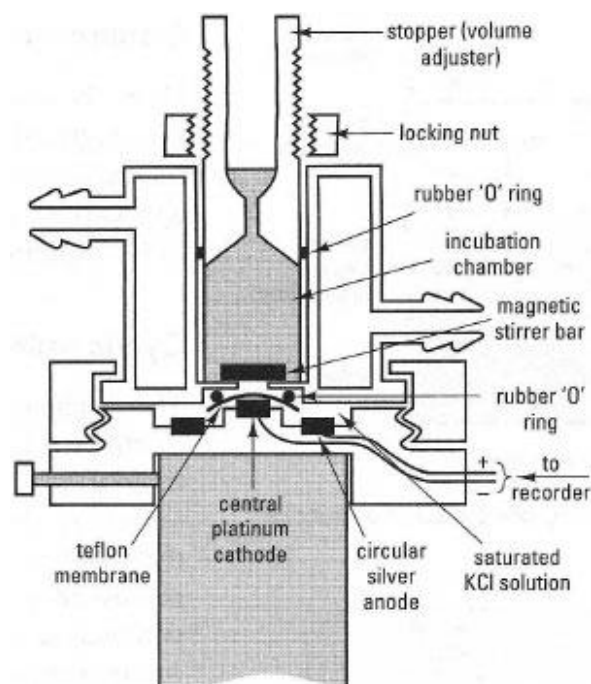


Figure 2.6 – Transverse section through a Clark (Rank) oxygen electrode (“Oxygen electrodes | Electroanalytical techniques,” n.d.).

3.1.2 Photosynthetic activity

In the chloroplast of cell, the chlorophyll pigment emits red light after the absorption of a photon. The fluorescence of chlorophyll can be used to quantify a stress under certain circumstances such as nutrient depletion or exposure to a toxic molecule. Far red light (λ of 735 nm, $10 \mu\text{mol m}^{-2} \text{s}^{-1}$) was applied to stimulate the activity of PSI.

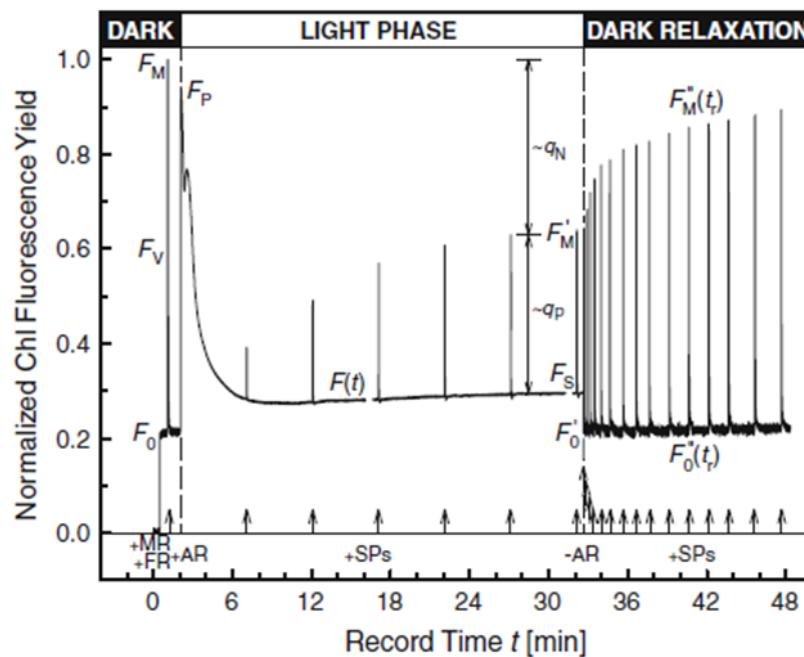


Figure 2.7 – Measurement of photosynthetic activity (Roháček, 2010).

To measure the minimum level of chlorophyll fluorescence, pulses of light are used (LED, PFD $< 0.1 \mu\text{mol m}^{-2} \text{s}^{-1}$, $3 \mu\text{s}$ or $1 \mu\text{s}$, 600Hz-100kHz, $\lambda < 670\text{nm}$). In the dark phase the fluorescence is called F_0 , in the dark relaxation phase it goes from F_0' to F_0'' .

The saturation pulses (halogen lamp, μs -scale, PFD $< 10,000 \mu\text{mol m}^{-2} \text{s}^{-1}$) make it possible to reduce Quinone A and the carriers of electrons and therefore to close all the reaction centers of

the PSII. The fluorescence intensity (FM, FM', FM'') is proportional to the number of acceptor / open centers (Figure 2.7).

3.2 β -carotene by spectrophotometry

To validate the protocol for measuring pigments by spectrophotometry, it is necessary to check that the extraction of the pigments by methanol is sufficient from the first exposure. β -carotene concentration in the methanol was measured using a double beam spectrophotometer Jasco V-530. For this purpose, 0.5 mL sample of cell culture at 1.2 g.L⁻¹ was centrifuged (4000g, 15°C, 10min), following this handling, the supernatant is carefully removed and replaced by 1.5ml methanol. The sample is passed through an ultrasonic bath and vortexed to break up the pellet and suspend the microalgae in 1.5mL of methanol (Sigma-Aldrich, >95%) at 44°C for 45min then centrifuged again and the absorbance of the supernatant was measured at 470 and 750nm. The β -carotene was quantified according to the equations of Lichtenthaler and Wellburn (1983), displayed as Equation 2.1, 2.2 and 2.3. According to Mojaat *et al.* (2008) the β -carotene represent the main carotenoid (>95%). Therefore, β -carotene concentration was approximated with total carotenoids concentration.

$$[\text{Chl.a}] = 15.65A_{666} - 7.3A_{653} \quad (\text{Eq. 2.1})$$

$$[\text{Chl.b}] = 27.05A_{653} - 11.21A_{666} \quad (\text{Eq. 2.2})$$

$$[\text{Car}] = (1000A_{470} - 2.05[\text{Chl.a}] - 114.8[\text{Chl.b}]) / 245 \quad (\text{Eq. 2.3})$$

After the pigment measurements, the samples are passed through the centrifuge to remove the supernatant. Then the extraction is performed again, this procedure is done once, twice or three times to assess the depletion of β -carotene in the biomass (Figure 2.8a). Results indicate

that 99.2% of β -carotene is extracted after the first cycle. In conclusion one extraction cycle will be used thereafter.

To access the possibility to store samples three storage conditions with methanol were tested and compared to direct extraction without storage. Biomass was directly at 44°C for 45 min, freeze at -12°C for 48h, put at 4°C for 45min or 4°C for 12h then each sample was incubated at 44°C for 45 min. Results summarized in Figure 2.8b suggest that no significant degradation happen during storage at -12°C for 48h, therefore sample can be store frozen before analysis.

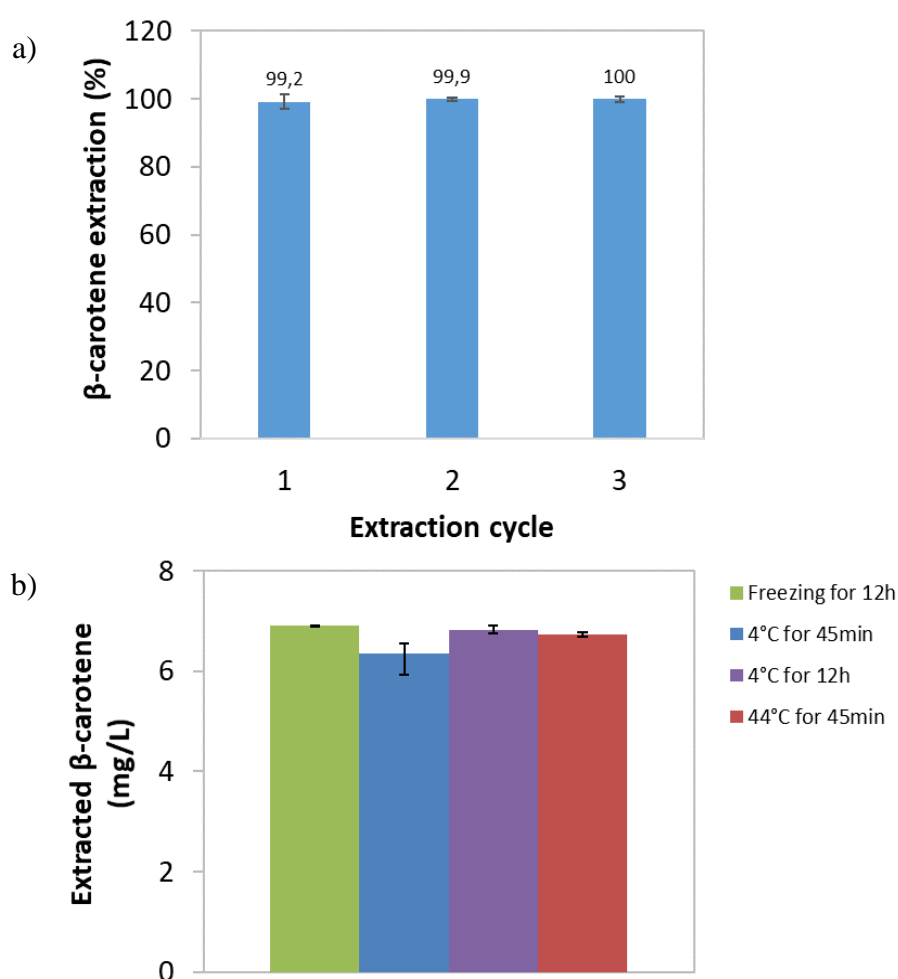


Figure 2.8 – Extraction of β -carotene with methanol. Effect of one, two or three extraction cycle on the extraction yield of β -carotene (a). Effect of incubating conditions with methanol on β -carotene extraction yield (b).

3.2.1 Mass balance with *n*-decane

To ensure that the β -carotene extracted from cells is effectively transferred in the solvent a mass balance for increasing extraction time was realized. The concentration of β -carotene was measured in cells as explained in the previous section. In the *n*-decane it was directly monitored with the absorbance at 480 nm. For that a calibration, with $R^2 > 0.99$, was made in the lab with commercial β -carotene (Sigma-Aldrich, >93%) (Figure 2.9a). The solubilization was achieved with sub saturation concentration below 5g/L.

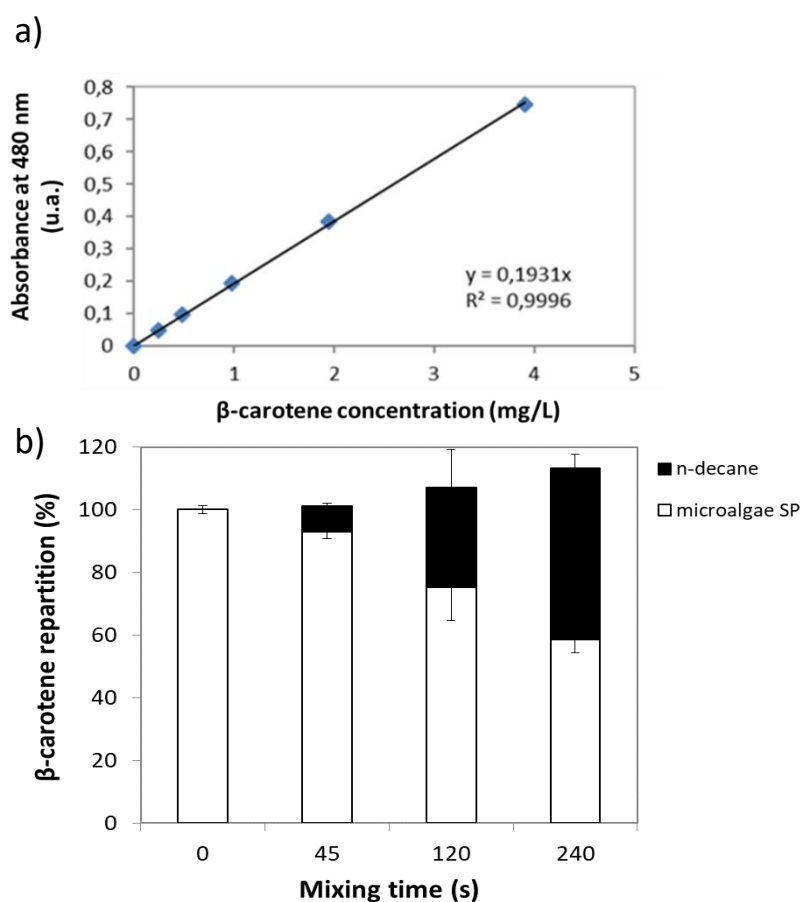


Figure 2.9 – The repartition of β -carotene between cells and the *n*-decane for increasing stirring time (a) and the calibration made in the lab for spectrophotometric measurement of β -carotene concentration in the *n*-decane, with $R^2 > 0.99$ (b).

The β -carotene extracted from biomass is recovered in the solvent (100%-110% of the mass), (Figure 2.9b). No significant loss of β -carotene was apparent ($p < 0.005$). Consequently, it can be considered to partition only between the inside of cells and the solvent phase. The emulsion or the supernatant (culture broth without cells) doesn't need to be considered for the mass balance of β -carotene.

3.3 Dry weight

Five mL of *D. salina* culture were filtered on pre-dried and pre-weighted fiberglass filters (Whatman GF / F, 0.7 μ m) using a Buchner funnel. To avoid overweighting due to salt crystallization; the filters were rinsed with 15ml of isotonic ammonium formate (100g L⁻¹, ACROS Organics, >99%), (Zhu and Lee, 1997). The filters were then dried in oven at 110°C for 24h, cooled in a desiccator for 10min and weighed (Sartorius, Secura).

3.4 Characterization of cell morphology

3.4.1 Counting chamber

Cell counting was performed on a Nageotte cell, this is a slide with a counting area of known depth (0.5 mm), (Figure 2.10). This cell is used for the purpose of counting microorganisms (under a microscope) using a grid engraved on the slide. Its use makes it possible to concentrate the cells by 2.5 compared to a Malassez cell. For example, for a culture at 3.10⁶ cells mL⁻¹ it reduces the number of images from 73 for Malassez cells to 25 to obtain 1600 cells. Natural settling or fixative agent concentrates the cells at the bottom of the counting chamber.



Figure 2.10 – Nageotte counting chamber.

The cell concentration must be in a certain range to have an accurate estimation: if the concentration is too low, the number of cells in the counting field may not be representative of the actual concentration in the stock solution. If the concentration is too high, then the cells may start to aggregate or overlap, leading to counting errors.

3.4.2 Cell fixation

Dunaliella salina cells which are motile have to be settle at the bottom of the slide in a homogeneous repartition to analyze cell density. In general, a fixative agent is added to the culture sample before pipetting the liquid in the counting chamber. Therefore, the effect of cell exposure with Lugol and Formaldehyde, two commonly used fixative, on the cell size and fluorescence were tested (Figure 2.11).

Lugol, a widely use solution, enters cells and fix to protein, this results in a freezing of cells that sink thereafter. However, the accumulation of Lugol hide the cell appearance because the cell become black and provoke a biggering in size after an exposure above 20 min (Zarauz and

Irigoien, 2008). Besides, Lugol is fluorescent which may cause interference in case of biological staining with fluorochromes. Formaldehyde is also commonly use and has the advantage to be transparent but is more toxic to the operator that Lugol, therefore precaution must be taken during the manipulation. No significant modification of cell size and fluorescence was observed (100%) with formaldehyde fixation at 2%.

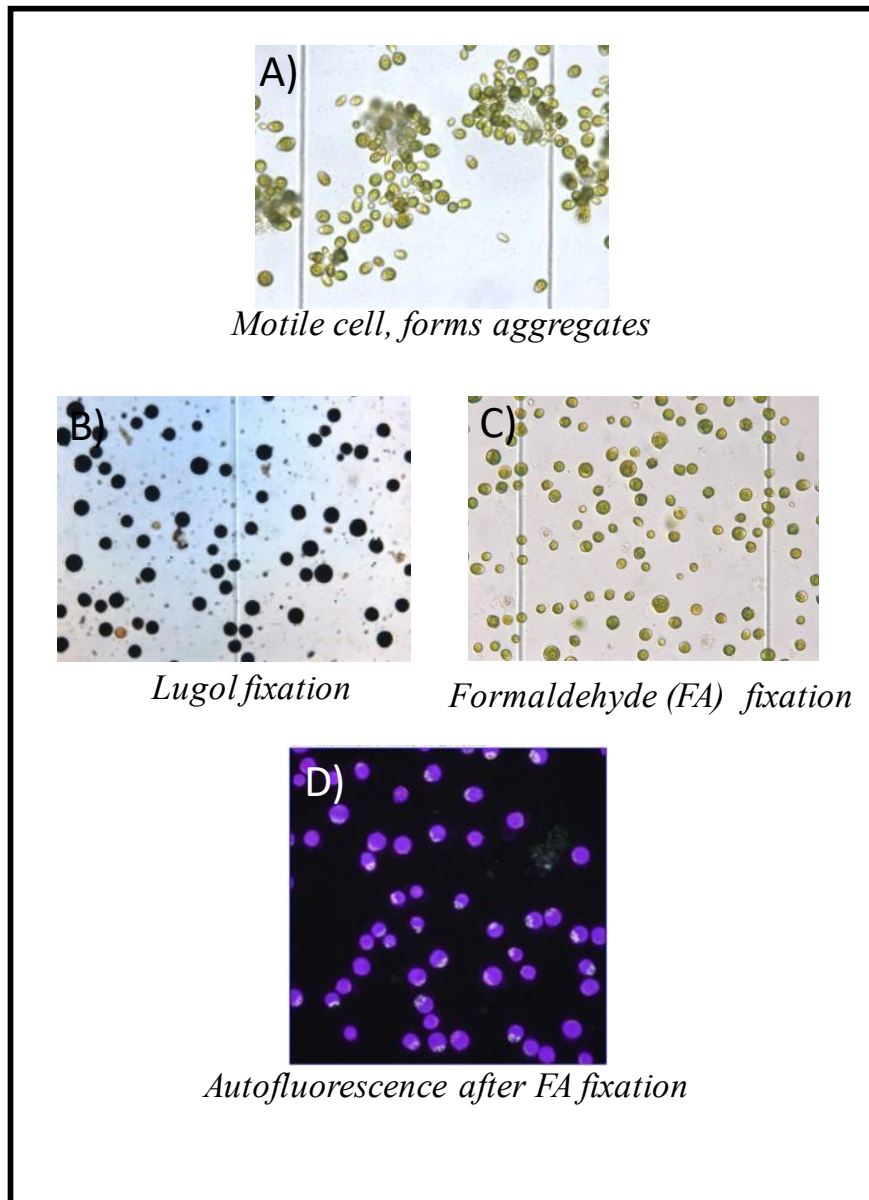


Figure 2.11 – Choice of fixative agents for cell counting size and fluorescence measurements of *Dunaliella salina*.

3.4.3 Automated particle analysis

It is possible to automate the counting of particles from photos previously taken under a microscope and analyzed with image processing software. To use these methods the sample volume in each photo must be constant. These techniques allow the concentration to be measured accurately (Appendix 1).

3.4.4 Digital imaging accuracy

An image is a matrix of digital numbers made up of small units called pixels (Figure 2.12). Each pixel is a value that can be converted to a square (in greyscale for example) to display the image. To activate a pixel a threshold of light must be reached. In the case of pictures taken with a microscope the 2D image is a representation of a real situation in 3D. Thus, a round shape is approximated by a certain number of pixels which are activated or not according to the camera threshold.

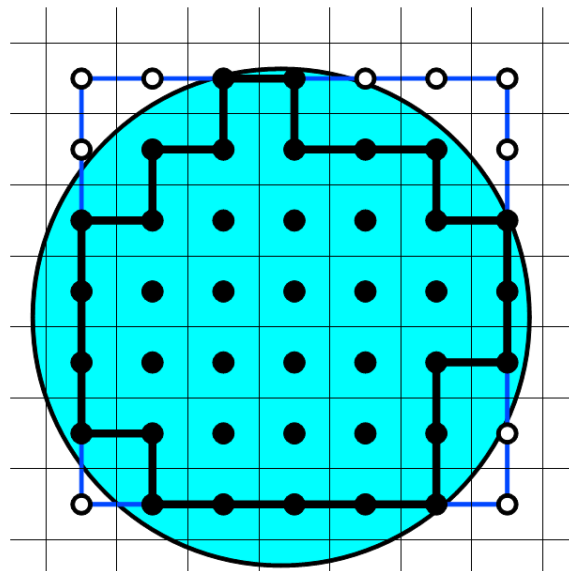


Figure 2.12 – Principle of pixel representation of a particle (INRA, 2021).

The resolution of an image corresponds to the number of pixels of the mesh which constitutes it, it corresponds to the fineness of spatial description. To measure small particles, an optical objective is used to reduce the optical field. The accuracy of measurement is given by the number of pixels per μm :

$$N_p (\text{px}/\mu\text{m}) = \text{Resolution} (\text{px}^2) * \text{Magnification} (\text{a.u.}) / \text{Optical field} (\mu\text{m}^2) \quad (\text{Eq. 2.1})$$

In theory the maximum measurement uncertainty on the diameter is 2 pixels. A resolution of $4\text{px } \mu\text{m}^{-1}$ (i.e. $0.5\mu\text{m}$ of uncertainty) results in an error of 20% for $5\mu\text{m}$ particles which is the smallest size of *D.salina* cells and therefore acceptable (Figure 2.13).

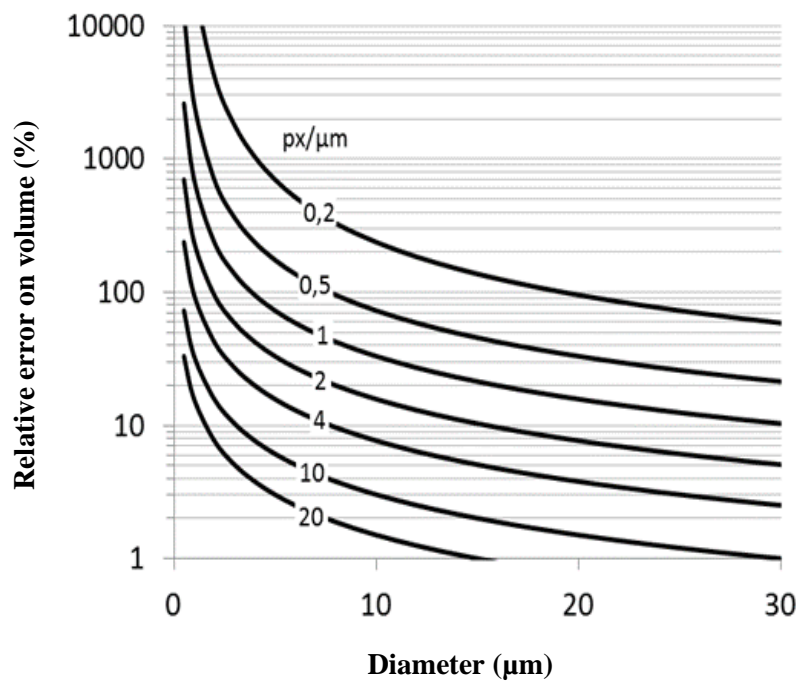


Figure 2.13 – Relative error on the estimation of cell volume regarding diameter for different resolution of image.

3.4.5 Size measurement

There is a wide variety of shapes and sizes of single-celled algae. Spherical and ovoid forms are quite common in microalgae. Since the cells settle on their cross section the shape obtained in the 2D projection allows the volume to be calculated. Nonstressed *Dunaliella* cells exhibit a prolate spheroid shape whereas the shape of stressed cells varies from oblong to spherical (Sun and Liu, 2003). Cells settle on their longitudinal section in the counting slide allowing the major axis (b) to be measured as the maximum Feret diameter and the semi-minor axis (a) as the minimum Feret diameter (Figure 2.14).

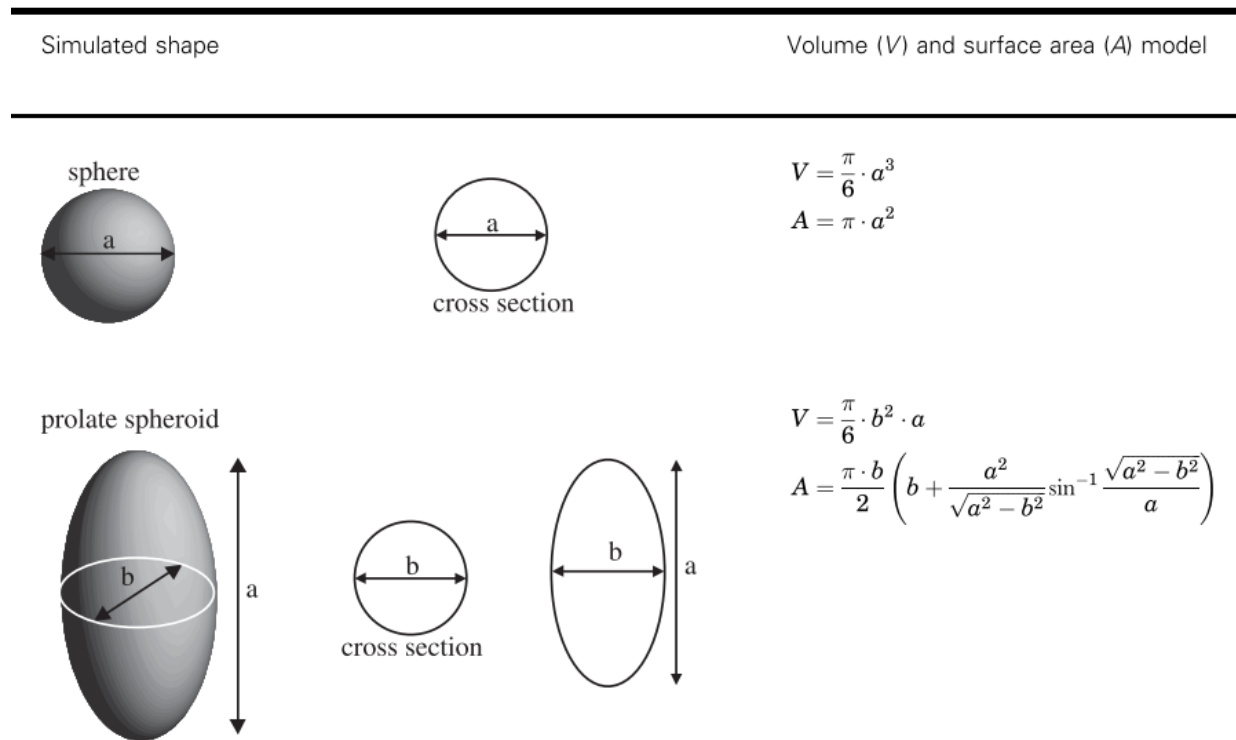


Figure 2.14 – Cell volume calculation from cross section for sphere and prolate spheroid shapes (Sun and Liu, 2003).

3.4.6 Shape factors

1) The aspect ratio makes it possible to characterize the shape anisotropy of the particle, i.e., its

elongation. Aspect ratio $RA = \frac{F_{min}}{F_{max}}$ (Eq. 2.2)

2) The compactness factor reflects the ratio of the area of the particle and the area of the smallest

rectangle that can contain it. Compactness factor $FC = \frac{A}{W*H}$ (Eq. 2.3)

3) The sphericity parameter highlights the difference between the shape of the particle compared

to a spherical particle. Sphericity $S = \frac{R_{in}}{R_{out}}$ (Eq. 2.4)

4) If the particles have a very irregular surface state, it is possible to use circularity (C).

Circularity $C = 4\pi\left(\frac{A}{p^2}\right)$ (Eq. 2.5)

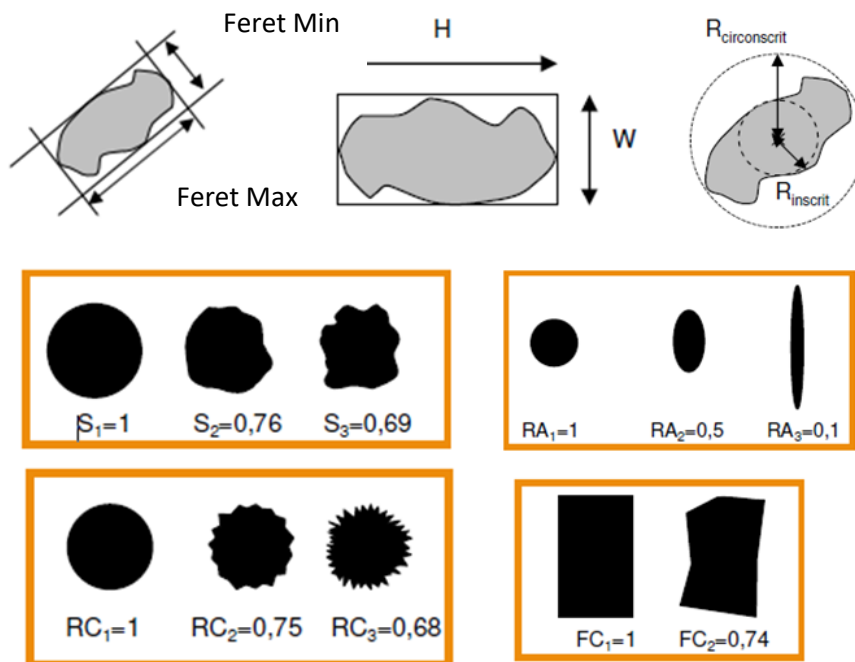


Figure 2.15 – The different size parameters of a particle and shape factors.

3.5 Biological activity

3.5.1 Enzymatic activity

Fluorescein diacetate (FDA) (Sigma Aldrich, >99% purity) was used to measure non-specific esterases activity. Esterases are hydrolase enzyme that splits esters into an acid and an alcohol. In the intracellular medium FDA is hydrolysed in fluorescein (excitation: 488nm, emission: 510nm) by non-specific esterases, which are produced by the respiratory activity of cells. Esterase activity is the most common way to measure the overall enzyme activity of cells. FDA is not fluorescent, and fluorescein fluoresces in green therefore fluorescence intensity represents the enzymatic activity. A stock solution of 5mg/mL of FDA in ethanol was prepared as indicated by the manufacturer. Separate samples of cells were incubated in the dark for 20 min with 5 μ L of the stock solution.

5-Cyano-2,3-Ditoyl Tetrazolium Chloride (CTC) (Sigma Aldrich, 99% purity) was used to evaluate cellular respiratory activity. This non-fluorescent dye freely penetrates cells and is absorbed via electron transport mechanisms and reduced with dehydrogenase into fluorescent insoluble formazan crystal (excitation: 488nm, emission: 630nm) by esterases. A stock solution of 5mg/mL of CTC in ethanol was prepared as indicated by the manufacturer. Separate samples of cells were incubated in the dark for 20 min with 5 μ L of the stock solution.

3.5.2 Permeability

Propidium Iodide (PI) is a small (660Da) hydrophilic dye that is unable to cross through intact cell membrane. Once in the cell it binds to DNA and fluoresces in red (excitation: 535nm,

emission: 625nm). A stock solution of 5mg/mL of PI (Sigma Aldrich, 99% purity) in distilled water was prepared as indicated by the manufacturer. Separate samples of cells were incubated in the dark for 20 min with 5 μ g/mL of the stock solution.

SYTOX green is a dye that only penetrates cell with compromised membrane integrity. Once in the cell it binds to DNA with a 500-fold increase in green fluorescence intensity (excitation: 502nm, emission: 523nm). Its spectral fluorescence properties allow its observations without interference from chlorophyll autofluorescence. A stock solution of 5mg/mL of Sytox Green in distilled water was prepared as indicated by the manufacturer. Separate samples of cells were incubated in the dark for 20 min with 5 μ g/mL of the stock solution.

Cell permeabilization with Evans blue dye (Sigma-Aldrich, >75%) was tested according to Hamer *et al.* (2002). To distinguish between irreversible and reversible permeabilization, Evans blue (EB) (120 μ l mL⁻¹ of solution in the cell culture) was added in three different conditions: (A) without treatment, (B) before the treatment, (C) after each solvent treatment time with *n*-decane (Luengo *et al.*, 2014).

3.5.3 Phase of cell division cycle

DAPI is used to determine the phase of cell division considering the amount of DNA in cell. DAPI is a dye that freely penetrates the membrane of intact cell. Once in the cell it binds to nucleic acids and fluorescence in blue (excitation: 358nm, emission: 461nm). A stock solution of 5mg/mL of DAPI (Sigma Aldrich, 99% purity) in acetone was prepared as indicated by the manufacturer. Separate samples of cells were incubated in the dark for 20min with 5 μ g/mL of the stock solution.

3.5.4 β -carotene fluorescence

The fluorescence of β -carotene was measured at 530nm with an excitation wavelength of 488 nm. In this flow cytometry experiment cell volume was estimated with the diameter and the shape of cells were considered as sphere. The stirring of n-decane on the β -carotene fluorescence in cells was studied regarding cell volume. The density plot of β -carotene content was estimated with the fluorescence intensity at 480nm (Kleinegris *et al.*, 2010b). Grown, stressed cells and stressed cells stirred for 120s with n-decane were compared.

Chapter 3.

*Effects of n-decane exposure on
metabolic activity of Dunaliella
salina*

1 Introduction

Microalgae have been identified as a promising resource for a wide spectrum of bioproducts for food, pharmaceutical, and cosmetic industries. Among the carotenoids family, the β -carotene molecules have properties of main interest: provitamin A, antioxidant and skin protection from UV damage (Gateau *et al.*, 2016). In contrast with synthetic products, natural β -carotene is extracted as a mixture of *cis*- and *trans*-isomers (Ben-Amotz *et al.*, 1988). The growing market of β -carotene, mostly natural, has risen the interest in extracting β -carotene from different natural sources (Scarsini *et al.*, 2020). Therefore, the economic viability of the β -carotene production and extraction from microalgae is a biotechnological challenge.

Indeed, microalgae are relatively slow growth micro-organisms (Darvehei *et al.*, 2018). The light availability inside the reactors is a major bottleneck for the industrialization of autotrophic production of microalgae (Pruvost *et al.*, 2016). In addition, carbon is mandatory for biomass production and for metabolites accumulation, thus these steps are separated in practice to improve overall efficiency. In current industrial processes, the pigment-enriched biomass is usually separated from water with technics like filtration, centrifugation and drying. Then, the targeted metabolites can be extracted, with organic solvent in the case of hydrophobic compounds. This biorefining strategy ultimately causes biomass losses and has high requirements in terms of time and energy (Hosseini Tafreshi and Shariati, 2009), (Vinayak *et al.*, 2015). It has been shown that it is possible in microalgae culture, to repeatedly extract hydrophobic metabolites *in situ* using immiscible organic solvents (Frenz *et al.*, 1989), (Vinayak *et al.*, 2015), (Atta *et al.*, 2016). Studies report that there was no significant toxicity of the solvent on the cell at the same time β -carotene was extracted (León *et al.*, 2003), (Mojaat *et al.*, 2008), (Kleinegris *et al.*, 2010a). In this case, a ‘milking’ could be envisioned provide cells are able to

synthesize *de novo* the metabolite that was extracted with the aim to extract them again. The circular use of matter might unlock saving of water and energy in bio production processes (Chaudry *et al.*, 2015).

To unlock the potential of microalgae and industrialize the production of high value substances the improvement of the productivity and the reproducibility of cultivation processes is mandatory (Guedes *et al.*, 2011). The understanding of the microalgal metabolism and production processes is therefore a key step. Environmental and toxicological studies of phytoplankton provide basic information on the toxicity of substances and treatments on microalgae (Adler *et al.*, 2007). Outside the laboratory conditions, the growth variability is caused by the non-homogeneous conditions, nutrient availability, competition and predation. In the laboratory conditions microbial culture still displays high heterogeneity in terms of growth rate and stress resistance. The most common method to monitor a culture is to measure an averaged characteristic of the population (cell density, dry weight, pigments content, photosynthetic activity) which may result in biased information not rendering the heterogeneity of the culture.

While many studies focus on solvent choice and extraction operating conditions, there is a lack of understanding about the impact of culture conditions on the single cell characteristics and *de facto* on the extraction biocompatibility. There is a general consensus that among the first measurable signs of cell death are the loss or reduction of membrane integrity and metabolic activity (Caron and Badley, 1995), (Hyka *et al.*, 2013). Therefore, the metabolic activity that quantifies vitality and the membrane permeability, the phase of cell division and the cell ability to pursue growth that quantifies the viability could influence single cell biocompatibility.

This study investigated the influence of *n*-decane exposure of *Dunaliella salina* on the single cell metabolic function that characterizes the viability and vitality. Cell density, oxygen production

and consumption, metabolic activity, membrane integrity and β -carotene fluorescence were monitored before and after extraction.

2 Materiel et methods

2.1 Strain and pre-culture

The green microalga *Dunaliella salina* CCAP 19/18 was cultivated in 500mL glass erlenmeyer fed with 200mL of Johnson growth medium modified according to Çelekli and Dönmez, (2006). Cultures were grown in a thermostated room ($20\pm 2^\circ\text{C}$) under a continuous photon flux density ($35\pm 5\mu\text{mol m}^{-2} \text{s}^{-1}$) and agitated manually once a day. The cultures were subcultured in fresh medium every four weeks to reach a cell density, and a dry weight of *circa* $2.1 \cdot 10^6 \text{ cell mL}^{-1}$, $0.70\text{g}_{\text{DW}} \text{ L}^{-1}$. This culture condition is referred as grown in erlenmeyer (GE).

To trigger β -carotene accumulation, GE cells were harvested in sterile Falcon tube, centrifuged ($6000\times g$, 10°C , 10min), resuspended in a glass erlenemeyer in the same medium but free of nitrogen (nitrogen depleted medium) and continuously illuminated from the bottom by using a photon flux density (PFD) of $800\mu\text{mol m}^{-2} \text{s}^{-1}$ provided by LED panels (neutral white, 4000–4500K) for four weeks to reach a cell density, a dry weight and a mean volume of *circa* $9.7 \cdot 10^5 \text{ cell mL}^{-1}$ and $0.63\text{g}_{\text{DW}} \text{ L}^{-1}$. Cells cultivated under these conditions are referred as stress in erlenemeyer condition (SE).

2.2 In-situ mixing experiment

Cells were mixed with n-decane for 120s to provoke a long exposure to the solvent. Cell culture was exposed to n-decane (ACROS Organics, >99%) in 50mL Falcon tube. Microalga culture

concentration was adjusted with fresh medium to reach 0.63-0.70g_{DW} L⁻¹ and then mixed with *n*-decane (1:1 v/v) for 120s using a vortex (Fischerbrand) vibrating at 25Hz. The Falcon tubes were then immediately centrifuged (4000xg, 15°C, 10min), then the pellet was resuspended in the same media resulting in the recovery of three phases: the lower aqueous phase (residue), the upper organic phase (extract) and a stable emulsion at the interface. The biomass was analyzed before and after extraction for each characterization methods.

2.3 Characterization of the impact on cell biology

2.3.1 Growth ability after extraction

After the mixing with *n*-decane for 120s, 50mL of stressed culture residue was reinoculated in 500mL erlenmeyer that contained 150mL of culture medium. Cultures were grown in a thermostated room (20±2°C) under a continuous photon flux density (35±5μmol m⁻² s⁻¹). Two conditions were tested, growth in nitrogen depleted and nitrogen repleted medium. The experiment was carried in triplicate. The behaviour of the culture was qualitatively analyzed after 2 weeks.

2.3.2 Oxygen production and consumption

Oxygen productivity is widely used as an indicator to measure photosynthesis in microalgae, as such it is also used to detect stress conditions that have impaired photosynthesis. To measure photosynthetic activity, the release of oxygen was measured using a Clark electrode. A volume of 1.5ml of culture was introduced into the chamber and 30μl of 0.2M NaHCO₃ was added to ensure sufficient carbon concentration for photosynthesis. The culture media was diluted if needed to adjust the cell density to 5 10⁵ cell mL⁻¹ for each sample tested. The intensity was set

to culture intensity conditions i.e., 400 μ E/m²/s for growth and 800 μ E/m²/s for stress. Nitrogen gas was bubbled to decrease the oxygen level up to 5mg/L for GE and 2mg/L for SE. When the oxygen level rises, the data acquisition started recording. The curve was smoothed with a mean point every 10s. After 5 minutes, the light was turned off and data were recorded for another 5min. As expressed in Equation Oxygen production and oxygen consumption (P) were obtained by linear regression of the oxygen concentration [O₂]_t between t=0 and t=5min with $\Delta t=5$ min and $C_x=5 \cdot 10^5$ cell mL⁻¹.

$$P(\mu\text{g}/\text{cell}/\text{s}) = ([\text{O}_2]_{t=0} - [\text{O}_2]_{t=5\text{min}}) / (\Delta t * C_x * 1000) \quad (\text{Eq 3.1})$$

2.3.3 Enzymatic activity

Fluorescein diacetate (FDA) (Sigma Aldrich, >99% purity) was used to measure non-specific esterases activity. Esterases are hydrolase enzyme that splits esters into an acid and an alcohol. In the intracellular medium FDA is hydrolysed in fluorescein (excitation: 488nm, emission: 510nm) by non-specific esterases, which are produced by the respiratory activity of cells. Esterase activity is the most common way to measure the overall enzyme activity of cells. FDA is not fluorescent, and fluorescein fluoresces in green therefore fluorescence intensity represents the enzymatic activity. A stock solution of 5mg/mL of FDA in ethanol was prepared as indicated by the manufacturer. Separate samples of cells were incubated in the dark for 20 min with 5 μ L of the stock solution. The fluorescence was measured in the whole culture (cell + media) and in the supernatant of the centrifuged culture. The 100% reference was fixed with grown cells and 0% reference was set to 0 fluorescence intensity.

5-Cyano-2,3-Ditolyl Tetrazolium Chloride (CTC) (Sigma Aldrich, 99% purity) was used to evaluate cellular respiratory activity. This non-fluorescent dye freely penetrates cells and is absorbed via electron transport mechanisms and reduced with dehydrogenase into fluorescent

insoluble formazan crystal (excitation: 488nm, emission: 630nm) by esterases. A stock solution of 5mg/mL of CTC in ethanol was prepared as indicated by the manufacturer. Separate samples of cell culture were incubated in the dark for 20 min with 5 μ L of the stock solution.

2.3.4 Permeability

Propidium Iodide (PI) is a small (660Da) hydrophilic dye that is unable to cross through intact cell membrane. Once in the cell it binds to DNA and fluorescence in red (excitation: 535nm, emission: 625nm). A stock solution of 5mg/mL of PI ((Sigma Aldrich, 99% purity))in distilled water was prepared as indicated by the manufacturer. Separate samples of cells were incubated in the dark for 20 min with 5 μ g/mL of the stock solution. The fluorescence was measured in the whole culture (cell + media) and in the supernatant of the centrifuged culture. The reference was fixed to 100% for cell culture with acetone treatment and 0% was set to 0 fluorescence intensity.

SYTOX green is a dye that only penetrates cell with compromised membrane integrity. Once in the cell it binds to DNA with a 500-fold increase in green fluorescence intensity (excitation: 502nm, emission: 523nm). Its spectral fluorescence properties allow its observations without interference from chlorophyll autofluorescence. A stock solution of 5mg/mL of Sytox Green in distilled water was prepared as indicated by the manufacturer. Separate samples of cells were incubated in the dark for 20 min with 5 μ g/mL of the stock solution.

2.3.5 Phase of cell division cycle

DAPI is a dye that freely penetrates the membrane of intact cell. Once in the cell it binds to nucleic acids and fluorescence in blue (excitation: 358nm, emission: 461nm). A stock solution of 5mg/mL of DAPI (Sigma Aldrich, 99% purity) in acetone was prepared as indicated by the

manufacturer. Separate samples of cells were incubated in the dark for 20min with 5 μ g/mL of the stock solution.

2.3.6 β -carotene fluorescence

The fluorescence of β -carotene was measured at 530nm with at excitation wavelength of 488 nm. In this flow cytometry experiment cell volume was estimated with the diameter and the shape of cells were considered as sphere. The stirring of n-decane on the β -carotene fluorescence in cells was studied regarding cell volume. The density plot of β -carotene content was estimated with the fluorescence intensity at 480nm (Kleinegris *et al.*, 2010b). Grown, stressed cells and stressed cells stirred for 120s with n-decane were compared.

2.4 Instrument for fluorescence measurement

2.4.1 Spectrofluorimetry

A spectrofluorometer (Fluoromax, Horiba) was used to measure the fluorescence intensity after staining. This method quantifies the average fluorescence intensity over the microalgae in suspension in the media. This experiment was realized at the Maine University.

2.4.2 Epifluorescence microscopy

For enzymatic activity, permeability and DNA content one optical field was picture in bright field and epifluorescence field (in the corresponding wavelength) to realize the single cell measurement of fluorescence intensity. To immobilize the algae culture aliquots were stirred (500:50 v/v) with a solution of paraformaldehyde (PF) in phosphate buffered saline (137 mM NaCl, 2.7 mM KCl, 10 mM Na₂HPO₄, 1.8 mM KH₂PO₄ at pH=7.4). This procedure did not

affect their morphology nor their colour (Hyka *et al.*, 2013). The bright field pictures (16bit) were transformed into B/W ones (2bit) using the Image J software (<https://imagej.nih.gov/ij/>, National Institutes of Health), which were then subjected to particle analysis using a default ImageJ routine. Briefly, cell debris and other small particles were first automatically removed from the analysis by setting the 'cell area' parameter to the range 20-400 μm^2 and by manual sorting. The bright field microscopy image analysis results in region of interest (ROI) which are closed regions corresponding to cell boundaries. The ROI were then applied to the fluorescence picture for the measurement of the mean fluorescence of each cell. The fluorescence level was then normalized between the minimal and maximal value obtained.

2.4.3 Flow cytometry

Data obtained from flow cytometry instruments were sorted with a gating strategy to remove unwanted event. In the case of microalgae, the aim is to obtain focused single cells that contain chlorophyll (Figure 3.1).

Cells out of focus in the picture are not suitable for analysis because the apparent value of size and fluorescence are not correct. Cell out of focus had roots mean square gradient value above 45 units and only 81.1% of cells were kept. Thereafter cells were discriminated by aspect ratio regarding area to remove the 17,4% of clumped cell (colony, flocs). Finally, out of the remaining cells 94.2% of them contained chlorophyll. The gating strategy kept 63.1% of cells. Within 5min 1892 cells were analysed out of the 3000 events pictured.

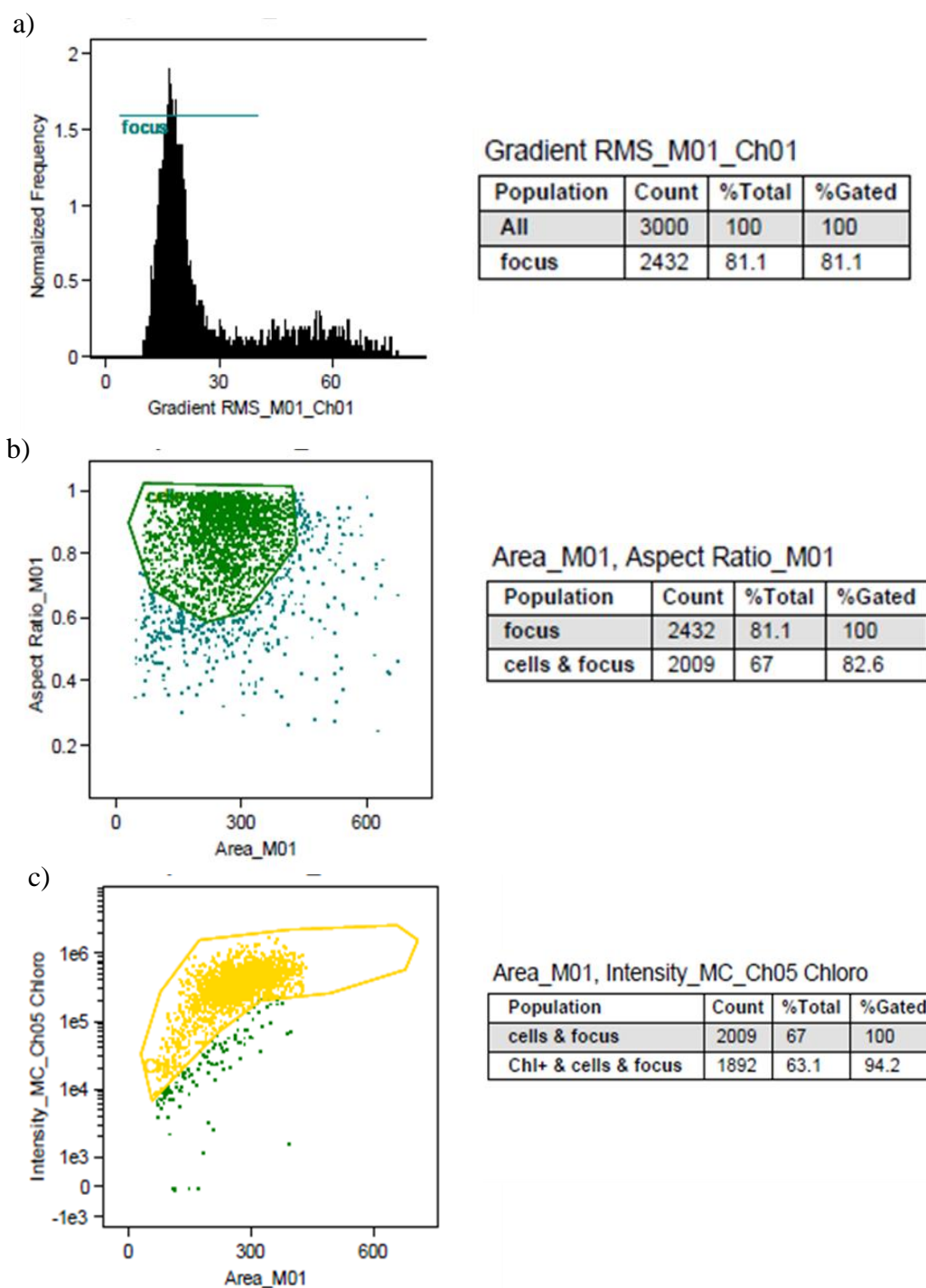


Figure 3.1 – The gating strategy in cytometric analysis. Cells outside the focus were not considered (a), isolated cells were analysed (b), cells with a chlorophyll content were kept (c).

2.5 Statistics

2.5.1 Population analysis

The percentage of fluorescence $F(\%)$ was calculated as the difference in fluorescence intensity between the culture F_{culture} and the supernatant F_{sn} divided by the fluorescence intensity of the arbitrary reference F_{ref} multiplied by 100.

$$F(\%) = (F_{\text{cell}} - F_{\text{sn}}) / F_{\text{ref}} * 100 \quad (\text{Eq 3.2})$$

For the results expressed on the population level for experiments that analyses the single cell fluorescence intensity. The sum of all individual cell intensity was used.

2.5.2 Single cells analysis

The metabolic activities (namely Sytox green permeability, DNA content and enzymatic activity) of each cell referred as MA (%) were calculated using the single cell fluorescence intensity F divided by the difference between the maximum fluorescence intensity F_{max} and the minimum fluorescence intensity F_{min} .

$$\text{MA} (\%) = F / (F_{\text{max}} - F_{\text{min}}) * 100 \quad (\text{Eq 3.4})$$

Cells were classed in 10% metabolic activity class width distribution.

The cell frequency in the class x $CF_x (\%)$ was calculated as the number of cells in the class x NC_x divided by the total number of cells before extraction TC_0 . This calculation renders the abundance of cell in each class considering the variation of cell density.

$$CF_x (\%) = NC_x / TC_0 \quad (\text{Eq 3.5})$$

3 Results and discussion

3.1 Characterization of the microalgae population

3.1.1 Photosynthetic oxygen production and respiration

In the absence of solvent exposure, stressed cells had lower specific oxygen productivity under light and higher consumption of oxygen rate in the dark than grown cells. The increase in oxygen consumption in the dark with stressful culture conditions compared to growth conditions was also reported by Lv *et al.* (2016). This can be explained metabolically by a more active respiratory system.

Exposure of *Dunaliella salina* to *n*-decane caused a decrease in oxygen production of 4% and 20% respectively for grown and stressed cells. In the dark, the oxygen consumption was also reduced by 25% for grown cells. The experiment showed that in the dark the oxygen concentration in the clarck electrode kept increasing for a long time for stressed cultures after solvent exposure, therefore, the measurement was not possible for this condition. However, this method of viability measurement after exposition to organic solvent must be discussed. The solubility of oxygen is higher in *n*-decane than in water, thus considering that the *n*-decane was balance with oxygen in the air the exposure to *n*-decane could have increase the oxygen in the medium. As results only show a decrease in oxygen thus the viability can only be underestimated.

León *et al.* (2003) showed a stimulation of the photosynthetic oxygen production activity of 111% after 15 min stirring with 5% of decane. In the previous study, cells grew at $100\mu\text{mol m}^{-2} \text{s}^{-1}$ and oxygen production was tested at $1500\mu\text{mol m}^{-2} \text{s}^{-1}$ whereas in our study, analysis were carried out at the same irradiance than the culture. Interestingly, Hejazi *et al.*, (2002) found that

the averaged oxygen productivity of cells grown between 24h and 96h in the presence of 12% *n*-decane was almost decrease by 100% at $350\mu\text{mol m}^{-2} \text{s}^{-1}$. Considering results from the two previous studies it can be concluded that low concentration and short exposure stimulated the cell and long-term exposure had high toxic effect on cells. Results from this work showed that high concentration and short exposure slightly inhibited cells. In fact, this conclusion is consistent with what is reported in the literature, for a review, see Miazek *et al.*, (2017).

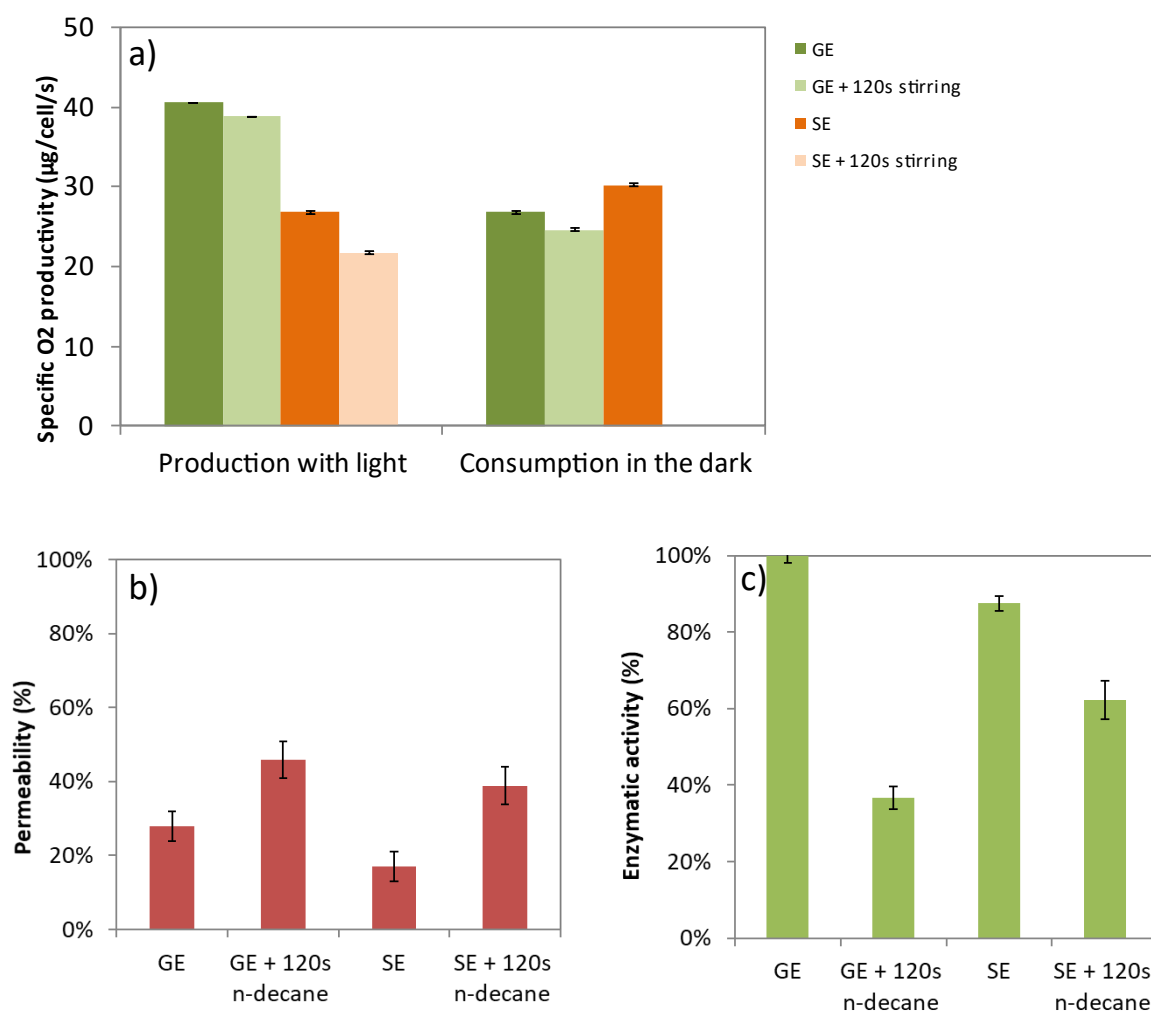


Figure 3.2 – Effect of *n*-decane stirring on the oxygen productivity (a), on the permeability (b) and on the enzymatic activity (c) of *Dunaliella salina* with and without *n*-decane stirring for 120 s for cells grown in erlenmeyer (GE) and stressed in erlenmeyer (SE).

3.1.2 Cell permeability to Propidium Iodide

Cell permeabilization was measured on cells that undergo 120s exposure to *n*-decane (Figure 3.2). The 0% value was set with 0 f.u. and 100% was arbitrary set with the value obtained with acetone exposure in each stress state. In the absence of the *n*-decane mixing, the natural permeability was lower in stressed cells (16%) than in grown cells (26%). The exposure of grown cells to *n*-decane for 120s increased the permeability by a factor two. It reached 50% permeability after agitation with solvent. Likely, stressed cells exhibited a 22% increase in permeability after mixing with *n*-decane.

In this experiment, two sources of free DNA could induce a background noise to the DNA present in the cell: (i) there is free DNA in the fresh culture coming from cell that died naturally and (ii) there is a released of DNA materials into the media after cell destruction by the solvent. For that purpose, the fluorescence was measured in the supernatant and in the resuspended cell in the fresh and in the treated culture. This induced a lot of laboratory operations that are time consuming. Therefore, this limits the use of the spectrofluorometer to measure the permeability of a cell population.

One of the drawbacks of staining with propidium iodide is the overlap of chlorophyll autofluorescence and PI emission spectrum (Hyka *et al.*, 2013). Nevertheless, it has been used to measure cell viability of *Chlorella vulgaris* after exposure to pulsed electric field where the authors do not describe any interference or quenching with autofluorescence (Luengo *et al.*, 2014). However, cell destruction was less important with the use of pulsed electric field than with stirring with *n*-decane.

3.1.3 Enzymatic activity

Enzymatic activity was measured on cell subjected to 120s *n*-decane mixing (Figure 3.2). The enzymatic activity was arbitrary set at 100% for the fresh green culture and 0% was arbitrary set for 0 u.a. in fluorescence intensity. As expected, the untreated stressed culture had a lower enzymatic activity (of 17%) than grown cells. Brookes *et al.*, (2000) showed that nitrogen concentration of 0, 2 and 5 μ M in the culture media of the cyanobacteria *Microcystis aeruginosa* results in a 50% to 30% decrease in the FDA conversion rate (fluorescence cell⁻¹ min⁻¹) after 6 days of cultivation compared to a concentration of 50 μ M.

Exposing the grown culture to *n*-decane for 120s decreased the esterases activity of the remaining cells by 63%. This could be the result of a deterioration of the enzyme production chain or the breakage of the enzymes themselves. For stressed cells, the enzymatic activity of the remaining cells decreased by 26%.

Microscope observation (data not shown) showed the leakage of green liquid from the cell that correspond to fluorescein and not chlorophyll. In fact, FDA can passively enter through the cell membrane. When hydrolysed the resulting fluorescein is only retained by intact membranes (Garvey *et al.*, 2007). Thus, for the measurement of enzymatic activity a fluorochrome that is retained in permeabilized cells is preconized.

3.1.4 Growth after solvent exposure

In order to repeatedly extract β -carotene from *Dunaliella salina*, cells need to be able to accumulate the metabolite again. Previous results showed that the mixing with *n*-decane provoke a decrease in cell density. In a stable loop cell would need to grow to compensate the loss in cell density. Therefore, SE cells were reinoculated in erlenmeyer in nitrogen depleted medium and

repleted medium to qualitatively show the reaccumulation and growth ability. Results showed that no reaccumulation happened in nitrogen depleted medium because of cell death. Growth was possible in nitrogen repleted medium and cells turned green. In conclusion, after mixing with n-decane cells need to be in growth conditions before undergoing another stress phase.

Condition after mixing with solvent	Growth ability	Observations
Nitrogen depleted	-	Bleaching of the culture
Nitrogen repleted	+	Growth happened, cells turned green

Figure 3.3 Growth ability of stressed cells in erlenmeyer (SE) after n-decane mixing for 120s in nitrogen depleted and nitrogen repleted medium.

3.2 Single cell characterization

3.2.1 Cytometry measurements with fluorescein

The measurement of esterases activity of cells stained with fluorescein diacetate (FDA) showed the presence of two categories of cells: cells with lower enzymatic activity (FDA+) and cells with higher enzymatic activity (FDA++), (Figure 3.4a). There was a slight trend of higher enzymatic activity with larger forward side scatter (FSC). The stirring with *n*-decane for 120s clearly decreases the enzymatic activity of the FDA++ subpopulation and increase the cell abundance in the FDA+ category from 16% to 37% (Figure 3.4b).

Fachet *et al.*, (2016) showed that in *Dunaliella salina* stressed with high light and nitrogen depletion and after 7 days of cultivation, two separate subpopulations were detected; approximately 50% of the culture emitted a lower fluorescent signal than the other half. They

also reported a strong cell breakage and lipid particle release. The authors presented two possible explanations: (i) the long-lasting stress could lead to a reduced esterase enzyme activity, (ii) the permeabilization of the mitochondrial or cell membranes could lead to an outflow of converted fluorescein from the cells. Therefore, the decrease in fluorescence intensity observed in our study could also be explained by a leakage of converted fluorescein in the media due to cell disruption.

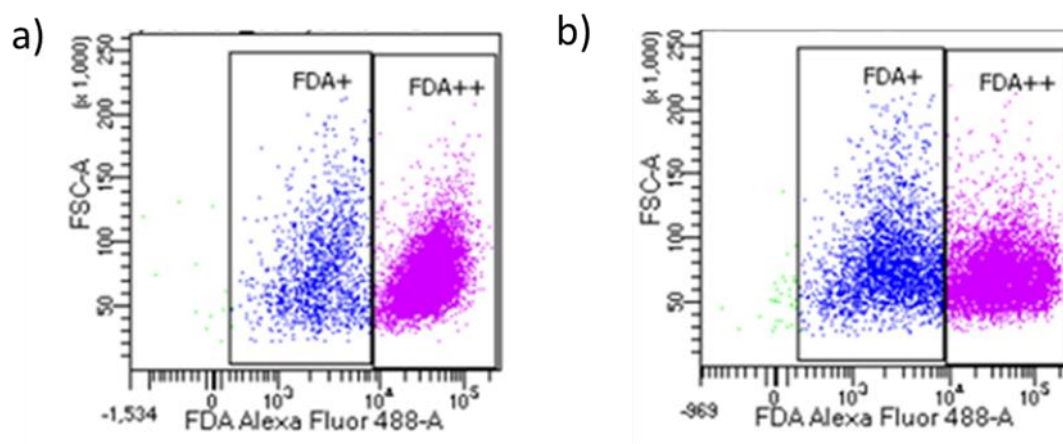


Figure 3.4 – Effect of n-decane stirring on esterases activity of stressed cells in erlenmeyer (SE). Cytogram of untreated stressed cells (a) and stressed cells exposed to 120s n-decane stirring (b). Cells were stained with fluorescein diacetate (FDA).

3.2.2 Epifluorescence measurement with CTC

Bright field and fluorescence of grown cells staining with CTC is shown in Figure 3.5a-b. Cells without mixing present a low and steady level of red fluorescence. Without mixing, cells approximately follow a normal distribution with a maximum of 30% of cells around 30% of enzymatic activity.

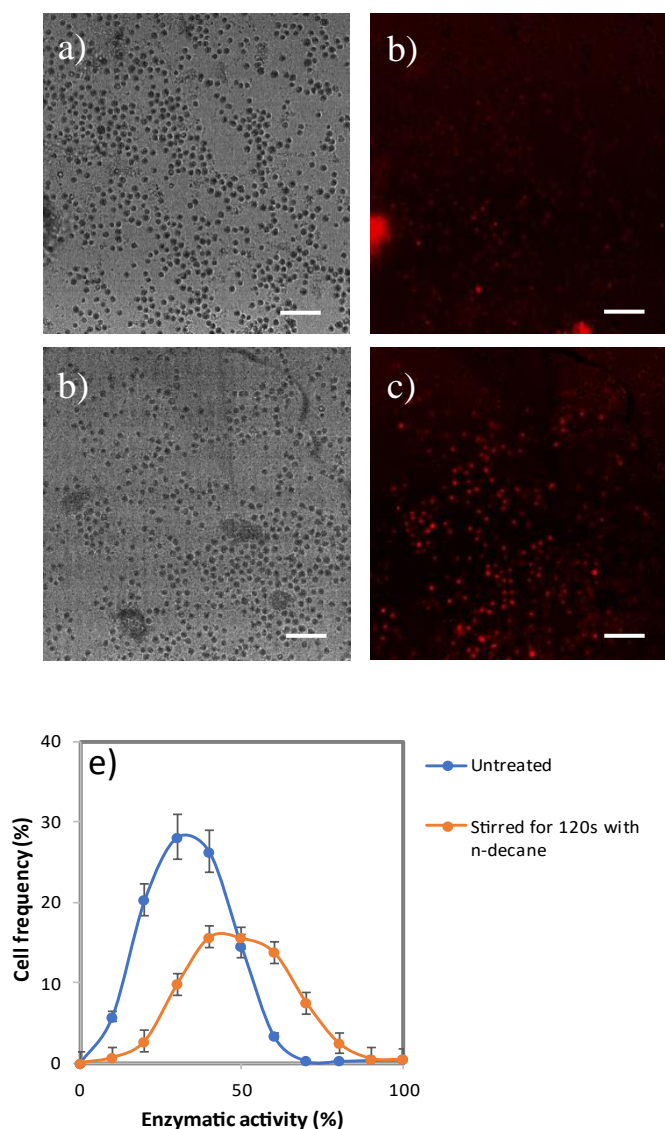


Figure 3.5 – Bright field picture of *Dunaliella salina* untreated stressed cell (a,b) and after 120s stirring with *n*-decane (c,d). Enzymatic activity of *Dunaliella salina* is indicated by the blue fluorescence intensity of CTC (formazan) (b,d). Scale bars in white indicate 50 μm. The normalized enzymatic activity distribution is plot in cell frequency (e).

After the stirring of cells with *n*-decane for 120s (Figure 3.5c-d), the cell density dropped by 53%. The enzymatic activity of the surviving cells shifts to a higher value and increases by 20% on average. Tashyreva *et al.*, (2013) observed that after breakage of colonies into fine suspension, the polar cells of the filaments turn SYTOX Green-positive, and accumulate higher amounts of CTC-formazan, apparently due to injuries to their plasma membranes. The use of CTC is

demonstrated to work on environmental study but might be biased by treatment that increase cell permeability. Therefore, three hypotheses remain: the exposure to *n*-decane increases the exchange of material across membranes that results in a stimulation of the metabolic activity (i), the increase of permeability increases the penetration of dye (ii) or the presence of holes in the membrane increase the diffusion of light through the membranes (iii).

3.2.3 Single cell permeability with Sytox Green

GE cells stained with SYTOX Green are pictured in Figure 3.6. Sytox green is supposed to enters only cells that are permeabilized. A lot of cells without treatment were emitting green fluorescence, therefore, the natural permeability of cells was elevated. Without mixing, cells approximately follow a normal distribution of SYTOX Green fluorescence intensity with a maximum of 25% of cell around 50% permeability. Therefore, the permeabilization state is heterogenous, this is probably due to the not well controlled culture condition in erlenmeyer. After the stirring of cells with *n*-decane for 120s, the cell density dropped by 53%. The quantity of cell below 20% permeability remain equal, one can say that the threshold for permeabilization could be set at 20%. Above the threshold, the higher the permeability the lower the survival rate, cells with permeability higher than 50 % were preferentially disrupted by the exposition to *n*-decane. Organic solvent is known to create pore in the membrane thus on a cell naturally-permeabilized the contact of a separate droplet will increase permeabilization and the threshold for phase toxicity will be reached easily (Sikkema *et al.*, 1995). Cell above 80% of permeability are as numerous, possibly due to an increase in permeability of some of the surviving cells.

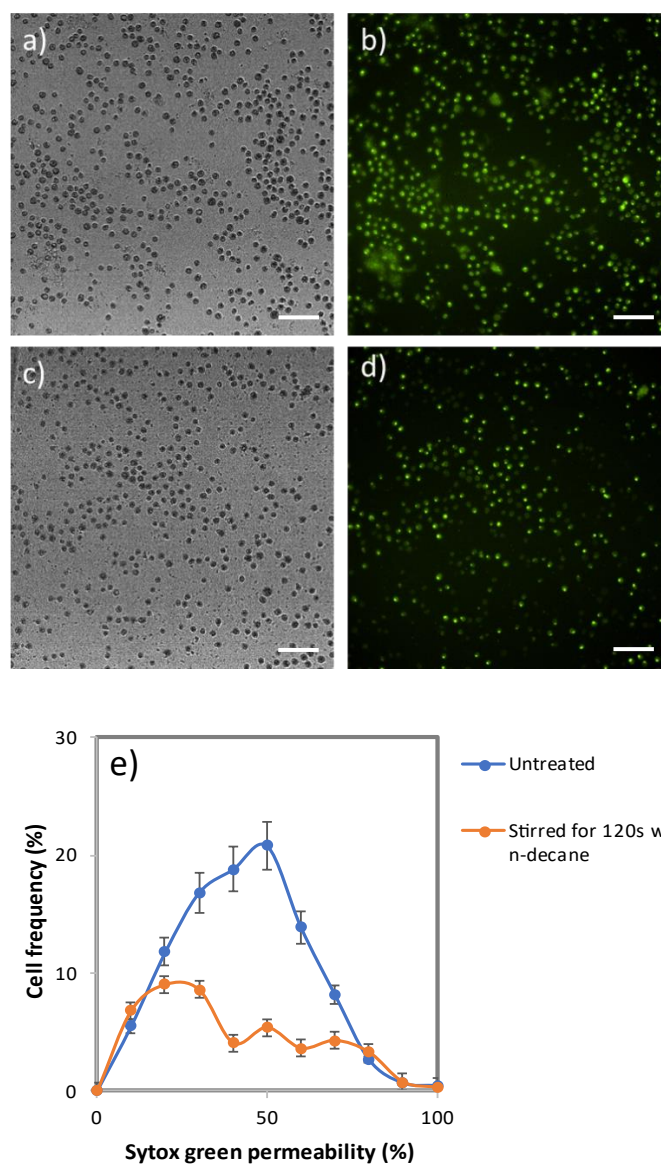


Figure 3.6 – Bright field picture of *Dunaliella salina* untreated stressed cell (a,b) and after 120s stirring with n-decane (c,d). Permeability of *Dunaliella salina* to Sytox Green is indicated by the green fluorescence intensity (b,d). Scale bars in white indicate 50 μ m. The normalized permeability distribution is plot in cell frequency (e).

3.2.4 Cell cycle analysis

GE cells stained with DAPI are pictured in Figure 3.7. Bright field and epifluorescence field pictures showed that cells stained with DAPI fluoresced differently: some from the whole cell, others from a large part of the cells and others from the cytoplasm near the flagella. This

repartition of the fluorescence in *Dunaliella salina* cells stained with DAPI is similar to the one in *Chroococcidiopsis* obtained by Tashyreva *et al.* (2013). The fluorescence of DAPI is proportional to the DNA content of the cell. Normally the fluorescence intensity curve allows to distinguish the three phases of the cell division cycle: a high peak corresponding to the growing cells (phase G1), then a low steady phase corresponding to the replication of DNA (phase S) and moderate peak corresponding to the preparation of cell division (phase G2).

Without mixing cells, the G1 peak is present among most of the curve, only a small shoulder is visible around 70% of DNA content. This curve shape is similar to the one of the diatom *Chaetoceros calcitrans* (Veldhuis *et al.*, 2001). This might be due to the slow growth nature of *Dunaliella salina* that widens the peak and hides the S phase. Therefore, most of the cells are in a state of cell growth. After the stirring of cells with n-decane for 120s, the cell density dropped by 53%. Interestingly the three phases of the cell division cycle are much more distinguishable. It can be concluded that cells in the G1 phase were more prone to cell destruction. Cells in the G1 phase are growing cells that are not in the process of cell division, defective cells that are not able to pursue division are found in this category.

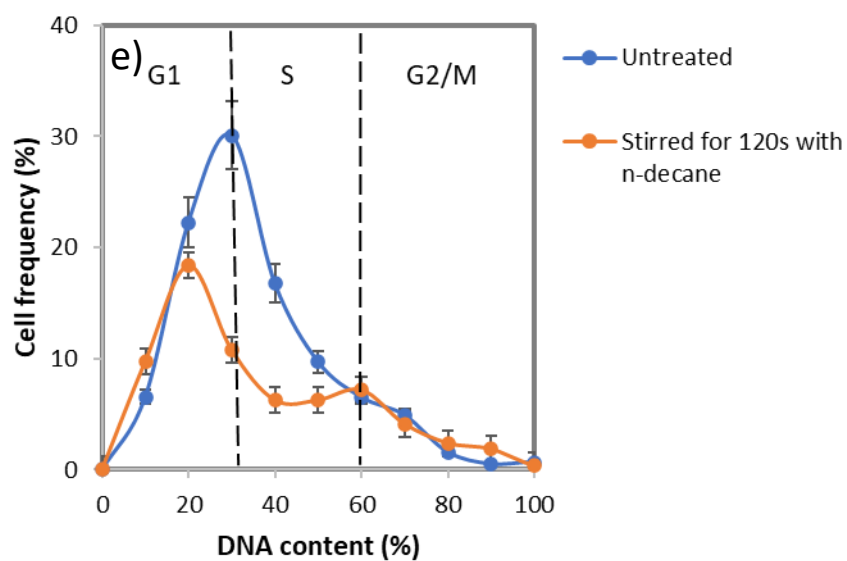
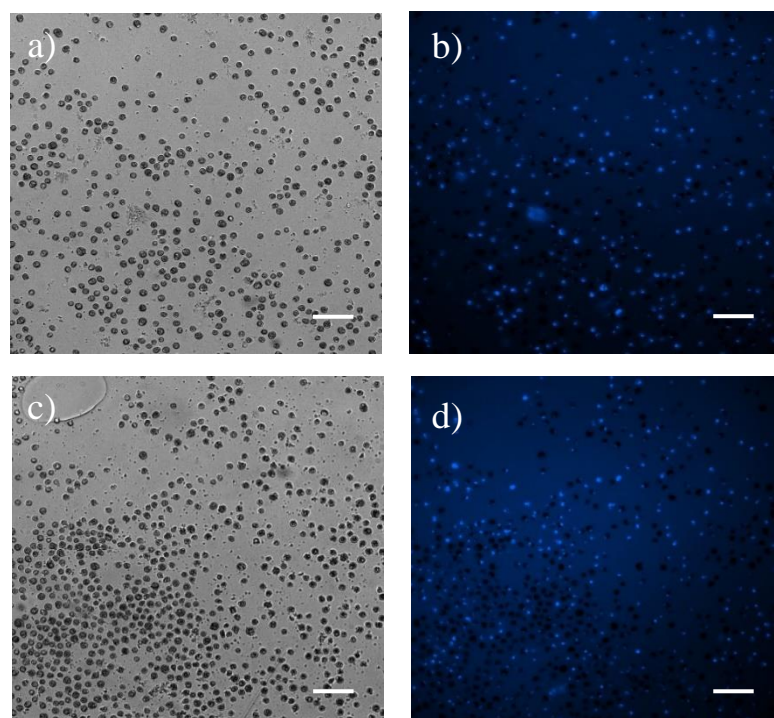


Figure 3.7 – Bright field picture of *Dunaliella salina* untreated stressed cell (a,b) and after 120s stirring with n-decane (c,d). DNA content of *Dunaliella salina* is indicated by the blue fluorescence intensity of DAPI (b,d). Scale bars in white indicate 50µm. The normalized DNA distribution is plot in cell frequency (e). The phase of cell division is indicated by dashed lines.

3.2.5 β -carotene content

The core of the culture of SE cells has a β -carotene fluorescence between $1.5 \cdot 10^4$ to $3.5 \cdot 10^4$ f.u and between 1500 and 3500 μm^3 (Figure 3.8). The results showed the trend that the larger the cell volume, the higher the β -carotene concentration (10^4 fluorescence unit per $1,5 \cdot 10^3 \mu\text{m}^3$). The concentration of β -carotene in the culture was 30 mg/L, the mean β -carotene fluorescence was $2.5 \cdot 10^4$ f.u. for 2200 cells, from there the ratio of conversion $5.5 \cdot 10^{-7}$ mg/L/f.u. It followed that the β -carotene concentration in cells was $3.6 \cdot 10^{-3}$ pg. μm^{-3} which corresponds to 6pg for a cell of 15 μm in diameter, considering a spherical shape. Mojaat Guemir, (2008) also showed that the higher the diameter the higher the β -carotene content, a ratio of 3.2 pg. μm^{-1} was found which correspond to 48pg for a cell of 15 μm in diameter, less that one order of magnitude higher than in our study.

It appeared that the largest cells are more impacted by the treatment, then two hypotheses can be made: (i) the solvent killed a part of the population, and some surviving cells shrank in size or (ii) the largest cells of the population are killed by the treatment. The coefficient between cell size and β -carotene content is relatively similar between treated and non-treated cells. Therefore, the decrease in β -carotene intracellular content of surviving cells is not confirmed. In those conditions, two explanation remains: (i) the treatment decrease the size of cells proportionally to the extracted β -carotene and (ii) the extracted β -carotene came from cells that disappeared during the treatment.

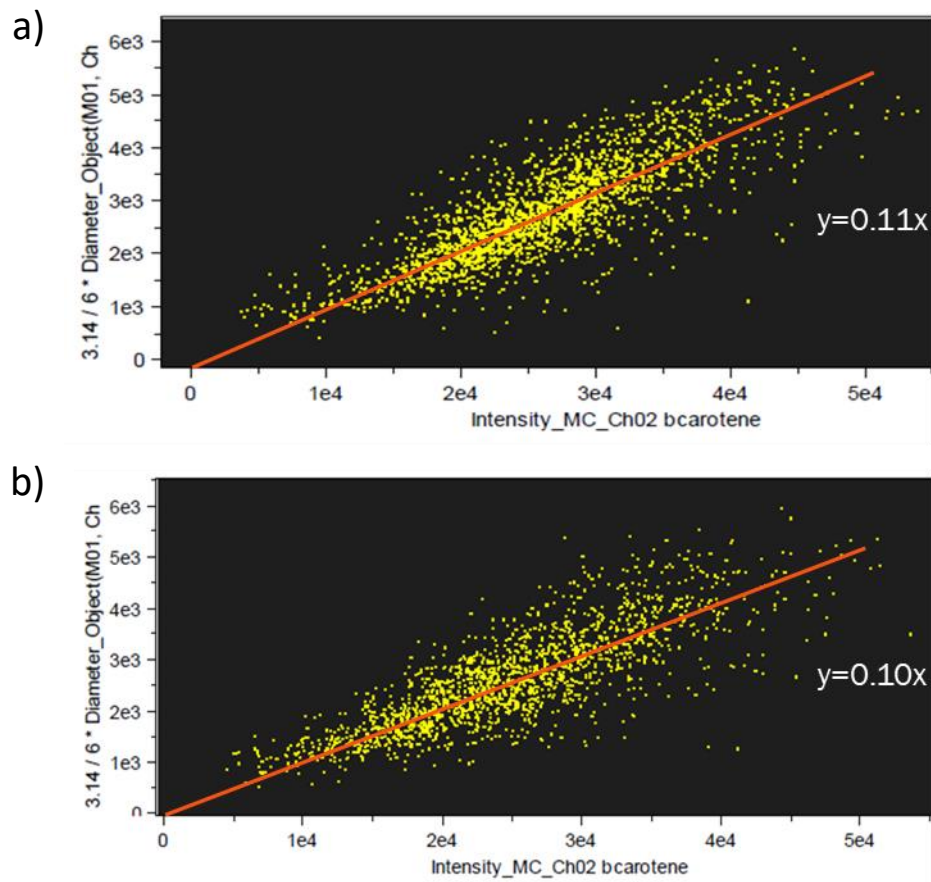


Figure 3.8 – Scatter plot of β -carotene content (x-axis) and volume (y-axis) for untreated stressed cells (a), after *n*-decane stirring for 120s (b).

3.3 Comparison of characterization methods

The advantages and drawbacks of instruments used to measure the fluorescence are presented in Figure 3.9. The spectrofluorometer allowed to measure the averaged value of biological activity of cell population. In addition to cells, the organic matter inside the medium is analysed, it can be removed by centrifugation and resuspension. But the handling is tedious and implies a lot of steps.

The flow cytometer allowed to obtain values for each individual enabling to differentiate the subpopulation heterogeneity. The cytometer thus exhibited an interesting cell analysis throughput. To analyse cells of a population, data obtained from flow cytometry instruments must be sorted with a gating strategy. But this strategy ultimately removed cells and therefore the information from those individuals. This can lead to the conclusion than only apply to a subpopulation and are thus biased.

Microscope allows to obtain values for each individual enabling to differentiate the sub population heterogeneity. The microscope method allowed to get images of focused and non-agglomerated cells. The main drawback is the necessity to analyse cell, if there is no pre-installed software. Finally, the optic method has the advantages of displaying images than can be used to monitor the aspect of cells.


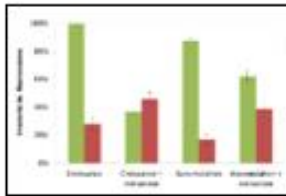


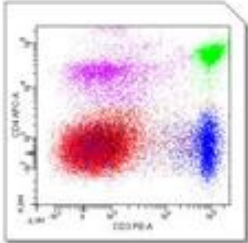

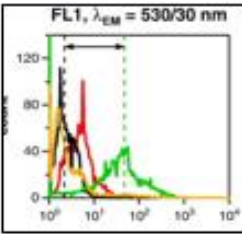

	Advantages	Inconvenient	Instruments	Data
Spectrophotometer	Cheap	Tough and inaccurate procedure (washing, exposition, washing, extraction). Whole population measure		
Fluorimeter	More sensitive	Tough procedure (washing, exposition, washing, extraction). Whole population measure		
Flow Cytometer	High number of cell analyzed, Quick	Debris, clumped cell, unfocused cell and cell without Chl.a are not analyzed Expensive		
Microscope w/Fluorescence	Affordable, Visualisation	High number of cell analyzed take long time		
Optic cytometer	Visualisation, Quick, High number of cell analyzed,	Expensive		

Figure 3.9 – Comparison of the characterization methods used to access biological parameters such as permeability, activity, cell cycle.

4 Conclusion

The study shown how the biological characteristics of *Dunaliella salina* cells influence the biocompatibility of the exposure to *n*-decane. The level of measurement (single cell or population average) can change the reliability of the results. On the whole population results showed that oxygen production slightly decreased with the exposure to *n*-decane. However, the presence of solvent residues might bias results. Results from single cell measurements showed that the permeability decrease; the higher the level of natural permeabilization, the higher the cell destruction. Cells in the phase of growth (G1) were more prone to cell destruction than dividing cells (S and G2). The exposure to *n*-decane triggered an increase in enzymatic activity possibly due to the increase in permeability. The type of instruments used gave results averaged on the population in the culture or for each individual. The flow cytometer and microscope allowed to obtain values for each individual enabling to differentiate the sub population heterogeneity and increase the reliability of the results.

Chapter 4.

*Selection of culture conditions
and cell morphology for
biocompatible extraction of β -
carotene from *Dunaliella salina***

**This chapter was accepted in the journal Marine Drugs.*

Some corrections were made based on the jury suggestions.

1 Introduction

Microalgae have been identified as promising sources for the production of biomolecules for energy, food, feed, health, pharmaceutical, and cosmetic industries (Mimouni *et al.*, 2012). Among the biomolecules extracted from microalgae, carotenoids occupy a historical and prominent place (Scarsini *et al.*, 2020) because they exhibit unique properties such as provitamin A, antioxidant and skin protection activities (Gateau *et al.*, 2016). The powerful antioxidative effect of carotenoids is due to the scavenging of the free radicals. Its positive effect on health has been proven in the treatment of a wide number of diseases with antidiabetic, antitumor, anti-inflammatory activities and benefits for cognitive function (Gateau *et al.*, 2016).

β -carotene is an ubiquitous pigment in microalgae due to its requirement for the photosynthetic process (Scarsini *et al.*, 2020). In a few taxa, such as the green microalga *Dunaliella* sp., the coupled application of nitrogen depletion and high light stress triggers the reorientation of the carbon metabolism toward the massive accumulation of β -carotene: up to 14% of DW, (Ben-Amotz *et al.*, 1988; da Silva and Lombardi, 2020). Current microalgal fractionation processes require several downstream steps such as dewatering, drying, solvent extraction and purification of the target biomolecules (Vinayak *et al.*, 2015). In addition, they generate residues that need to be treated. Most of these steps consume time and energy intensively (Hosseini Tafreshi and Shariati, 2009), which jeopardizes the ecology and economic viabilities of these processes unless the prices of this type of biomolecules are very high. The expensive market prices of those active compounds from microalgae ultimately reduce their uses for medical treatment and favour the use of chemically synthesized molecules (Scarsini *et al.*, 2020). To reduce production residues, *in situ* extraction methods or milking; have been proposed. This includes the use of pre-

Chapter 4: Selection of culture conditions and cell morphology for biocompatible extraction of β -carotene from *Dunaliella salina*

treatments as electric pulses (Zhang *et al.*, 2020; Gateau *et al.*, 2021) or resonance frequency (Vinayak *et al.*, 2017), and biocompatible solvents (Frenz *et al.*, 1989; Hejazi *et al.*, 2002; León *et al.*, 2003; Atta *et al.*, 2016). In *Dunaliella*, by comparing β -carotene solubility, solvent extraction ability and biocompatibility of organic solvents, León *et al.* (2003) established that the best compromised for β -carotene biocompatible extraction is achieved with hydrophobic solvents exhibiting a log P_{octanol} around 5 like *n*-decane, provided that the solvent/culture ratio (v/v) remains less than 1 (Mojaat *et al.*, 2008). Nevertheless, for *Dunaliella*, *n*-decane was considered either as noncompatible (Hejazi *et al.*, 2002) with a direct correlation between cell destruction and β -carotene extraction (Kleinegris *et al.*, 2011b), or biocompatible (Mojaat *et al.*, 2008) with proportionally more β -carotene extracted than cells disrupted. It has also been reported that lipid extraction from microalgae with organic solvent depends on the contact time and area between the culture media and the organic solvent, but the higher the extraction the lower the biocompatibility (Frenz *et al.*, 1989; Hejazi *et al.*, 2003; Atta *et al.*, 2016; Miazek *et al.*, 2017).

While many studies focus on solvent choice and extraction operating conditions there is a lack of understanding of the impact of culture conditions on the single cell characteristics and *de facto* on the extraction biocompatibility. *D. salina* is a cell wall less microalga meaning that the cells is limited by a thin and elastic plasma membrane (Dodge, 1973) that acts as the sole selective barrier to compounds (León *et al.*, 2001). In theory, the extraction can only be biocompatible for a cell if its membrane permeabilization is reversible. Indeed, the biological membranes are the preferential places where organic solvents like *n*-alkanes can accumulate (Bar, 1988), disturbing membrane fluidity (Sikkema *et al.*, 1995) and leading to the permeabilization of the membrane (Lorente De Nó, 1934).

The influence of *D. salina* morphology on the β -carotene extraction with n-decane as well as cell preservation during the process was investigated using a multi-disciplinary approach including cell biology, biochemistry, physiology and processing. These data will be crucial for the establishment of future biotechnological processes aiming at extracting β -carotene from microalgae.

2 Material and methods

2.1 Strain and cultures in flask

The green microalga *Dunaliella salina* CCAP 19/18 was cultivated in 500mL glass erlenmeyer fed with 200mL of Johnson growth medium modified according to Çelekli and Dönmez, (2006). Cultures were grown in a thermostated room ($20\pm 2^\circ\text{C}$) under a continuous photon flux density ($35\pm 5\mu\text{mol m}^{-2} \text{s}^{-1}$) and agitated manually once a day. The cultures were subcultured in fresh medium every four weeks to reach a cell density, a dry weight and a mean volume of *circa* $2.1 \cdot 10^6 \text{ cell mL}^{-1}$, $0.70\text{g}_{\text{DW}} \text{ L}^{-1}$ and $1100\mu\text{m}^3$. This culture condition is referred as grown in erlenmeyer (GE).

To trigger β -carotene accumulation, GE cells were harvested in sterile Falcon tube, centrifuged ($6000\times g$, 10°C , 10min), resuspended in a glass erlenmeyer in the same medium but free of nitrogen (nitrogen depleted medium) and continuously illuminated from bottom using a photon flux density (PFD) of $800\mu\text{mol m}^{-2} \text{s}^{-1}$ provided by LED panels (neutral white, 4000–4500K) for four weeks to reach a cell density, a dry weight and a mean volume of *circa* $9.7 \cdot 10^5 \text{ cell mL}^{-1}$.

¹, 0.63g_{DW} L⁻¹ and 1700 μ m³. Cells cultivated under these conditions are referred as stress in erlenmeyer condition (SE).

2.2 Culture in photobioreactor

To produce cells in a photobioreactor (PBR), 100mL of the GE culture were added into 1L airlift flat panel PBR in the previous medium with doubled concentration of nitrogen, sulphur and phosphorus and maintained at pH=7.5 and at 400 \pm 35 μ mol m⁻² s⁻¹ supplied by LED panels (neutral white, 4000–4500K) to reach a cell density of 8.2 10⁶ cell mL⁻¹ after one week. Then, cells were harvested and resuspended in nitrogen free medium in PBR for one week, as described in the previous section, but the PFD was increased to 1200 μ mol m⁻² s⁻¹ to reach a cell density, a dry weight and a mean volume of *circa* 1.6 10⁶ cell mL⁻¹, 2.2g_{DW} L⁻¹ and 600 μ m³. This culture condition is referred as stress in photobioreactor (SPBR). A sample of 200mL of SPBR culture was then harvested, transferred in an erlenmeyer without medium modification and the GE conditions were applied to allow the development under less controlled conditions, these cells are referred as SPBR+E.

The specific irradiance I_{sp} (μ mol g_{DW}⁻¹ s⁻¹) was adapted from Pruvost *et al.* (2016) and can be defined as the photon flux density PFD (μ mol m⁻² s⁻¹) divided by the dry weight of the biomass DW (g_{DW} L⁻¹) and multiplied by the specific illuminated area a_{light} (m² m⁻³) as expressed in equation 4.1:

$$I_{sp} = \text{PFD} / (\text{DW} * 1000) * a_{light} \quad (\text{Eq. 4.1})$$

The specific illuminated area a_{light} can be calculated with the culture depth L using the equation 4.2. The culture depth in PBR was 0.03m. Due to the illumination from the bottom and to simplify calculation the same equation was used for erlenmeyer, the light path was also 0.03m.

$$a_{\text{light}} = 1/L \quad (\text{Eq. 4.2})$$

2.3 In situ extraction experiment

β -carotene was extracted in 50mL Falcon tube using *n*-decane (ACROS Organics, >99%). Microalga culture concentration was adjusted with fresh medium to reach 0.63-0.70g_{DW} L⁻¹. The extraction consisted in two phases: mixing and separation. (i) 25mL of microalgae culture was mixed with 25mL *n*-decane (1:1 v/v) for 45, 120 or 240s using a vortex (Fischerbrand) vibrating at 25Hz. (ii) the Falcon tubes were then immediately centrifuged (4000xg, 15°C, 10min), resulted in the recovery of three phases: the lower aqueous phase (residue), the upper organic phase (extract) and a stable emulsion at the interface.

For a 1st order-like extraction kinetic, concentration profile (%) can be described by a single parameter model k (s⁻¹) following equation 4.3:

$$C_{\text{b-carot}} (\%) = e^{-k \cdot t} \quad (\text{Eq. 4.3})$$

2.4 Characterization of the aqueous and solvent phases

2.4.1 Photosynthetic activity

Previous studies (e.g. (León *et al.*, 2001)) have regularly used the light-dependent oxygen emission from the photosynthetic apparatus for evaluating the biocompatibility of solvent

treatment on microalgae. However, these results might be biased as the solubility of oxygen in aqueous media is lower than in organic solvents (Xu *et al.*, 2007). To avoid this difficulty, the biocompatibility of the treatment with *n*-decane was studied from the microalgal physiology point of view using the variations of the chlorophyll fluorescence quantum yield, a non-destructive tool for measuring the photosynthetic activity (Roháček *et al.*, 2008). Photosynthetic activity was measured according to Roháček *et al.* (2014). Cell concentration was adjusted to reach a fluorescence intensity of 2000 u.a. Maximum quantum efficiency of the photosystem II (Fv/Fm), photochemical (qP) and non-photochemical quenching (NPQ) were calculated according to Roháček *et al.* (2008). The maximum quantum efficiency (Fv/Fm) of the photosystem II (PSII) photochemistry quantifies the maximum photochemical efficiency of open reaction centers.

2.4.2 β -carotene quantification in biomass

β -carotene concentration in the biomass was measured before and after each solvent treatment time. For this purpose, 0.5mL sample of cell culture was centrifuged (4000g, 15°C, 10min) and the pellet was resuspended in 1.5mL of methanol (ACROS Organics, >99%) at 44°C for 45min then centrifuged again and the absorbance of the supernatant was measured at 470, 653, 666 and 750nm. The β -carotene was quantified spectrophotometrically according to the equations of Lichtenthaler and Wellburn (1983):

$$[\text{Chl.a}] = 15.65A_{666} - 7.3A_{653} \quad (\text{Eq. 4.4})$$

$$[\text{Chl.b}] = 27.05A_{653} - 11.21A_{666} \quad (\text{Eq. 4.5})$$

$$[\text{Car}] = (1000A_{470} - 2.05[\text{Chl.a}] - 114.8[\text{Chl.b}]) / 245 \quad (\text{Eq. 4.6})$$

*Chapter 4: Selection of culture conditions and cell morphology for biocompatible extraction of β -carotene from *Dunaliella salina**

According to Mojaat *et al.* (2008) the β -carotene represent the main carotenoid (>95%). Therefore, β -carotene concentration was approximated with total carotenoids concentration measured by spectrophotometry.

2.4.3 Dry mass

Five mL of *D. salina* culture were filtered on pre-dried and pre-weighted fiberglass filters (Whatman GF / F, 0.7 μ m) using a Buchner funnel. To avoid overweighting due to salt crystallization; the filters were rinsed with 15ml of isotonic ammonium formate (100g L⁻¹, ACROS Organics, >99%), (Zhu and Lee, 1997). The filters were then dried in oven at 110°C for 24h, cooled in a desiccator for 10min and weighed (Sartorius, Secura).

2.4.4 Cell density, volume and circularity

2.4.4.1 Cell density

Cell density, cell volume and cell circularity were determined on a Nageotte slide after cell immobilization (500:50 v/v) with a 4% solution of paraformaldehyde (PF), (ACROS Organics, >96%) in saline phosphate buffer. The treatment did not affect the morphology or the color of the microalgae (Hyka *et al.*, 2013). Sixty microscopy bright fields (AxioVision A1, Zeiss, Iena, Germany; magnification: x400, picture resolution: 0.25 μ m px⁻¹) were pictured randomly. The color pictures (16bit) were transformed into B/W ones (8bit) using the Image J software (<https://imagej.nih.gov/ij/>, National Institutes of Health), which were then subjected to particle analysis using a default ImageJ routine. Briefly, cell debris and other small particles were first automatically removed from the analysis by empirically setting the ‘cell area’ parameter to the

range 20-400 μm^2 and by manual sorting. A minimum of 1600 cells was counted, limiting the standard error of cell concentration estimation to 5% (Lund *et al.*, 1958). Cell density was calculated as the number of cells (N_{cells}) in the corresponding volume of the image sample ($V_{\text{image}} = 4.75 \cdot 10^{-2} \mu\text{L}$) multiplied by the number of images (N_{images}), adjusted with the PF dilution coefficient (dil_{PF}) as shown in equation 4.4:

$$\text{Cell density (cell mL}^{-1}\text{)} = N_{\text{cells}} / (V_{\text{image}} * N_{\text{images}}) * (\text{dil}_{\text{PF}}) \quad (\text{Eq. 4.4})$$

2.4.4.2 Circularity

The circularity quantifies the regularity of the outer surface of a particle and has been used to highlight changes in cell morphology due to contact with organic solvent in gram-positive bacteria (De Carvalho and Da Fonseca, 2004). The circularity is calculated with the area (A) and perimeter (P) of the particle using equation 4.5 and ranges between 0 and 1 (Syed *et al.*, 2018).

$$\text{Circularity} = 4\pi * A / P^2 \quad (\text{Eq. 4.5})$$

Cells were classified into 21 classes of 0.05 width for the distribution analysis.

2.4.4.3 Cell volume

Nonstressed *Dunaliella* cells exhibit a prolate spheroid shape whereas the shape of stressed cells varies from oblong to spherical (Sun and Liu, 2003). Cells settle on their longitudinal section in the counting slide allowing the major axis (b) to be measured as the maximum Feret diameter and the semi-minor axis (a) as the minimum Feret diameter. Individual cell volume was calculated using equation 4.6.

$$\text{Volume (}\mu\text{m}^3\text{)} = (\pi/6) * a * b^2 \quad (\text{Eq. 4.6})$$

Estimated cell volumes were classified into 27 classes of $200\mu\text{m}^3$ width for distribution analysis.

The biomass volume was calculated as the sum of all individual volumes.

2.4.4.4 Index of potential disruption

An index of potential cell disruption (IPCD) was calculated as the product of normalized cell volume (V_n) and normalized cell circularity (C_n) following equation 4.8. The cell volume V_x was normalized between 0 and 1 with minimum and maximum values set to 0 and $2600\mu\text{m}^3$ (more than 90% of the cells were in this interval for all the distribution), respectively (equation 4.7).

The cell circularity C_x was normalized between 0 and 1 with minimum and maximum values set to 0.5 and 0.9, respectively (equation 4.8). Cells with volume or circularity outside of the respective ranges - which represented less than 10% of the population - were not accounted.

$$V_n = (V_x - V_{\min}) / (V_{\max} - V_{\min}) = (V_x - 0) / (2600 - 0) \quad (\text{Eq. 4.7})$$

$$C_n = (C_x - C_{\min}) / (C_{\max} - C_{\min}) = (C_x - 0.5) / (0.9 - 0.5) \quad (\text{Eq. 4.8})$$

$$\text{IPCD} = V_n * C_n \quad (\text{Eq. 4.9})$$

2.4.4.5 Biomass integrity, cell disruption yield and rate

Biomass integrity (%) was calculated relative to the fresh biomass for cell density, biomass volume β -carotene concentration and dry weight (equation 4.10), where X_0 is the initial amount and X_t is the amount after t seconds of extraction:

$$B_t (\%) = 100 * X_t / X_0 \quad (\text{Eq. 4.10})$$

Cell disruption yield (%) for each IPCD class was calculated following equation 11 between the initial state (0s) and the end of the treatment (240s).

Chapter 4: Selection of culture conditions and cell morphology for biocompatible extraction of β -carotene from *Dunaliella salina*

$$DY (\%) = 100 * (X_0 - X_{240}) / X_0 \quad (\text{Eq. 4.11})$$

First order model (equation 4.12) was used to calculate cell disruption rate for each volume class with X_0 the initial cell concentration and X_{240s} the concentration after 240s. Only value with $R^2 > 0.95$ were plotted.

$$\text{Cell disruption rate (s}^{-1}\text{)} = -\ln(X_{240s}/X_0)/240 \quad (\text{Eq. 4.12})$$

2.4.5 Cell membrane permeabilization

Cell permeabilization with Evans blue dye (Sigma-Aldrich, >75%) was tested according to Hamer *et al.* (2002). To distinguish between irreversible and reversible permeabilization, Evans blue (EB) ($120 \mu\text{l mL}^{-1}$ of solution in the cell culture) was added in three different conditions: (A) without treatment, (B) before the treatment, (C) after each solvent treatment time with *n*-decane (Luengo *et al.*, 2014). Thirty bright fields were represented in color as explained in the section 2.4.4.1 and the cell counter plug-in from Image J was used to manually count the cells which have led the dye (bluish cells) and those which did not. The number of cells shown varied from 300 to 1200 cells per sample.

Table 4.1 – Cell response to the staining with Evans blue.

Cell category	Abreviation	EB alone (A)	EB before solvent (B)	EB after solvent (C)
Non-affected	NA	-	-	-
Reversibly permeabilized	RP	-	+	-
Irrreversibly permeabilized	IP	-	+	+
Naturally permeabilized	NAT-P	+	+	+
Disrupted cells	DC	/	/	/

In agreement with Gateau *et al.* (2020) cells can range into 5 categories i.e. (1) the irreversibly permeabilized (IP), (2) the reversibly permeabilized (RP), (3) the naturally permeabilized (NAT-P), (4) the non-affected cells (NA) and (5) disrupted cells (DC), (Table 4.1). Thus, after mixing

Chapter 4: Selection of culture conditions and cell morphology for biocompatible extraction of β -carotene from Dunaliella salina

with solvent, a sample contained a certain proportion of each cell category. In addition, it is considered that each cell could exist under two states: non permeabilized (non-stained) or permeabilized (stained). Therefore, one can write after a time of t seconds the equation 4.13 and 4.14:

$$100\% = IP_t(\%) + RP_t(\%) + NA_t(\%) + DC_t(\%) \quad (\text{Eq. 4.13})$$

$$100\% = \text{Non-stained cells}_t(\%) + \text{Stained cells}_t(\%) + DC_t(\%) \quad (\text{Eq. 4.14})$$

Because the number of cells is not fixed disrupted cells percentage after t seconds of mixing with the solvent was calculated with the cell density after t seconds of mixing (C_t) relative to initial cell density (C_0) as follow in equation 4.15:

$$DC_t (\%) = 100.(C_0 - C_t)/ C_0 \quad (\text{Eq. 4.15})$$

In the absence of mixing with solvent (A) all the cells remain by definition non permeabilized, but only NAT-P cells will be stained with Evans blue as expressed in equation 4.16a and 4.16b:

$$\text{Non-stained cells } (\%) = NA (\%) \quad (\text{Eq. 4.16a})$$

$$\text{Stained cells } (\%) = \text{NAT-P } (\%) \quad (\text{Eq. 4.16b})$$

During mixing with the solvent, cells can turn from non-permeabilized state to the permeabilized state resulting in the formation of IP and RP categories. Among the permeabilized cells, those that were able to reseal the plasma membrane form the RP category the other forms the IP one. When Evans blue was added before mixing with solvent (B) only IP, RP and NAT-P cells should be stained with Evans blue. The categories of IP, RP and NAT-P cells cannot be distinguished individually but can be grouped together and defined as stained cells as expressed in equation 4.17a and 4.17b:

$$\text{Non-stained cells (\%)} = \text{NA (\%)} \quad (\text{Eq. 4.17a})$$

$$\text{Stained cells (\%)} = \text{NAT-P (\%)} + \text{RP (\%)} + \text{IP (\%)} \quad (\text{Eq. 4.17b})$$

When Evans blue has been added after mixing with solvent (C), cells that resealed their membranes i.e. the RP should not be stained as expressed in equation 4.18a and 4.18b:

$$\text{Non- stained cells (\%)} = \text{NA (\%)} + \text{RP (\%)} \quad (\text{Eq. 4.18a})$$

$$\text{Stained cells (\%)} = \text{NAT-P (\%)} + \text{IP (\%)} \quad (\text{Eq. 4.18b})$$

By definition, NA and RP cells are alive after the treatment with *n*-decane. Their values can be combined to define the biocompatibility index (BI) which can be calculated using equation 4.19:

$$\text{BI}_t (\%) = \text{NA}_t (\%) + \text{RP}_t (\%) \quad (\text{Eq. 4.19})$$

2.4.6 Statistics and plots

Extraction experiments were performed in triplicate. Error bars represent the standard deviation of the three replicates. Results were considered statistically different when the p value was under 0.05. It has been calculated using the software excel. Boxplots were graphed on MATLAB, density scatter plots were made with Eilers and Goeman (2004) algorithm on MATLAB.

3 Results and discussion

3.1 β -carotene extraction from cells

The ability of *n*-decane to extract β -carotene from cells of *D. salina* GE, SE and SPBR was determined through the establishment of the extraction kinetic (Fig. 1c-e). GE, SE cells initially

Chapter 4: Selection of culture conditions and cell morphology for biocompatible extraction of β -carotene from *Dunaliella salina*

have a β -carotene content of 4 and 38pg cell⁻¹, respectively. Interestingly however, SPBR cells only had 20% less intracellular β -carotene with 33pg cell⁻¹. For GE and SE, the β -carotene extraction follows a 1st order kinetic with up to 60% recovery in *n*-decane in 240s for GE and 88% for SE. For SPBR, the extraction yield is lower, with a maximum of 30% recovery after 120s. The extraction rate was twice higher for SE cells than for GE cells ($k_{SE}=7.3 \cdot 10^{-3} \text{ s}^{-1}$, $k_{GE}=3.3 \cdot 10^{-3} \text{ s}^{-1}$), in the same mixing-settling conditions indicating a pigment extraction mechanism with lower resistance when it is over-accumulated. 90% extraction yield is then expected to be obtained in 315s and 700s for SE and GE, respectively.

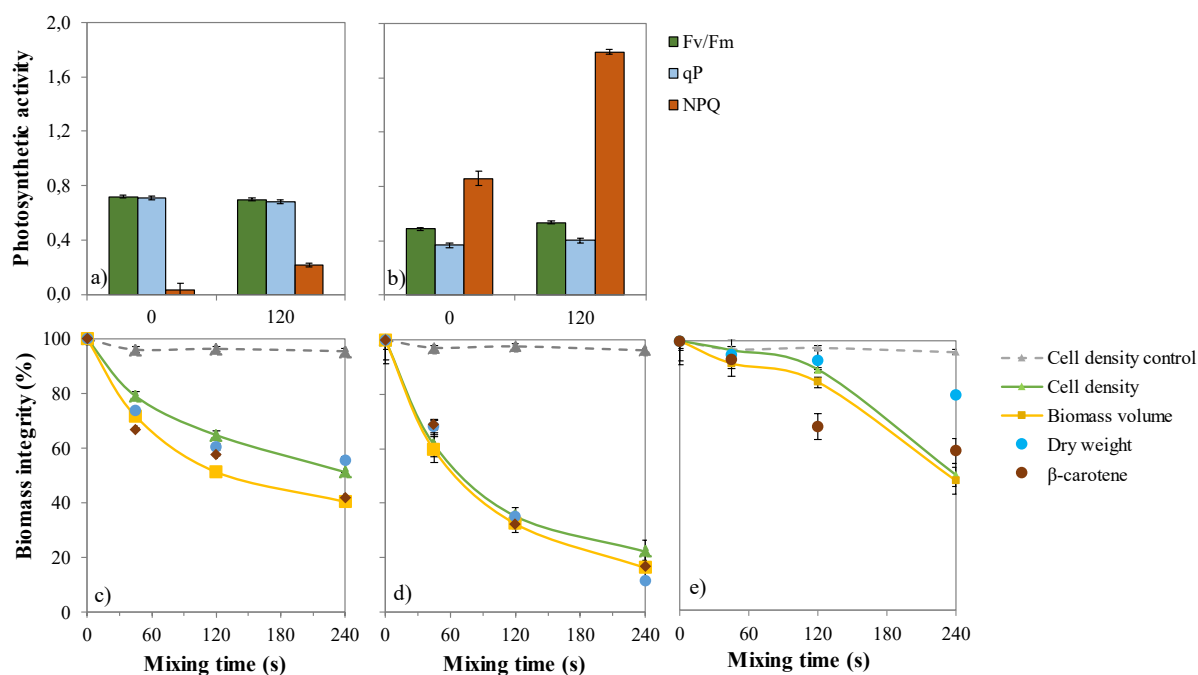


Figure 4.1 – Biocompatibility of n-decane treatment. Photosynthetic activity (a-b) before stirring (0s) and after 120 s mixing time for (a) grown cells (GE) and (b) stressed cells (SE). Biomass integrity (%) (c-e) expressed as cell density (control: stirring without solvent), biomass volume, dry weight and β -carotene content for GE (c), SE (d) and SPBR (e) cells with solvent mixing time. Scale bars indicate standard deviation error (n=3).

3.2 Impact of β -carotene extraction on photosynthetic activity

Before solvent treatment, Fv/Fm reached 0.7 values typical of GE cells (Figure 4.1 a-b). Under the irradiance used, most of the absorbed photons are used for photochemistry as shown by the high value of photochemical quenching (qP) and therefore, the need to dissipate excessive photons is very reduced as shown by the low value of NPQ. The values of these parameters are contrasted in SE cells (Figure 4.1 b). Fv/Fm value of 0.5 indicates that PSII reaction centers have been damaged and that their ability to use the energy associated with the absorbed photons for photosynthesis is reduced. Altogether, these results fit with the dismantling of the photosynthetic membranes (Ben-Amotz *et al.*, 1988) as reflected by the reduction of the photosynthetic oxygen emission capacity (Ben-Amotz and Avron, 1983) and reduction of Fv/Fm (Masuda and Melis, 2002) during β -carotene accumulation. Therefore, the need to dissipate this excess of energy as heat using NPQ mechanism is strongly increased. This increase is tremendously larger when after mixing with *n*-decane (Figure 4.1 b). This is probably due to the decreased light filtering effect exerted by the β -carotene included in the droplets. In its absence the amount of photons reaching the light-harvesting antenna complexes is higher, increasing the photon excitation pressure (1-qP), (Gray and Huner, 1995). The absence of decrease in Fv/Fm after 120s of mixing indicates that the solvent did not significantly impair the photosynthetic machinery. Our results confirm the low toxicity of *n*-decane on the photosynthetic activity of GE and SE cells reached by several other studies (e.g., (Hejazi *et al.*, 2002; León *et al.*, 2003)).

3.3 Impact of *n*-decane treatment on cell integrity

To evaluate the effect of the *n*-decane extraction on GE, SE and SPBR cells integrity, β -carotene content, dry weight, cell density and biomass volumes were measured throughout the treatment.

*Chapter 4: Selection of culture conditions and cell morphology for biocompatible extraction of β -carotene from *Dunaliella salina**

First, as a control sample, regardless the cell stress status, there was no significant cell disruption (<3%) using vortex treatment alone (Figure 4.1c-e). Then for GE, the comparison of the β -carotene release and cell density decrease kinetics (65% of remaining β -carotene and 78% of the intact cells at 45s) indicates that a part of carotenoids are extracted without any cell disruption or that there is a possible heterogeneity in cell content (disrupted cells contain more carotenoids than intact ones) or in the cell disruption (cells that contain more carotenoids are preferentially disrupted). For SPBR cells, while a slight biocompatible extraction seemed to be possible at 120s (Figure 4.1e), (30% of carotenoids recovery with 15% cell disruption) an opposite result appeared at 240s (40% of carotenoids recovery with 50% cell disruption). This indicates a difference in the fragility of cells before 120s, but a similar level of cell destruction than GE after 240s.

For SE cells, the β -carotene release and cell density decrease kinetics are similar (83% extracted β -carotene and 78% cell disruption at 120s), indicating in this case that extraction and disruption are directly correlated or that the culture content is homogeneous.

For GE cells, after 240s of mixing, the biomass volume had a 60% decrease while the cell density decrease was 49% (Figure 4.1c). The difference was less pronounced for SE cells: 88% biomass volume decrease and 80% cell density decrease (Figure 4.1b). Except for SPBR after 240s, the decrease in biomass dry weight and volume were similar; no cell shrinkage occurred during extraction. In the three culture conditions, after 120s of mixing, the higher decrease in volume is related to the higher extraction yield. The decrease in average cell volume of *D. salina* cultured in the presence of *n*-dodecane was previously reported by Kleinegris *et al.* (2011a) and this behaviour extends the correlation between β -carotene extraction and cell death established by Kleinegris *et al.* (2011b) to cell disruption as a prerequisite for β -carotene extraction. Because the larger cells have the higher carotenoids content (Mojaat Guemir, 2008) the most likely

hypothesis to explain GE and SPBR behavior is that they are preferentially disrupted during the liquid-liquid extraction with *n*-decane.

3.4 Impact of the cell size distribution

As usual, the cell size distribution by volume classes does not follow a normal distribution (Halter *et al.*, 2009) (Figure 4.2a-b). The skewness is due to the presence of a higher number of volume classes larger than the median *i.e.* $1000\mu\text{m}^3$, $1500\mu\text{m}^3$ and $500\mu\text{m}^3$ for GE, SE and SPBR cultures, respectively. As shown by the quantile values, the population heterogeneity was larger in SE culture than in GE culture. Regardless the stress state, contact with *n*-decane reduced the number of cells in each individual cell volume classes (Figure 4.2c-d), with the larger cell volume classes being the most affected *i.e.* those above the median and third quartile of the distribution ($p < 0.05$). For the GE cells, disruption rate by volume class increased linearly ($R^2 > 0.99$) from $5.4 \cdot 10^{-4} \text{ s}^{-1}$ for the $200\mu\text{m}^3$ class to $5.9 \cdot 10^{-3} \text{ s}^{-1}$ for the $2200\mu\text{m}^3$ class (Figure 4.2e). Values for higher cell volumes are not calculated because of insufficient data. Large volume *D. salina* cells were disrupted ten time faster than the small ones, confirming the heterogeneity hypothesis of the previous section and disallowing the biocompatible extraction one. For SE cells, the *D. salina* cells were bigger with a wider cell size distribution (Figure. 4.2a-b at 0s). The disruption rate by volume class increased also linearly ($R^2 > 0.99$) according to the cell size (Figure 4.2f) up to $k_d = 1.4 \cdot 10^{-2} \text{ s}^{-1}$ for $3500\mu\text{m}^3$ cells. Interestingly SPBR cells were smaller and more homogeneous than cells from the two other culture conditions. Because SPBR cells received less light energy ($18\mu\text{mol g}_{\text{DW}}^{-1} \text{ s}^{-1}$) than SE cells ($42\mu\text{mol g}_{\text{DW}}^{-1} \text{ s}^{-1}$), their volumes were smaller as shown by Xu *et al.* (2016). The destruction rate after 120s increase by volume class but seems constant after

Chapter 4: Selection of culture conditions and cell morphology for biocompatible extraction of β -carotene from Dunaliella salina

240s indicating that cells were smaller and thus less fragile during the extraction but that the extraction duration plays a significant role in the ability of cell to survive the treatment.

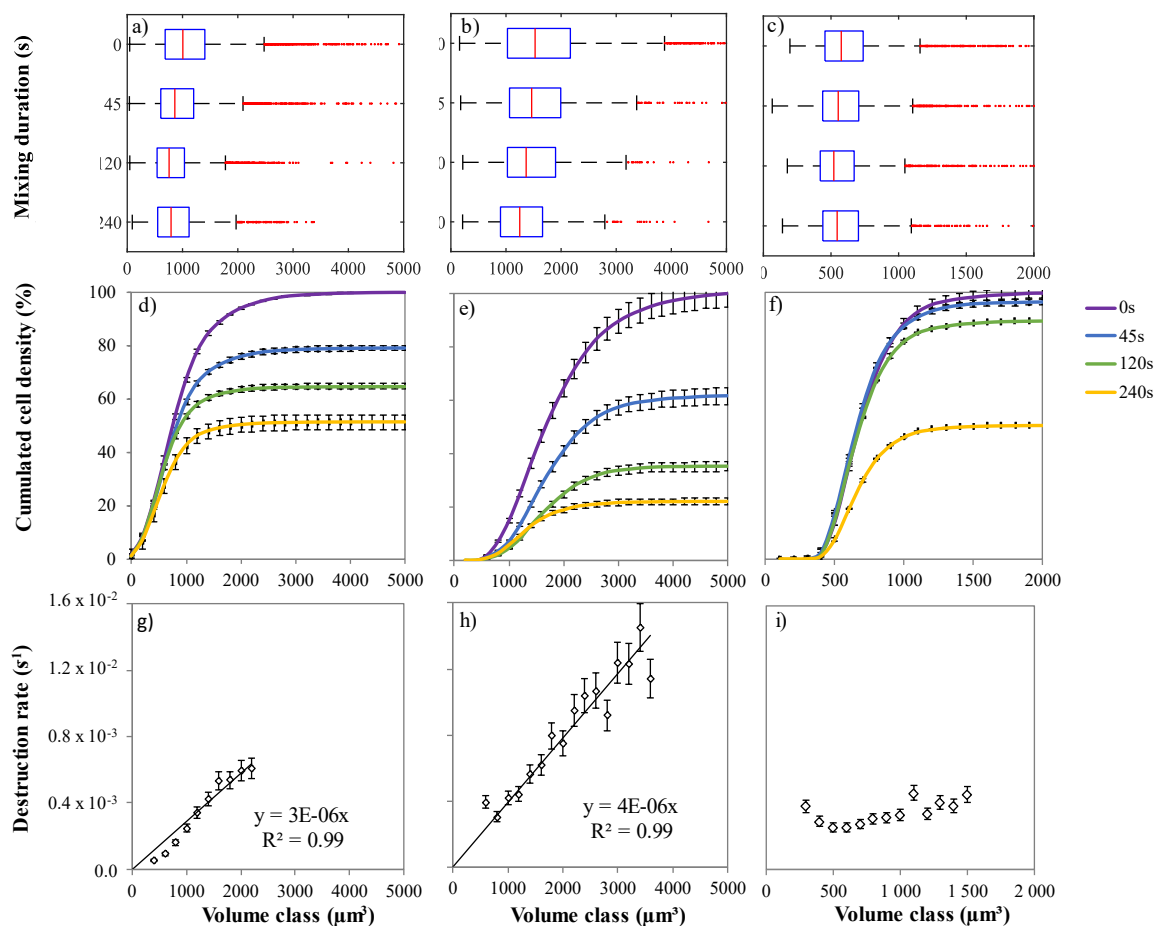


Figure 4.2 – Cell volume dependant disruption for (GE) grown cells (a,d,g), (SE) stressed cells (b,e,h) and (SPBR) stressed cells in erlenmeyer (c,f,i). Box plot of the distribution (a-c). Cumulated cell density per volume class (d-f). Cell disruption rate by volume class (μm^3) after 240s (g-i). Scale bars indicate standard error (n=3). Median and third quartile of the distribution were more affected than first quartile ($p < 0.05$).

3.5 Influence of volume and circularity on cell disruption

The density scatter plots displayed in Figure 4.3a-h show the distribution of cell volume and cell circularity throughout the liquid-liquid extraction with *n*-decane. As expected, GE cells are mainly characterized by high circularity, ranging in 0.85-0.95 and with an initial mean cell volume around $1000\mu\text{m}^3$ (Figure 4.3a). After 45s of mixing with the solvent, 15% of GE cells dropped in circularity between 0.60 and 0.80 (Figure 4.3b, Figure 4.4a) while the cells that initially had a cell volume greater than $1500\mu\text{m}^3$ decreased significantly. Low circularity cells progressively disappeared (Figure 4.3c-d). The transient decrease in circularity for short contact time with the solvent (less than 45s) induced a cell distortion may be due to a cell membrane alteration as confirmed by electron microscope observations by Hejazi *et al.* (2004) and Li *et al.* (2015). Cells that survived to longer exposure (up to 240s) to *n*-decane were a few, small and showed circularity ranging between 0.70-0.90. As shown by the light blue contour (Figure 4.3e), the 80% core population of SE cells is distributed in a more diffuse pattern in terms of circularity and volume. All categories of cells were altered by the solvent treatment, but obviously those characterized by a circularity less than 0.50 or cell volume greater than $1500\mu\text{m}^3$ were almost absent after 240s. Unlike for GE cells, the transient decrease in single cell circularity was not observed for SE and SPBR cells (Figure 4.4b). The density scatter plot displayed in Figure 4.3a shows the distribution of cell volume and cell circularity for the SPBR cells. The applied culture conditions led to more homogeneous cell characteristics than in erlenmeyer with about 0.9 in circularity (Figure 4.3f) and $600\mu\text{m}^3$ mean cell volume (Figure 4.3e), which was 3 times smaller than for SE cells. The improved design of photobioreactors allows to culture microalgae under controlled conditions such as pH, agitation and CO_2 supply to increase their growth rate (Hadj-

Romdhane *et al.*, 2012). In the three culture conditions cells that survive were concentrated around 0.9 in circularity and below $1000\mu\text{m}^3$ in volume.

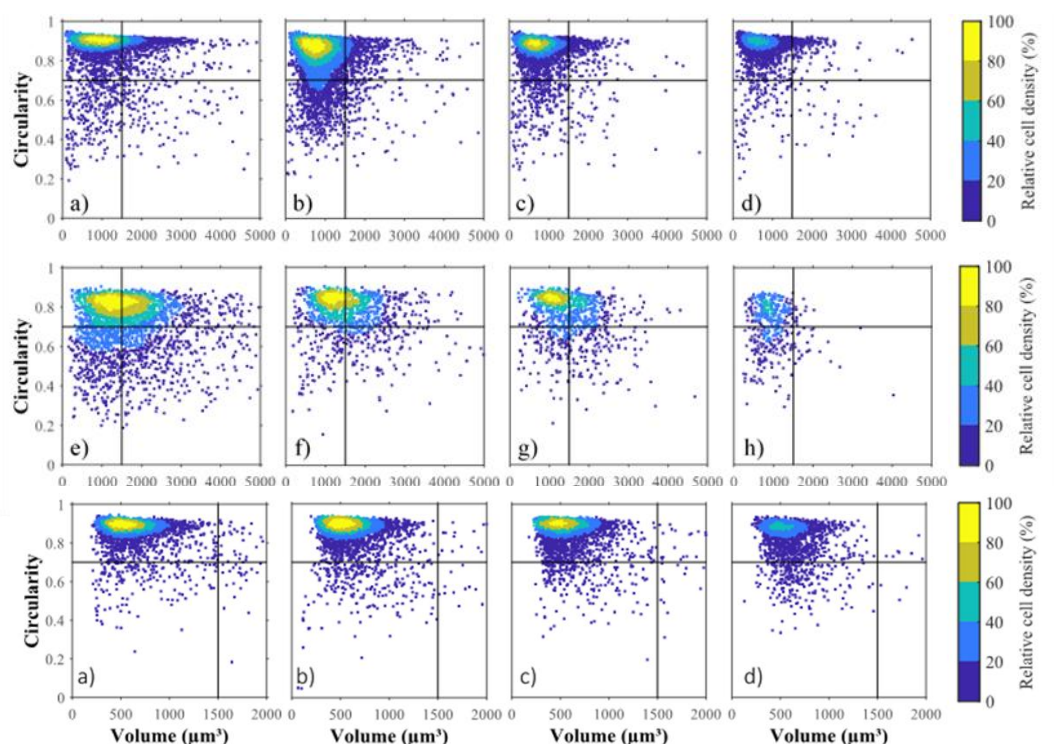


Figure 4.3 – Effect of n-decane extraction on circularity and volume. Density scattering plots of grown cells (GE), (a-d) for 0s (a), 45 s (b), 120s (c) and 240s (d), stressed cells in erlenmeyer (SE), (e-h) for 0s (e), 45s (f), 120s (g) and 240s (h) and stressed cells in PBR (SPBR), (i-l) for 0s (i), 45s (j), 120s (k) and 240s (l).

The volume and circularity criteria were unified with an index of potential cell disruption (IPCD) (equation 8), that varies between 0 and 1, to model the overall disruption pattern. It was calculated as the product of normalized volume (equation 6) by the normalized circularity (equation 7) (Section 2.4.4.5). Regardless the stress state, the higher the IPCD the higher the disruption yield ($p < 0.005$) (Figure 4.4). Similar sigmoidal curves with inflection point around $\text{IPCD} = 0.4$ were found. They differ however in the initial relative destruction, it is much higher for SE than for GE ones, suggesting that there are other biological parameters that influence cell disruption. The

Chapter 4: Selection of culture conditions and cell morphology for biocompatible extraction of β -carotene from *Dunaliella salina*

index of potential cell disruption (IPCD) for SPBR and GE cells were similar (Figure 4.3h). At $IPCD=0.4$, the disruption rate was 60%, 80% and 70% for GE, SE and SPBR respectively. This indicate that apart from the difference in volume and circularity, cells SPBR were slightly more robust than SE cells. In the SPBR culture conditions, cells were constantly agitated, increasing the access to nutrient and light limiting or favouring cellular maintenance. The pH was controlled for SPBR cells limiting toxic effect on cells. The cell disruption and β -carotene extraction did not follow a 1st order kinetic anymore. Small cells (around $600\mu\text{m}^3$) with a circular membrane (around 0.9 in circularity) were able to maintain their membrane integrity for extraction time up to 120s while 240s extraction led to a loss in cell density and biomass volume (50%).

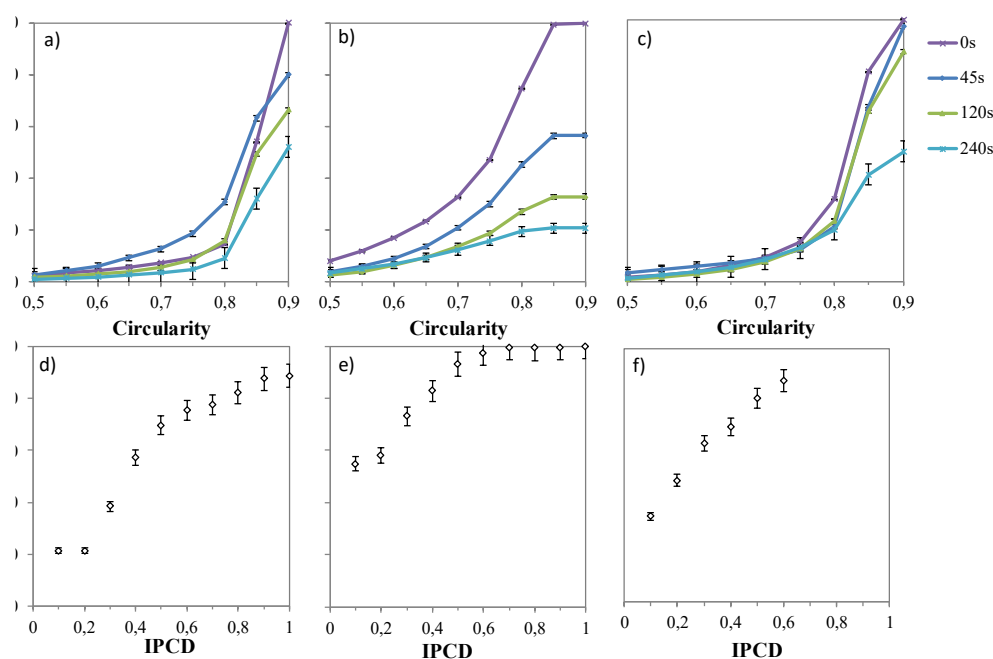


Figure 4.4 – The index of potential disruption. Cumulated cell density per circularity class (a-c) for (a) grown cells (GE), (b) stressed cells (SE) and (c) SPBR cells. Disruption yield (%) per index of potential disruption class (IPCD), (d-f) for GE cells (d), SE cells (e) and SPBR cells (f). Scale bars indicate standard deviation (n=3). The higher the IPCD the higher the disruption yield ($p < 0.05$).

3.6 Cell permeabilization with solvent

To highlight the kinetic of permeabilization and understand the higher IPCD values of SE compared to SPBR culture conditions, the mixing of *D. salina* with *n*-decane was carried out with cells that were robust (SPBR) but then cultured in erlenmeyer (SPBR+E) to increase the abundance of fragile cells like in the SE cell state. Cells were stained with Evans blue (EB) to measure the percentage of permeabilized cells. Representative picture of samples with EB added before or after extraction are shown in Figure 4.5a. In the absence of contact with the solvent, many cells loaded EB and appeared dark in color, meaning that NAT-P sub-population accounted for 36% of the microalgae tested (Figure 4.5e). This proportion is similar to that reported in literature (Gateau *et al.*, 2021). Among the NAT-P sub-population, some cells presented an irregular membrane and were partially opened (Figure 4.5a). Interestingly compared to SPBR cells SPBR+E present a higher proportion of cells with low circularity.

As seen with the color contour the core population of NAT-P cells (Figure 4.5d) overlap the one of NA (Figure 4.5c), thus in average NAT-P and NA had the same volume and circularity. In consequence the natural permeabilization is independent of the circularity and the volume. Therefore, to predict the cell destruction with *n*-decane extraction, the permeabilization level needs to be quantified in addition to the volume and the circularity.

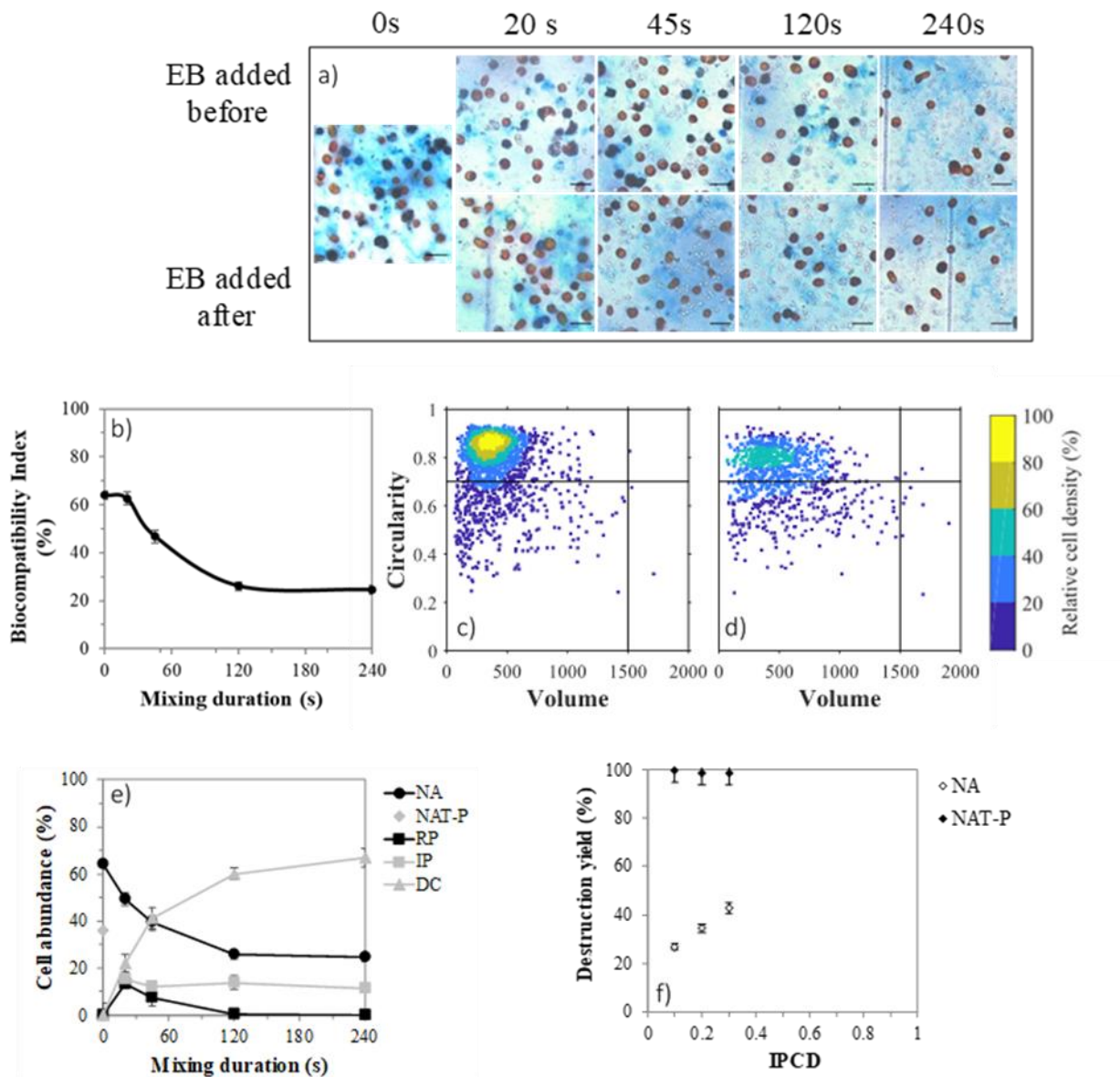


Figure 4.5 – Membrane permeabilization with n-decane of SPBR+E cells. Pictures of the different permeabilization categories of cells (a), black line represent 20 μ m. Cell abundance (%) in disrupted cells (DC), non-affected cells (NA), irreversibly permeabilized cells (IP) and reversibly permeabilized cells (RP) for the different extraction time (b). Biocompatibility index throughout the treatment (c). Density scatter plots of non-affected cells (d) and naturally permeabilized cells (e). Cell disruption yield per index of potential disruption (IPCD), (f).

After 20s, 21% of cells were disrupted (DC), 15% of cells were IP, 13% turned RP, NA decreased from 64% to 50%. Because they are both stained when EB was added after mixing, NAT-P and

*Chapter 4: Selection of culture conditions and cell morphology for biocompatible extraction of β -carotene from *Dunaliella salina**

IP cannot be distinguished. However, the DC (21%) correspond to the difference between NAT-P (36%) and IP (15%) and the decrease in NA (14%) correspond to the increase in RP (13%).

Therefore, it can be hypothesized that: (i) the NAT-P were more fragile and disappeared the first (turned DC), (ii) some IP cells stayed in the category and (ii) NA cells that were more robust turned RP. For longer mixing time, the RP cells progressively became less abundant while that of IP remained constant and DC cells increased (Figure 4.5e). To summarize, NAT-P are disrupted first, and NA seems to follow a gradual permeabilization process: RP→IP→DC. The presence of RP cells is only transient as its proportion decreased when the treatment time exceeds 20s. Gateau *et al.* (2021) have coined the biocompatibility index (BI) to describe the evolution of such populations during a permeabilizing treatment. Figure 4.5b displays the evolution of BI along the *n*-decane treatment. An exposure time longer than 45s led to a decrease in NA and BI. But the NAT-P cells are considered as dying cells, their death will not effectively decrease the biocompatibility. Therefore, the treatment could be considered as mainly biocompatible for very short extraction time *i.e.* <45s. The disruption yield for NAT-P cells was around 100% for all IPCD (Figure 4.5f), indicating that regardless the volume and circularity if the cells is naturally permeabilized it is disrupted by the mixing with *n*-decane. However, NA and RP cells are considered alive based on the membrane integrity and not on the ability to divide again.

The IPCD curve of non-affected (NA) SPBR+E cells (Figure 4.5f) was similar to that of SPBR cells. The curve for all SPBR+E cells was similar to that of SE cells. In consequence the presence of naturally permeabilized cells in SPBR+E and probably in SE increased the destruction yield for all IPCD class compared to SPBR cells. Results shows that the permeability is a crucial parameter for the characterization of the fragility of cell and the upper time limit to ensure a biocompatible treatment.

4 Conclusions

This study revealed that the culture conditions and the associated morphology (around 0.9 in circularity and cell volume below $600\mu\text{m}^3$) of *Dunaliella salina* were important factors to be considered to drive the extraction of β -carotene with n-decane. The different culture conditions used highlighted the relationship between the disruption yield in a population, the cell volume, circularity and abundance of naturally permeabilized cells. New carotenoid production schemes can be envisioned by the growth of robust cells enriched in β -carotene cells under controlled pH, mixing and CO_2 conditions to ensure biocompatible extraction. The behaviour of cells of different morphology at the liquid-liquid interface seems to govern both extraction efficiency and cell viability. Further, the ability of the cells to grow and re-accumulate β -carotene after one extraction step have to be studied before suggesting a biocompatible extraction process. Finally, the use of green solvents to extract β -carotene need to be investigated as a benefit for future applications, including those related to medicine and pharmacy.

General discussion

General discussion

The results presented in this thesis were focused on the biocompatibility of β -carotene extraction from *Dunaliella salina* with the organic solvent *n*-decane. The small scale and reproducible extraction in Falcon allowed to characterize the impact of the solvent mixing on cells with various protocols. The effect of extraction on cell cultured with different conditions and on the cell morphology was investigated. In addition, metabolic activity of cells altered by the exposure to *n*-decane were examined.

One criteria of biocompatible extraction retained from the literature is that the proportion of β -carotene extracted must be higher than the proportion of disrupted cells by the extraction. In these conditions it can be hypothesized that all the metabolites were extracted from disrupted cell and that the remaining quantity of metabolites was extracted from intact cells. For grown cells, the extraction was all along slightly biocompatible with up to 60% recovery in *n*-decane for 45% of cell disruption. For stressed cells after 240s, the extraction was efficient but poorly biocompatible: up to 88% of carotenoid recovery for 87% cell disruption. Interestingly, for SPBR cells after 120s there was 30% of carotenoid recovery for 15% of cell disruption. Even though the biocompatible criterion was filled, it globally appears that high extraction yield is linked to higher cell destruction. This confirms the correlation between β -carotene extraction and cell death to cell disruption as a prerequisite for β -carotene extraction reach by several other studies.

From the analysis on the impact of extraction of the cell size distribution the main result is that the cell disruption rate increased linearly ($R^2 > 0.99$) with cell volume. It was validated that the larger cells have the higher carotenoids content. Therefore, the extraction rate on SE cells was faster than GE because it had larger cells. Considering that *n*-decane droplet size is around 1mm in diameter during extraction (microscope measurement, data not shown), the difference in cell diameter (4 to 25 μ m) is not significant to result in a selective mechanism based on contact probability between cells and solvent droplets. It can be concluded that, for a given culture

condition, larger cell required less energy to break. A better criterion to verify the biocompatibility would be that the proportion of β -carotene extracted must be higher than the proportion of cell volume loss. However, it should be verified that it is effectively possible to extract β -carotene from surviving cells on a significant number of cells. The only way to perform this test is to operate the extraction and the biocompatibility measurement on a single cell, possibly with microfluidic techniques.

Low circularity was associated with a low surviving rate. The circularity was lower for SE cells, both resulting in a higher IPCD for SE. The transient decrease in circularity for short contact time with the solvent (less than 45s) induced a cell distortion may be due to a cell membrane alteration may be a consequence of cell permeabilization. For GE and SE cells the contribution of the natural permeabilization to cell fragility was not measured. The cells' permeabilization increased with n-decane exposure as shown with propidium iodide staining and measured with a spectrofluorometer. The use of microalgae spectrally compatible SYTOX Green and single-cell analysis showed on the contrary that the permeability of cells decreases after exposure to n-decane. Above the threshold of 20% of permeability, the higher the permeability the higher the disruption. This result is contrasted with the increased permeability due to organic solvent exposure encountered in the literature, often measured as an average on the population. However, the mechanism of organic solvent toxicity is based on the membrane formation of pores. Cells that are naturally permeabilized are closer to the critical threshold of pore area on the membrane and more prone to cell disruption. Single-cells measurement of permeabilization carried with Evans blue dye confirmed the results and allowed to highlight the mechanism of cell disruption. The proportion of naturally permeabilized cells was high for cells cultures in erlenmeyer. An exposure time longer than 45s led to a decrease in cells with membrane integrity (non-affected) and in the biocompatibility index. The naturally permeabilized cells are disrupted first, but they

General discussion

are considered as non-viable dying cells, their death won't effectively decrease the biocompatibility. Therefore, the treatment could be considered as mainly biocompatible for very short extraction time *i.e.* <45s. To summarize, naturally permeabilized cells are disrupted first, and the non-affected seems to follow a gradual permeabilization process: reversible permeabilization → irreversible permeabilization → disrupted cells. The presence of reversibly permeabilized cells is only transient as its proportion decreased when the treatment time exceeds 20s.

For the measurement of enzymatic activity, a fluorochrome than is retained in permeabilized cell is preconized. However, the increase in cell permeability might increase the entry of the Fluorochrome molecules in the cell and decrease the blocking effect of outgoing fluorescence from the cell. Consequently, it is not possible to conclude on the effect of *n*-decane exposure on the enzymatic activity of cells with these methods. The cytometric and microscope measurements had the advantages to measure the biological characteristics at the individual cell level over spectrofluorometric and Clark electrode measurement that acquires results as a population average. The results shown how the biological activity of *Dunaliella salina* cells influences the biocompatibility of the exposure to *n*-decane and how the level of measurement (population average or individual cell value) can change the reliability of the results. The oxygen production slightly decreases by 20% in average. However, the higher oxygen solubility in the solvent compared to the culture media might cause overestimation of oxygen production at light and underestimate the oxygen consumption in the dark from the cell. The absence of decrease in Fv/Fm after 120s of mixing indicates that the solvent did not significantly impair the photosynthetic machinery. Our results confirm the low toxicity of *n*-decane on the photosynthetic activity of GE and SE cells reached by several other studies (e.g., (Hejazi *et al.*, 2002; León *et al.*, 2003)). As measured with CTC dye, the respiratory activity is stimulated, possibly due to

General discussion

higher exchange across the membrane. This method confirmed the low toxicity of *n*-decane on the photosynthetic activity. The *n*-decane exposure decrease the esterase activity of grown and stressed cells as measured on average by spectrofluorimetry. Cytometry experiment shown that in stressed culture there was two subpopulations that had their enzymatic activities decreased by the *n*-decane exposure, in particular the subpopulation with higher enzymatic activity. Concerning the impact of *n*-decane exposure on the cell division cycle, cells that were not in the process of cell division were more prone to cell disruption. Because growth was stopped due to cell malfunctioning or to unfavourable culture conditions (pH, nutrient, light). Altogether, results suggest that weak cells, that were already permeabilized and unable to pursue cell division, were disrupted preferentially (Figure 5.1).

Metabolic activity	Measurment	Fluorochromes	Conclusion
Photosynthesis	Oxygen production	/	Low toxicity on photosynthesis
Respiration	Oxygen consumption Respiratory chain	/ CTC	Low toxicity on respiration Stimulation of respiration
Enzymatic	Non specific esterases activity	FDA	Decrease in enzymatic activity
Membrane integrity	Permeability to hydrophile nucleic acid stains	Sytox Green Evans Blue	Decrease in permeability Gradual permeabilization
Cell division	Hydrophobe Nucleic acid stains Growth after <i>n</i> -decane mixing	DAPI /	G1 phase impaired Only possible with nitrogen repleted medium

Figure 5.1 Influence of β -carotene extraction with *n*-decane on the metabolic activity of *Dunaliella salina*

Considering results from previous studies and ours, it can be concluded that low concentration and short exposure stimulated the cell, high concentration and short exposure slightly inhibited survival cells and long-term exposure had high toxic effect on cells. Selective death of the non-viable cells inside the culture and the increase in exchange across permeabilized membrane could explain the metabolic stimulation after the exposure to organic solvent that were reported in the

General discussion

literature. This study revealed that the culture conditions and the associated morphology (around 0.9 in circularity and cell volume below $600\mu\text{m}^3$) of *Dunaliella salina* were important factors to be considered to drive the extraction of β -carotene with n-decane. The different culture conditions used highlighted the relationship between the disruption yield in a population, the cell volume, circularity and abundance of naturally permeabilized cells. Because a high proportion of cells die after 120s the extraction need to be limited to this value.

Culture conditions	Influence on cell in literature	Reference	Proposed strategy for biocompatibility
Salinity	Turn cell hydrophobe > 3M	(Curtain and Snook, 1982)	<3M
Temperature	Provoke cell death if too high	(Abu-rezq et al., 2010)	Close but below optimal
Agitation	Shear stress if too high Limited nutrient access if too low	(Barbosa et al., 2004)	Minimized
Light intensity	Cell volume correlated to it	(Xu et al., 2016)	Minimized
NaNO ₃	Needed for cell division	(Lamers et al., 2012)	Nitrogen limitation or other method for stress

Figure 5.2 Suggested strategy for the optimization of culture conditions of *Dunaliella salina* to improve the biocompatibility of β -carotene extraction.

The ideal case for the milking of β -carotene could be all the molecules are extracted from all cells without cell death, then the cells reaccumulated, the fastest possible, the extracted molecules. Cells use the carotenoids as a protection from the light. As such a minimal quantity should be left in the cells. Because cell death happens to fragile cells, cells need to regrow to keep a constant cell density and avoid the crash of the culture. Then the cells need to be recycled in a media with nitrogen. To meet this need, two processes are possible (i) there is a relaxation

step with nitrogen enriched medium to trigger cell growth, or (ii) only one photobioreactor is used with a medium limited in nitrogen to maintain growth. This second solution may result in less fragile cells because they would have sufficient material for cell maintenance compared to depleted medium. The strategy for the choice of culture conditions in order to improve the biocompatibility of the extraction is presented in Figure 5.2.

However, to industrially produced β -carotene the extraction rate per culture volume is a criterion to be maximized. One way to maximized it is to increase culture density, the other way is to maximize extraction rate per cell. Nevertheless, for industrial process to be viable the cost and energy to obtain the targeted metabolites need to be minimized

Another efficient extraction process could produce, on the contrary, fragile β -carotene-enriched cells, in this case, the cell disruption would be facilitated but non-selective. It would be relevant to determine the most efficient strategy for β -carotene production between the linear high destruction and the biocompatible extraction in loop.

Conclusion and perspectives

Conclusion

This thesis aims to study the biocompatible extraction of β -carotene from the model organism *Dunaliella salina* with the organic solvent *n*-decane. The influence of *n*-decane exposure on the biologic activity of individual cells of *Dunaliella salina* was investigated. Culture conditions are then chosen to obtain the appropriate cell morphology to ensure the biocompatibility of β -carotene extraction from *D. salina*.

For GE and SE cells, the biocompatibility of the extraction was low. Interestingly, the biocompatibility was the highest for SPBR cells after 120s with 30% of carotenoid recovery for 15% of cell disruption. Even though the biocompatible criterion was filled, it globally appears that high extraction yield is linked to higher cell destruction. This confirms the correlation between β -carotene extraction and cell death to cell disruption as a prerequisite for β -carotene extraction reach by several other studies. From the analysis on the impact of extraction of the cell size distribution the main result is that the cell disruption rate increased linearly ($R^2 > 0.99$) with cell volume. It was validated that the larger cells have the higher carotenoids content. Therefore, a better criterion to verify the biocompatibility would be that the proportion of β -carotene extracted must be higher than the proportion of cell volume loss. However, it should be verified that it is effectively possible to extract β -carotene from surviving cells on a significant number of cell.

Permeabilization measurements performed at the single-cell level with SYTOX Green and Evans blue were consistent, indicating that naturally permeabilized cells were more prone to cell disruption. A mechanism of gradual permeabilization explained the cell disruption; upon solvent

exposure cells with membrane integrity become reversibly permeabilized up to 45s, then become irreversibly permeabilized after 120s and finally die. Cells that were not in the process of cell division were more damaged by mixing with n-decane. It is still unclear whether the mixing with n-decane provoke an inhibition or a stimulation or the metabolism.

In conclusion, the culture conditions highly influence cell morphology and the robustness of *Dunaliella salina* cells to the extraction of β -carotene. Surviving cells were small ($<600\mu\text{m}^3$), with a high circularity (0.7-0.9) and non-naturally permeabilized. This finding opens new carotenoid production schemes based on growing robust β -carotene-enriched cells under controlled conditions, such as pH, mixing and CO_2 in photobioreactor, to ensure biocompatible extraction.

Perspectives

To continue the study of biocompatible extraction, cell sorting by volume, circularity, permeability and enzymatic activity with a cytometer might be a useful tool to understand in detail the influence of morphology and biological activity on the biocompatibility. Further, the ability of the cells to grow and re-accumulate β -carotene after one extraction step must be studied before suggesting a biocompatible extraction process.

Further work could be focus on the culture conditions to produce the most robust cells. The coupled application of light stress and nitrogen depletion is the most common method to trigger the accumulation of lipids (carotenoids included) in microalgae. However, the growth of cells is stopped, and the maintenance of cells is limited. Hence, it may be possible to maintain growth and intracellular maintenance, to increase cell robustness, under moderate light stress and nitrogen limitation. *Dunaliella salina* is lacking a cell wall thus is subject to cell lysis in high

shear stress environment, therefore, a special attention must be provided to limit cell death and impairment due to the agitation of the culture without compromising mass transfer.

Other wall less strains can be used for biocompatible extraction with organic solvents. The main advantages of *Dunaliella salina* for extraction are the absence of cell wall and therefore organic solvent enters in direct contact with the cell membrane. The extraction of carotenoids from cells still needs the penetration of solvents inside the chloroplast. Extraction on strains that lack cell wall but accumulate lipids inside the cytoplasm, like *Dunaliella tertiolecta* (Hoshaw and Maluf, 1981; Priyanka *et al.*, 2020), could be facilitated. Interestingly, within the strain the cytoplasmic lipid droplet contain zeaxanthin, which has a higher market value compared to β -carotene. In addition, cells are smaller than *D.salina* ones, which can improve the survival rate of extraction.

Solvent choice for the efficient extraction and downstream processes of valuable compounds from microalgae is also of main importance. A category of switchable solvents can switch from a hydrophobic to hydrophilic form by a simple process like CO₂ addition or heat treatment. The use of switchable solvent would allow to use the hydrophobic form for the extraction and turn it to the hydrophilic form to back extract the metabolites (D'Elia *et al.*, 2021). In this case, solvent recovery consumes less energy than vacuum evaporation suitable for organic solvents. The use of a different type of solvent might involve a different cellular reaction to the exposure and might allow new extraction processes.

Conclusion

Cette thèse vise à étudier l'extraction biocompatible du β -carotène de l'organisme modèle *Dunaliella salina* avec le solvant organique n-décane. L'influence de l'exposition au n-décane sur l'activité biologique des cellules individuelles de *Dunaliella salina* a été étudiée. Les conditions de culture sont ensuite choisies pour obtenir la morphologie cellulaire appropriée pour assurer la biocompatibilité de l'extraction du β -carotène de *D. salina*.

Pour les cellules GE et SE, la biocompatibilité de l'extraction était faible. Fait intéressant, la biocompatibilité était la plus élevée pour les cellules SPBR après 120 secondes avec 30 % de récupération des caroténoïdes pour 15 % de rupture cellulaire. Même si le critère de biocompatibilité était rempli, il apparaît globalement qu'un rendement d'extraction élevé est lié à une destruction cellulaire plus élevée. Cela confirme la corrélation entre l'extraction du β -carotène et la mort cellulaire à la perturbation cellulaire comme condition préalable à l'extraction du β -carotène portée par plusieurs autres études. De l'analyse sur l'impact de l'extraction de la distribution de la taille des cellules, le principal résultat est que le taux de rupture des cellules a augmenté de manière linéaire ($R^2 > 0,99$) avec le volume des cellules. Il a été validé que les cellules les plus grandes ont la teneur en caroténoïdes la plus élevée. Par conséquent, un meilleur critère pour vérifier la biocompatibilité serait que la proportion de β -carotène extraite soit supérieure à la proportion de perte de volume cellulaire. Cependant, il convient de vérifier qu'il est effectivement possible d'extraire le β -carotène des cellules survivantes sur un nombre significatif de cellules.

Les mesures de perméabilisation effectuées au niveau de la cellule unique avec SYTOX Green et Evans blue étaient cohérentes, indiquant que les cellules naturellement perméabilisées étaient plus sujettes à la perturbation cellulaire. Un mécanisme de perméabilisation progressive expliquait la rupture cellulaire ; lors de l'exposition au solvant, les cellules avec l'intégrité de la membrane deviennent réversiblement perméabilisées jusqu'à 45 s, puis deviennent irréversiblement perméabilisées après 120 s et meurent finalement. Les cellules qui n'étaient pas en cours de division cellulaire étaient plus endommagées par le mélange avec du n-décane. On ignore encore si le mélange avec le n-décane provoque une inhibition ou une stimulation du métabolisme.

En conclusion, les conditions de culture influencent fortement la morphologie cellulaire et la robustesse des cellules de *Dunaliella salina* à l'extraction du β -carotène. Les cellules survivantes étaient petites ($<600 \mu\text{m}^3$), avec une circularité élevée (0,7-0,9) et non naturellement perméabilisées. Cette découverte ouvre de nouveaux schémas de production de caroténoïdes basés sur la croissance de cellules robustes enrichies en β -carotène dans des conditions contrôlées, telles que le pH, le mélange et le CO₂ dans un photobioréacteur, pour assurer une extraction biocompatible.

Perspectives

Pour poursuivre l'étude de l'extraction biocompatible, le tri cellulaire par volume, circularité, perméabilité et activité enzymatique avec un cytomètre pourrait être un outil utile pour comprendre en détail l'influence de la morphologie et de l'activité biologique sur la biocompatibilité. De plus, la capacité des cellules à croître et à réaccumuler du β -carotène après une étape d'extraction doit être étudiée avant de proposer un procédé d'extraction biocompatible.

D'autres travaux pourraient être axés sur les conditions de culture pour produire les cellules les plus robustes. L'application couplée d'un stress lumineux et d'une déplétion azotée est la méthode la plus courante pour déclencher l'accumulation de lipides (caroténoïdes inclus) dans les microalgues. Cependant, la croissance des cellules est arrêtée et le maintien des cellules est limité. Par conséquent, il peut être possible de maintenir la croissance et le maintien intracellulaire, d'augmenter la robustesse cellulaire, sous un stress léger modéré et une limitation de l'azote. *Dunaliella salina* n'a pas de paroi cellulaire et est donc sujette à la lyse cellulaire dans un environnement à forte contrainte de cisaillement. Par conséquent, une attention particulière doit être portée pour limiter la mort cellulaire et l'altération due à l'agitation de la culture sans compromettre le transfert de masse.

D'autres souches sans paroi peuvent être utilisées pour une extraction biocompatible avec des solvants organiques. Les principaux avantages de *Dunaliella salina* pour l'extraction sont l'absence de paroi cellulaire et donc le solvant organique entre en contact direct avec la membrane cellulaire. L'extraction des caroténoïdes des cellules nécessite encore la pénétration de solvants à l'intérieur du chloroplaste. L'extraction sur des souches dépourvues de paroi cellulaire mais accumulant des lipides à l'intérieur du cytoplasme, comme *Dunaliella tertiolecta* (Hoshaw et Maluf, 1981 ; Priyanka *et al.*, 2020), pourrait être facilitée. Fait intéressant, au sein de la souche, la gouttelette lipidique cytoplasmique contient de la zéaxanthine, qui a une valeur marchande plus élevée que le β -carotène. De plus, les cellules sont plus petites que celles de *D.salina*, ce qui peut améliorer le taux de survie de l'extraction.

Le choix du solvant pour l'extraction efficace et les processus en aval de composés précieux à partir de microalgues est également d'une importance capitale. Une catégorie de solvants commutables peut passer d'une forme hydrophobe à une forme hydrophile par un processus simple comme l'ajout de CO₂ ou le traitement thermique. L'utilisation d'un solvant commutable

Conclusion and perspectives

permettrait d'utiliser la forme hydrophobe pour l'extraction et de la transformer en forme hydrophile pour extraire les métabolites (D'Elia *et al.*, 2021). Dans ce cas, la récupération des solvants consomme moins d'énergie que l'évaporation sous vide adaptée aux solvants organiques. L'utilisation d'un type de solvant différent pourrait impliquer une réaction cellulaire différente à l'exposition et pourrait permettre de nouveaux procédés d'extraction.

Bibliography

- Abu-rezq, T.S., Al-hooti, S., Jacob, D.A., 2010. Optimum culture conditions required for the locally isolated *Dunaliella salina*. *J. Algal Biomass Util.* 1, 12–19.
- Adler, N.E., Schmitt-Jansen, M., Altenburger, R., 2007. Flow cytometry as a tool to study phytotoxic modes of action. *Environ. Toxicol. Chem.* 26, 297–306. <https://doi.org/10.1897/06-1636R.1>
- Ahmed, F., Fanning, K., Netzel, M., Schenk, P.M., 2015. Induced carotenoid accumulation in *Dunaliella salina* and *Tetraselmis suecica* by plant hormones and UV-C radiation. *Appl. Microbiol. Biotechnol.* 99, 9407–9416. <https://doi.org/10.1007/s00253-015-6792-x>
- Alaswad, A., Dassisti, M., Prescott, T., Olabi, A.G., 2015. Technologies and developments of third generation biofuel production. *Renew. Sustain. Energy Rev.* 51, 1446–1460. <https://doi.org/10.1016/J.RSER.2015.07.058>
- Alder, A., Jamil, M., Marzorati, M., Bruno, M., Vermathen, M., Bigler, P., Ghisla, S., Bouwmeester, H., Beyer, P., Al-Babili, S., 2012. The path from β -carotene to carlactone, a strigolactone-like plant hormone. *Science* (80-.). 335, 1348–1351. <https://doi.org/10.1126/science.1218094>
- Ambati, R.R., Gogisetty, D., Aswathanarayana, R.G., Ravi, S., Bikkina, P.N., Bo, L., Yuepeng, S., 2019. Industrial potential of carotenoid pigments from microalgae: Current trends and future prospects. *Crit. Rev. Food Sci. Nutr.* 59, 1880–1902. <https://doi.org/10.1080/10408398.2018.1432561>
- Arrieta, J., Barreira, A., Chioccioli, M., Polin, M., Tuval, I., 2017. Phototaxis beyond turning: persistent accumulation and response acclimation of the microalga *Chlamydomonas*

Bibliography

- reinhardtii. *Sci. Reports* 2017 7 1–7. <https://doi.org/10.1038/s41598-017-03618-8>
- Atta, M., Bukhari, A., Idris, A., 2016. Enhanced lipid selective extraction from *Chlorella vulgaris* without cell sacrifice. *Algal Res.* 20, 7–15. <https://doi.org/10.1016/j.algal.2016.09.014>
- Bar, R., 1988. Effect of interphase mixing on a water–organic solvent two-liquid phase microbial system: ethanol fermentation. *J. Chem. Technol. Biotechnol.* 43, 49–62. <https://doi.org/10.1002/jctb.280430106>
- Barbosa, M.J., Hadiyanto, Wijffels, R.H., 2004. Overcoming Shear Stress of Microalgae Cultures in Sparged Photobioreactors. *Biotechnol. Bioeng.* 85, 78–85. <https://doi.org/10.1002/bit.10862>
- Baroli, I., Melis, A., 1996. Photoinhibition and repair in *Dunaliella salina* acclimated to different growth irradiances. *Planta* 198, 640–646. <https://doi.org/10.1007/BF00262653>
- Ben-Amotz, A., 1996. Effect of low temperature on the stereoisomer composition of β -carotene in the halotolerant alga *Dunaliella bardawil* (Chlorophyta). *J. Phycol.* 32, 272–275. <https://doi.org/10.1111/j.0022-3646.1996.00272.x>
- Ben-Amotz, A., 1995. New mode of *Dunaliella* biotechnology: two-phase growth for β -carotene production. *J. Appl. Phycol.* 7, 65–68. <https://doi.org/10.1007/BF00003552>
- Ben-Amotz, A., Avron, M., 1983. On the Factors Which Determine Massive β -Carotene Accumulation in the Halotolerant Alga *Dunaliella bardawil*. *Plant Physiol.* 72, 593–597. <https://doi.org/10.1104/pp.72.3.593>
- Ben-Amotz, A., Avron, M., 1979. Osmoregulation in the halophilic algae *Dunaliella* and *Asteromonas*. *Basic Life Sci.* 14, 91–99. https://doi.org/10.1007/978-1-4684-3725-6_8
- Ben-Amotz, A., Lers, A., Avron, M., 1988. Stereoisomers of β -Carotene and Phytoene in the
-

Bibliography

- Alga *Dunaliella bardawil*. *Plant Physiol.* 86, 1286–1291.
<https://doi.org/10.1104/pp.86.4.1286>
- Ben-Amotz, A., Shaish, A., Avron, M., 1989. Mode of Action of the Massively Accumulated β -Carotene of *Dunaliella bardawil* in Protecting the Alga against Damage by Excess Irradiation. *Plant Physiol.* 91, 1040–1043. <https://doi.org/10.1104/pp.91.3.1040>
- Ben-Amotz, A., Katz, A., Avron, M., 1982. Accumulation of B-Carotene in Halotolerant Algae: Purification and Characterization of B-Carotene-Rich Globules From *Dunaliella Bardawil* (Chlorophyceae). *J. Phycol.* 18, 529–537. <https://doi.org/10.1111/j.1529-8817.1982.tb03219.x>
- Benedetti, M., Vecchi, V., Barera, S., Dall’Osto, L., 2018. Biomass from microalgae: The potential of domestication towards sustainable biofactories. *Microb. Cell Fact.* 17, 173. <https://doi.org/10.1186/s12934-018-1019-3>
- Bertrand, M., 2010. Carotenoid biosynthesis in diatoms. *Photosynth. Res.* 2010 1061 106, 89–102. <https://doi.org/10.1007/S11120-010-9589-X>
- Bicas, J.L., Kleinegris, D.M.M., Barbosa, M.J., 2015. Use of methylene blue uptake for assessing cell viability of colony-forming microalgae. *Algal Res.* 8, 174–180. <https://doi.org/10.1016/j.algal.2015.02.004>
- Boender, L.G.M., De Hulster, E.A.F., Van Maris, A.J.A., Daran-Lapujade, P.A.S., Pronk, J.T., 2009. Quantitative physiology of *Saccharomyces cerevisiae* at near-zero specific growth rates. *Appl. Environ. Microbiol.* 75, 5607–5614. <https://doi.org/10.1128/AEM.00429-09>
- Bogacz-Radomska, L., Harasym, J., 2018. β -Carotene—properties and production methods. *Food Qual. Saf.* 2, 69–74. <https://doi.org/10.1093/FQSAFE/FYY004>
-

Bibliography

- Borowitzka, L., Borowitzka, M., 1990. Commercial Production of β -Carotene by *Dunaliella Salina* in Open Ponds. *Bull. Mar. Sci.* 47, 244–252.
- Borowitzka, L.J., 1981. The microflora. *Salt Lakes* 33–46. https://doi.org/10.1007/978-94-009-8665-7_4
- Borowitzka, L.J., Borowitzka, M.A., 1989. β -Carotene (Provitamin A) Production with Algae, in: *Biotechnology of Vitamins, Pigments and Growth Factors*. Springer Netherlands, pp. 15–26. https://doi.org/10.1007/978-94-009-1111-6_2
- Borowitzka, M.A., 1999. Commercial production of microalgae: ponds, tanks, and fermenters. *Prog. Ind. Microbiol.* 35, 313–321. [https://doi.org/10.1016/S0079-6352\(99\)80123-4](https://doi.org/10.1016/S0079-6352(99)80123-4)
- Borowitzka, M.A., Huisman, J.M., 1993. The Ecology of *Dunaliella salina* (Chlorophyceae, Volvocales): Effect of Environmental Conditions on Aplanospore Formation. *Bot. Mar.* 36, 233–244. <https://doi.org/10.1515/botm.1993.36.3.233>
- Borowitzka, M.A., Siva, C.J., 2007. The taxonomy of the genus *Dunaliella* (Chlorophyta, Dunaliellales) with emphasis on the marine and halophilic species. *J. Appl. Phycol.* 19, 567–590. <https://doi.org/10.1007/s10811-007-9171-x>
- Brink, L.E.S., Tramper, J., 1985. Optimization of organic solvent in multiphase biocatalysis. *Biotechnol. Bioeng.* 27, 1258–1269. <https://doi.org/10.1002/bit.260270822>
- Brookes, J.D., Geary, S.M., Ganf, G.G., Burch, M.D., 2000. Use of FDA and flow cytometry to assess metabolic activity as an indicator of nutrient status in phytoplankton. *Mar. Freshw. Res.* 51, 817–823. <https://doi.org/10.1071/MF00048>
- Caron, G.N.-V., Badley, R.A., 1995. Viability assessment of bacteria in mixed populations using flow cytometry*. *J. Microsc.* 179, 55–66. <https://doi.org/10.1111/j.1365->
-

Bibliography

2818.1995.tb03612.x

Çelekli, A., Dönmez, G., 2006. Effect of pH, light intensity, salt and nitrogen concentrations on growth and β -carotene accumulation by a new isolate of *Dunaliella* sp. *World J. Microbiol. Biotechnol.* 22, 183–189. <https://doi.org/10.1007/s11274-005-9017-0>

Cell Cycle Assay Principle - Beckman Coulter [WWW Document], n.d. URL <https://www.beckman.com/reagents/coulter-flow-cytometry/cell-health-research-assays/assay-principle> (accessed 11.6.21).

Chaudry, S., Bahri, P.A., Moheimani, N.R., 2015. Proposal of a New Pathway for Microalgal Oil Production and its Comparison with Conventional Method, in: *Computer Aided Chemical Engineering*. pp. 377–382. <https://doi.org/10.1016/B978-0-444-63578-5.50058-X>

Choudhari, S., Singhal, R., 2008. Media optimization for the production of β -carotene by *Blakeslea trispora*: A statistical approach. *Bioresour. Technol.* 99, 722–730. <https://doi.org/10.1016/j.biortech.2007.01.044>

Cifuentes, A.S., González, M.A., Inostroza, I., Aguilera, A., 2001. Reappraisal of physiological attributes of nine strains of *Dunaliella* (chlorophyceae): Growth and pigment content across a salinity gradient. *J. Phycol.* 37, 334–344. <https://doi.org/10.1046/j.1529-8817.2001.037002334.x>

Colusse, G.A., Mendes, C.R.B., Duarte, M.E.R., Carvalho, J.C. de, Nosedá, M.D., 2020. Effects of different culture media on physiological features and laboratory scale production cost of *Dunaliella salina*. *Biotechnol. Reports* 27, e00508. <https://doi.org/10.1016/j.btre.2020.e00508>

CRC Handbook of Chemistry and Physics, 2009–2010, 90th ed., 2009. . J. Am. Chem. Soc. 131,

Bibliography

12862–12862. <https://doi.org/10.1021/ja906434c>

Curtain, C., 2000. PLANT BIOTECHNOLOGY- The growth of Australia's algal β -carotene industry.

Curtain, C.C., Snook, H., 1982. Method for harvesting algae.

D'Ambrosio, D.N., Clugston, R.D., Blaner, W.S., 2011. Vitamin A metabolism: An update. *Nutrients*. <https://doi.org/10.3390/nu3010063>

D'Elia, L., Imbimbo, P., Liberti, D., Bolinesi, F., Pollio, A., Mangoni, O., Brilman, W., Olivieri, G., Monti, D.M., 2021. Switchable Solvent Selective Extraction of Hydrophobic Antioxidants from *Synechococcus bigranulatus*. *ACS Sustain. Chem. Eng.* 9, 13798–13806. <https://doi.org/10.1021/ACSSUSCHEMENG.1C04400>

da Silva, J.C., Lombardi, A.T., 2020. Chlorophylls in Microalgae: Occurrence, Distribution, and Biosynthesis, in: *Pigments from Microalgae Handbook*. Springer International Publishing, pp. 1–18. https://doi.org/10.1007/978-3-030-50971-2_1

Darvehei, P., Bahri, P.A., Moheimani, N.R., 2018. Model development for the growth of microalgae: A review. *Renew. Sustain. Energy Rev.* <https://doi.org/10.1016/j.rser.2018.08.027>

Davidi, L., Shimoni, E., Khozin-Goldberg, I., Zamir, A., Pick, U., 2014. Origin of β -carotene-rich plastoglobuli in *Dunaliella bardawil*. *Plant Physiol.* 164, 2139–2156. <https://doi.org/10.1104/pp.113.235119>

De Carvalho, C.C.C.R., Da Fonseca, M.M.R., 2004. Solvent toxicity in organic-aqueous systems analysed by multivariate analysis. *Bioprocess Biosyst. Eng.* 26, 361–375. <https://doi.org/10.1007/s00449-004-0381-1>

Bibliography

- Del Campo, J.A., García-González, M., Guerrero, M.G., 2007. Outdoor cultivation of microalgae for carotenoid production: Current state and perspectives. *Appl. Microbiol. Biotechnol.* 74, 1163–1174. <https://doi.org/10.1007/s00253-007-0844-9>
- Delgado Vargas, F., Jimenez, A.R., Paredes Lopez, O., 2010. Natural Pigments: Carotenoids, Anthocyanins, and Betalains — Characteristics, Biosynthesis, Processing, and Stability, *Critical Reviews in Food Science and Nutrition*.
- Dodge, J.D., 1973. *The Fine Structure of Algal Cells*, The Fine Structure of Algal Cells. Elsevier. <https://doi.org/10.1016/b978-0-12-219150-3.x5001-8>
- Druesne-Pecollo, N., Latino-Martel, P., Norat, T., Barrandon, E., Bertrais, S., Galan, P., Hercberg, S., 2010. Beta-carotene supplementation and cancer risk: a systematic review and metaanalysis of randomized controlled trials. *Int. J. Cancer* 127, 172–184. <https://doi.org/10.1002/IJC.25008>
- Eilers, P.H.C., Goeman, J.J., 2004. Enhancing scatterplots with smoothed densities. *Bioinformatics* 20, 623–628. <https://doi.org/10.1093/BIOINFORMATICS/BTG454>
- Einsparh, K.J., Maeda, M., Thompson, G.A., 1988. Concurrent changes in *Dunaliella salina* ultrastructure and membrane phospholipid metabolism after hyperosmotic shock. *J. Cell Biol.* 107, 529–538. <https://doi.org/10.1083/jcb.107.2.529>
- Fachet, M., Hermsdorf, D., Rihko-Struckmann, L., Sundmacher, K., 2016. Flow cytometry enables dynamic tracking of algal stress response: A case study using carotenogenesis in *Dunaliella salina*. *Algal Res.* 13, 227–234. <https://doi.org/10.1016/j.algal.2015.11.014>
- Farhat, N., Rabhi, M., Falleh, H., Jouini, J., Abdelly, C., Smaoui, A., 2011. Optimization of salt concentrations for a higher carotenoid production in *dunaliella salina* (Chlorophyceae). *J. Phycol.* 47, 1072–1077. <https://doi.org/10.1111/j.1529-8817.2011.01036.x>
-

Bibliography

- Frenz, J., Largeau, C., Casadevall, E., 1989. Hydrocarbon recovery by extraction with a biocompatible solvent from free and immobilized cultures of *Botryococcus braunii*. *Enzyme Microb. Technol.* 11, 717–724. [https://doi.org/10.1016/0141-0229\(89\)90120-8](https://doi.org/10.1016/0141-0229(89)90120-8)
- García-González, M., Moreno, J., Cañavate, J.P., Anguis, V., Prieto, A., Manzano, C., Florencio, F.J., Guerrero, M.G., 2003. Conditions for open-air outdoor culture of *Dunaliella salina* in southern Spain. *J. Appl. Phycol.* 2003 152 15, 177–184. <https://doi.org/10.1023/A:1023892520443>
- Garvey, M., Moriceau, B., Passow, U., 2007. Applicability of the FDA assay to determine the viability of marine phytoplankton under different environmental conditions. *Mar. Ecol. Prog. Ser.* 352, 17–26. <https://doi.org/10.3354/meps07134>
- Gateau, H., Blanckaert, V., Veidl, B., Burlet-Schiltz, O., Pichereaux, C., Gargaros, A., Marchand, J., Schoefs, B., 2021. Application of pulsed electric fields for the biocompatible extraction of proteins from the microalga *Haematococcus pluvialis*. *Bioelectrochemistry* 137, 107588. <https://doi.org/10.1016/j.bioelechem.2020.107588>
- Gateau, H., Solymosi, K., Marchand, J., Schoefs, B., 2016. Carotenoids of Microalgae Used in Food Industry and Medicine. *Mini-Reviews Med. Chem.* 17. <https://doi.org/10.2174/1389557516666160808123841>
- Gillet, J.N., 2015. Ultrafast molecular dynamics of biofuel extraction for microalgae and bacteria milking: Blocking membrane folding pathways to damaged lipid-bilayer conformations with nanomicelles. *J. Biomol. Struct. Dyn.* 33, 690–705. <https://doi.org/10.1080/07391102.2014.907544>
- Ginzburg, M., Ginzburg, B.Z., Wayne, R., 1998. Ultrarapid endocytotic uptake of large molecules in *Dunaliella* species. *Protoplasma* 206, 73–86.
-

Bibliography

<https://doi.org/10.1007/bf01279254>

Giordano, M., Pezzoni, V., Hell, R., 2000. Strategies for the allocation of resources under sulfur limitation in the green alga *Dunaliella salina*. *Plant Physiol.* 124, 857–864.

<https://doi.org/10.1104/pp.124.2.857>

Glikson, M., Lindsay, K., Saxby, J., 1989. *Botryococcus*—A planktonic green alga, the source of petroleum through the ages: Transmission electron microscopical studies of oil shales and petroleum source rocks. *Org. Geochem.* 14, 595–608. [https://doi.org/10.1016/0146-6380\(89\)90039-9](https://doi.org/10.1016/0146-6380(89)90039-9)

Gómez, P.I., González, M.A., 2005. The effect of temperature and irradiance on the growth and carotenogenic capacity of seven strains of *Dunaliella salina* (Chlorophyta) cultivated under laboratory conditions. *Biol. Res.* 38, 151–162. <https://doi.org/10.4067/s0716-97602005000200005>

Grand View Research, 2018. Beta-carotene market size, share, global industry growth report, 2024. *Food Addit. Nutr.* 1–6.

Gray, G.R., Huner, N.P.A., 1995. Excitation Pressure Determines Tolerance to Photoinhibition of Photosynthesis, in: *Photosynthesis: From Light to Biosphere*. Springer Netherlands, pp. 3335–3338. https://doi.org/10.1007/978-94-009-0173-5_784

Griehl, Carola, Kleinert, C., Griehl, Christoph, Bieler, S., 2015. Design of a continuous milking bioreactor for non-destructive hydrocarbon extraction from *Botryococcus braunii*. *J. Appl. Phycol.* 27, 1833–1843. <https://doi.org/10.1007/s10811-014-0472-6>

Guedes, A.C., Amaro, H.M., Malcata, F.X., 2011. Microalgae as sources of high added-value compounds—a brief review of recent work. *Biotechnol. Prog.* 27, 597–613. <https://doi.org/10.1002/BTPR.575>

Bibliography

- Guiry, M.D., 2012. How many species of algae are there? *J. Phycol.* 48, 1057–1063.
<https://doi.org/10.1111/j.1529-8817.2012.01222.x>
- Hadj-Romdhane, F., Jaouen, P., Pruvost, J., Grizeau, D., Van Vooren, G., Bourseau, P., 2012. Development and validation of a minimal growth medium for recycling *Chlorella vulgaris* culture. *Bioresour. Technol.* 123, 366–374. <https://doi.org/10.1016/j.biortech.2012.07.085>
- Halter, M., Elliott, J.T., Hubbard, J.B., Tona, A., Plant, A.L., 2009. Cell volume distributions reveal cell growth rates and division times. *J. Theor. Biol.* 257, 124–130.
<https://doi.org/10.1016/J.JTBI.2008.10.031>
- Hamer, P.W., McGeachie, J.M., Davies, M.J., Grounds, M.D., 2002. Evans Blue Dye as an in vivo marker of myofibre damage: Optimising parameters for detecting initial myofibre membrane permeability. *J. Anat.* 200, 69–79. <https://doi.org/10.1046/j.0021-8782.2001.00008.x>
- Harrop, A.J., Woodley, J.M., Lilly, M.D., 1992. Production of naphthalene-cis-glycol by *Pseudomonas putida* in the presence of organic solvents, *Enzyme and Microbial Technology*. [https://doi.org/10.1016/0141-0229\(92\)90112-2](https://doi.org/10.1016/0141-0229(92)90112-2)
- Harvey, P.J., Ben-Amotz, A., 2020. Towards a sustainable *Dunaliella salina* microalgal biorefinery for 9-cis β -carotene production. *Algal Res.* 50, 102002.
<https://doi.org/10.1016/j.algal.2020.102002>
- Hejazi, M., 2003. Milking of microalgae: Production and selective extraction of Beta-carotene in two-phase bioreactors.
- Hejazi, M.A., Andrysiewicz, E., Tramper, J., Wijffels, R.H., 2003. Effect of Mixing Rate on β -Carotene Production and Extraction by *Dunaliella Salina* in Two-Phase Bioreactors. *Biotechnol. Bioeng.* 84, 591–596. <https://doi.org/10.1002/bit.10791>
-

Bibliography

- Hejazi, M.A., De Lamarliere, C., Rocha, J.M.S., Vermuë, M., Tramper, J., Wijffels, R.H., 2002. Selective extraction of carotenoids from the microalga *Dunaliella salina* with retention of viability. *Biotechnol. Bioeng.* 79, 29–36. <https://doi.org/10.1002/bit.10270>
- Hejazi, M.A., Kleinegris, D., Wijffels, R.H., 2004. Mechanism of extraction of β -carotene from microalga *Dunaliella salina* in two-phase bioreactors. *Biotechnol. Bioeng.* 88, 593–600. <https://doi.org/10.1002/bit.20238>
- Hejazi, M.A., Wijffels, R.H., 2003. Effect of light intensity on β -carotene production and extraction by *Dunaliella salina* in two-phase bioreactors, in: *Biomolecular Engineering*. Elsevier, pp. 171–175. [https://doi.org/10.1016/S1389-0344\(03\)00046-7](https://doi.org/10.1016/S1389-0344(03)00046-7)
- Helena, S., Zainuri, M., Suprijanto, J., 2016. Microalgae *Dunaliella salina* (Teodoresco, 1905) Growth Using the LED Light (Light Limiting Diode) and Different Media. *Aquat. Procedia* 7, 226–230. <https://doi.org/10.1016/j.aqpro.2016.07.031>
- Hirano, K., Hara, T., Ardianor, Nugroho, R.A., Segah, H., Takayama, N., Sulmin, G., Komai, Y., Okada, S., Kawamura, K., 2019. Detection of the oil-producing microalga *Botryococcus braunii* in natural freshwater environments by targeting the hydrocarbon biosynthesis gene SSL-3. *Sci. Rep.* 9. <https://doi.org/10.1038/s41598-019-53619-y>
- Ho, T.Y., Quigg, A., Finkel, Z. V., Milligan, A.J., Wyman, K., Falkowski, P.G., Morel, F.M.M., 2003. The elemental composition of some marine phytoplankton. *J. Phycol.* 39, 1145–1159. <https://doi.org/10.1111/j.0022-3646.2003.03-090.x>
- Horiuchi, J.-I., Ohba, I., Tada, K., Kobayashi, M., Kanno, T., Kishimoto, M., 2003. Effective cell harvesting of the halotolerant microalga *Dunaliella tertiolecta* with pH control. *J. Biosci. Bioeng.* 95, 412–415. [https://doi.org/10.1016/S1389-1723\(03\)80078-6](https://doi.org/10.1016/S1389-1723(03)80078-6)
- Hoshaw, R.W., Maluf, L.Y., 1981. Ultrastructure of the green flagellate *Dunaliella tertiolecta*
-

Bibliography

- (Chlorophyceae, Volvocales) with comparative notes on three other species. *Phycologia* 20, 199–206. <https://doi.org/10.2216/i0031-8884-20-2-199.1>
- Hosseini Tafreshi, A., Shariati, M., 2009. *Dunaliella* biotechnology: Methods and applications. *J. Appl. Microbiol.* 107, 14–35. <https://doi.org/10.1111/j.1365-2672.2009.04153.x>
- Hyka, P., Lickova, S., Přibyl, P., Melzoch, K., Kovar, K., 2013. Flow cytometry for the development of biotechnological processes with microalgae. *Biotechnol. Adv.* 31, 2–16. <https://doi.org/10.1016/j.biotechadv.2012.04.007>
- Iglina, T., Iglin, P., Pashchenko, D., 2022. Industrial CO₂ Capture by Algae: A Review and Recent Advances. *Sustain.* 14. <https://doi.org/10.3390/su14073801>
- INRA, 2021. Plateforme Logicielle Cépia - Morphologie de particules [WWW Document]. URL <https://www.pfl-cepia.inra.fr/index.php?page=tutoImg-morphologie> (accessed 10.11.21).
- Jamers, A., Lenjou, M., Deraedt, P., van Bockstaele, D., Blust, R., de Coen, W., 2009. Flow cytometric analysis of the cadmium-exposed green alga *Chlamydomonas reinhardtii* (chlorophyceae). *Eur. J. Phycol.* 44, 541–550. <https://doi.org/10.1080/09670260903118214>
- Joannes, C., Sipaut, C.S., Dayou, J., Yasir, S.M., Mansa, R.F., 2015. The potential of using pulsed electric field (PEF) technology as the cell disruption method to extract lipid from microalgae for biodiesel production. *Int. J. Renew. Energy Res.* 5, 598–621. <https://doi.org/10.20508/ijrer.20627>
- Johnson, M.K., Johnson, E.J., MacElroy, R.D., Speer, H.L., Bruff, B.S., 1968. Effects of salts on the halophilic alga *Dunaliella viridis*. *J. Bacteriol.* 95, 1461–1468. <https://doi.org/10.1128/jb.95.4.1461-1468.1968>
- Joyard, J., Morot-Gaudry, J.-F., 2020. Shedding light on photosynthesis. *Encycl.*
-

Bibliography

- l'Environnement, [en ligne ISSN 2555-0950] url <http://www.encyclopedie-environnement.org/?p=10812>.
- Khademi, H., Morowvat, M.H., Ghasemi, Y., 2018. Effects of Nitrogen and Sulfur Deprivation on β -Carotene and Fatty Acid content of *Dunaliella salina*. *Trends Pharm. Sci.* 4, 187–196.
- Khoo, K.S., Leong, H.Y., Chew, K.W., Lim, J.W., Ling, T.C., Show, P.L., Yen, H.W., 2020. Liquid biphasic system: A recent bioseparation technology. *Processes* 8. <https://doi.org/10.3390/pr8020149>
- Kleinegris, D.M.M., Janssen, M., Brandenburg, W.A., Wijffels, R.H., 2011a. Continuous production of carotenoids from *Dunaliella salina*. *Enzyme Microb. Technol.* 48, 253–259. <https://doi.org/10.1016/j.enzmictec.2010.11.005>
- Kleinegris, D.M.M., Janssen, M., Brandenburg, W.A., Wijffels, R.H., 2010a. The selectivity of milking of *dunaliella salina*. *Mar. Biotechnol.* 12, 14–23. <https://doi.org/10.1007/s10126-009-9195-0>
- Kleinegris, D.M.M., van Es, M.A., Janssen, M., Brandenburg, W.A., Wijffels, R.H., 2011b. Phase toxicity of dodecane on the microalga *Dunaliella salina*. *J. Appl. Phycol.* 23, 949–958. <https://doi.org/10.1007/s10811-010-9615-6>
- Kleinegris, D.M.M., van Es, M.A., Janssen, M., Brandenburg, W.A., Wijffels, R.H., 2010b. Carotenoid fluorescence in *Dunaliella salina*. *J. Appl. Phycol.* 22, 645–649. <https://doi.org/10.1007/s10811-010-9505-y>
- Koller, M., 2015. Design of Closed Photobioreactors for Algal Cultivation. *Algal Biorefineries Vol. 2 Prod. Refin. Des.* 133–186. https://doi.org/10.1007/978-3-319-20200-6_4
- Kunal Ahuja, Amit Rawat, 2021. Beta Carotene Market outlook 2021-2027 | Industry Statistics.
-

Bibliography

- Lamers, P.P., Janssen, M., De Vos, R.C.H., Bino, R.J., Wijffels, R.H., 2012. Carotenoid and fatty acid metabolism in nitrogen-starved *Dunaliella salina*, a unicellular green microalga. *J. Biotechnol.* 162, 21–27. <https://doi.org/10.1016/j.jbiotec.2012.04.018>
- Lamers, P.P., Janssen, M., De Vos, R.C.H., Bino, R.J., Wijffels, R.H., 2008. Exploring and exploiting carotenoid accumulation in *Dunaliella salina* for cell-factory applications. *Trends Biotechnol.* 26, 631–638. <https://doi.org/10.1016/j.tibtech.2008.07.002>
- Lamers, P.P., Van De Laak, C.C.W., Kaasenbrood, P.S., Lorier, J., Janssen, M., De Vos, R.C.H., Bino, R.J., Wijffels, R.H., 2010. Carotenoid and fatty acid metabolism in light-stressed *Dunaliella salina*. *Biotechnol. Bioeng.* 106, 638–648. <https://doi.org/10.1002/bit.22725>
- León, R., Garbayo, I., Hernández, R., Vígara, J., Vilchez, C., 2001. Organic solvent toxicity in photoautotrophic unicellular microorganisms. *Enzyme Microb. Technol.* 29, 173–180. [https://doi.org/10.1016/S0141-0229\(01\)00370-2](https://doi.org/10.1016/S0141-0229(01)00370-2)
- León, R., Martín, M., Vígara, J., Vilchez, C., Vega, J.M., 2003. Microalgae mediated photoproduction of β -carotene in aqueous-organic two phase systems. *Biomol. Eng.* 20, 177–182. [https://doi.org/10.1016/S1389-0344\(03\)00048-0](https://doi.org/10.1016/S1389-0344(03)00048-0)
- Leonardi, P.I., Cáceres, E.J., 1997. Light and electronmicroscope observations of the life cycle of *Dunaliella salina*(Polyblepharidaceae, Chlorophyceae). *Nov. Hedwigia* 621–633. <https://doi.org/10.1127/NOVA.HEDWIGIA/64/1997/621>
- Lers, A., Biener, Y., Zamir, A., 1990. Photoinduction of massive β -carotene accumulation by the alga *Dunaliella bardawil*: Kinetics and dependence on gene activation. *Plant Physiol.* 93, 389–395. <https://doi.org/10.1104/pp.93.2.389>
- Li, Z., Li, Y., Zhang, X., Tan, T., 2015. Lipid extraction from non-broken and high water content microalgae *Chlorella* spp. by three-phase partitioning. *Algal Res.* 10, 218–223.
-

<https://doi.org/10.1016/j.algal.2015.04.021>

Lichthentaler, H.K., Wellburn, A.R., 1983. Determinations of total carotenoids and chlorophylls a and b of leaf extracts in different solvents. *Biochem. Soc. Trans.* 11, 591–592.

<https://doi.org/10.1042/bst0110591>

Lindblad, P., Fuente, D., Borbe, F., Cicchi, B., Conejero, J.A., Couto, N., Čelešnik, H., Diano, M.M., Dolinar, M., Esposito, S., Evans, C., Ferreira, E.A., Keller, J., Khanna, N., Kind, G., Landels, A., Lemus, L., Noirel, J., Ocklenburg, S., Oliveira, P., Pacheco, C.C., Parker, J.L., Pereira, J., Pham, T.K., Pinto, F., Rexroth, S., Rögner, M., Schmitz, H.J., Benavides, A.M.S., Siurana, M., Tamagnini, P., Touloupakis, E., Torzillo, G., Urchueguía, J.F., Wegelius, A., Wiegand, K., Wright, P.C., Wutschel, M., Wünschiers, R., 2019. CyanoFactory, a European consortium to develop technologies needed to advance cyanobacteria as chassis for production of chemicals and fuels. *Algal Res.* 41.

<https://doi.org/10.1016/J.ALGAL.2019.101510>

Lorente De Nó, R., 1934. Studies on the structure of the cerebral cortex. II. Continuation of the study of the ammonic system. *J. für Psychol. und Neurol.* 46, 113–117.

Luengo, E., Condón-Abanto, S., Álvarez, I., Raso, J., 2014. Effect of Pulsed Electric Field Treatments on Permeabilization and Extraction of Pigments from *Chlorella vulgaris*. *J. Membr. Biol.* 247, 1269–1277.

<https://doi.org/10.1007/s00232-014-9688-2>

Lund, J.W.G., Kipling, C., Le Cren, E.D., 1958. The inverted microscope method of estimating algal numbers and the statistical basis of estimations by counting. *Hydrobiologia* 11, 143–

170. <https://doi.org/10.1007/BF00007865>

Lv, H., Cui, X., Wahid, F., Xia, F., Zhong, C., Jia, S., 2016. Analysis of the physiological and molecular responses of *Dunaliella salina* to macronutrient deprivation. *PLoS One* 11, 1–19.

Bibliography

<https://doi.org/10.1371/journal.pone.0152226>

Lv, H., Qiao, C., Zhong, C., Jia, S., 2018. Metabolic fingerprinting of *Dunaliella salina* cultured under sulfur deprivation conditions. *J. Appl. Phycol.* 30, 355–365.

<https://doi.org/10.1007/s10811-017-1230-3>

Marín, N., Morales, F., Lodeiros, C., Tamigneaux, E., 1998. Effect of nitrate concentration on growth and pigment synthesis of *Dunaliella salina* cultivated under low illumination and preadapted to different salinities. *J. Appl. Phycol.* 1998 104 10, 405–411.

<https://doi.org/10.1023/A:1008017928651>

Marino, T., Casella, P., Sangiorgio, P., Verardi, A., Ferraro, A., Hristoforou, E., Molino, A., Musmarra, D., 2020. Natural beta-carotene: A microalgae derivate for nutraceutical applications. *Chem. Eng. Trans.* 79, 103–108. <https://doi.org/10.3303/CET2079018>

Masuda, T., Melis, A., 2002. Biosynthesis and Distribution of Chlorophyll among the Photosystems during Recovery of the Green Alga. *Society* 128, 603–614.

<https://doi.org/10.1104/pp.010595.1>

McIntosh, T.J., Simon, S.A., MacDonald, R.C., 1980. The organization of n-alkanes in lipid bilayers. *BBA - Biomembr.* 597, 445–463. [https://doi.org/10.1016/0005-2736\(80\)90219-9](https://doi.org/10.1016/0005-2736(80)90219-9)

Metzger, P., Largeau, C., 2005. *Botryococcus braunii*: A rich source for hydrocarbons and related ether lipids. *Appl. Microbiol. Biotechnol.* <https://doi.org/10.1007/s00253-004-1779-z>

Miazek, K., Kratky, L., Sulc, R., Jirout, T., Aguedo, M., Richel, A., Goffin, D., 2017. Effect of organic solvents on microalgae growth, metabolism and industrial bioproduct extraction: A review. *Int. J. Mol. Sci.* 18, 1429. <https://doi.org/10.3390/ijms18071429>

Mie, A., Andersen, H.R., Gunnarsson, S., Kahl, J., Kesse-Guyot, E., Rembiałkowska, E.,

- Quaglio, G., Grandjean, P., 2017. Human health implications of organic food and organic agriculture: a comprehensive review. *Environ. Heal.* 2017 161 16, 1–22. <https://doi.org/10.1186/S12940-017-0315-4>
- Mimouni, V., Ulmann, L., Pasquet, V., Mathieu, M., Picot, L., Bougaran, G., Cadoret, J.-P., Morant-Manceau, A., Schoefs, B., 2012. The Potential of Microalgae for the Production of Bioactive Molecules of Pharmaceutical Interest. *Curr. Pharm. Biotechnol.* 13, 2733–2750. <https://doi.org/10.2174/138920112804724828>
- Moheimani, N.R., Cord-Ruwisch, R., Raes, E., Borowitzka, M.A., 2013. Non-destructive oil extraction from *Botryococcus braunii* (Chlorophyta). *J. Appl. Phycol.* 25, 1653–1661. <https://doi.org/10.1007/s10811-013-0012-9>
- Mojaat Guemir, M., 2008. Production par *Dunaliella salina* et extraction en continu de β -carotène par couplage d'un photobioréacteur et d'une chromatographie de partage centrifuge.
- Mojaat, M., Foucault, A., Pruvost, J., Legrand, J., 2008. Optimal selection of organic solvents for biocompatible extraction of β -carotene from *Dunaliella salina*. *J. Biotechnol.* 133, 433–441. <https://doi.org/10.1016/j.jbiotec.2007.11.003>
- Molina Grima, E., Belarbi, E.H., Acién Fernández, F.G., Robles Medina, A., Chisti, Y., 2003. Recovery of microalgal biomass and metabolites: Process options and economics. *Biotechnol. Adv.* 20, 491–515. [https://doi.org/10.1016/S0734-9750\(02\)00050-2](https://doi.org/10.1016/S0734-9750(02)00050-2)
- Nezammahalleh, H., Nosrati, M., Ghanati, F., Shojaosadati, S.A., 2017. Exergy-based screening of biocompatible solvents for in situ lipid extraction from *Chlorella vulgaris*. *J. Appl. Phycol.* 29, 89–103. <https://doi.org/10.1007/s10811-016-0921-5>
- Nikolova, P., Ward, O.P., 1993. Whole cell biocatalysis in nonconventional media. *J. Ind. Microbiol.* 12, 76–86. <https://doi.org/10.1007/BF01569905>
-

Bibliography

- Oren, A., 2005. A hundred years of *Dunaliella* research: 1905-2005. *Saline Systems* 1, 2–2. <https://doi.org/10.1186/1746-1448-1-2>
- Orset, S., Young, A.J., 1999. Low-temperature-induced synthesis of α -carotene in the microalga *Dunaliella salina* (Chlorophyta). *J. Phycol.* 35, 520–527. <https://doi.org/10.1046/j.1529-8817.1999.3530520.x>
- Oxygen electrodes | Electroanalytical techniques [WWW Document], n.d. URL https://biocyclopedia.com/index/chem_lab_methods/oxygen_electrodes.php (accessed 11.2.21).
- Paalme, T., Elken, R., Kahru, A., Vanatalu, K., Vilu, R., 1997. The growth rate control in *Escherichia coli* at near to maximum growth rates: The A-stat approach. *Antonie van Leeuwenhoek, Int. J. Gen. Mol. Microbiol.* 71, 217–230. <https://doi.org/10.1023/A:1000198404007>
- Pasqualetti, M., Bernini, R., Carletti, L., Crisante, F., Tempesta, S., 2010. Salinity and nitrate concentration on the growth and carotenoids accumulation in a strain of *Dunaliella salina* (Chlorophyta) cultivated under laboratory conditions. *Transitional Waters Bull.* 4, 94–104. <https://doi.org/10.1285/i1825229Xv4n2p94>
- Perrin, D., Examiner-John Rollins, A.W., 1985. Process for producing a naturally-derived carotene/oil composition by direct extraction from algae. *Bailey's Ind. Oil Fat Prod.* 1, 69.
- Phadwal, K., Singh, P.K., 2003. Effect of nutrient depletion on β -carotene and glycerol accumulation in two strains of *Dunaliella* sp. *Bioresour. Technol.* 90, 55–58. [https://doi.org/10.1016/S0960-8524\(03\)00090-7](https://doi.org/10.1016/S0960-8524(03)00090-7)
- Phillips, L.G., Cowan, A.K., Rose, P.D., Logie, M.R.R., 1995. Operation of the Xanthophyll Cycle in Non-Stressed and Stressed Cells of *Dunaliella salina* Teod. in Response to Diurnal
-

Bibliography

- Changes in Incident Irradiation: A Correlation with Intracellular β -Carotene Content. *J. Plant Physiol.* 146, 547–553. [https://doi.org/10.1016/S0176-1617\(11\)82022-5](https://doi.org/10.1016/S0176-1617(11)82022-5)
- Polle, J.E.W., Roth, R., Ben-Amotz, A., Goodenough, U., 2020. Ultrastructure of the green alga *Dunaliella salina* strain CCAP19/18 (Chlorophyta) as investigated by quick-freeze deep-etch electron microscopy. *Algal Res.* 49, 101953. <https://doi.org/10.1016/j.algal.2020.101953>
- Pourkarimi, S., Hallajisani, A., Nouralishahi, A., Alizadehdakhel, A., Golzary, A., 2020. Factors affecting production of beta-carotene from *Dunaliella salina* microalgae. *Biocatal. Agric. Biotechnol.* 29, 101771. <https://doi.org/10.1016/j.bcab.2020.101771>
- Praveenkumar, R., Gwak, R., Kang, M., Shim, T.S., Cho, S., Lee, J., Oh, Y.K., Lee, K., Kim, B., 2015. Regenerative Astaxanthin Extraction from a Single Microalgal (*Haematococcus pluvialis*) Cell Using a Gold Nano-Scalpel. *ACS Appl. Mater. Interfaces* 7, 22702–22708. <https://doi.org/10.1021/acsami.5b07651>
- Priyanka, S., Kirubakaran, R., Mary Leema, J.T., 2020. Optimization of Algal Culture Medium for Zeaxanthin Production by *Dunaliella tertiolecta*: An RSM based Approach. *Curr. Sci.* 119, 1997. <https://doi.org/10.18520/cs/v119/i12/1997-2005>
- Pruvost, J., Cornet, J.-F., 2012. Knowledge models for the engineering and optimization of photobioreactors, *Microalgal Biotechnology: Potential and Production.* <https://doi.org/10.1515/9783110225020.181>
- Pruvost, J., Cornet, J.-F., Pilon, L., 2016. Large-Scale Production of Algal Biomass: Photobioreactors 10. https://doi.org/10.1007/978-3-319-12334-9_3i
- Pulz, O., 2001. Photobioreactors: Production systems for phototrophic microorganisms. *Appl. Microbiol. Biotechnol.* 57, 287–293. <https://doi.org/10.1007/S002530100702>
-

Bibliography

- Rajvanshi, M., Sagaram, U.S., Subhash, G.V., Krishna Kumar, G.R., Kumar, C., Govindachary, S., Dasgupta, S., 2019. Biomolecules from Microalgae for Commercial Applications, Sustainable Downstream Processing of Microalgae for Industrial Application. <https://doi.org/10.1201/9780429027970-1>
- Ramachandra, T. V, Mahapatra, D.M., Karthick, B., Gordon, R., 2009. Milking diatoms for sustainable energy: Biochemical engineering versus gasoline-secreting diatom solar panels. *Ind. Eng. Chem. Res.* 48, 8769–8788. <https://doi.org/10.1021/ie900044j>
- Roháček, K., 2010. Method for resolution and quantification of components of the non-photochemical quenching (qN). *Photosynth. Res.* 105, 101–113. <https://doi.org/10.1007/s11120-010-9564-6>
- Roháček, K., Bertrand, M., Moreau, B., Jacquette, B., Caplat, C., Morant-Manceau, A., Schoefs, B., 2014. Relaxation of the non-photochemical chlorophyll fluorescence quenching in diatoms: Kinetics, components and mechanisms. *Philos. Trans. R. Soc. B Biol. Sci.* 369. <https://doi.org/10.1098/rstb.2013.0241>
- Roháček, K., Soukupová, J., Barták, M., 2008. Chlorophyll fluorescence: a wonderful tool to study plant physiology and plant stress, *Plant Cell Compartments - Selected Topics*.
- Saha, S.K., Moane, S., Murray, P., 2013. Effect of macro- and micro-nutrient limitation on superoxide dismutase activities and carotenoid levels in microalga *Dunaliella salina* CCAP 19/18. *Bioresour. Technol.* 147, 23–28. <https://doi.org/10.1016/j.biortech.2013.08.022>
- Salguero, A., León, R., Mariotti, A., De La Morena, B., Vega, J.M., Vílchez, C., 2005. UV-A mediated induction of carotenoid accumulation in *Dunaliella bardawil* with retention of cell viability. *Appl. Microbiol. Biotechnol.* 66, 506–511. <https://doi.org/10.1007/s00253-004-1711-6>
-

Bibliography

- Salter, G.J., Kelt, D.B., 1995. Solvent selection for whole cell biotransformations in organic media. *Crit. Rev. Biotechnol.* 15, 139–177. <https://doi.org/10.3109/07388559509147404>
- Sathasivam, R., Juntawong, N., 2013. Modified medium for enhanced growth of *Dunaliella* strains. *Int J Curr Sci* 5, 67–73. <https://doi.org/10.13140/2.1.1362.4326>
- Sato, M., Murata, Y., Mizusawa, M., Iwahashi, H., Oka, S., 2004. A simple and rapid dual-fluorescence viability assay for microalgae. *Microbiol Cult Coll* 20, 53–59.
- Scarsini, M., Marchand, J., Manoylov, K.M., Schoefs, B., 2019. Photosynthesis in Diatoms. *Diatoms Fundam. Appl.* 191–211. <https://doi.org/10.1002/9781119370741.CH8>
- Scarsini, M., Marchand, J., Schoefs, B., 2020. Carotenoid Overproduction in Microalgae: Biochemical and Genetic Engineering, in: *Pigments from Microalgae Handbook*. Springer International Publishing, Cham, pp. 81–126. https://doi.org/10.1007/978-3-030-50971-2_5
- Shaish, A., Avron, M., Pick, U., Ben-Amotz, A., 1993. Are active oxygen species involved in induction of β -carotene in *Dunaliella bardawil*? *Planta* 190, 363–368. <https://doi.org/10.1007/BF00196965>
- Shapiro, H.M., 2005. Using Flow Cytometers: Applications, Extensions, and Alternatives, in: *Practical Flow Cytometry*. John Wiley & Sons, Inc., Hoboken, NJ, USA, pp. 443–542. <https://doi.org/10.1002/0471722731.ch10>
- Shete, V., Quadro, L., 2013. Mammalian metabolism of β -carotene: Gaps in knowledge. *Nutrients* 5, 4849–4868. <https://doi.org/10.3390/NU5124849>
- Sikkema, J., De Bont, J.A.M., Poolman, B., 1995. Mechanisms of membrane toxicity of hydrocarbons. *Microbiol. Rev.* 59, 201–222. [https://doi.org/0146-0749/95/\\$04.00+0](https://doi.org/0146-0749/95/$04.00+0)
- Sikkema, J., Poolman, B., Konings, W.N., De Bont, J.A.M., 1992. Effects of the membrane
-

Bibliography

- action of tetralin on the functional and structural properties of artificial and bacterial membranes. *J. Bacteriol.* 174, 2986–2992. <https://doi.org/10.1128/jb.174.9.2986-2992.1992>
- Solymosi, K., Latruffe, N., Morant-Manceau, A., Schoefs, B., 2015. Food colour additives of natural origin, *Colour Additives for Foods and Beverages*. <https://doi.org/10.1016/B978-1-78242-011-8.00001-5>
- Sourkes, T.L., 2009. The discovery and early history of carotene. *Bull. Hist. Chem* 34, 33.
- Subba Rao, D., 2009. Cultivation, Growth Media, Division Rates and Applications of *Dunaliella* Species. *Alga Dunaliella* 45–89. <https://doi.org/10.1201/B10300-4>
- Sun, J., Liu, D., 2003. Geometric models for calculating cell biovolume and surface area for phytoplankton. *J. Plankton Res.* 25, 1331–1346. <https://doi.org/10.1093/plankt/fbg096>
- Syed, M.S., Rafeie, M., Vandamme, D., Asadnia, M., Henderson, R., Taylor, R.A., Warkiani, M.E., 2018. Selective separation of microalgae cells using inertial microfluidics. *Bioresour. Technol.* 252, 91–99. <https://doi.org/10.1016/j.biortech.2017.12.065>
- Takahashi, T., 2020. Potential of an automated- and image-based cell counter to accelerate microalgal research and applications. *Energies* 13. <https://doi.org/10.3390/en13226019>
- Takaichi, S., 2011. Carotenoids in algae: Distributions, biosyntheses and functions. *Mar. Drugs* 9, 1101–1118. <https://doi.org/10.3390/md9061101>
- Taleb, A., 2015. Production de biodiesel à partir des microalgues : recherche des souches accumulatrices des lipides et optimisation des conditions de culture en photobioréacteurs. <http://www.theses.fr>.
- Tanaka, Y., 1990. Vacuum-packed food containing *dunaliella* algae and process for the
-

Bibliography

production thereof.

Tashyreva, D., Elster, J., Billi, D., 2013. A Novel Staining Protocol for Multiparameter Assessment of Cell Heterogeneity in Phormidium Populations (Cyanobacteria) Employing Fluorescent Dyes. *PLoS One* 8, e55283. <https://doi.org/10.1371/JOURNAL.PONE.0055283>

Teodoresco, E.C., 1905. Organisation et developpement du *Dunaliella*, nouveau genre de Volvocacee-Polyblepharidee. *Bot Zentralbl Beih* 18, 215–232.

Torregrosa-Crespo, J., Montero, Z., Fuentes, J.L., García-Galbis, M.R., Garbayo, I., Vílchez, C., Martínez-Espinosa, R.M., 2018. Exploring the Valuable Carotenoids for the Large-Scale Production by Marine Microorganisms. *Mar. Drugs* 16. <https://doi.org/10.3390/MD16060203>

Uriarte, I., Farías, A., Hawkins, A.J.S., Bayne, B.L., 1993. Cell characteristics and biochemical composition of *Dunaliella primolecta* Butcher conditioned at different concentrations of dissolved nitrogen. *J. Appl. Phycol.* 1993 54 5, 447–453. <https://doi.org/10.1007/BF02182737>

Varsano, T., Kaftan, D., Pick, U., 2003. Effects of iron deficiency on thylakoid membrane structure and composition in the alga *Dunaliella salina*. *J. Plant Nutr.* 26, 2197–2210. <https://doi.org/10.1081/PLN-120024275>

Veldhuis, M., Kraay, G., Timmermans, K., 2001. Cell death in phytoplankton: Correlation between changes in membrane permeability, photosynthetic activity, pigmentation and growth. *Eur. J. Phycol.* 36, 167–177. <https://doi.org/10.1080/09670260110001735318>

Vinayak, V., Gordon, R., Gautam, S., Rai, A., 2014. Discovery of a diatom that oozes oil. *Adv. Sci. Lett.* 20, 1256–1267. <https://doi.org/10.1166/asl.2014.5591>

Bibliography

- Vinayak, V., Kumar, V., Kashyap, M., Joshi, K.B., Gordon, R., Schoefs, B., 2017. Fabrication of resonating microfluidic chamber for biofuel production in diatoms (Resonating device for biofuel production), in: 2016 3rd International Conference on Emerging Electronics, ICEE 2016. Institute of Electrical and Electronics Engineers Inc. <https://doi.org/10.1109/ICEmElec.2016.8074628>
- Vinayak, V., Manoylov, K.M., Gateau, H., Blanckaert, V., Hérault, J., Pencreac'H, G., Marchand, J., Gordon, R., Schoefs, B., 2015. Diatom milking? A review and new approaches. *Mar. Drugs* 13, 2629–2665. <https://doi.org/10.3390/md13052629>
- Wongsansilp, T., Juntawong, N., Wu, Z., 2016. Effects of phosphorus on the growth and chlorophyll fluorescence of a *Dunaliella salina* strain isolated from saline soil under nitrate limitation. *J. Biol. Res.* 89, 51–55. <https://doi.org/10.4081/jbr.2016.5866>
- Xu, F., Yuan, Q.P., Zhu, Y., 2007. Improved production of lycopene and β -carotene by *Blakeslea trispora* with oxygen-vectors. *Process Biochem.* 42, 289–293. <https://doi.org/10.1016/j.procbio.2006.08.007>
- Xu, Y., Ibrahim, I.M., Harvey, P.J., 2016. The influence of photoperiod and light intensity on the growth and photosynthesis of *Dunaliella salina* (chlorophyta) CCAP 19/30. *Plant Physiol. Biochem.* 106, 305–315. <https://doi.org/10.1016/j.plaphy.2016.05.021>
- Y. Shen, W. Yuan, Z. J. Pei, Q. Wu, E. Mao, 2009. Microalgae Mass Production Methods. *Trans. ASABE* 52, 1275–1287. <https://doi.org/10.13031/2013.27771>
- Yao, S., Lu, J., Sárossy, Z., Baggesen, C., Brandt, A., An, Y., 2016. Neutral lipid production in *Dunaliella salina* during osmotic stress and adaptation. *J. Appl. Phycol.* 28, 2167–2175. <https://doi.org/10.1007/s10811-016-0794-7>
- Ye, Z.W., Jiang, J.G., Wu, G.H., 2008. Biosynthesis and regulation of carotenoids in *Dunaliella*:
-

Bibliography

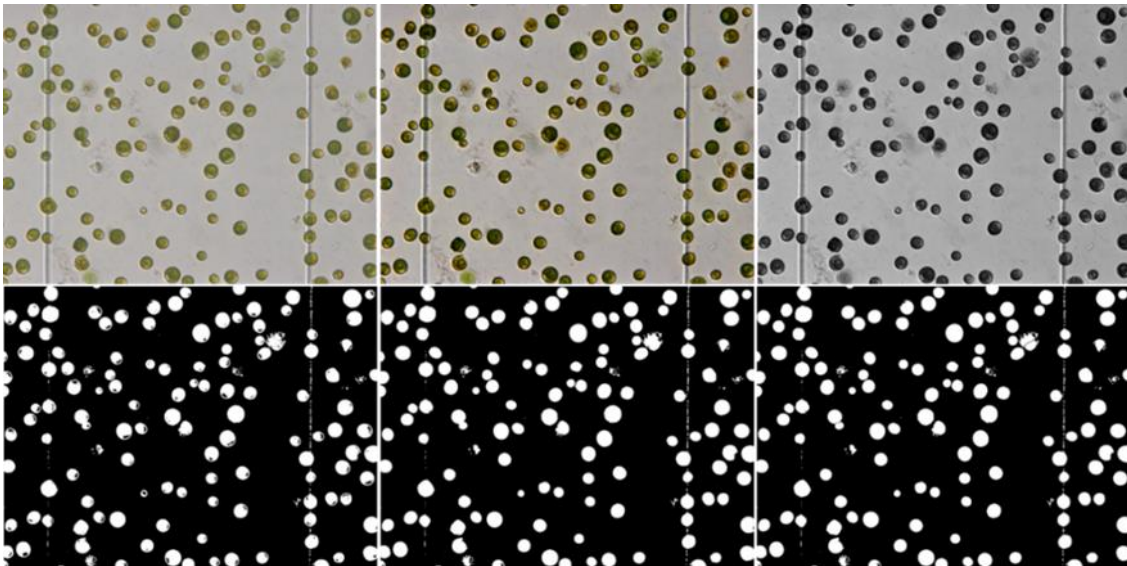
- Progresses and prospects. *Biotechnol. Adv.* 26, 352–360.
<https://doi.org/10.1016/j.biotechadv.2008.03.004>
- Ying, K., Gilmour, D.J., Zimmerman, W.B., 2014. Effects of CO₂ and pH on growth of the microalga *Dunaliella salina*. *J. Microb. Biochem. Technol.* 6, 167–173.
<https://doi.org/10.4172/1948-5948.1000138>
- Zarauz, L., Irigoien, X., 2008. Effects of Lugol's fixation on the size structure of natural nano-microplankton samples, analyzed by means of an automatic counting method. *J. Plankton Res.* 30, 1297–1303. <https://doi.org/10.1093/plankt/fbn084>
- Zetsche, E.M., Meysman, F.J.R., 2012. Dead or alive? Viability assessment of micro- and mesoplankton. *J. Plankton Res.* 34, 493–509. <https://doi.org/10.1093/plankt/fbs018>
- Zhang, F., Cheng, L.H., Xu, X.H., Zhang, L., Chen, H.L., 2013. Application of membrane dispersion for enhanced lipid milking from *Botryococcus braunii* FACHB 357. *J. Biotechnol.* 165, 22–29. <https://doi.org/10.1016/j.jbiotec.2013.02.010>
- Zhang, F., Cheng, L.H., Xu, X.H., Zhang, L., Chen, H.L., 2011. Screening of biocompatible organic solvents for enhancement of lipid milking from *Nannochloropsis* sp. *Process Biochem.* 46, 1934–1941. <https://doi.org/10.1016/j.procbio.2011.06.024>
- Zhang, R., Marchal, L., Lebovka, N., Vorobiev, E., Grimi, N., 2020. Two-step procedure for selective recovery of bio-molecules from microalga *Nannochloropsis oculata* assisted by high voltage electrical discharges. *Bioresour. Technol.* 302, 122893.
<https://doi.org/10.1016/J.BIORTECH.2020.122893>
- Zhu, C.J., Lee, Y.K., 1997. Determination of biomass dry weight of marine microalgae. *J. Appl. Phycol.* 9, 189–194. <https://doi.org/10.1023/A:1007914806640>
-

Appendixes

Appendix 1

Phase A: Image processing

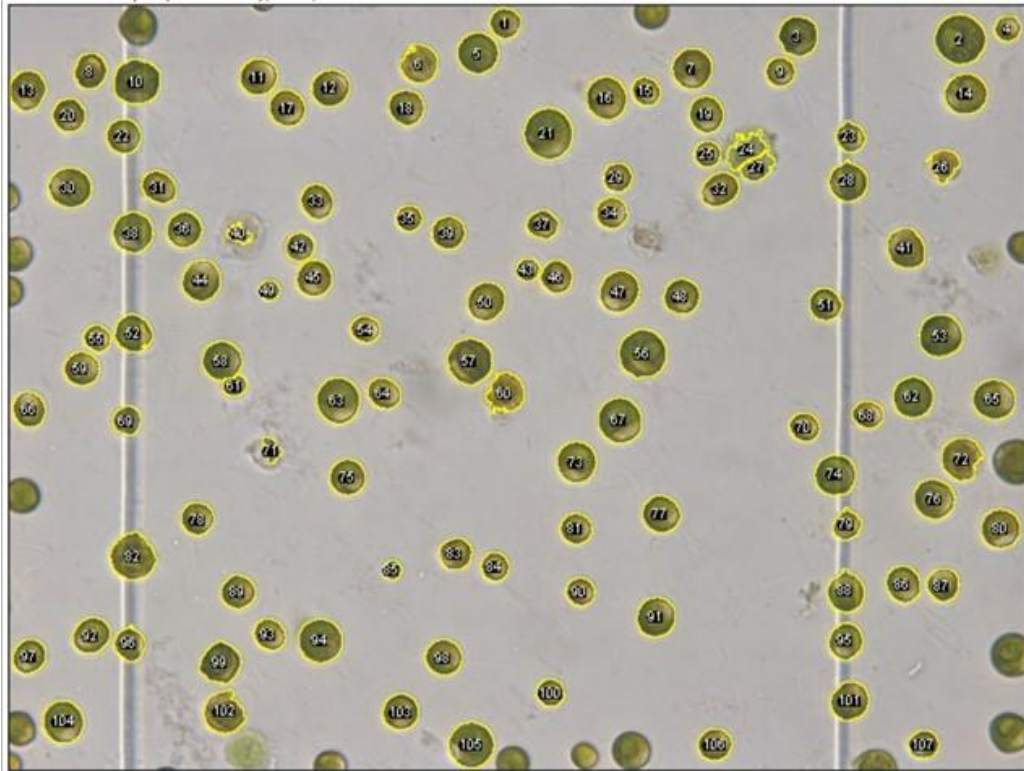
- 1) Import the image sequence
- 2) Enhanced contrast
- 3) Convert to 8-bit
- 4) Convert to black and white
- 5) Separate linked particle
- 6) Fill holes in particle



Appendix

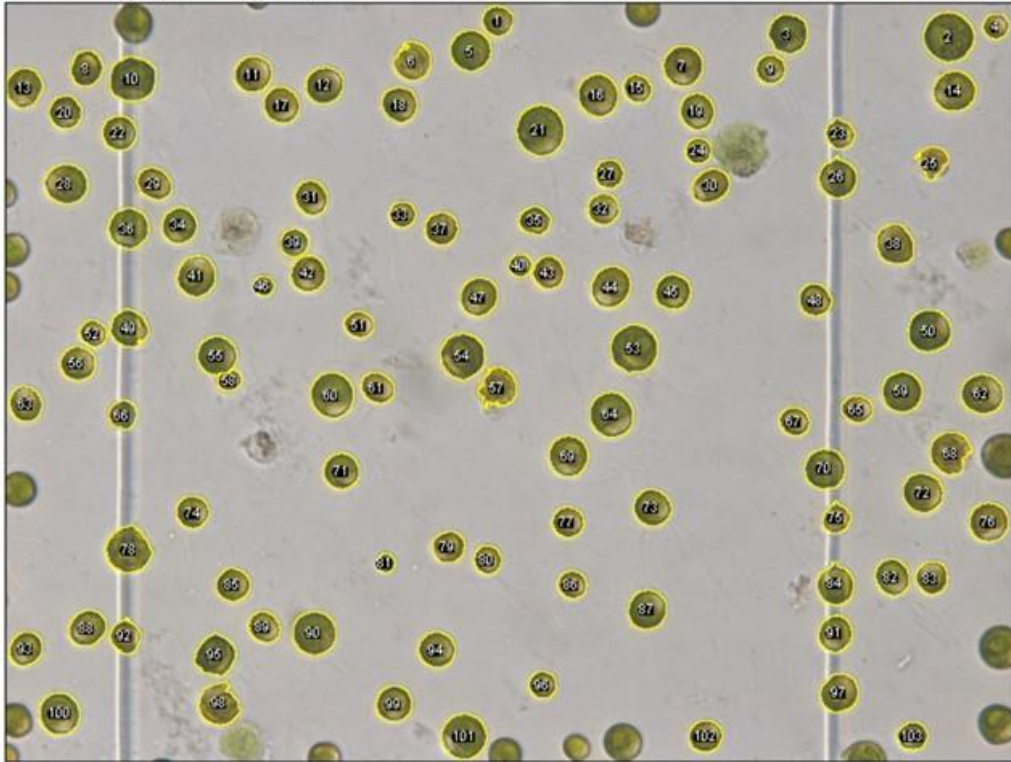
Phase B1: Automatic analysis

- 7) Set scale (was measured with a scale on the image)
- 8) Set the measurement
- 9) Run the particles size=40.00-600.00 circularity=0.00-1.



Phase B2: Manual cleaning

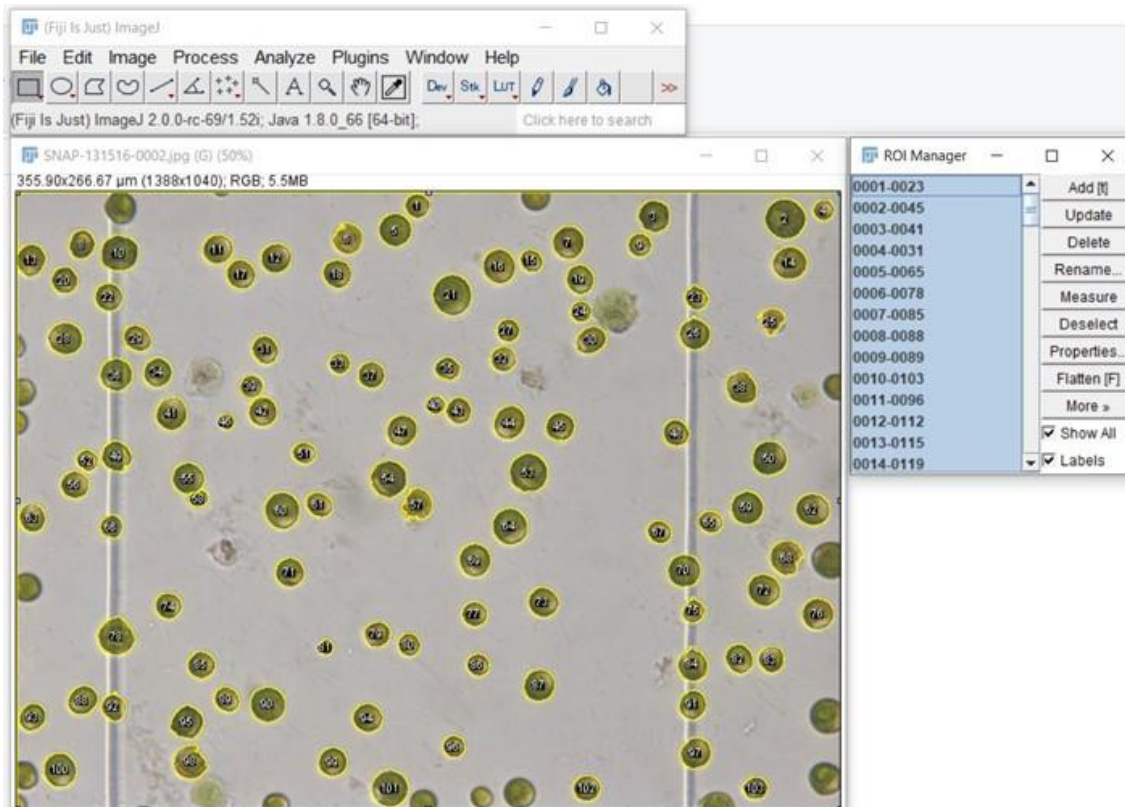
10) Particles n°24, 27, 40 and 71 are removed from picture below



Phase C: Particle analysis

11) Select remaining particles in the “ROI manager”

12) Run the particles analysis



Appendix 2

Fluorescence measurement

Fluorescence principle

The term fluorescence was coined by Stokes circa 1850 to name a phenomenon causing the emission of light at a wavelength longer than the absorbed light (Figure 5.1).

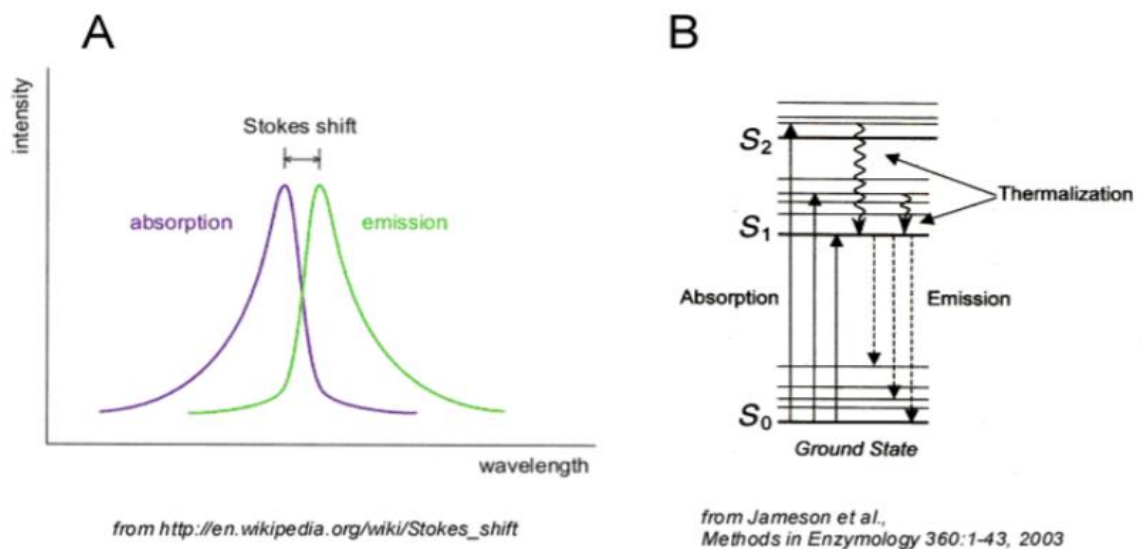


Figure 5.1– The stokes wavelength shift in fluorescence phenomenon, the excited the excited electrons emit a particle with different wavelength.

The fluorescence intensity depends on the laboratory conditions and in particular on the temperature and light perturbation.

Spectrofluorometer

A spectrofluorometer is a device used to measure the characteristic of fluorescence in the visible spectrum: the distribution of intensity regarding the wavelength over the emission spectrum of the sample after the excitation by a certain spectrum of light. It is useful for the detection of the presence or the quantification of a specific molecule in the sample.

Most fluorometers utilize a double beam. These two beams work in association to decrease the noise created by light fluctuations. The upper beam goes through a filter or monochromator before passing through the sample. The lower beam is passed through an attenuator and adjusted to match the fluorescent intensity going out from the sample. Light from the fluorescence of the sample and the attenuated beam are detected by separate photodetector and converted to an electrical signal that is interpreted by a computer system. The fluorometer used was a Fluoromas plus Horiba (Figure 5.2).



Figure 5.2 – A spectrofluorometer Horiba fluoromax plus.

Epifluorescence microscope

A fluorescence microscope is an optical microscope that uses fluorescence to study the properties of a microscopic object. The epifluorescent microscope is the simplest version of fluorescence microscope

The specimen is illuminated with a specific wavelength of light which is absorbed by the molecules sensitive to excitation (fluorophore), causing them to emit light of longer wavelengths.

The excitation light is separated from the emitted fluorescence with the help of spectral filter.

a) Typical components of a fluorescence microscope are a light source (xenon arc lamp or mercury-vapor lamp are common; more advanced forms are high-power LEDs and lasers), the excitation filter, the dichroic mirror (or dichroic beamsplitter), and the emission filter (Figure 5.3a). The filters and the dichroic beamsplitter are chosen to match the spectral excitation and emission characteristics of the fluorophore used to label the specimen. The instrument used was a Nikon TiE eclipse inverted epifluorescence microscope (Figure 5.3b).

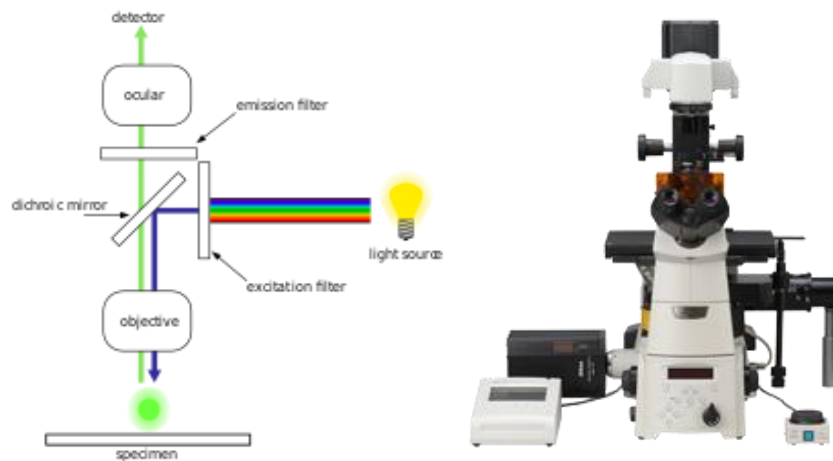


Figure 5.3 – Rays of light in an epifluorescence microscope (a) and a Nikon TiE eclipse inverted epifluorescence microscope (b).

Flow cytometer

A flow cytometer is an instrument used to detect and measure physical and chemical characteristics of a population of cells. In this device, a sample containing a suspension of cells is injected into the detection chamber (Figure5.4a). The light scattered is characteristic to the cells and their components. Cells are often labelled with fluorescent markers so light is absorbed and then emitted in a band of wavelengths. Tens of thousands of cells can be quickly examined, and the data gathered are processed by a computer. Two systems were used: an imaging flow cytometry Amnis Image Stream Mk II (Figure5.4b) and a laser flow cytometer BD Accuri C6 plus (Figure5.4c).

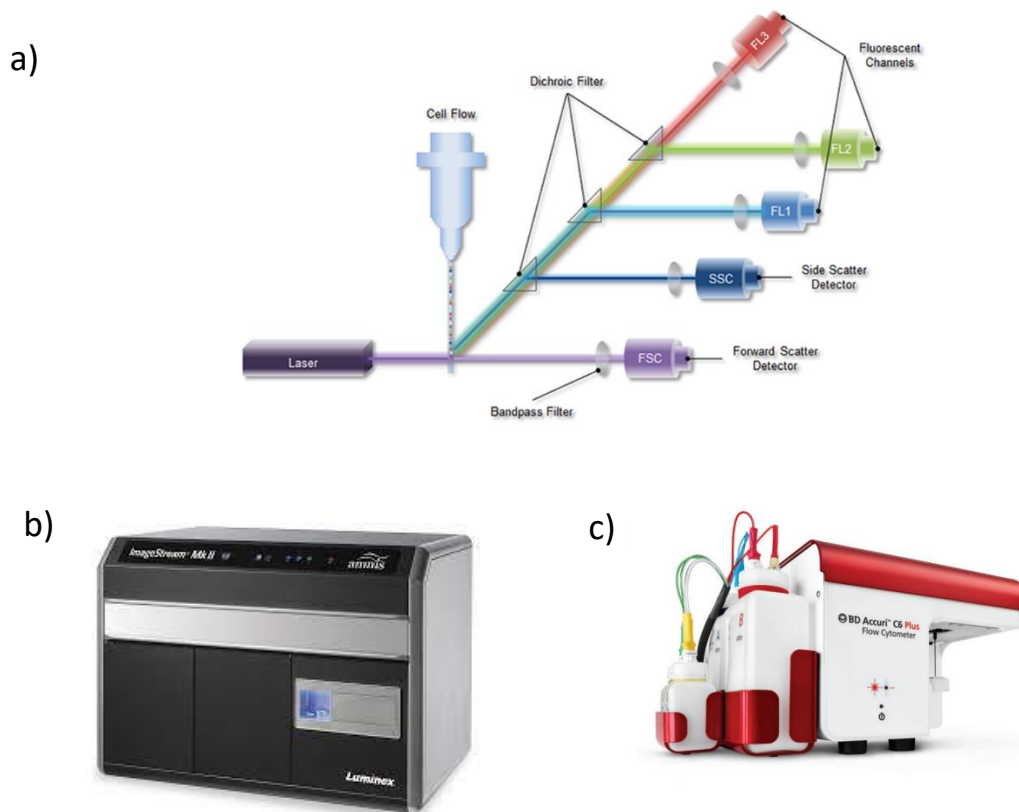


Figure5.4 – Cytometry working principle. Multiple laser source excites the sample, the fluorescence intensity is then read by a photodiode detector (a). An imaging flow cytometry Amnis Image Stream Mk II (b) and a laser flow cytometer BD Accuri C6 plus (c).

Titre : Extraction biocompatible de métabolites de microalgues

Mots clés : Microalgues, bioraffinage, caroténoïdes, solvant organique, granulométrie

Résumé : Cette thèse vise à déterminer les paramètres biologiques qui influencent la biocompatibilité de l'extraction de β -carotène par solvant organique chez la microalgue *Dunaliella salina*. La molécule de β -carotène est un pigment d'intérêt avec des applications industrielles en agroalimentaire, cosmétique et pharmaceutique. Contrairement aux procédés de production actuels, destructif pour la biomasse, l'extraction biocompatible permet de soutirer continuellement le métabolite sans mort cellulaire. Néanmoins, les études scientifiques ont principalement étudié la biocompatibilité à l'échelle de la culture mais manquent d'informations au niveau des cellules individuelles. Pour cela, une méthode robuste d'extraction avec du n-decane et découplée de la culture a été développée en tube Falcon.

Des méthodes de mesure morphologiques et de marquage cellulaire ont été sélectionnées ou améliorées pour obtenir de plus amples informations sur l'exposition des cellules au solvant organique. L'analyse biologique révèle que l'impact photosynthétique est faible, une stimulation de l'activité respiratoire a été observé. Les cellules en phase de division sont moins impactées et les cellules déjà perméabilisées le sont plus. Les résultats ont montré que le taux de destruction était corrélé au volume cellulaire. Ils ont souligné que les cellules les plus fragiles, qui était sélectivement détruites, était plus grande que $1500 \mu\text{m}^3$ et avec une circularité supérieure à 0,7. L'extraction était biocompatible avec des cellules petites ($600\mu\text{m}^3$) et circulaire (0.7), stressées en photobioréacteur. En conclusion, la recherche des conditions de cultures pour obtenir des cellules robustes est une piste à privilégier.

Title : Biocompatible extraction of metabolites from microalgae

Keywords : Microalgae, biorefining, carotenoids, organic solvent, granulometry

Abstract : This thesis aims to determine the biological parameters that influence the biocompatibility of β -carotene extraction by organic solvent in the microalga *Dunaliella salina*. The β -carotene molecule is a pigment of interest with industrial applications in food, cosmetics and pharmaceuticals. Unlike current production processes, which are destructive to the biomass, biocompatible extraction allows continuous extraction of the metabolite without cell death. Nevertheless, scientific studies have mainly investigated biocompatibility at the culture scale but lack information at the single cell level. For this purpose, a robust method of extraction with n-decane and decoupled from the culture was developed in Falcon tubes.

Morphological measurements and cell labelling methods were selected or improved to obtain more information on the exposure of the cells to the organic solvent. The biological analysis reveals that the photosynthetic impact is low, a stimulation of the respiratory activity was observed. Cells in division phase are less impacted and cells already permeabilized are more impacted. The results showed that the rate of destruction was correlated to the cell volume. He pointed out that the most fragile cells, which were selectively destroyed, were larger than $1500 \mu\text{m}^3$ and with a circularity higher than 0.7. The extraction was biocompatible with small ($600\mu\text{m}^3$) and circular (0.7) cells, stressed in photobioreactor. In conclusion, the research of culture conditions to obtain robust cells is a track to be follow for biocompatible extraction.

